Manufacturing of hybrid composites based on polypropylene matrix

A dissertation submitted to The University of Manchester
For the Degree of
MPhil Polymers and Composites
in the Faculty of Science and Engineering

2021

Duriyang Thongsoon

Student ID: 10546917

School of Natural Sciences

Department of Materials

List of contents

Word count: 51,321

List of figures

Chapter 1

Chapter 2

Chapter 3

Chapter 5

Appendix A

Appendix C

Appendix D

Appendix E

List of tables

Chapter 2

Chapter 3

Chapter 4

Chapter 5

Chapter 6

Appendix C

Appendix D

Appendix E

List of abbreviations

AGC	Oleic-Acid modified geopolymer concrete
ANN	Artificial Neural Networks method
ANOVA	Analysis of variance
ASCE	American Society of Civil Engineers
ASEAN	Association of Southeast Asian Nations
ATR-FTIR	Attenuated total reflectance - Fourier Transform Infrared
Au−Pd	Gold-Palladium
$CaCO_3$	Calcium Carbonate
CFRP/GFRP	Carbon fibre reinforced polymer/ Glass fibre reinforced polymer
CH_4	Methane
CE	Circular Economy
CMCs	Ceramic matrix composites
CNTs	Carbon Nanotubes
CO_2	Carbon dioxide
CV	Coefficient of variation
DSC	Differential scanning calorimetry
DOE	Design of experiments
et al.	and others
FRP	Fiber Reinforced Polymers
FTIR	Fourier Transform Infrared Spectroscopy
GFRP-UHPFRC	Glass Fibre Reinforced Plastic - Ultra High-Performance Fiber-Reinforced Concrete
GNPs	Graphene Nanoplateletes
HC	Hybrid composites
HDT	Heat deflection temperature, Heat distortion temperature
IR	Infrared
L/D	Length-diameter ratio of extruder
LGF	Long glass fibre
MAH	Maleic anhydride
MFI	Melt flow index

MMCs	Metal matrix composites
MWCNT	Multi-Walled Carbon Nanotubes
N_2O	Nitrous oxide
NH_3	Ammonia
NO_x	Other oxides of nitrogen
PCW	Post-Consumer Waste
PE	Polyethylene
PLA	Polylactic Acid
PMCs	Polymer matrix composites
PP	Polypropylene
PP/CC	Polypropylene/calcium carbonate composite
PP/CF	Polypropylene/carbon fibre composite
PP/GB	Polypropylene/glass bead composite
PP/GF	Polypropylene/glass fibre composite
PP/GN	Polypropylene/Graphene nanoplatelets composite
PP/KL	Polypropylene/kaolin composite
PP-g-MA	Polypropylene grafted maleic anhydride
pph	parts per hundred
R.H.	Relative humidity
RTM	Resin transfer molding
RSM	Response Surface Methodology model
rHC	Recycled hybrid composite
rPP	Recycled PP
SEC	Specific energy comsumption
SEM	Scanning electron microscopy
SSE	Single screw extruder
TSE	Twin screw extruder
TP	Temperatures profiles
TGA	Thermogravimetric Analysis
vol%	Percentage by volume
wt%	Percentage by weight

List of symbols

Symbol	Description	Unit
A	The initial cross-sectional area of the specimen	mm^2
A	Sample weight in air	g
B	Sample weight in the auxiliary liquid	g
b_1	Width at narrow portion	mm
b_2	Width at ends	mm
E_t	Tensile modulus	MPa
F	Measured force concerned	N
$\overline{h}$	Average thickness of samples	mm
H , h	Thickness of the specimen	mm
ΔH_c	Crystallization enthalpy	J/g
ΔH_m	Melting enthalpy	J/g
ΔH_o	Theoretical melting enthalpy of the 100% crystalline	J/g
m	Mass	g, kg
ΔL_o	The increase of the specimen length between the gauge marks	mm
L_0	Gauge length	mm
L	Initial distance between grips	mm
L	The length of span	mm
l_1	Length of narrow parallel-sided portion	mm
l_2	Distance between broad parallel-sided portions	mm
l_3	Overall length	mm
S_i	Deflections	mm
S.D.	Standard deviation	
T_c	Crystallization temperature	^oC
T_m	Melting temperature	^oC
V	Volume	
X_c	Percentage of the crystallinity	%
$\overline{x}$	Average of the dataset	
σ	Tensile stress	MPa

σ_{f1}	Flexural stress	MPa
$\varepsilon_{f\,i}$	Flexural strain	
ρ	Density of sample	kg/m^3,g/cm^3
ρ_o	Density of the auxiliary liquid	kg/m^3,g/cm^3
ρ_L	Density of air (0.0012 g/cm^3)	kg/m^3,g/cm^3
η	Shear viscosity	Pa.s
ϕ	Diameter	mm

Abstract

Composites are becoming widely popular in wide range of applications due to their superior properties. Based on the key learnings from number of literatures, this present work aimed to explore potential methodologies to improve and to maximize the performance of recycled PP matrix composites via hybrid reinforcement systems by adapting methods overcome the knowledge gaps and limitations. The novelty of this research was created by the consideration of processibility and cost, the suitable compatibilizer dosage, the maximum filler content and maximum ratio of recycled PP to obtain the acceptable range to the composite in the market. To achieve the best possible combinations, a comprehensive study was carried out to explore the effect of filler types and loading via a number of screening tests. Fillers from both fibre family (i.e., carbon fibre and glass fibre), and particle family (i.e., $CaCO_3$, glass bead, kaolin and Graphene Nanoplatelets (GNPs)) were processed using a twin screw extruder. Firstly, the effect of filler types and loading on mechanical and thermal properties of neat PP composite systems were investigated as a reference result. The filler contents were varied from 10 – 30 % by weight. Mechanical properties such as the tensile modulus, flexural modulus and Izod impact strength were evaluated. For the particle family, PP/glass bead composites had the best overall mechanical properties. Mechanical properties such as tensile, flexural modulus and Izod impact strength showed maximum improvements by 37%, 47% and 6%, respectively compared to neat PP. These PP/glass bead composites were improved with a simple compounding process and with an acceptable cost. Therefore, the most suitable filler from the particle family was the “Glass Bead”. For the fibrous family, PP/glass fibre was selected as the most suitable fillers due to the incorporation of glass fibre could promote the mechanical properties up compared to neat PP more than carbon fibre especially for Izod impact strength. At the second stage, the best performing fillers from each family which were glass fibre and glass bead were used to manufacture hybrid composite systems. These hybrid composite systems were investigated on neat PP resin. Then, thirteen sets of experimental trials were carried out by varying the ratios of glass bead and glass fibre combinations. Based on the experimental results, it can be concluded that PP hybrid composites with 10 wt% of glass bead and 40 wt% of glass fibre and 7.5 wt% of PP-g-MA (HC13) was the most suitable formulation among all of hybrid composite formulations tested. This is considering their superior mechanical properties e.g. tensile, flexural modulus and Izod impact strength with 250%, 330% and 34% improvement respectively compared to the extruded neat PP. Moreover, it was also cheaper and its density and melt flow index were acceptable for injection moulding application in the current market.

At the final stage of the project, the selected combination of glass fibre and glass bead reinforcements (HC13) was used to manufacture recycled PP based composites. Composites were manufactured by varying the percentage of recycled PP from 5 to 100 wt% in order to investigate the mechanical properties. In conclusion, the implementation of the formulation HC13 by replacing neat PP with rPP, could be effective since the performance of rPP was demonstrated to be comparable to that of neat PP in term of the mechanical properties.

Furthermore, all the test samples were validated through thermal and rheology properties. Fractured surfaces were studied by employing scanning electron microscopes (SEM). These types of hybrid filler systems can be considered as promising reinforcing materials to increase the performance of thermoplastics. Hence, the results achieved in this work with these composite systems should encourage recycled thermoplastics to be applied for high-end applications at a significant rate in the near future.

Declaration

The author of this thesis declares that no portion of the work referred to in the thesis has been submitted in support of an application for another degree or qualification of this or any other university or other institute of learning.

Copyright Statement

i. The author of this thesis (including any appendices and/or schedules to this thesis) owns certain copyright or related rights in it (the "Copyright") and s/he has given the University of Manchester certain rights to use such Copyright, including for administrative purposes.

ii. Copies of this thesis, either in full or in extracts and whether in hard or electronic copy, may be made only in accordance with the Copyright, Designs and Patents Act 1988 (as amended) and regulations issued under it or, where appropriate, in accordance with licensing agreements which the University has from time to time. This page must form part of any such copies made.

iii. The ownership of certain Copyright, patents, designs, trademarks and other intellectual property (the "Intellectual Property") and any reproductions of copyright works in the thesis, for example graphs and tables ("Reproductions"), which may be described in this thesis, may not be owned by the author and may be owned by third parties. Such Intellectual Property and Reproductions cannot and must not be made available for use without the prior written permission of the owner(s) of the relevant Intellectual Property and/or Reproductions.

iv. Further information on the conditions under which disclosure, publication and commercialisation of this thesis, the Copyright and any Intellectual Property and/ or Reproductions described in it may take place is available in the University IP Policy (see http://documents.manchester.ac.uk/DocuInfo.aspx?DocID=24420), in any relevant Thesis restriction declarations deposited in the University Library, the University Library's regulations (see http://www.library.manchester.ac.uk/about/regulations/) and in the University's policy on Presentation of Theses.

Acknowledgements

This dissertation is accomplished by kind supports and assistances from many individuals. I would like to express my special appreciation to all of them.

It is a great pleasure to express my deepest gratitude towards my supervisor, Dr.Chamil Abeykoon who always provided the guidance, dedication and constant supervisions as well as willingness to facilitate this research under difficult circumstances. I would like to express my very great appreciation to Dr. Ivan Vera marun and Prof. Prasad Potluri, my co-supervisors for their very useful advice and encouragement. Your kind supports and dedication from all of you are invaluable to me.

I am particularly grateful to Andrij Zadoroshnyi for his kind trainings and suggestions on all polymer processing machines. Also, I would like to thank Stuart Morse for his supports in mechanical testing. My special thanks are extended to all friends and staffs in James Lighthill building for their kind greeting and assistance.

I would like to express my deepest appreciation and acknowledge the contribution of SCG Chemicals Co., Ltd. for financial support during my MPhil study. I am highly indebted to my mentors, Dr. Butra Boonliang and Dr. Wareerom Polrut for their guidance, kind cooperation and encouragement which helped me in completion of this project. Moreover, I wish to acknowledge the willingness to support and help, which have been provided by members of the Application Development Centre and Application Development Support Team from SCG Chemicals Co., Ltd.

Lastly, I would like to express my sincere gratitude towards my beloved parents, brother and my girlfriend for love and encouragement. You are the reason why I keep pushing to overcome all the struggles and obstacles during this difficult circumstance.

1. Introduction

1.1 Background of global composite usage and applications

The development of composite materials and their various applications have expanded rapidly since the middle of the 20th century [1]. Generally speaking, a composite material is a combination of two or more materials, consisting of matrix material and reinforcing materials with different properties and forms such as particles, fibres [1-3]. The matrix material is a continuous phase, and it includes metal, inorganic non-metallic matrix and polymer matrix composites. For the reinforcing materials, they may be considered as assistant ingredients or compounding agents. They refer to auxiliary materials which are physically dispersed within the polymer matrix without significantly affecting the polymer molecular structure. Their main functions are to improve performance of the polymer matrix, such as mechanical properties, enhancing the stability, etc as it carries the applied load to the material [4, 5].

In terms of classification composites, there are several ways to classify composite materials. They can be categorized in accordance with the type of matrix material such as Metal Matrix Composites (MMCs), Ceramic Matrix Composites (CMCs) and Polymer Matrix Composites (PMCs) [4]. Typically, the classification of composites is usually made with respect to the matrix constituent. However, polymer matrix composites have been widely used and have become the fastest growing composite materials for various applications [4]. Polymer composites are used extensively in aerospace, automotive, marine, building and construction, furniture, sports goods, telecommunication, and railway industries, etc. [6].

It is difficult to accurately state about when composites originated but their first uses were estimated back to the 1500s in order to create durable buildings [1, 5]. In 1935, Owens Corning introduced the first glass fibre and launched the fibre reinforced polymer resin. This was the beginning of the Fibre Reinforced Polymers (FRP) as we know today. In the 1970s, the composites industry began to mature since a number of improved reinforcing fibres and plastic resins and were developed such as Aramid, Kevlar [1]. In the 1990s and 2000s, composite materials became more common in mainstream manufacturing and construction due to their specific strength, cost-effectiveness, replacing engineering thermoplastics. From the mid-2000s, composite materials have been used in aerospace and marine applications. Nowadays, research on composite materials attracts significant amount of funding from governments and is expected to continue this growth over the coming years [5].

A review of the applications of the composites industry within the global composites market revealed that in 2016 the top three industries in terms of volume and value were logistic, construction & building and electrical & electronic goods, as shown in Figure 1.1(a) and (b) [7].

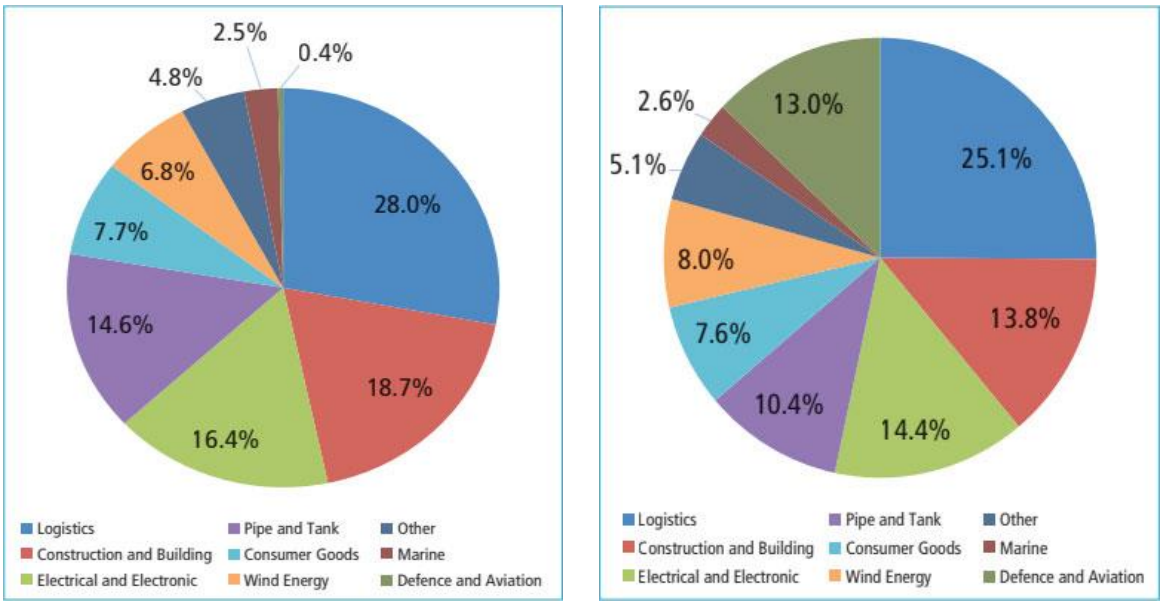

(a) (b)

Figure 1.1: Distribution of the global composites market in 2016 by application in terms of (a) volume and (b) value [7]

The global composites market revenue was valued at 78,400 million USD in 2020. It is expected to reach 110,910 million USD by the end of 2026. Grand View Research Inc, has forecasted 5% of annual growth rate of composites usage over the period of 2021-2026 [8]. The global composites market size is consistently expanding owing to their myriad applications, including construction, industrial, automotive, defense, sports, and aerospace, etc.

For these applications, polymer matrix composites (PMCs) have been selected. This is due to the functions of the polymer matrix in helping to distribute or transfer loads, control chemical properties of composites, carry interlaminar shear, hold all reinforcements together as a binder, and protect the fibres from mechanical damage due to crack propagation within the material, both during fabrication and in the finished component [6].

In terms of polymer matrix composites, the two main types of polymer are thermoplastics and thermosettings [4]. Thermosetting polymers are composed of long chains of molecules that are strongly cross-linked to other long chains of molecules after curing. However,

thermoset composites are very difficult to recycle due to the irreversible reaction occurs during processing. On the contrary, thermoplastic polymers are not chemically cross-linked, which allows them to be re-melted and reformed a few times. They do not require a catalyst, oven or autoclave to recycle. They are composed of long polymer chains that are entangled from the joining together of monomer units [6].

The polymer matrix composites can be made by using thermoset or thermoplastic polymers but there are some differences between both of them. For thermoset composite, once thermoset polymer has been catalyzed, it cannot be reversed or returned to their original form. Its shape cannot be altered. Therefore, thermosetting composite would be beneficial in terms of strong material, very good fatigue strength and can be used for high-heat applications because the thermoset matrix does not melt like thermoplastics. However, the drawbacks of thermoset composites are the extremely brittleness and low impact toughness. Moreover, the recycling of thermoset composites is extremely difficult. While, thermoplastic composites can be melted, molded and remolded. They offer tougher and very good impact resistance and damage tolerance compare to thermoset composite. Since the thermoplastic can be re-melted, it can be recycled and repaired easily. However, the disadvantages of thermoplastic composites are more energy consumption for manufacturing process comparing to traditional thermoset composite manufacturing process. Both of thermoset and thermoplastic polymer have different properties and pros and cons. It depends on which one is best suited to any given applications [9, 10].

From the pros and cons of thermoset or thermoplastic composites, researchers prefer thermoplastic polymeric matrices than thermosets due to performance of materials, lower cost of processing, and high reparability [11]. Among of thermoplastic, Polypropylene (PP) is one of the important polymers in the group of commodity thermoplastics produced in large quantities which has great efforts to utilize PP in the advanced engineering applications such as aerospace engineering, automotive, electrical appliance, renewable energy [12]. There are some reasons why work on PP could be applied to wider engineering. PP has been selected as the most suitable material in many applications since it possesses several properties such as high heat distortion temperature, transparency and dimensional stability which widen its application. For works of composite PP is widely used as polymer matrix because it has some excellent characters for composite fabrication which is very suitable for filling, reinforcing and blending [11].

Polymer composite materials offer a wide range of advantages to industries. Examples of composites have been described in many aspects which can improve mechanical properties, enhance chemical corrosion resistance, good moldability, low manufacturing cost due to low part count, longer fatigue resistance, retain properties at high temperature, good electrical and thermal insulation and can be pigmented easily.

However, polymer composites suffer from some drawbacks such as lack of ductility, variation in properties of parts due to the nature of fabrication, degradation by solvents and moisture, and propagation of crack in fibre direction [1]. Besides these drawbacks, sometimes an attempt to improve the tensile property would lead to the simultaneous decline of impact property [4]. Furthermore, these significant drawbacks and limitations include the deterioration in impact resistances or other properties such as optical, thermal properties and moisture barrier properties [13]. It appeared that these limitations could be overcome by using “hybrid composites”.

1.2 Hybrid composites

Hybrid is the Greek-Latin word which means something of mixed origin or composition. This term has been used in numerous researches and has been clarified in various definitions [14]. A hybrid composite is defined as a combination of at least two different materials or reinforcement materials are incorporated and embedded into a single matrix material [12, 14-17]. The incorporation of hybrid fillers was shown to enhance the physical and mechanical properties of the hybrid composites or aids in achieving a balance between performance and cost of composites [14]. Research and application of hybrid composites have greatly increased since the 1970s. Firstly, hybrid composite materials were mainly used as structural materials. Between 1985 and 1990, their applications grew relatively fast and had an increase of up to 10 times in 5 years [4]. Hybrid polymer composites were fabricated as new and effective alternative materials having better performance, lighter weight and more cost effectiveness than composite materials with single reinforcement [12]. The hybrid fibres in the composites can withstand higher loads compared to single-fibre reinforcements in different direction, acting as a higher load transfer medium between them [2]. Extensive research supported that hybridization was one of the methods used by researchers to overcome the negatives of one fibre with the introduction of secondary reinforcement [16].

Currently, there is a growing demand for hybrid composites in the advanced engineering applications such as aerospace engineering, secondary structures applications, aircraft interior, solar cells and in wind energy generation [12, 14]. Applications of the hybrid composites in various industries are as follow;

1.2.1. Application of hybrid composites in the aerospace industries

The application of hybrid composites in the aerospace industry includes their use in aircrafts, spacecrafts, satellites, helicopters, missiles, and booster rockets [18]. Hybrid composites are sought after by the aerospace industry because there are lightweight materials that can improve aircraft's performance and hence reduce costs. Another reason for the high demand for hybrid composites in aerospace sector include their excellent strength, stiffness, fatigue resistance and ability to be tailored-made for specific purposes. Reinforcement materials have been used in this area are carbon fibre, aramid, and glass fibre. For example, the application of composites in the body of the Airbus A350 and Boeing 787 Dreamliner, in which the proportion of hybrid composites of carbon fibre with other materials is more than 50%, as shown in Figure 1.2 [19, 20].

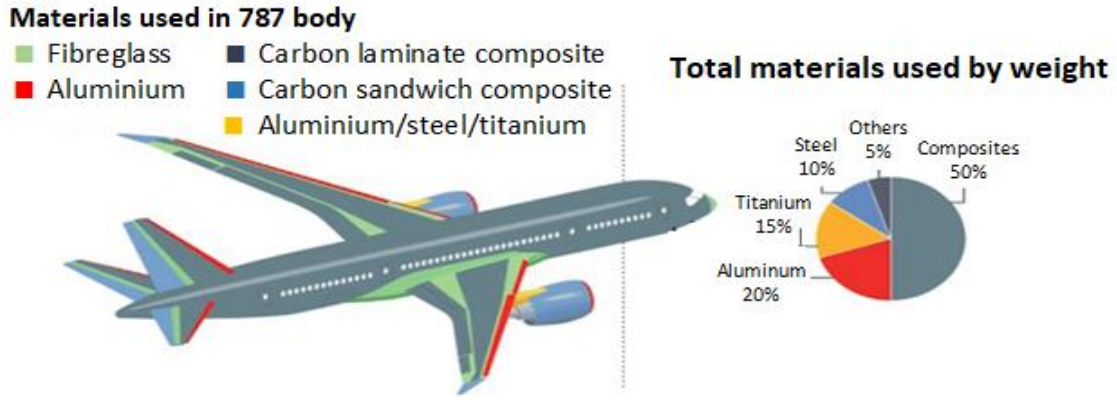

Figure 1.2: Usage of various materials in the Boeing 787 Dreamliner by comparison, the 777 uses 12 percent of composites and 20 percent aluminum [19]

In 2019, the market size of aerospace composites was 12.7 billion USD and it has been predicted to register over 9% growth in the period between 2020 and 2026, as depicted in Figure 1.3.

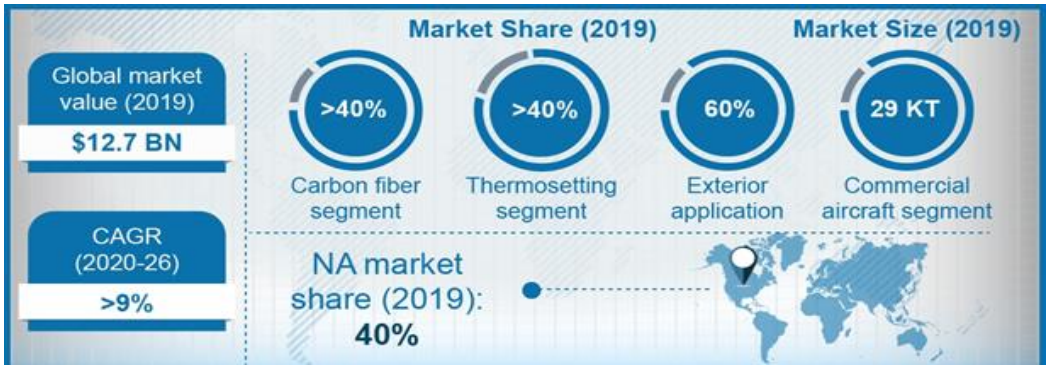

Figure 1.3: Details of the composites market relating to aerospace industry in 2019 [21]

However, the COVID-19 pandemic has adversely affected the aviation industry leading to shutdown of aircraft production and cancellation of new orders. Global air traffic reached to an almost standstill in the early 2020, thus affecting the aerospace industry. The reduction in air transportation together with shutdown of the manufacturing will negatively impact the market size of this segment [21].

1.2.2. Application of hybrid composites in the automotive industry

Regarding the automotive industry, hybrid composite materials have been widely used in various components such as engine covers, doors, floors, seats, and so forth. In railway transport, composite materials are used in passenger carriage doors, windows and various communication equipment [4]. One of the key properties is their light weight because lighter vehicles require less energy to start and stop, improving fuel efficiency. Stringent fuel economy and emission regulations from 2020 to 2022 will continue to drive demand for lightweight materials [3, 22].

In consideration of the automotive market, over 2 million tons of composite materials have been sold into automotive applications on an annual basis [22]. The vast majority of this volume is thermoplastic composites. Growth in global vehicle production was modest in 2019, with an annual growth rate of about 2% expected in the near future [3, 22]. The implementations of polymer composites in automobiles cover both interior and exterior parts, as seen in Figures 1.4 – 1.6.

(a) (b)

Figure 1.4: (a) Car window regulators made from kenaf fibre composites (b) Samples of carbon and glass fibre reinforced epoxy composite automotive drive shafts [6]

Figure 1.5: Side panels on John Deere hay balers incorporate polyurethane resins derived from corn and soy beans [23]

Figure 1.6: Glass fibre reinforced plastic has been replaced by flax/polypropylene composite for under body components of the Mercedes Benz A-Class[23]

1.2.3. Application of hybrid composites in infrastructure industry

In the infrastructure industry, hybrid composites have been extensively used in a variety of large building structures. The key areas that must be addressed are initial cost, durability, fire resistance, ease of erection and retrofitting in-service structures. Furthermore, the development of smart manufacturing of composites must focus on the capability to retrofit existing infrastructure and new modular systems, resulting in high labour productivity and high-quality of finished products [22]. Examples of usage of polymer composites are shown in Figures 1.7 – 1.8.

Figure 1.7: Repairing of a corroded concrete column by using fibre reinforced polymer [24]

Figure 1.8: Glass Fibre Reinforced Plastic - Ultra High-Performance Fibre-Reinforced Concrete (GFRP-UHPFRC) pedestrian bridge in Miyagi, Japan [12]

U.S. infrastructure is projected to replace conventional construction materials in areas of high corrosion with composite materials [22]. Fibre reinforced composites have inherent advantages such as corrosion resistance, durability, magnetic transparency, high strength and high stiffness-to-weight ratio. Over the next 10 years, the American Society of Civil Engineers

(ASCE) projects a 1.4 trillion USD funding gap between revenue and needs. The export market of U.S. composites is expected to grow of up to 4.9 % annually by 2022 [22].

1.2.4. Application of hybrid composites in the marine industry

Hybrid composite materials are used in the production of different work boats, such as fishing boats, transport boats, cruises, military minesweepers and submarines, mostly in anti-corrosion equipment as seen in Figures 1.9 and 1.10 [12, 25]. The fibre-reinforced polymer composites have gained wide acceptance in the marine industry due to their high strength-to-weight ratio, ability to withstand harsh off-shore conditions, resistance against corrosion and erosion, good protection from environmental degradation and impact loads [11].

Figure 1.9: Hybrid Carbon fibre reinforced polymer/ Glass fibre reinforced polymer (CFRP/GFRP) composite laminate as face skin of Visby Class corvette [12]

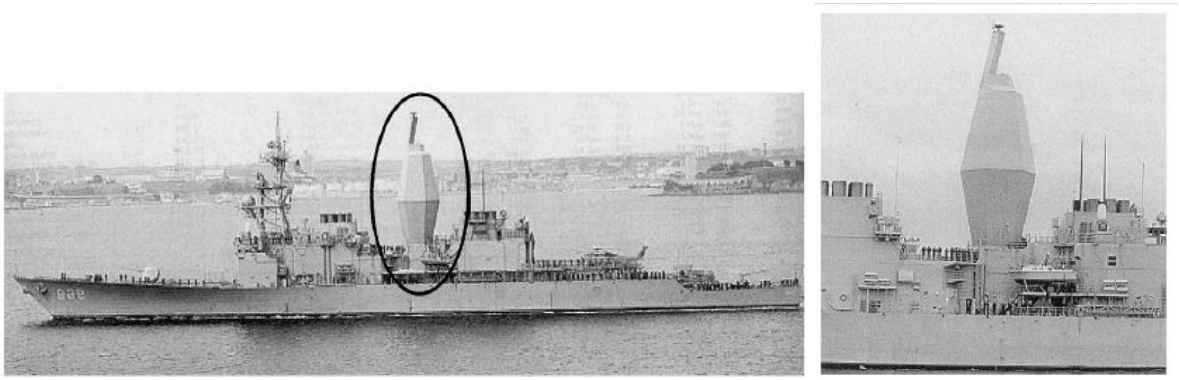

Figure 1.10: The Advanced Enclosed Mast Sensor System was installed aboard the Spruance class destroyer USS Arthur W. Radford [25]

1.2.5. Application of hybrid composites in sporting goods and leisure

Hybrid composite materials have been used in various sporting goods which require light weight and strength. Carbon/Glass/Kevlar fibre reinforced composites and carbon nanomaterials (e.g., carbon nanotubes, nanoclay, nanoparticles, and fullerenes) are of great

interests for this market [12]. For example, squash racquets have consisted of composite materials due to their light weight, stiffness, and toughness. Moreover, hybrid composite has been applied for the golf club to balance of compression and tension forces, consistency of feel, light weight, and durability. Boron, carbon, and aramid fibre hybridization allow the aramid fibre to dampen vibration and reduce weight. Furthermore, carbon and glass fibre hybrids play to the key properties of each and offer affordability [26]. Other applications of composite materials in the sport industry include the making of bicycle frames, golf shafts, tennis rackets, fishing rods, snow skis, ski boots, racing cars, hockey sticks and pole vaults [6]. Some sporting goods from composites are shown in Figure 1.11 – 1.12.

(a)

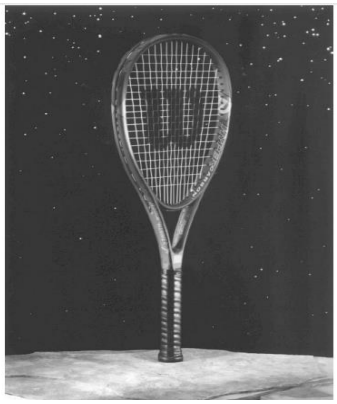

(b)

Figure 1.11: (a) Mandrel wrapped golf club shafts from S-2 glass fibre in the laminate (b) Millennium racket made with high stiffness carbon fibres from Toray [26]

Figure 1.12: Bicycle featuring carbon-based composite components ridden by some cyclists in 2008 Tour de France race [12]

1.2.6. Application of hybrid composites in other industries

There are many industries that require composites in order to improve performance such as electrical and electronic industries. Composite materials are used in the production of laminates, insulated pipes, tools of live operation and fishery [4]. Moreover, the hybrid composites have been used in sophisticated applications such as composite scaffolds for tissue engineering, hydrogel for fabricating nanocomposites, metal filled conducting

polymers, etc. Hybrid composites represent the advanced next generation of engineered materials, with functions such as carrying mechanical loads along with delivering or storing electrical energy [12].

1.3 Plastic recycling and Circular Economy (CE)

Nowadays, people are increasingly concerned about comfort of life and the pursuit of health, while environmental damage is becoming intolerable. The rapid increase of global population is directly associated with the growing consumption of natural resources and negative environmental impacts [27]. It is estimated that of around 8.3 billion metric tons of plastic have been produced worldwide since plastic was introduced in the 1950s [28-31]. At present, the annual global plastic production is approximately 359 million metric tons [32].

Although it is being said that up to 90% of solid plastic waste is recyclable, there is only less than 10% of plastic waste actually recycled each year [13, 33, 34]. The rest is sent either to landfill or to incineration plants. These incineration processes can cause serious consequences to the environment as they produce greenhouse gases such as CO_2 (Carbon dioxide), N_2O (Nitrous oxide), NO_x (other oxides of nitrogen), NH_3 (ammonia), CH_4 (methane) and organic carbon, measured as total carbon [35]. For instance, landfill liners can break by allowing harmful pollutants to mix with soil and underground water [36]. Moreover, many reports showed that solid plastic waste in the sea and the subsequent fragments can enter the environment and eventually be ingested into the bodies of living organisms, including humans [37, 38]. The best known consequence of this problem is The Great Pacific Garbage Patch which is the highest density of marine debris has been created by the effect of ocean current and the accumulation plastic wastes and other litters which end up in the North Pacific Ocean. These patches are almost entirely made up of tiny bits of plastic, called “microplastics” [39]. However, reports revealed that the average composition of the polymer waste streams is dominated by Polyethylene (PE) and Polypropylene (PP) which have been calculated as about 60% of the plastic materials we use in the current decade [40, 41]. There are great efforts undertaken to transform PP into a specific type of thermoplastic suitable for engineering use. Research works have been focused on upgrading the mechanical performance of PP by toughening, filling and reinforcing. The advantages of PP composite for replacing more conventional automotive materials offer short processing time, excellent corrosion resistance and potential for rapid repair [42].

There are several opportunities and challenges for the development of composite materials, with one of the important challenges being their environment management. A sustainable approach is making polymer composites from recycled polymers. This way, we can decrease massive bulk volume of the polymers and obtain high quality products. Recycling process is one of the alternatives increasingly promoted to achieve a Circular Economy (CE) [27, 43, 44]. Many scholars considered that the circular economic system was primarily introduced since the 1970s by the environmental economists, Pearce and Turner [27]. The overall objective of the circular economy was mainly to promote the sustainable development of economy and society, while it also helps to achieve sustainable environmental protection and also prevent losses and reduce the demand for primary raw materials [27, 44, 45].

The current concept of circular economy formulated by practitioners and businesses is depicted in Figure 1.13. The circular economy prefers product reuse, remanufacturing and refurbishment, therefore demanding less resources and energy and being more economical. Then, recovered material will be prepared for remanufacturing, which has been the main focus in traditional recycling. According to the circular economy, landfill should be the last option. In this way, the product value chain and life cycle retain the highest possible value and quality, as well as being as energy efficient as it can be [43]. From the principle of circular economy, recycling of materials is considered as the one of the main pillars and is also expected to be economical and to discharge fewer pollutants [44].

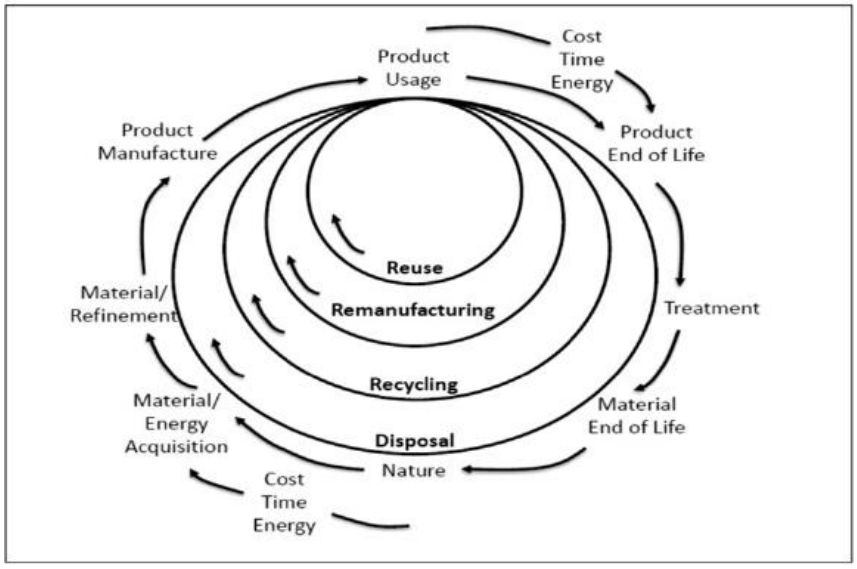

Figure 1.13: The current concept of circular economy [43]

The advantages of recycling cover aspects regarding both the environment and the economy. For example, recycling can assist to conserve finite natural resources. Furthermore, recycling prevents waste from going into oceans and it encourages to significantly reduce the use of fossil fuel energy and CO_2 emissions. With regards to the economy, the process of recycling can create valuable resources for manufacturing and also generates more jobs [46, 47].

However, the quality of recycled plastic is a limitation that restricts usage in single plastic applications such as trash bags and shopping bags. This is due to the degradation of recycled plastic by chain scission causing the deterioration of the mechanical properties such as tensile strength and modulus, together with the increase of melt flow index which is due to decrease in molecular weight. Moreover, the increasing processing cycles effect directly to additive consumption [48, 49]. The appearance and color of the material is also affected. As degradation can cause a discoloration of the material, the pellets change color (turn yellow) and become darker with every processing cycle [50].

In consideration of Polypropylene (PP), it is a commodity thermoplastic produced in large quantities. In 2018, 1.06 million metric tons of polypropylene were lost to the environment worldwide [51]. Given these issues, there are a number of attempts by many research groups to improve the performance of recycled PP. Conventionally, the performance of recycled PP can be promoted by incorporating particles, fibres reinforcing agents. In some single-component composite systems, specific properties have been improved while another properties have been demoted. Several studies showed that strength and impact toughness of recycled PP have been decreased compared to neat PP in PP/glass fibre composites [52, 53].

In order to enhance and compensate such properties, hybrid composite systems have been introduced by combining various fillers in a composite system. These methods exploit pros and cons that each component contributes to composite materials such as fibre/calcium carbonate system or glass fibre/graphene [54, 55]. Several components have been combined in PP composite systems in order to promote performances of PP. Therefore, maximizing the performance of recycled PP in hybrid composites is a challenging topic.

1.4 Aims and objectives

This study aims to explore potential methodologies that can improve the performance of recycled PP to be comparable to neat PP which can be used in potential applications via hybrid

reinforcement systems. The most suitable hybrid composites have been determined from criteria that are the improvement of mechanical properties, processability and cost.

The following objectives are set to achieve the aims of this study. First, for achieving the best possible performance of recycled PP hybrid composites, a comprehensive study will be carried out to investigate the effect of different families of fibres and filler types, as well as loading, by a number of screening tests. Then, the best performing candidate in each family will be selected and combined to manufacture a hybrid composite. All the specimens will be validated through analytical, mechanical and thermal properties including failure mode and fracture surfaces. The project is separated into three stages of experiments.

Stage 1: Screening experiments for selecting the best suited fillers for hybrid composites

This stage will focus to study reinforcing performances of candidate fillers from fibre and particle families with neat PP resin in various composites systems. Here it is expected:

- to study the best processing conditions for neat PP based composites.
- to evaluate the performance of neat PP based composites from various fillers by investigating mechanical properties (such as tensile, flexural, impact testing), thermal properties, rheological properties, density and melt flow index (MFI).
- to study the morphology of PP composites including fracture mode by scanning electron microscopy (SEM).
- to study the presence of chemical functional groups fracture mode by Fourier transform infrared spectroscopy (FTIR).

Stage 2: Determination of the best formulation of the neat PP based hybrid composites

The main purpose of stage 2 is to study the effect of ratio of selected reinforcing agents in order to find out the best possible formulation in terms of mechanical properties through flexural modulus, tensile strength, Izod impact strength. Here, it is expected:

- to evaluate the performance of hybrid composites by investigating thermal properties, rheological properties, density and MFI.
- to study the morphology of PP hybrid composites including fracture modes by SEM.
- to study the presence of chemical functional groups fracture mode by FTIR.

Stage 3: Recycled PP based hybrid composites

This final stage is to study the performance of recycled PP based from hybrid composites and main focus will be:

- to study the effects of blending ratio of Recycled PP (rPP) to neat PP.
- to evaluate the performance of rPP based composites from various ratio of rPP by investigating mechanical properties (such as tensile, flexural, impact testing), thermal properties, rheological properties, density and MFI.
- to study the morphology of recycled PP hybrid composite including fracture mode at break area by SEM.
- to study the presence of chemical functional groups by FTIR.

2. Literature review

2.1 Polypropylene based composites

Polypropylene (PP) is a crystalline thermoplastic polymer that can be made by polymerizing propylene molecules [11]. It is well known that PP is one of the important polymers in the group of commodity thermoplastics produced in large quantities. Nowadays, there are great efforts to utilize PP in the advanced engineering applications such as aerospace engineering, automotive, electrical appliance, renewable energy [12]. There are plenty of works have focused on upgrading the mechanical performance of PP by toughening, filling, and reinforcing [56]. PP has been selected as the most suitable material in many applications since it has valuable properties such as the dimensional stability, high temperature resistance, high heat distortion temperature (typical value in the range of 93 – 100^{o}C) [57, 58]. Moreover, it is relatively easy to mould into shapes and has good performance in processing. Therefore, it is one of the most versatile polymers which is used widely in everyday objects. PP is also very suitable for filling, reinforcing and blending. There are a number of researches that have explored the possible use of PP as a matrix in manufacturing of polymer matrix composites.

2.2 Reinforcing materials

In the development process of polymeric materials, the reinforcing agents have become the second major component of polymer materials which have been considered to be essential. There are a plenty of reinforcing materials which have been studied as an auxiliary material that improves the performance of the matrix materials such as mechanical properties, dimensional stability, thermal resistance, etc [4]. In general, reinforcing agents are in the form of fibre, particles and flakes sizing from macro to nano scale. Some of the examples for fibrous type are carbon fibre, glass fibre, carbon nanotube, etc. while many materials belong to the particle family such as $CaCO_3$, kaolin, glass beads, carbon black. Moreover, they can be in the form of flakes such as mica flake, glass flake, aluminium flake, and so forth. In this study, ubiquitous fibrous (glass fibre, carbon fibre) and a few particle reinforcing agents ($CaCO_3$, kaolin, glass beads, GNPs) that have been widely used in polymer composite industries are chosen to be investigated. The basic information of these selected reinforcing agents have been described in Appendix A.

2.3 Previous studies on the preparation and properties of PP composites

2.3.1 PP/fibre reinforced composites

2.3.1.1 PP/glass fibre composites

Glass fibre is one of the well-known fillers to be added in thermoplastics [59]. Over the last five decades, short fibre reinforced thermoplastics have replaced traditional materials in many high-performance applications such as transportation, environmental protection, petrochemical, electronic and electrical appliances, machinery, aerospace, nuclear power, weapons, and many others [4, 60, 61]. A great amount of work has been done to understand the structure-properties relationship in PP/glass fibre composites. This is because of the fast growing rate of PP applications in automotive and other industries [59, 62]. Not only the low cost of PP but also the case of its comparatively ease of fabrication, fast processability and recyclability motivate its widespread use [62].

Addition of glass fibre as a reinforcing material improves mechanical properties of the resulting composites due to their high tensile and flexural properties [59, 63-65]. Zebarjad et al. [59] supported that yield stress and tensile modulus were increased with addition of glass fibre. The incorporation of 30 wt% of glass fibre can improve yield stress and tensile modulus by 41% and 200% higher than neat PP, respectively. This is because glass fibres have high tensile strength and modulus compared with neat polypropylene. The primary function of the fibre–matrix interface is to transmit stress from the weak polymer matrix to the high-strength fibres [59]. Caring et al. [65] found that nylon/glass fibre at 30 wt% increases its toughness by an average of 18%. This improvement is due to the longer fibres themselves beginning to play a significant reinforcing role in the matrix [65]. Ramsteiner et al. [66] revealed that tensile and impact strength depend on several parameters such as fibre content, fibre orientation and geometry, as well as interfacial adhesion between fibre and polymer matrix [66]. Interfacial adhesion appeared to be of significance in determining stiffness, work by Gupta et al. [67] revealed that the shear strength of the samples prepared from short fibre with a coupling agent had the highest values at all temperatures because the interfacial bond between the fibre and the matrix is strong and the fibres can consequently carry higher load. While the samples prepared from long fibre granules without coupling agent had the lowest value at all temperatures (from -43, 20, 55, 90^{o}C). This is a consequence of the poor bonding between the fibre and the matrix [67]. Earlier works have shown a significant increase of both fibre/matrix adhesion and composite properties with the addition of a coupling agent such as

maleic anhydride (MAH), which is grafted onto the PP backbone (PP-g-MA) [62, 63, 68]. The level of improvement has been shown to depend on the concentration of the coupling agent. Moreover, it can be seen that yield stress, modulus of elasticity and elongation to failure were highly dependent on the surface treatment of glass fibres, that is, the fibre–matrix interface [55, 59]. Etcheverry et al. [63] conducted by adding untreated and treated fibres with 0.5 wt% to 2.0 wt%, with the results evidencing that samples from the PP/treated glass fibre composites had tensile strain increased three times from 2% up to 7% [63].

Besides the interfacial adhesion between fibre and matrix, other factors that are also very important to composite performance are fibre length, orientation and uniformity. In general, toughness is the highest in the composite with the longest fibres. Some researchers proved that the strength of short-fibre-reinforced thermoplastics increases rapidly with the increase of the mean fibre length [64, 67] However, in case of samples having higher average fibre length, the dispersion of fibres is usually not uniform. While longer fibres are expected to provide higher stiffness, the agglomeration due to poor dispersion of fibres apparently has an adverse effect [67]. If the fibres are very short, then a coupled, well-bonded interface is an advantage. Regarding fibre orientation, the composite strength increases with the increase of fibre orientation coefficient [64].

On the other hand, a number of limitations of glass fibre have emerged. One of the major disadvantages of reinforced plastics with glass fibre is the embrittlement of the materials, especially if the matrix material is ductile. This deterioration in impact behaviour often limits the application of fibre-reinforced materials [66]. Some researchers found that the tendency of the material to draw was reduced by increasing the glass fibre content. Zebarjad et al. [59] indicated that the addition of glass fibres to PP matrix suppresses its tendency to neck [59].

The deterioration of glass fibre composite properties have mainly been from the breakage of the glass fibre. The fibre length attrition can be considered as a two-stage phenomenon. Firstly, the fibres are exposed by surface melting of the granules close to the barrel wall of the extruder. Furthermore, they interact with flow of the molten polymer and experience a bending moment which can result in fibre breakage. The broken pieces flow with the polymer melt and can experience further breakage [69]. Gupta and coworkers reported that additional breakages occur in the mold and runners, but that most of the length reduction occurs in the injection unit [69]. The average fibre length might be affected by fibre volume fraction or process conditions, screw speed including barrel/die set temperature [69]. Not only the

processing conditions affect to the fibre breakage, but the fibre ends are also good places for craze initiation because they act as stress concentrators as a result of their weak bonding to the matrix [59]. Moreover, a number of authors have considered and analyzed the schematic representation of stages in crack growth in a fibre composite, as shown in Figure 2.1. The schematic of stages in crack growth in a fibre composite have been divided into five steps. First of all, the fibre is gripped by resin in uncracked composite as shown in step (a). In step (b) the crack of resin is held by the fibre. After that, the interfacial shearing and lateral contraction of the fibre result in debonding and further increment of crack extension (c). After a considerable level of debonding, the fibre breaks at the weakest spot within resin and further crack extension occurs as shown in step (d). Finally, in stage (e) the broken fibre end must be pulled out against frictional grip of resin if total separation of sample is to occur [70].

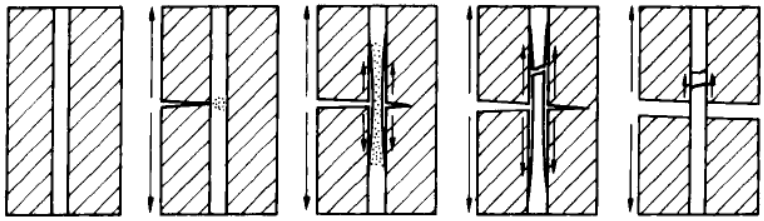

Figure 2.1: A schematic representation of five stages in crack growth in a fibre composite (a) uncracked composite (b) crack initiation (c) debonding (d) crack extension (e) broken [70]

2.3.1.2 PP/carbon fibre composites

There has been a great interest for using carbon fibre-reinforced plastic in many applications especially in aerospace, civil engineering and automotive industries. It has a potential to become one of the most important commercial materials in coming years mainly due to its superior mechanical properties [71, 72]. Nowadays, carbon fibres have been commercially available to be used with PP composites that are produced in different forms, like homopolymer or copolymer PP composites [72]. Recently attention have been focused on improvement of the performance of carbon fibre-reinforced PP based composites [71, 73-75]. Rocha et al. [71] revealed that Young's modulus of compression molding samples was enhanced up to 147% when adding 5 pph (parts per hundred) of carbon fibre. This is because the content of the filler was high enough to enhance the rigidity to the polymer matrix [71]. Work by Altay et al. [73] showed that the tensile and flexural moduli of PP increase with addition of recycled carbon fibre up to 40 wt% the tensile and flexural moduli were increased

by about 177% and 359%, respectively. The results indicated that the tensile and flexural strength of PP increase because the recycled carbon fibre acts as the load carrier where stress is being transferred from the PP matrix to the recycled carbon fibre [69]. Xiaochun et al. [74] found that the increase of carbon fibre loadings significantly increased the tensile modulus from 1,500 to 5,000 MPa at 10 wt% of carbon fibre. For flexural modulus, they found a marked increase in flexural strength and flexural modulus compared to neat PP and PP/carbon fibre at 10 wt%. Flexural modulus increased from 1,300 MPa – 3,500 MPa. This was because the fibre and matrix phases are pressed together and may touch each other. At this juncture, the interface can transfer load more efficiently, which could be the reason for the increase in flexural strength and modulus [74]. This is similar to the study from Huang et al.[75] that showed the improvement of tensile modulus from 1,621 MPa of neat PP to 4,207 MPa of PP/carbon fibre at 20 wt%, or approximately a 159% increment [55, 75].

Not only, it is very interesting in the aspects of low cost, high-performance, lightweight structural composites with low carbon footprints but it has been also outstanding for high electrical and thermal conductivities. Yılmaz et al. [72] investigated that the average softening temperature of PP copolymer with the incorporation of carbon fibre at 5 vol% increased from 110 – 124^{o}C with increasing heat treatment temperature from 100 to 150^{o}C [72]. Huang et al.[75] reported that the optimal conductivity of 10^{-6} S/m occurs when the PP/carbon fibre composites contain more than 3 wt% of carbon fibre, while the optimal EMI SE (the value of the correlation of the conductivities such as electrical conductivity and magnetic conductivity of composites) occurs when containing 20 wt% of carbon fibre [75].

Beside tensile and flexural properties, thermal stability can also be increased with the addition of carbon fibre. Xiaochun et al. [74] reported that the increase of carbon fibre loadings can contribute to higher degradation temperatures, also Thermogravimetric Analysis (TGA) results showed the composites' thermal stability improved with the increasing carbon fibre loadings at 10 wt%, temperature at 5 wt% weight loss increased from 418.8 to 428.5°C [74].

Furthermore, one of the major challenges in the area of carbon fibre-reinforced PP base-composites is to improve the fibre matrix adhesion and interfacial strength of such composites. This is because the interfacial adhesion has a significant impact on the composite performance. A number of researchers attempted to enhance the properties of carbon-fibre PP based-composite by addition of PP-g-MA. PP-g-MA is well-known as a one of the popular coupling agents for PP composites which improves the adhesion between phases in

composite materials [76]. Moreover, it can increase dispersability of the carbon fibre in the PP matrix which allowed the composite blends to crystallize in a smaller time. This can be used as a compatibiliser for composite blending. This is because PP-g-MA can enhance the interfacial adhesion between the carbon fibre and matrix material because chemical functional groups were formed at the PP/carbon fibre interface by reaction between PP and maleic anhydride (MAH) [77-79]. Therefore composites showed improved performance when the filler content was increased [78]. The addition of carbon fibre related to an increase in the crystallinity and density. More evidences were found that as the carbon fibre content was increased in those samples containing PP-g-MAH as compatibiliser, indicating the formation of nuclei due to a synergistic effect between PP-g-MAH and the carbon fibre [71]. This contributed to the increase in the crystallinity and density [73].

Despite the advantages of carbon fibre as a reinforcing agent, there are some limitations too. The incorporation of carbon fibre into PP material can cause to make it more brittle by indicating a dramatic reduction of elongation at break [71, 73, 74]. This is because fillers usually restrict the chain mobility of polymer molecules. Since the polymer chains cannot move freely, the strain at break is reduced with increasing the carbon fibre content [71]. The impact strength is one of the properties that can be reduced compared to neat polymers with the increase of weight fraction of carbon fibre because of the stress concentration regions that can be formed around fillers [71, 73, 74].

2.3.2 PP/particle reinforced composites

A particulate reinforced composite is a composite system which consists of particles suspended or embedded in a matrix [1, 80]. Particulate composites are economically attractive and a number of systems have received attention and have been investigated [81]. In industry, PP is usually filled with various organic or inorganic particles to improve the mechanical properties and also to reduce its cost. This is because some fillers are typically cheaper than polymer resins, the addition of these materials can reduce cost of composite. These can be minerals or can be synthesized from economical sources such as calcium carbonate, kaolin, mica, talc, glass bead, etc [2, 6].

2.3.2.1 PP/$CaCO_3$ composites

The incorporation of $CaCO_3$ in polypropylene can enhance mechanical properties. Elastic modulus and yield stress were increased with the incorporation of nanoparticles of $CaCO_3$ [82-84]. This is because $CaCO_3$ acted as a load carrier in the composites [85]. The maximum elastic modulus enhancement was reached with loadings 15 – 20 wt% [86]. This advancement has been investigated based on a number of aspects such as the particle size and filler contents. Some articles indicated that PP/$CaCO_3$ composite showed a higher tensile modulus than neat PP with regarding to the particle size distribution. Thio et al. [82] investigated that the size of agglomeration tends to increase with increasing the fraction of small particles, by studying three different $CaCO_3$ average particle sizes of 0.07, 0.7 and 3.5 micron. They found that increasing the volume fraction from 5 to 30 vol% of 0.07-micron, 0.7-micron and 3.5-micron $CaCO_3$ particles, changed the average agglomeration size from 47 to 56 micron, 28 to 36 micron and 12 to 63 micron, respectively [82]. The addition of small content of $CaCO_3$ can contribute to great increases in mechanical properties [84]. Eiras et al. [84] observed a great increase in elastic modulus from 1.8 GPa to 2.6 GPa with the addition of 3 wt% of $CaCO_3$ nanoparticles. A similar result was observed for the yield stress which increased from 31 MPa to 35 MPa [84].

Another significant development on mechanical properties from PP/$CaCO_3$ composite is the improvement of the flexural modulus [87-89]. Yang et al. [89] found that the flexural strength and modulus of PP/$CaCO_3$ composites increased with increasing $CaCO_3$ content. They investigated three PP/$CaCO_3$ systems, the improvement were about 50 – 60% with increasing $CaCO_3$ content to 40 wt% [89].

However, limitations have also been found, such as that high loadings with poor dispersion can worsen the mechanical properties [83, 84]. Eiras et al. [84] reported that the elastic modulus decreased by 5% when the nanoparticle content reached 10 wt%. They suggested that $CaCO_3$ nanoparticles have a strong influence in elastic modulus in low contents due to their high surface contact area. When $CaCO_3$ content was increased, the nanoparticles tended to form agglomerates that can be described as particles with higher dimensions, with smaller surface contact area [84].

Good dispersion of particles can be achieved by coating the particles with a monolayer of stearic acid. PP/$CaCO_3$ could significantly improve the impact strength when its content was lower than an optimum value [82, 89-91]. Yang et al. [89] found that the highest Izod impact

strength from the three systems of the PP/$CaCO_3$ composites at 30 wt% was increased to 44.5 kJ/m^2 from 10.3 kJ/m^2 [89]. Work by Lin et al. [91] supported that $CaCO_3$ can improve the impact strength and yield strength. The average Izod impact strength of the 150 °C annealed nanocomposite, containing 20 wt % of coated $CaCO_3$ nanoparticles with 6 wt% stearic acid, was 168 J/m, which was 3.5 times higher than neat PP [91]. Thio et al. [82] reported that the incorporation of 0.7-micron $CaCO_3$ particles at higher than 30 vol.% can improve impact strength about 2.5—3 times higher than neat PP [82].

On the other hand, some studies contradicted the aforementioned improvement of impact strength. Some researches revealed that the addition of $CaCO_3$ increased modulus but decreased impact strength and elongation at break in comparison to the neat PP resin [83]. There is evidence that the impact strength decreased once filler content was higher than that of a certain critical value [84, 89, 92]. Yang et al. [89] reported that the impact strength of PP/$CaCO_3$ composites increased with increasing $CaCO_3$ content until a critical value of about 20 – 30 wt%, with further increases in $CaCO_3$ content leading to a decrease in impact strength [89].

Moreover, the particle size is important to impact strength, work by Thio et al. [82] showed that the 0.07 and 3.5 micron diameter $CaCO_3$ failed to toughen the matrix. They found that the too small (0.07 micron) and too large size (3.5 micron) can initiate the brittle behaviour. This is because they found where many agglomeration larger than 25 micron were presented in the PP filled 0.07-micron PP/Composites. These agglomeration can trigger brittle fracture due to their large sizes and sharp edges. In terms of larger $CaCO_3$ particles of 3.5-micron, the irregularities in particle shapes and sizes acted in a similar roles as agglomerates in the smaller particles [82]. Thenepalli et al. [87] reviewed the studies which referred to fine grade of $CaCO_3$, with surface area about 5-7 m^2/g, that can improve the toughness compared to other grades, which typically have a broader particle size distribution [87]. The toughness was increased with initial addition of $CaCO_3$. They found that $CaCO_3$ can act as a plastic constraint which can trigger the plastic deformation of the matrix [90]. However, the toughness decreased with increasing filler content because the composition of the material changed due to the coalescence of distributed voids which were created by the nanofiller, as they are difficult to disperse uniformly in a polymer matrix [91].

Normally, the surface treatment is essential for improving the interfacial adhesion of composites. Work by Mitsuishi et al. [83] analyzed the mechanical properties of PP/$CaCO_3$

composites in terms of the surface contact area, which related to the filler dispersion [83]. It can be seen that the incorporation of larger contents of $CaCO_3$ did not lead to any considerable successive increase in mechanical properties [84]. If the $CaCO_3$ was too high (over 35 wt%), it related to poor dispersion and increased in composite viscosity [93]. Work by Rocha et al. [91], revealed that at the high level of $CaCO_3$ content at 35 wt%, the $CaCO_3$ tended to agglomerate and increase the composite viscosity [93]. This was because these particles had high surface energy that made them easy to agglomerate. This agglomeration affected to impact strength with much lower yield strength than PP matrix [83, 89]. In order to overcome this restriction, the studies on the effect of surface treatment of $CaCO_3$ were investigated with chemicals such as sodium tripolyphosphate. Sodium tripolyphosphate was used as a crystallization inhibitor and then the surface was modified with stearic acid. These systems can prevent agglomeration and improve the ability to disperse in PP matrix. This can enhance the thermal stability while increasing the yield and tensile strengths of composite with loading 15 – 20 wt% [86].

Additionally, $CaCO_3$ has been selected in some applications where a high wear resistance is required. Palanikumar et al. [85] investigated in the system of PP/$CaCO_3$ composite by defining the loss of material due to abrasive. This experiment studied the $CaCO_3$ content in PP in the range of 1 – 10 wt%. They found that the wear resistance was improved with the increase the content of $CaCO_3$. The addition of 10 wt% of $CaCO_3$ has improved the wear resistance by 70%. This result was reported by tests that were conducted with varying load in the range of 10 N to 50 N at the velocity 1 m/s and time 10 min as constant [85]. It can be shown that $CaCO_3$ acted as a load carrier in the composites since it has better elastic properties than PP [85, 86]. Moreover, work by Leong et al. [88] reported that $CaCO_3$ fillers and the matrix would lessen crack propagation from the surface to the interior of the samples, thus minimizing the internal damage [88].

2.3.2.2 PP/kaolin composite

Some scientists revealed that PP/kaolin composites showed improvement of tensile strength, flexural modulus and impact strength [94-96]. Ariffin et al. [96] indicated that the PP/kaolin composite (with 30 wt% kaolin) could enhance by up to 47% the impact strength [96]. However, one of the major complications of PP/kaolin composite is the possible high level of agglomeration [97]. This is because kaolin is an inorganic rigid material with a high surface

energy or polarity which is in the range of 250 – 255 mJ/m^2 [98] comparing to PP which has very low surface energy and the polarity in the range of 25 - 37 mJ/m^2 [99]. When kaolin was mixed with the hydrophobic PP, the agglomeration of kaolin particles can become crucial [100]. Furthermore, the interfacial adhesion of kaolin particles and PP matrix is also poor.

The dewetting process of kaolin contributes to debonding between filler and polymer matrix to occur prior to fully-developed plastic deformation. The debonding relates to the formation of large voids that can lead to failures. It was claimed that if the debonding is dominant, the deformation mechanism may cause to deteriorate the mechanical properties. This phenomena can lead to the formation of weak points within the composite materials. The average kaolin's particle size of 2 - 3 micron can be agglomerated to form the particles with sizes of 5 - 6 micron by developing sharp corners of the agglomerate [95, 96]. These points can be considered as stress concentration locations causing non-homogeneous behaviours in the structure [96]. Therefore, the result from Ariffin and coworkers also indicates the PP/kaolin at high kaolin content at 30 wt% exhibited brittle failure behaviour [96].

Based on these previous studies, a key challenge in compounding the polymer composites with kaolin is to get uniform dispersion and to avoid agglomeration. Many specialists attempted to solve this by surface modification or treatment to improve the compatibility in polymer matrix [96]. Not only, surface modification, but also the use of coupling agents was also explored in order to improve the compatibility between filler and matrix which is expected to improve the interfacial adhesion characteristic of the polymeric resins [97].

2.3.2.3 PP/glass bead composites

Recently, one of the main particles that has been widely used to enhance toughness and rigidity of composites is the glass bead. Glass bead particles are isotropic due to their spherical shape. Therefore the induced polymer orientation due to the filler should also be reduced [101]. Some studies investigated the mechanical properties by varying the glass bead content. The results showed that the elastic modulus increased until a critical concentration which was in the range of 10 – 20 wt% and then decreased [101, 102]. This was because of the interaction between the inclusion and the matrix, the defects in the composites increased obviously in the case of higher filler content. The treated glass bead with the silane coupling agent can improve the interfacial adhesion, dispersion and distribution of the particles in the PP matrix. The surface treatment can also enhance the tensile and impact properties of the composites.

This is because the end of the molecular silane coupling agent can create a chemical reaction with glass beads' surface. Whereas the organic function of the other end can interact with the PP molecule. This promotes enhancement of the interfacial bond strength between the matrix and the filler [102].

The size of glass beads is one important factor on the determination of the mechanical properties of a composite [101]. The typical particle size of glass bead is in the range of 2.7 – 49 micron and its percentage by volume in PP composite can be in the range of 5 – 20% [102-105]. Kwok et al. [103] showed that the PP composite with an average glass bead diameter of 2.7 micron provided the better performance comparing to 3, 5.7 and 8.9 micron. It was found that the impact strength has increased of up to 4.5 times as the glass bead volume fraction increases from 0 to 0.25, while the tensile modulus did not change significantly. For the aspect of bead size, the impact strength of the composites with larger diameter and narrower size distribution increases only slightly with increasing glass bead content from 0 – 20% by volume [103]. This is because the good interfacial interaction contributed to the pinning effect in the case of crack propagation. The beads would hinder and block the crack propagation [101, 104]. The PP-based composite from smaller glass bead particles had a higher flexural strength and modulus including impact strength than of the composites filled with bigger ones [101, 104]. Yang et al. [101] investigated the tensile and impact strength of PP/glass beads composite which had average particle sizes of 2.5, 5, 10 and 15 micron, and found that the 2.5-micron glass bead had the best toughening effect to improve the tensile and impact strength of the PP matrix. The reason was that smaller particles could form a strong interfacial adhesion between the fillers and PP matrix, and therefore achieve better mechanical properties [101]. Tsui et al. [105] observed the effects of glass-bead content and glass-bead size on strain damage of PP/glass bead composites. They studied two sizes of glass beads, 4 and 49 micron, and five different volume percentages from 5% to 25%. According to their results, the stiffness of all of the composites was found to decrease with increasing strain after a certain threshold strain due to the debonding-induced damage occurring in the composites. This became serious as the glass-bead content and glass-bead size were increased. The larger bead size cause to lower fracture toughness since it could be related to their differences in interparticle spacing. This implied that interaction between the stress fields around the large particles may be much larger than around the smaller ones [105].

Moreover, the thermal conductivity was reduced with increasing the volume fraction of hollow glass bead when the volume fraction was less than 20%. This was because there is more gas in hollow bead, leading to improvement of the heat insulation properties of composites. Furthermore, they revealed the prediction modeling in order to anticipate the thermal conductivity of the polymer/hollow microsphere composites, especially for low filler concentration [106].

2.3.2.4 PP/Graphene nanoplatelets (GNPs) composites

The benefits of GNPs have also been examined especially on mechanical properties which are the properties focused on in this study. It has been found that increasing GNPs loading improves mechanical properties [107]. There are a lot of factors affecting the tensile mechanical properties of polymer composites, such as the shape, size, and content of the fillers, the interfacial adhesion between the fillers and the matrix, the dispersion of the filler particles in the matrix [108]. Studies over a few years have provided important information on the suitable GNPs characteristics. The GNPs with big flake thickness and layers number were beneficial to improve the Young's modulus and the tensile yield strength of the composites. Moreover, the GNPs with large specific surface area and small particle lateral dimension were beneficial to improve elongation at break of the composites [109].

Various articles found the notable limitations and disadvantages of the incorporation of GNPs. They found that tensile elongation at break of GNPs-based composites decreases with increasing GNPs content in the polymer matrix [107, 108, 110]. The scientific evidence supported that decrease in elongation could be from restacking phenomenon and high restriction in the chain movement within the polymer matrix due to higher loading of GNPs filled in the system, which eventually causes stiffness reduction in the nano-composite [108]. Some works [108, 111] have offered contradictory findings about the decrease in mechanical properties. They found that this deterioration of strength can be associated with several factors, such as degree of filler dispersion, orientation of fillers, and defects of the composite originating from poor surface interaction between filler and polymer matrix, which leads to failure in effective load transfer. As the GNPs content increased to 12 wt%, they can widely distribute in the PP matrix, and hence partial agglomeration can occur [111]. To address this limitation, it would be good to use a compatibilizer to enhance adhesion between polymer matrix and GNPs phases [108]. For instance, the addition of PP-g-MA compatibilizer improved

the tensile and impact strength of resulting composite when compared to the one without the PP-g-MA [108].

The improvement in impact strength indicated the increase of composite ductility and toughness due to the enhanced adhesion [108]. However, GNPs loading and compatibilizers have no significant influence on crystallization of neat PP. However, it was found that increasing the GNPs loading had a significant influence on improving the thermal behaviour of neat PP [108, 112]. Gopakumar et al. [112] reported that the degradation temperature of PP/PP-g-MA/GO/G nanocomposites increased by about 55°C compared to the neat PP. This evidences that the thermal stability of PP increases [112].

Not only the existence of compatibilizer in PP/GNPs composite is important, but the consideration about screw configurations for extruder would also be beneficial for improving both the dispersion and distribution. The concept of screw configurations adjustment is aimed to increase the residence time, and mixing elements. The various screw elements in set of screw can specify the flow behaviour of molten polymer. For example, many kneading elements resulted in the high shear stress, a larger shear region and reduce viscosity [113].

Furthermore, previous work [114] revealed that applying GNPs can improve the photo-stabilization of the PP. This is because the presence of GNPs can be attributed to the UV absorption ability and the radical scavenging action.

2.4 Preparation of PP Composites

Conventionally, there are plenty of manufacturing methods for preparing hybrid composite components such as Brabender mixer, two - roller mixer, three - roller mixer, hand lay-up, vacuum infusion, resin transfer molding (RTM), and compression molding including single screw extruder (SSE), twin screw extruder (TSE), injection moulding and other melt mixing processes (compounding) [1, 11, 115-117]. These methods have been well-developed and have been successful in producing composites with exceptional quality. Each type of machine has its own characteristics in terms of mixing performance which depend on the shear rate and batch size.

Compounding is a melt mixing technique and is defined as the mixing of two or more components in the molten state to produce pellets that can be used in subsequent processes, such as extrusion, injection molding. The compounding processes are also important which

directly affect the final properties of composites especially for which manufacture with any fibre and particular filler system. Twin screw extrusion is one of the typical methods that has been widely used in order to prepare composites via compounding.

Twin screw extruders can be classified based on the direction of rotation and degree of intermeshing. Twin screw extruders with screws rotating in the same direction are termed 'co-rotating' while those with screws rotating in the opposite direction is called 'counter-rotating extruder, as shown in Figure 2.2 [116]. A general comparison between co-rotating and counter - rotating twin screw extruders are provided in Table 2.1 [117].

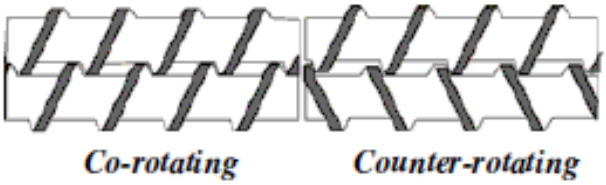

Figure 2.2: Direction of rotation of twin screw extruder

Table 2.1: Comparison between Co-rotating and Counter-Rotating twin screw extruders [117]

Co-rotating	Counter-Rotating
• Screws have equal pitch • Effective self-wiping action • Limited number of screw geometries allow fully self-wiping action • Sliding occurs in intermeshing region, most material will bypass intermeshing region • Fair pumping capability, limited pressure development capability • Good melting characteristics • Good distributive mixing with effective distributive mixing elements • Good dispersive mixing with effective dispersive mixing elements • Can run at very high screw speeds, up to 1400 rpm • Good degassing • Large market share in compounding application, very small market share in profile extrusion • Large market share in polymer industry	• Screws have opposite pitch • Less effective self-wiping action • Wider range of screw geometries possible • For milling type of intermeshing, material likely to be drawn into intermeshing region • Good pumping capability, Good pressure development capability • Excellent melting capability • Good distributive mixing with effective distributive mixing element • Inherently better dispersive mixing capability • Can run at moderately high screw speeds, up to about 500 rpm • Excellent degassing • Small market share in compounding application, very large market share in profile extrusion (low speed extruders) • Large market share in polymer industry

Furthermore, one of the factors which affects the shear force that will be applied to molten polymer is the degree of intermeshing. Typically, twin screw extruders can be fully intermeshing, partially intermeshing, and non-intermeshing. The last can be further subdivided into non - intermeshing with distance and non-intermeshing without distance, as shown in Figure 2.3. A general comparison between intermeshing and non - intermeshing twin screw extruders is shown in Table 2.2 [117].

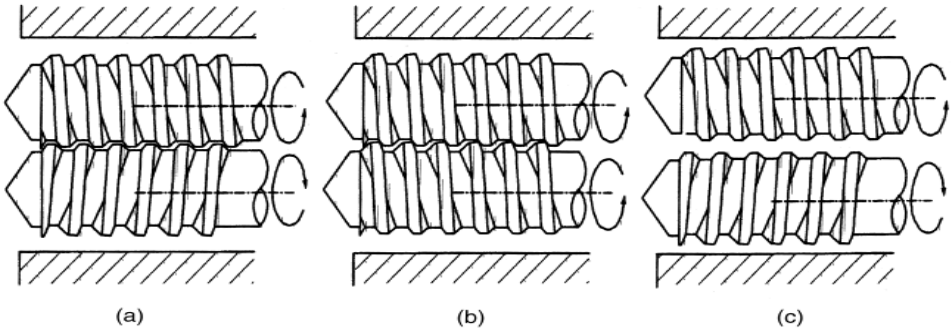

Figure 2.3: Various types of twin screw extruder (a) counterrotating intermeshing elements, (b) co-rotating intermeshing elementsand (c) counterrotating nonintermeshing elements [116]

Table 2.2: Comparison between Intermeshing and Non - Intermeshing Twin Screw Extruders [117]

Intermeshing TSE	Non - intermeshing TSE
• Self-wiping action possible • Good melting characteristics • Good distributive mixing • Good dispersive mixing • Good degassing • L/D up to about 60:1 • Large market share in polymer industry	• Self-wiping action impossible • Fair melting capability • Good distributive mixing • Poor dispersive mixing • Good degassing • L/D up to over 100:1 • Small market share in polymer industry

2.4.1 Effect of processing condition

For the compounding processes, processing conditions have an important role in influencing the composite properties. The key processing conditions that should be controlled for compounding processes are set temperature, screw speed, residence time (mixing time), throughput and screw configuration [118, 119]. If these various factors of process conditions in preparation process have not been controlled efficiently, this can be influenced on fibre breakage, orientation and distribution of fibre which are the critical properties. These directly

affect the performance of the fibre composite and would be considered stringently in this works.

2.4.1.1 Temperature

The initial setting of the temperature profile is one of the steps that have to be paid more attention. If the temperature of the barrel is too high this can result in burning of the plastic. This burnt plastic will manifest itself as small black pieces in the finished product [120]. While, a too cool temperature can result in the flowability and inhomogeneities in the molten polymer. From a fundamental perspective, there are some factors that have to be considered for setting of the temperature profile, which are the softening temperature of the material, the glass transition temperature, the crystallization temperature (for semi-crystalline materials) and the processing temperature [121]. These temperature profile in each barrel can be set depending on the barrels of extruder's position. For the first zone of barrel, the set temperature should therefore be above the softening temperature or even above the crystalline melting temperature of the material. As a rule of thumb, in Zone 1, it can be applied a temperature slightly above the melt temperature. Processing temperature of typical semi-crystalline materials is 50°C – 75°C above the melting temperature [121].

Typically, increasing the mixing temperature by increasing the barrel temperature (within the limits of the polymer stability) can decrease viscosity of molten polymer [119, 122]. This can be beneficial to composite due to the lower shear was applied into the material. Moreover, high mixing temperature leads to low polymer viscosity which contributes to a better infiltration into polymer chains. Due to easier polymer chain diffusion into the agglomeration of fillers, this can improve the dispersion of composites [122]. Villmow et al. [123] studied the influence of temperature profile, screw configuration (profile) and rotation speed in a twin screw extruder used to produce PLA/MWCNT composites. They studied two different temperature profiles (TP1 and TP2 on Table 2.3). The experimental results showed that the better distribution was promoted by TP2 which was higher temperature profile. Moreover, secondary MWCNT agglomerations formed at the end of the extrusion process due to lower melt viscosity comparing to TP1.

Table 2.3 Temperatures profiles TP1 and TP2 designed to perform different mixing tasks [123]

	Heating Zone (°C)					
	1	**2**	**3**	**4**	**5**	**6**
TP1	200	190	190	190	180	180
TP2	200	190	180	180	220	200
Extrusion Direction	→					

2.4.1.2 Screw speed

Screw Speed of extruder screw rotation is very important to composite quality. At a constant throughput, higher screw speed can generate higher shear forces to materials. This effect to dispersability which can increase of dispersion and reduce the number and size of filler agglomerations. Good dispersion of composite can be improve their properties such as mechanical properties, electrical properties and many others [123-126]. However, too high screw speed can also give the opposite results. Krause et al. [123] found that too high screw rotation caused the disruption of the electrical network structure. Moreover, there are some researchers studied the fibre length as critical parameter that is a direct effect of compounding process. The possible factors of fibres breakage along the twin screw extruder are from screw configuration, screw speed etc. Increasing screw speed was found to increase the extent of fibre breakage [118, 127]. Therefore, the increase of screw speed does not always improve composite properties. The tuning the suitable screw speed is required for each composite manufacturing.

Furthermore, there are some researchers investigated the effect of processing conditions on composite properties [118, 127]. Xiaochun et al. [74] found that the screw rotation rate had a significant impact on mechanical properties. The tensile strength of PP/carbon fibre composite with the combination of 10 wt% of carbon fibre decreased from 37 MPa to 35.75 MPa when increasing screw rotation rate from 40 rpm to 120 rpm. There are two possible factors, which cause this phenomenon. This is because the fibres became shorter with the increase in screw rotation rate and the thermal–mechanical history from increased screw rotation that the materials suffered will cause the fracture of the molecular chain. On the other hand, the fibres that are relatively long may not disperse in the matrix when the screw rotation rate is too low [74]. Ozkoc et al. [128] reported that screw speed affected to

unnotched charpy impact strength and average fibre length. The average fibre length decreases from 418 micron to 230 micron with increasing screw speed from 100 to 250 rpm. Moreover, unnotched charpy impact strength also decreased from 2.8 kJ/m^2 to 1.8 kJ/m^2 when increasing screw speed from 100 rpm to 250 rpm. This is because the fibre ends acted as points of stress concentrators that weakened the composite by acting as crack initiators. It was obvious that composites of longer fibres had higher impact strength compared to short ones due to the lower number of fibre ends at the same content [128]. Work presented by Cantor et al. [129] reported that the contribution of heaters towards the extruder SEC was higher at low screw speeds than the drive motor and this trend changed as screw speed increased. The author claimed that the heaters waste over 95% of the supplied energy and hence suggested consideration of new barrel heating technologies [129].

2.4.1.3 Residence time (mixing time)

Residence time has an influence on composite properties. In the case of twin screw extruders, the residence time is a function of screw configuration, screw speed and throughput [126, 130]. The influence of screw configuration, throughput and rotational speed on the residence time in a twin screw extruder was studied on polycaprolactone/MWCNT composites by Villmow et al. [126]. They found that the residence time reduced from an increase of the screw rotational speed and throughput. While, the use of backward-conveying elements can increase of mixing time since polymer processing length was increased [126].

Pötschke et al.[130], investigated that increasing the rotor speed can improve dispersion of MWCNT in polymer matrix but the length of MWCNT was reduced due to breakage. The variation of residence time has to be adjusted for each composites manufacturing process.

2.4.1.4 Throughput (Output rate)

Throughput represents amount on materials passing through the mixing machine per unit of time. The higher the throughput, the lower the residence time [126]. The study of Villmow et al. [126] found that a higher throughput decreased the residence time of mixed ingredients in the extruders. Too much of throughput can reduce the mixing quality required for both of dispersion and distribution. Villmow et al. [124] revealed that interesting result that even though higher throughput may lead to large agglomerated Carbon Nanotubes (CNTs), but if the agglomerated CNTs can be infiltrated by polymer chains then it will lead to good

dispersion and distribution of CNTs. This can promote the formation of electrical pathways causing to enhance the electrical conductivity [126].

2.4.1.5 Screw configuration

Overall, a number of experimental results indicated that the selection of screw element was an important factor to control dispersion and that screw configuration could be tailored to improve specific properties of the composites [118, 119, 123, 126, 127, 131]. Screw configuration is a main factor to be concerned to achieve target properties of composites. To obtain a suitable screw configuration for particular compounding, well understanding of screw design should be required. There are various types of screw elements which are dispersive and distributive mixing. Distributive mixings so-called flow direction changes, while dispersive mixing was designed for breaking up agglomerates or large particles [130]. Therefore, screw configuration including processing conditions have to be specially designed and controlled.

Lekube et al. [119] investigated the screw configuration in compounding on the properties of glass fibre reinforced polypropylene. They varied the screw geometry and configurations and reported that the screw set which contained least shear intensive elements can cause improved final composite properties. This is due to less damage to glass fibres. While a combination of reverse and kneading elements that led to high shear effect and less conveying effect, this contributed to higher residence time and caused a higher depletion of the stabilizer. Ezatet et al. [131] found that the use of a screw configuration consisted of reverse and kneading elements can be beneficial in decreasing the electrical percolation threshold from 6 wt% nanotube contents to 2 wt%. Villmow et al. [126] designed five different screw configurations and found that the use of screws containing mixing elements (distributive screw configuration), led to a higher degree of MWCNT dispersion and distribution. Hence, this can improve electrical properties [123, 126].

2.5 Hybrid composites

Hybrid composite has been clarified in various definition by numerous researches [115, 132-135]. Feng et al. [132] defined hybrid composites as the materials that consist of two or more types of fibres embedded in a single polymer matrix [132]. Jamir et al. [115] explained the definition of hybrid composites are materials that are fabricated by combining two or more

different types of fibres within a common matrix [115]. Thwe et al. [133] defined hybrid composites as a reinforcing material incorporated in a mixture of different matrices [133] . Fu et al. [134] explained that these composites are a reinforcing material that is incorporated into two or more reinforcing and filling materials that are present in a single matrix [134]. Saba et al. [136] proposed more comprehensive descriptions as the material system integrates the functions of more than two different components and/or composites/materials/structures increasing the total system's efficiency [136].

Hybrid composites can be categorized by referring various criterions but there are some common approaches that can be used for grouping hybrid composites with synthetic and natural fibres. Synthetic fibres are made by human through chemical processes such as polymerization. The examples of synthetic fibres are some of the most widely accepted reinforcement material due to their good mechanical properties and low cost are glass fibre, carbon fibre, Aramid fibre, and so forth. Natural fibres can be obtained from stem, leaf, and seed of plants, animals or mineral sources such as Jute, Flax, Hemp, Sisal, Cotton, Silk. Natural fibres possess a number of benefits such as biodegradability, less abrasiveness, high fatigue resistance and low cost [132]. However, even if natural fibres have a lot of attractive features, their mechanical properties are relatively lower than synthetic fibres due to the hydrophilic nature of natural fibre. This is a main cause of weak bonding between fibres and matrix, which directly affects mechanical strength of polymer composites [137]. Therefore, hybrid composites can lead to enhanced performance of composites. There are some common approaches that can be used for grouping hybrid composites, which are synthetic/synthetic, synthetic/natural, and natural/natural hybridization. The most commonly explored hybrid composites are synthetic/natural fibre-reinforced hybrid composites due to the balance of environmental friendliness and mechanical strength [132]. Meanwhile, scientists have offered ways to classify hybrid composite into two groups based on their functional properties: structural and nonstructural [136].

Researches and applications about hybrid composites have experienced great development since the 1970s. In the past, hybrid composite materials were mainly used as structural materials. Their applications have grown fast, with an increase of 10 times in 5 years between 1985 and 1990 [4]. Furthermore, the continuous improvement motivates the interest in development of hybrid materials and structures. Researchers would like to find new and

effective alternative for existing materials, in terms of better performance, lightweight, and cost effectiveness, by fabricating promising hybrid polymer composites [15, 136, 138].

Hybrid composite materials can offer extensive engineering capabilities with a combination of properties which cannot be found in polymers or single-fibre reinforced polymer composite materials. The hybrid composites show diverse functional applications ranging from environmental, automotive, space, etc [136]. On a fundamental level, they have been created as an appropriate conventional composites containing more than one filler. The main purpose of hybrid polymer composite materials is to provide combination of various properties in one polymer composite materials [15]. For example, the hybrid fibres in the composites can withstand higher load compared to single-fibre reinforcements in different directions based on the reinforcement, and the surrounding matrix keeps them in the desired location and orientation, acting as a higher load transfer medium between them [2]. Although natural fibres are environmentally friendly, but these natural fibre-reinforced composite materials may not be able to withstand heavy loading. For this purpose, researchers have found a few methods to enhance the mechanical properties of the natural fibre reinforced composite materials. Among them, hybridization was one of the methods used for overcoming the negatives of using one reinforcement [138].

Currently, there is a growing demand for hybrid composites in the advanced engineering applications such as in airplanes, space shuttles, secondary structure for solar cells and in wind energy generation [136]. Moreover, there are novel applications where hybrid composites are used to improve further performance, such as composite scaffolds for tissue engineering, hydrogel for fabricating nanocomposite, having conducting polymers filled with different metals shows numerous nonstructural and structural functions, exclusive applications in aerospace industries. Hybrid composites represent the advanced, hi-tech, and next generation of engineered materials. They perform two or more functions simultaneously, such as carrying the mechanical loads while delivering or storing electrical energy [136].

2.6 Previous studies on the preparation and properties of PP hybrid composites

Nowadays great efforts are undertaken to transform PP into a specialty thermoplastic that can be used in engineering applications. Advantages have been forwarded as arguments for replacing more conventional automotive materials such as short processing times, low

density, excellent corrosion resistance, and potential for rapid repair [42]. Several studies showed that strength and impact toughness have been decreased compared to virgin PP in PP/glass fibre composite [52, 53]. In order to enhance and compensate such properties, hybrid composite systems have been introduced by applying various fillers combinations. Many hybrid composites based on a combination of various inorganic fillers have been developed.

Hybrid composite PP materials have currently received great attention from researchers because they offer a number of enhanced properties and various advantages over traditional composite materials. This can serve for diverse requirements for modern composite materials which desire more sophisticated properties such as in aircraft structures, energy sector components (solar cells, wind energy generation), aerospace engineering, marine transportation, sporting goods (golf shafts, squash racquets, kayaks, surfboards, hockey sticks, fishing rods) [4, 6, 12, 18, 20, 25, 139, 140].

In terms of hybrid polymer matrix composites, hybrid composites can be produced into various approaches which are particle/particle hybrid composite, fibre/fibre hybrid composite and particle/fibre hybrid composites. In regard to particle hybrid composites, the most common particulate fillers are inorganic minerals such as $CaCO_3$, talc, kaolin, wollastonite, colemanite [2]. Leong et al. [88], reported that the hybridization between talc and $CaCO_3$ can enhance the weather resistance of composite to severe environmental degradation based on tropical climate in Penang for 6 months. Talc acted as the main reinforcing fillers to hold composite together while the incorporation of $CaCO_3$ acted as damper to absorb energies from crack propagation before it reached the part and retard chain scission. Furthermore, Abu Bakar et al. [141] found that the hybridization between talc and kaolin with PP base composite can produce an economically advantageous material with promising mechanical properties (tensile, flexural, and impact) comparable to those of the single talc-filled PP composites. Ghasemi et al. [56] investigated that the talc and GNPs played a significant role in the enhancement of mechanical properties such as tensile strength, impact resistance. The Response Surface Methodology (RSM) models predicted that the suitable formulation to maximize these mechanical properties had to be 30 wt% for talc, 4 wt% for PP-g-MA and 0.69 wt% for GNPs. Furthermore, statistical models were used to anticipate the composite performance. İnal et al. [142] tried to optimize and model the Young's modulus properties of PP hybrid composite materials with talc/colemanite. The

results obtained were compared with the ANOVA results obtained from the Taguchi experiment design method. It was found that the Artificial Neural Networks (ANN) method provided the modelling of Young's Modulus was quite close to experimental results.

In regard to fibre/fibre hybrid composites, some scientific articles categorized the fibre/fibre hybrid composites into three main categories which are synthetic/synthetic, synthetic/natural, and natural/natural hybridization [132]. Examples of the synthetic /synthetic hybrid system include PP based composite. Yan et al. [143] developed a model to anticipate the mechanical properties of a glass and carbon fibre reinforced PP composite fabricated by the direct fibre feeding injection molding process. It has been found that when the average fibre length was lower than 0.7 mm. the tensile modulus became larger with increasing average fibre length. At 25 wt% of glass fibre, they found that the tensile modulus increased from 4.5 GPa to 7 GPa at length of 0.2 mm. to 0.7 mm. The tensile modulus of the composites decreases with increasing fibre orientation angle. Moreover, the predicted tensile strength of the hybrid composites was larger than the experimental results due to the interfacial bonding between carbon fibre and PP being weaker than that of glass fibre and PP [143]. Research by Khan. et al. [144] found that the stiffness and heat distortion temperatures (HDT) of the composites were improved when incorporation of jute fibre and cellulose. But impact strength was reduced with increasing jute portion due to the presence of too many jute fibre ends within the body of the composites, which could cause crack initiation and increase the probability of fibre agglomeration. Treated jute fibres led to moderate improvements in tensile modulus by 6% with respect to the untreated fibre composites [144].

Numerous research studies [54, 55, 145] were carried out in order to investigate various properties of hybrid PP based composites by addition of particulate fillers and fibres. For example, the main fibre which was the major component in hybrid composite was glass fibre. Papageorgiou et al. [54] investigated the effect of the addition glass fibres and GNPs in PP and found that the Young's modulus of the hybrid material was three times higher than that of the materials containing the individual fillers. The presence of GNPs at the interface between the PP and glass fibres may lead to better interfacial stress transfer between the PP and glass fibres [54]. Hartikainen et al. [55] studied the structure and fracture behaviour of the rPP based composite by adding long glass fibre (LGF) and $CaCO_3$. They found that the acoustic activity of PP/LGF/$CaCO_3$ hybrid samples was much higher compared to PP/LGF without a

filler as the fibre pullouts occurred more easily due to the reduction of fibre-matrix adhesion [55] .

Another type of filler that has been added as the combination of glass fibre is wollastonite. Joshi et al. [146] prepared the combination of glass fibres and wollastonite. While elongation at maximum force and failure strain of the hybrid composites increases slightly with an increase in wollastonite content. This may be from the less brittle nature of wollastonite fibre compared to glass fibre. The tensile strength and modulus, flexural strength and modulus and impact strength of hybrid composites were similar to the single glass fibre composites [146]. Moreover, there were various attempts to develop hybrid PP based composites with nanosilica and glass fibre PP composites [147]. Jacob et al. [147] reported that the maximum hybrid composite performance was at a fibre loading of 30 wt% by measuring the storage modulus of glass fibre-precipitated nanosilica/PP composite [147]. Furthermore, the thermal stability of PP composite was also improved by the addition of glass fibre and nanosilica. Rasana et al. [148] investigated the effect of incorporation of glass fibre and nanosilica separately and in combination in a thermoplastic matrix [148]. They found the presence of nanosilica surrounding the glass fibres and the improvement in tensile strength and modulus for hybrid composite. AlMaadeed et al. [149] studied the performance of rPP based hybrid composites of date palm wood flour/glass fibre in different weight ratios. They found that rPP properties were firstly improved by reinforcing it by ground wood. The tensile strength and Young's modulus of wood flour reinforced rPP increased further by adding glass fibre. Glass fibre reinforced composites showed a higher hardness than other composites. The studies indicated that glass fibre has good adhesion with rPP supporting the improvement of the mechanical properties of hybrid composites. There was about 18% improvement of the tensile strength from the addition of 5wt% glass fibre to wood flour/rPP composite relative to the wood flour/rPP composite alone [149].

Beside the hybrid composites between glass fibre and particulate fillers have been paid widely attention, the hybridization between carbon fibre and various particulate fillers were also investigated. Wang et al. [61] reported that mechanical properties such as tensile, flexural and impact strengths of the graphene oxide/carbon fibre PP composite were obviously improved. It could be observed that the PP composite of 0.5 wt% of graphene oxide 10 wt% of short carbon fibre had a maximum flexural, tensile and impact strength, with an increase of 31%, 30%, and 54% as compared to PP/short carbon fibre at 10 wt%. This is due to the

chemical reaction and mechanical interlocking between the graphene oxide on carbon fibre surface and PP. Moreover, the results also showed that this hybrid composite had good thermal stability. Therefore, the multiscale and synergistic effects of graphene oxide/carbon fibre PP composite showed the extensive potential in improving mechanical and thermal performance for various fields [61]. However, Gogoi et al. [145] was interested in the study on the effect of hybrid PP composites with carbon fibre and hollow glass bead. They investigated by varying concentration of both carbon fibre (0 – 8 wt%) and hollow glass microspheres (0 – 40 wt%) on various physical and mechanical properties. It was revealed that there was improvement in the specific strength using carbon fibre and hollow glass microspheres. Synergistic effect of hybrid inclusion on tensile properties was observed as the tensile strength improved up to 10 wt%. Hybrid composites with 8wt% of short carbon fibre and 10 wt% of hollow glass beads showed comparatively higher tensile strength and modulus. Furthermore, the flexural test for hybrid composites showed a positive synergistic effect of two fillers as improved flexural strength and modulus were observed compared to PP [145]. Furthermore, Oladele et al. [150] reported the enhancement of mechanical properties of the hybridization between natural fibre and $CaCO_3$. They found that the hybrid PP based composite from bagasse fibre and $CaCO_3$ had improved mechanical properties comparing to the single-component samples and the control. They found that the flexural modulus of hybrid composite was 70% higher than the control sample. The percentage improvement of the tensile modulus was higher than the control is 49.5%. Furthermore, the results also showed that this hybrid composite had an increased degradation temperature from 285^{o}C to 329^{o}C [150].

From the aforementioned works it can be seen that the hybridization can improve some mechanical properties, including thermal conduction and morphology. However, there are significant drawbacks and limitations which are associated with the hybrid PP based composite. These limitations include reductions in the strength to failure, impact resistance at high loading of reinforcing materials. It appeared that these problems are common in various systems of hybrid composites. Therefore, the challenges of this research were to establish the most suitable hybrid PP based composite to enhance or compensate some of the deteriorated properties. The synergy of various types of fillers and combinations of reinforcing materials from particle and fibre family have been evaluated.

2.7 Previous studies on the properties of recycled PP composites

As a matrix material, PP is widely used because it has some excellent characters for composite fabrication such as good stiffness, low density, and high resistance to aging and it is recyclable. It has been widely used to replace numerous metals in many industries including automotive parts in order to achieve light weight and cost savings [151]. The rapid increasing of plastic materials in various application may be the one of main reason causing plastics to environmental impact after discarding them following the utilization. Therefore, the recycling of PP can be an effective way of reducing large amount of plastic waste in plastic manufacturing industry [152-154]. Moreover, PP is really suitable for recycle process because it is a thermoplastic material which can be remelted or reshaped several times. This gives various possibilities to manufacture a new product from reused and generates small losses in material strength when being recycled [48, 155]. Recycling of PP can also assist to minimize cost for the manufacturing industries, increase profit as well as maintaining the mechanical performance of PP [154].

Composites can be one approach to enhance rPP properties by adding filler materials and/or blending rPP with the virgin one [149, 156-159]. The performance of blended PP product was determined whether they are better when compared to its original mechanical properties. Jmal et al. [151] revealed that the effects of the contaminants contained in the rPP from waste origin and additives added by suppliers influenced to the final composite properties such as $CaCO_3$ and rigid fillers can improve Young's modulus and yield stress [151]. Hyie et al. [154] investigated that the blending of 75 wt% of virgin PP and 25 wt% of rPP were optimum composition that had positive influence on tensile strength, percentage of elongation at break and Young's modulus [154].

On the other hand, the rPP composites has some limitations. Some researchers revealed that rPP are still ending up in low-value products [160]. This is due to the degradation of polymer structure, which can cause the deterioration of composite performance [159]. Moreover, they reported that another important reason are the deformation mechanisms of rPP depends on contaminants and high temperature profile during recycling process [151, 159, 161]. To overcome these limitations, it seems that the easiest way to recycle the waste plastics is by utilizing the development of blends and composites from recycle materials or apply more auxiliary additive and reinforcing materials [151, 159].

Recently, the development of rPP composite have been getting more attention. The main purpose of the making of rPP composites is the improvement of composite performance. The mechanical properties can be used to estimate the service life of composite materials. Therefore, the improvement of mechanical properties can lead to an extended service life of composites [159]. However, the multiple reprocessing cycles influences the rheological, thermal and mechanical properties of PP. Moreover, earlier studies [48, 50, 161] reported that recycling induced a reduction of PP molecular weight as well as a narrowing of the molecular weight distribution. This is due to the degradation mechanisms of PP contributing to chain scission mechanism [48, 50, 161]. Moreover, the deterioration of mechanical properties can be detected in which yellowness increased with increasing the processing cycles [50]. Therefore, many scientists attempted to enhance the strength of rPP by adding the reinforcing materials. However, one of the limitations of this method is the incompatibility between PP matrix and reinforcing materials. This leads to poor interfacial adhesion between matrix and fillers and cause composite failure. Adding of PP-g-MA has been applied to some rPP composites [52, 155, 158]. The addition of PP-g-MA has proven to act as a compatibilizer that promotes interfacial adhesion between fillers and rPP matrix [52]. The addition of antioxidant may be used in some processes for preventing further degradation. Moreover, it has been found that it did not change the mechanical properties of the polymer matrix material [155]. Zheng et al. [162] reported that there was an observable improvement for tensile and flexural modulus by adding 20 wt% of Talc about 42.2% and 19.3%, respectively [162]. Mekap et al. [52] revealed that the tensile strength and flexural modulus increased with increasing amounts of reinforcing fibre in composites as compared to rPP matrix [52]. Moreover, rPP composite has be addressed is the system with the addition of geopolymer concrete waste particles. Study of Ramos et al. [163] reported that the elastic modulus was better than neat PP. The elastic modulus enhanced up from 529.1 MPa to 618.2 MPa at 40 wt% of oleic acid modified geopolymer concrete waste (AGC) [163]. Moreover, the presence of silica and graphite in rPP can improve the hardness, tensile and flexural modulus and thermal behaviour but decrease in elongation because graphite makes material more brittle according to the investigation of Kumar et al. [156]. The rPP composites can be improved in term of Izod impact strength. Li et al. [158] demonstrated that the Izod strength was increasing at higher wood flour contents by reinforcing with PP-g-MA as compatibilizer. The Izod impact strength increased about 10% with increasing filler content to 40 wt% [158].

Besides the investigation of single rPP composites, there are a number of works on hybrid rPP composite. According to the study of Al-Maadeed et al. [149, 157] rPP properties were improved by wood flour and glass fibre. The tensile and shear modulus of binary composites were increased by 71% and 53%, respectively, relative to the wood flour reinforcement alone [149, 157]. An interesting work by Soy et al. [152] found that there was an increment in 300% of elastic modulus by the incorporation of glass fibre, talc and $CaCO_3$ [152]. Furthermore, the increase of tensile strength can be obtained by containing cellulose and newsprint fibres with the addition of impact modifier and compatibilizer, as per the findings from Bogataj et al. [164].

2.8 Conclusions

2.8.1 Key learnings

From the number of literatures were mentioned previously, it has been seen that various functions of each filler from many endeavors. These key learnings were taken from these studies were summarized in the Table 2.4 – 2.6.

Table 2.4 Mechanical and other properties of polymers/reinforcements studied on single composite system

Sample details	Key finding	Comments	Ref
Glass fibre reinforcement			
PP + glass fibre (average length and diameter of 6 mm and 13 µm)	PP/glass fibre at 30 wt% can improve yield stress and tensile modulus by 41% and 200% higher than neat PP	Glass fibres have high tensile strength and modulus compared with neat PP. The primary function of the fibre–matrix interface is to transmit stress from the weak polymer matrix to fibre	[59]
PP + untreated and treated glass fibres	Adding untreated and treated glass fibres with 0.5 wt% to 2.0 wt%, with the results evidencing that samples from the PP/treated glass fibre composites had tensile strain increased three times from 2% up to 7%		[63]

Sample details	Key finding	Comments	Ref
Nylon + glass fibre (fibre length 0.25 mm and few fibers are longer than 0.5 mm*)*	Increases toughness by an average of 18%. at 30 wt% of glass fibre	This improvement is due to the longer fibres themselves beginning to play as significant reinforcing role in the matrix	[65]
Polyamide 6 (nylon 6), PP and Polymethylmethacrylate (PMMA) + Glass fibre (diameter of 10 or 14 μm)	Tensile and impact strength depend on several parameters such as fibre content, fibre orientation and geometry, as well as interfacial adhesion between fibre and polymer matrix		[66]
PP+ short glass fibre (average length of around 0.5 mm), PP+ long glass fibre (average length of around 9 mm)	- Shear strength of the samples prepared from short fibre with a coupling agent had the highest values at all temperatures	- The interfacial bond between the fibre and the matrix is strong and the fibres can consequently carry higher load.	[67]
	- Long fibre granules without coupling agent had the lowest value at all temperatures (from -43, 20, 55, 90^{o}C).	- This is a consequence of the poor bonding between the fibre and the matrix - Higher average fibre length, the dispersion of fibres is usually not uniform. While longer fibres are expected to provide higher stiffness, the agglomeration due to poor dispersion of fibres apparently has an adverse effect	
Glass fiber-reinforced PP 30%wt	Additional breakages occur in the mold and runners, but that most of the length reduction occurs in the injection unit	The average fibre length might be affected by fibre volume fraction or process conditions, screw speed including barrel/die set temperature	[69]
Carbon fibre reinforcement			
PP+ Carbon fibre (150 μm, diameter of 8 μm)	Young's modulus of compression molding samples was enhanced up to 147% when adding 5 pph (parts per hundred) of carbon fibre.	This is because the content of the filler was high enough to enhance the rigidity to the polymer matrix.	[71]

Sample details	Key finding	Comments	Ref
PP + milled carbon (length of 130 µm and diameter of 8 µm)	The average softening temperature of PP copolymer with the incorporation of carbon fibre at 5 vol% increased from 110 – 124^{o}C with increasing heat treatment temperature from 100 - 150^{o}C		[72]
PP + recycled carbon fibre (length of 6 mm and diameter of 7 µm)	Tensile and flexural moduli of PP increase with addition of recycled carbon fibre up to 40 wt% the tensile and flexural moduli were increased by about 177% and 359%, respectively.	The results indicated that the tensile and flexural strength of PP increase because the recycled carbon fibre acts as the load carrier where stress is being transferred from the PP matrix to the recycled carbon fibre.	[73]
PP + carbon fibre (length of 6 mm and diameter of 7 µm)	- The increase of carbon fibre loadings significantly increased the tensile modulus from 1,500 to 5,000 MPa at 10 wt% of carbon fibre. - For flexural modulus, they found a marked increase in flexural strength and flexural modulus compared to neat PP and PP/carbon fibre at 10 wt%. Flexural modulus increased from 1300 MPa – 3500 MPa. - The increase of carbon fibre loadings can contribute to higher degradation temperatures also TGA results showed the composites' thermal stability improved with the increasing carbon fibre loadings at 10 wt%, temperature at 5 wt% weight loss increased from 418.8 to 428.5°C	This was because the fibre and matrix phases are pressed together and may touch each other. At this juncture, the interface can transfer load more efficiently, which could be the reason for the increase in flexural strength and modulus	[74]

Sample details	Key finding	Comments	Ref
PP + carbon fibre (length of 6.2 mm and diameter of 7 µm)	- improvement of tensile modulus from 1621 MPa of neat PP to 4207 MPa of PP/carbon fibre at 20 wt%, or approximately a 159% increment - the optimal conductivity of 10^{-6} S/m occurs when the PP/carbon fibre composites contain more than 3 wt% of carbon fibre, while the optimal EMI SE (the value of the correlation of the conductivities such as electrical conductivity and magnetic conductivity of composites) occurs when containing 20 wt% of carbon fibre		[75]
$CaCO_3$ reinforcement			
PP + $CaCO_3$ (0.07 µm , 0.7 µm and 3.5- µm)	- The increasing the volume fraction from 5 to 30 vol% of 0.07-micron, 0.7-micron and 3.5-micron $CaCO_3$ particles, changed average agglomeration size from 47 - 56 µm, 28 to 36 µm and 12 to 63 µm, respectively - The incorporation of 0.7-micron $CaCO_3$ particles at higher than30 vol.% can improve impact strength about 2.5—3 times higher than neat PP	The size of agglomeration tends to increase with increasing the fraction of small particles, by studying three different $CaCO_3$ average particle sizes of 0.07, 0.7 and 3.5 micron.	[82]
PP + $CaCO_3$ (mean diameter of the nanoparticles is between the range of 70-90 nm and the surface treatment was stearic acid*)*	Great increase in elastic modulus from 1.8 GPa to 2.6 GPa with the addition of 3 wt% of CaCO3 nanoparticles. A similar result was observed for the yield stress which increased from 31 MPa to 35 MPa		[84]

Sample details	Key finding	Comments	Ref
PP + $CaCO_3$	- The wear resistance was improved with the increase the content of $CaCO_3$. - This experiment studied the CaCO3 content in PP in the range of 1 – 10 wt%.	The addition of 10 wt% of $CaCO_3$ has improved the wear resistance by 70%. This result was reported by tests that were conducted with varying load in the range of 10 N to 50 N at the velocity 1 m/s and time 10 min as constant	[85]
PP + $CaCO_3$ (surface area about 5-7 m^2/g)	the studies which referred to fine grade of $CaCO_3$ can improve the toughness compared to other grades, which typically have a broader particle size distribution		[87]
PP + $CaCO_3$ untreated and the other treated with stearic acid	$CaCO_3$ fillers and the matrix would lessen crack propagation from the surface to the interior of the samples, thus minimizing the internal damage		[88]
PP + $CaCO_3$ (average particle size of 0.07 µm)	Investigated three PP/$CaCO_3$ systems, the improvement were about 50 – 60% with increasing $CaCO_3$ content to 40 wt% - The highest Izod impact strength from the three systems of the PP/$CaCO_3$ composites at 30 wt% was increased to 44.5 kJ/m^2 from 10.3 kJ/m^2 - The impact strength of PP/$CaCO_3$ composites increased with increasing $CaCO_3$ content until a critical value of about 20 – 30 wt%, with further increases in $CaCO_3$ content leading to a decrease in impact strength	The flexural strength and modulus of PP/$CaCO_3$ composites increased with increasing $CaCO_3$ content.	[89]

Sample details	Key finding	Comments	Ref
PP + coated $CaCO_3$ with 2 wt % stearic acid.	$CaCO_3$ can improve the impact strength The average Izod impact strength of the 150 °C annealed nanocomposite, containing 20 wt % of coated $CaCO_3$ nanoparticles with 6 wt% stearic acid, was 168 J/m, which was 3.5 times higher than neat PP		[91]
PP, PP/$CaCO_3$ composite (Particle diameter 4 and 2.9 µm)	the high level of $CaCO_3$ content at 35 wt%, the $CaCO_3$ tended to agglomerate and increase the composite viscosity	If the $CaCO_3$ was too high (over 35 wt%), it related to poor dispersion and increased in composite viscosity	[93]
Kaolin reinforcement			
PP+ Kaolin	- PP/kaolin composite (with 30 wt% kaolin) could enhance by up to 47% the impact strength - PP/kaolin at high kaolin content at 30 wt% exhibited brittle failure behaviour	- These points can be considered as stress concentration locations causing non-homogeneous behaviours in the structure - Key challenge in compounding the polymer composites with kaolin is to get uniform dispersion and to avoid agglomeration. - Many specialists attempted to solve this by surface modification or treatment to improve the compatibility in polymer matrix	[96]
PP + Kaolin (density of 2.59 g/cm^3 and mean particle diameter of 3.0 µm)	Use of coupling agents was also explored in order to improve the compatibility between filler and matrix which is expected to improve the interfacial adhesion characteristic of the polymeric resins		[97]

Sample details	Key finding	Comments	Ref
Glass bead reinforcement			
PP + glass bead (average particle sizes of 5, 10, 15µm)	Tensile and impact strength of PP/glass beads composite which had average particle sizes of 2.5, 5, 10 and 15 micron, and found that the 2.5-micron glass bead had the best toughening effect to improve the tensile and impact strength of the PP matrix.	The reason was that smaller particles could form a strong interfacial adhesion between the fillers and PP matrix, and therefore achieve better mechanical properties	[101]
PP + glass bead (average particle sizes of 27 µm)	PP composite with an average glass bead diameter of 2.7 µm provided the better performance comparing to 3, 5.7 and 8.9 µm. It was found that the impact strength has increased of up to 4.5 times as the glass bead volume fraction increases from 0 to 0.25, while the tensile modulus did not change significantly.	For the aspect of bead size, the impact strength of the composites with larger diameter and narrower size distribution increases only slightly with increasing glass bead content from 0 – 20% by volume	[103]
PP + glass bead (average particle sizes of 4, 49 µm)	Effects of glass-bead content and glass-bead size on strain damage of PP/glass bead composites. They studied two sizes of glass beads, 4 and 49 micron, and five different volume percentages from 5% to 25%.	According to their results, the stiffness of all of the composites was found to decrease with increasing strain after a certain threshold strain due to the debonding-induced damage occurring in the composites. This became serious as the glass-bead content and glass-bead size were increased. The larger bead size cause to lower fracture toughness since it could be related to their differences in interparticle spacing. This implied that interaction between the stress fields	[105]

Sample details	Key finding	Comments	Ref
		around the large particles may be much larger than around the smaller ones	
PP + hollow glass bead (average particle sizes of 35, 70 µm)	Thermal conductivity was reduced with increasing the volume fraction of hollow glass bead when the volume fraction was less than 20%.	This was because there is more gas in hollow bead, leading to improvement of the heat insulation properties of composites they revealed the prediction modeling in order to anticipate the thermal conductivity of the polymer/hollow microsphere composites, especially for low filler concentration.	[106]
GNPs Reinforcement			
PP+ graphite flakes (0.3 mm x 3 mm)	The degradation temperature of PP/PP-g-MA/GO/G nanocomposites increased by about 55°C compared to the neat polypropylene. This evidences that the thermal stability of PP increases		[112]
PP + GNP-M-5 (average of 5 µm in diameter and a thickness of 6 nm)	- The deterioration of strength can be associated with several factors, such as degree of filler dispersion, orientation of fillers, and defects of the composite originating from poor surface interaction between filler and polymer matrix, which leads to failure in effective load transfer. The GNPs content increased to 12 wt%, they can widely distribute in the PP matrix, and hence partial agglomeration can occur	- Decrease in elongation could be from restacking phenomenon and high restriction in the chain movement within the polymer matrix due to higher loading of GNPs filled in the system, which eventually causes stiffness reduction in the nano-composite	[108]
	- The addition of PP-g-MA compatibilizer improved the tensile and impact	- The improvement in impact strength indicated the increase of composite	

Sample details	Key finding	Comments	Ref
	strength of resulting composite when compared to the one without the PP-g-MA	ductility and toughness due to the enhanced adhesion. - However, GNPs loading and compatibilizers have no significant influence on crystallization of neat PP. However, it was found that increasing the GNPs loading had a significant influence on improving the thermal behaviour of neat PP	
PP/ GNPs (average thickness lower than 2 nm; average diameter between 1 -2 mm and a specific surface area of about 750m^2/g)	GNPs can improve the photo-stabilization of the PP.	This is because the presence of GNPs can be attributed to the UV absorption ability and the radical scavenging action.	[114]

From a number of literatures which have been investigated on the hybrid composites, the most of experimental finding supported that the positive synergistic effect can improve the performance of polymer especially in terms of mechanical properties. The key findings from the literature reviews have been summarized in the Table 2.5.

Table 2.5 Mechanical and other properties of polymers/reinforcements studied on hybrid composite system

Sample details	Key finding	Comments	Ref
PP + GNPs + glass fibre	Young's modulus of the hybrid material was three times higher than that of the materials containing the individual fillers.	The presence of GNPs at the interface between the PP and glass fibres may lead to better interfacial stress transfer between the PP and glass fibre.	[54]
PP + long glass fibre (LGF) + $CaCO_3$.	The acoustic activity of PP/LGF/CaCO3 hybrid samples was much higher compared to PP/LGF without a filler as the fibre pullouts occurred more easily due to the reduction of fibre-matrix adhesion		[55]

Sample details	Key finding	Comments	Ref
PP + graphene oxide + carbon fibre	Mechanical properties such as tensile, flexural and impact strengths were obviously improved. It could be observed that the PP composite of 0.5 wt% of graphene oxide 10 wt% of short carbon fibre had a maximum flexural, tensile and impact strength, with an increase of 31%, 30%, and 54% as compared to PP/short carbon fibre at 10 wt%.	This is due to the chemical reaction and mechanical interlocking between the graphene oxide on carbon fibre surface and PP. Moreover, the results also showed that this hybrid composite had good thermal stability. Therefore, the multiscale and synergistic effects of graphene oxide/carbon fibre PP composite showed the extensive potential in improving mechanical and thermal performance for various fields	[61]
PP+ talc + $CaCO_3$	Enhance the weather resistance of composite to severe environmental degradation based on tropical climate in Penang for 6 months.	Talc acted as the main reinforcing fillers to hold composite together while the incorporation of $CaCO_3$ acted as damper to absorb energies from crack propagation before it reached the part and retard chain scission.	[88]
PP+ talc + kaolin	PP base composite can produce an economically advantageous material with promising mechanical properties (tensile, flexural, and impact) comparable to those of the single talc-filled PP composites.		[141]
PP + glass fibre + carbon fibre	- Average fibre length was lower than 0.7 mm. the tensile modulus became larger with increasing average fibre length. At 25 wt% of glass fibre, the tensile modulus increased from 4.5 GPa to 7 GPa at length of 0.2 to 0.7 mm. - The tensile modulus of the composites decreases	Model to anticipate the mechanical properties of a glass and carbon fibre reinforced PP composite fabricated by the direct fibre feeding injection molding process.	[143]

Sample details	Key finding	Comments	Ref
	with increasing fibre orientation angle.		
PP + Jute + Cellulose	The stiffness and heat distortion temperatures (HDT) of the composites were improved when incorporation of jute fibre and cellulose. But impact strength was reduced with increasing jute portion	-Due to the presence of too many jute fibre ends within the body of the composites, which could cause crack initiation and increase the probability of fibre agglomeration. -Treated jute fibres led to moderate improvements in tensile modulus by 6% with respect to the untreated fibre composites	[144]
PP + carbon fibre and hollow glass bead	- It was revealed that there was improvement in the specific strength using carbon fibre and hollow glass microspheres. - Synergistic effect of hybrid inclusion on tensile properties was observed as the tensile strength improved up to 10 wt%. - Hybrid composites with 8wt% of short carbon fibre and 10 wt% of hollow glass beads showed comparatively higher tensile strength and modulus.	They investigated by varying concentration of both carbon fibre (0 – 8 wt%) and hollow glass microspheres (0 – 40 wt%) on various physical and mechanical properties. Furthermore, the flexural test for hybrid composites showed a positive synergistic effect of two fillers as improved flexural strength and modulus were observed compared to PP	[145]
PP + glass fibres + wollastonite	Elongation at maximum force and failure strain of the hybrid composites increases slightly with an increase in wollastonite content.	This is because the less brittle nature of wollastonite fibre compared to glass fibre. The tensile strength, modulus, flexural strength and modulus and impact strength of hybrid composites were similar to the single glass fibre composites	[146]
PP + glass fibre + nanosilica	The maximum hybrid composite performance was at a fibre loading of 30 wt% by measuring the storage modulus of glass		[147]

Sample details	Key finding	Comments	Ref
	fibre-precipitated nanosilica/PP composite		
rPP + date palm wood flour + glass fibre in different weight ratios.	The studies indicated that glass fibre has good adhesion with rPP supporting the improvement of the mechanical properties of hybrid composites. There was about 18% improvement of tensile strength from the addition of 5wt% glass fibre to wood flour/rPP composite relative to the wood flour/rPP composite alone	The tensile strength and Young's modulus of wood flour reinforced rPP increased further by adding glass fibre. Glass fibre reinforced composites showed a higher hardness than other composites.	[149]
PP + bagasse fibre + $CaCO_3$	The hybrid PP based composite from bagasse fibre and $CaCO_3$ had improved mechanical properties comparing to the single-component samples and the control. They found that the flexural modulus of hybrid composite was 70% higher than the control sample. The percentage improvement of the tensile modulus was higher than the control is 49.5%. Furthermore, the results also showed that this hybrid composite had an increased degradation temperature from 285^{o}C to 329^{o}C		[150]

Table 2.6 Mechanical and other properties of polymers/reinforcements studied on recycled PP and recycled PP composite system

Sample details	Key finding	Comments	Ref
rPP + regenerated fiber from waste newspapers, magazines	The tensile strength and flexural modulus increased 35% and 64% respectively with increasing amounts of reinforcing fibre in composites as compared to rPP matrix		[52]
rPP + wood flour + glass fibre.	The tensile and shear modulus of hybrid composites were increased by 71% and 53%, respectively, relative to the wood flour reinforcement alone		[150]
Three rPP references	The effects of the contaminants contained in the rPP from waste origin and additives added by suppliers influenced to the final composite properties such as $CaCO_3$ and rigid fillers can improve Young's modulus and yield stress	The rigid particles can act as toughness agent or as structural defects which initiate material break depending to its microstructures. Adding Peroxide during recycling process allows control the melt flow index of recycled PP by modifying microstructures.	[151]
rPP + glass fibre + talc + CaCO3	An increment in 300% of elastic modulus by the incorporation of glass fibre, talc and $CaCO_3$		[152]
Virgin and recycled PP	The blending of 75 wt% of virgin PP and 25 wt% of rPP were optimum composition that had positive influence on tensile strength, percentage of elongation at break and Young's modulus	The polymer degradation occurred when the macromolecule of PP was submitted to thermal and mechanical stresses which promoted chemical reaction. Hence, the polymer degradation can deteriorate the physical properties of the polymer.	[154]

Sample details	Key finding	Comments	Ref
rPP + silica and graphite.	The presence of silica and graphite in rPP can improve the hardness, tensile and flexural modulus and thermal behaviour but decrease in elongation because graphite makes material more brittle		[156]
PP, rPP + sawdust	The Izod strength was increasing at higher wood flour contents by reinforcing with PP-g-MA as compatibilizer. The Izod impact strength increased about 10% with increasing filler content to 40 wt%		[158]
rPP + talc	There was an observable improvement for tensile and flexural modulus by adding 20 wt% of Talc about 42.2% and 19.3%, respectively		[162]
rPP + geopolymer concrete waste (GCW)	The elastic modulus was better than neat PP. The elastic modulus enhanced up from 529.1 MPa to 618.2 MPa at 40 wt% of oleic acid modified geopolymer concrete waste (GCW)		[163]
rPP + Cellulose (CF) + newsprint (NP) fibres	The increase of tensile strength can be obtained by containing cellulose and newsprint fibres with the addition of impact modifier and compatibilizer		[164]

2.8.2 The limitations and knowledge gaps of the hybrid composites from recycled PP

Based on the majority of previous works that have been mentioned, there are some limitations and knowledge gaps on preparation and properties of PP hybrid composites. For example, regarding some single or hybrid component composite systems, specific properties

have been improved while another properties have been demoted, such as the deterioration in impact resistances, ductility or other strengths [48, 52, 53, 151]. The deteriorations of mechanical properties of composites were occurred from the reasons that were supported by various literatures are listed below:

- The improper preparation process including the process conditions. This contributed to worsen the mechanical properties from non-uniform filler dispersions due to agglomeration [113, 118, 119, 126, 127].
- The incorporation of unsuitable filler contents that led to embrittlement and reduced mechanical properties [74, 89, 96, 111].
- The poor interfacial force between filler and polymer matrix [71, 108, 159, 165, 166].
- The limitations of recycled quality and recycled polymer usage. The quality of recycled plastic is one of the main limitations that restrict the usage in single used plastic applications, due to the degradation of recycled plastic and the subsequent deterioration of the mechanical properties [48, 151, 154, 159, 167-169].
- The effect of contaminants, inorganic components, residual additive which have an important impact on mechanical properties, even more than the MFI [151, 170-173].

In order to overcome these limitations and balance such properties, this study will investigate a hybrid composite system by applying various reinforcement materials from particle and fibre families into a composite system. The experiments will be performed in order to evaluate synergy of the various types of reinforcing materials in the hybridization that can improve the composite performance. However, the challenges of this research are establishing the most proper hybrid PP based composite to enhance or compensate some of the deteriorated properties.

2.8.3 The novelty of the research

From the key learnings and limitations from the a number of literatures which were mentioned in the 2.8.1 and 2.8.2, these findings have been adapted to this present work and create the novelty of this research as follows.

- The main objective of this paper is to find out methodologies that can improve the performance of recycled PP to be comparable to neat PP which can be used in potential applications via hybrid reinforcement systems. Even though many researchers were worked on the hybrid composites, very few researchers were

reported about the evaluation of hybrid composite based on recycled polymer. The investigation on the recycled PP hybrid composite was the main criteria for evaluating the performance of composites. The three properties which were tensile, flexural modulus and Izod impact strength were taken into consideration. These properties are very important to be considered for implementation in each application. Very few literatures were investigated all of these properties in the literature.

- Many researchers compared the only performance of single and hybrid composites in their work. Though there are similar work, but the processibility and composite cost were considered in the present work. These factor are the essential factors for industrial production which were very few researcher reported. These can exhibit the feasibility of each hybrid composite system to be implemented for the application market. The optimum processing conditions were investigated in this study to balance the optimum output rate with the suitable machine capacity.
- The recommended dosage is very important from the literatures the typical dosage were around 5 – 30 wt%. However, this typical values were varied in this study. These dosages were used for studying the performance of filler and hybrid composite. From this study the higher filler concentrations (40 – 50 wt% of total filler content) were tested in order to investigate trend of composite performance whether they would be in the acceptable range to the composite in the market.

3. Materials and methods

The objective of this study aims to explore potential methodologies that can improve the performance of recycled PP to be comparable to neat PP which can be used in potential applications via hybrid reinforcement systems in terms of the improvement of mechanical properties, processability and cost. The experiments were developed to achieve the aims of this study. First, screening tests were conducted to evaluate the effect of fillers in different families and types, as well as loading. This stage was designed to study reinforcing performances of candidate fillers from fibre and particle families with neat PP resin in various composites systems. The best processing conditions for neat PP based composites were evaluated. While, the performance of neat PP based composites from various fillers by investigating mechanical properties, thermal properties, rheological properties, density, MFI, the presence of chemical functional groups fracture mode by FTIR including composite structure by SEM. Then, the best performing candidate in each family will be selected and combined to manufacture a hybrid composite by studying the effect of ratio of selected reinforcing agents in order to find out the best possible formulation in terms of mechanical properties, thermal properties, rheological properties, density, MFI. This final stage was to study the performance of recycled PP based from hybrid composites by studying the effects of blending ratio of rPP to neat PP. All the specimens will be validated through mechanical and thermal properties including failure mode and fracture surfaces.

3.1. Materials

3.1.1 Polypropylene resin (PP resin) (Trade name; EL-Pro P739ET in Figure 3.1 (a)) was supplied by SCG Chemicals Co., Ltd., Thailand. It is a copolymer polypropylene resin which is designed for compounding and injection moulding process. The average particle size is 3 mm. This resin was chosen from various grades as base resin for composites in this study due to it is a high flow rate impact copolymer polypropylene resin which is suitable for injection moulding for targeted applications such as electrical appliances and automotive parts. This resin was also the good reference since its properties have been suitable and versatile for various injection moulding applications.

3.1.2 Recycled Polypropylene resin (rPP resin in Figure 3.1(b)) (Trade name; MOPLEN QCP300P Ivory) was purchased from LyondellBasell Industries, USA. This resin was chosen as

base resin for recycled PP based composites in this study since it is designed for compounding and injection moulding process and contains at least 99 % of recycled material that is fully based on Post-Consumer Waste (PCW) from pre-sorted municipal plastic waste.

3.1.3 Coupling agent (or compatibilizer) has been used in these experiments in order to enhance compatibility between fillers and Polypropylene matrix. For this research Polypropylene grafted Maleic Anhydride (PP-g-MA; (Trade name; Polybond 3200 in Figure 3.1 (c)) was selected as coupling agent. It was sponsored by Addivant UK, Ltd, United Kingdom. Polybond 3200 is a maleic anhydride modified on homo-polymer polypropylene. The percentage of Maleic Anhydride is in the range of 0.8 – 1.2 wt%. This coupling agent was selected to use in this study since it has been used in previous experiment that can be proven the compatibility between fillers and PP matrix [174]. The values of MFI and density were also determined and are given in Table 3.1.

Table 3.1: Melt flow index (MFI) and density of selected polymers used in the study

Resin ***(Trade name)***	**MFI** (g/10 min)	**Density** (g/cm^3)
Polypropylene resin (PP resin), *(EL-Pro P739ET)*	55*	0.910
Recycled Polypropylene resin (rPP resin), *(MOPLEN QCP300P IVORY)*	16*	0.917
Coupling agent (PP-g-MA*), (Polybond 3200)*	115**	0.910

** MFI tested at 230 °C, 2.16 kg loading ** MFI tested at 190 °C, 2.16 kg loading*

(a) (b) (c)

Figure 3.1: (a.) Polypropylene resin (PP resin), (EL-Pro P739ET) (b) Recycled Polypropylene resin (rPP resin), (MOPLEN QCP300P Ivory) and (c) Coupling agent (Polybond 3200)

Reinforcing agents; various reinforcing agents have been selected to be used as the fillers in this research. These fillers have been selected from fillers that have significant high consumption in polymer industries and interesting materials that have been developed recently. From many fillers using in plastic industries, six different reinforcing agents have been selected as the representatives from fibre and particles families.

For the fibrous fillers, there are different fibres used in polymer matrix composites. However, glass and carbon fibres are the most promising reinforcements in polymer matrix composites. There are a huge consumption for glass fibre and carbon fibre. The global glass fibre market reached approximately 14.27 billion USD by 2019 [175]. Similarly, by the same year, the annual global demand for carbon fibres was expected to increase from 72,000 tons to 140,000 tons and the carbon fibre-reinforced composite global revenue expected to increase from 28.2 billion USD to 48.7 billion USD. Given these considerations both glass and carbon fibres have been selected as the representatives fibrous fillers.

The values of average fibre length and average fibre diameter were also determined by suppliers are given in Table 3.2. More information of these fibrous reinforcing materials are shown in Appendix B. The following two fibrous materials were used and shown in the Figure 3.2 and 3.3.

Table 3.2: Average fibre length and diameter of fibrous fillers

Fibre (Trade name)	**Average Fibre length** (micron)	**Average fibre diameter** (micron)
Glass fibre (CS331)	4,000	13
Milled Carbon fibre (FP-MCF-2)	100	7

Figure 3.2: Glass fibre (CS331)

Figure 3.3: Milled Carbon fibre (FP-MCF-2)

For the fibrous filler, there are both short and long types of fibres. The main reasons that short fibre has been selected in this experiment was because short-fibre-reinforced polymer are generally extrusion-compounded, whereas long-fibre-reinforced polymers are fabricated in proprietary impregnation processes and then chopped into 8 – 12 mm long fibres that is a more complicated process [176].

3.1.4 Glass fibre

For glass fibre was manufactured in-line process. After chopping process glass fibre bundles were pelletized to make that filaments bond well in the pelletizer. This glass fibre is silane-

based water-soluble coated resin. This can be the key features to protect the glass fibres against abrasion, fracture during manufacturing and processing. Moreover, it can impose compatibility to glass fibre with the resin in bonding and ensure that the monofilaments bond to give a single glass fibre. The selected glass fibre is CS331, (as shown in Figure 3.2) which was provided by KCC corporation, Korea.

3.1.5 Carbon fibre

For milled carbon fibre it is a very short strand length (100 μm) fibrous powder manufactured from recycled carbon fibre. The use of milled carbon fibre in a range of applications can significantly improve mechanical properties (tensile strength and modulus), dimensional stability and electrical/electrostatic conductivity. The CARBISO™ MF SM45R-100 (as shown in Figure 3.3) was provided by ELG Carbon Fibre Ltd., United Kingdom.

For particle family, fillers were chosen either due to their huge consumption or for being interesting materials. There are four various reinforcing agents which were used to represent the particle family. These are:

- Calcium Carbonate ($CaCO_3$),
- Kaolin,
- Glass bead,
- Graphene Nanoplateletes (GNPs).

The average fibre length and bulk density of these reinforcing agents were also determined by suppliers are given in Table 3.3. More information of these reinforcing materials are shown in Appendix B.

Table 3.3: Average fibre length and bulk density of particulate fillers

Fillers (Trade name)	**Average particle size** (micron)	**Bulk Density** (g/cm^3)
Calcium Carbonate: $CaCO_3$ (OMYACARB-2T)	2	1.35
Kaolin (SILFIT Z 91)	2	0.33
Glass bead (EGB731A)	20	1.00
Graphene nanoplatelets (900420)	15	0.0215

3.1.6 Calcium Carbonate ($CaCO_3$)

Calcium Carbonate was selected to be used as one of candidate of fillers because it has been used widely, especially in most countries in Association of Southeast Asian Nations (ASEAN), along with India, Japan, and South Korea, which have been major consumers of $CaCO_3$ [177]. It is used in plastic, pharmaceuticals, and paper industries. Hence, demand for calcium

carbonate is expected to increase at approximately 6% in 2019 – 2027 [177]. However, companies are expanding into developing markets such as China, India, Indonesia, Australia, and Saudi Arabia. These countries are expected to provide lucrative opportunities to market players due to the growth of various end-use industries.

Selected $CaCO_3$ (OMYACARB-2T, as shown in Figure 3.4) was purchased from Surint Omya Chemicals, Thailand. This particular type is a ground calcium carbonate which was coated with < 2 % fatty acid. This is because fatty acid-coated $CaCO_3$ is more compatible with polymers than bare $CaCO_3$ [178].

Figure 3.4: Calcium Carbonate: $CaCO_3$ (OMYACARB-2T)

3.1.7 Kaolin

Kaolin was considered as the candidate in particle family because it is a natural mineral which is ubiquity and has been investigated from many previous literatures that they can improve mechanical properties of polymers [92-94, 180]. It is the combination of corpuscular silica and lamellar kaolinite, which has been subjected to a heat treatment. The components and the thermal process lead to a product that offers special performance benefits as a functional filler. The SIlfit Z 91 (as shown in Figure 3.5) was provided by Hoffmann mineral, Germany.

Figure3.5: Kaolin (SILFIT Z 91)

3.1.8 Glass bead

Glass beads are the one of candidates for fillers in particle family because it is mainly used as a filler for engineering thermoplastic compound. A main purpose to use glass bead for plastic compound is to have better dimensional stability (lower warpage), heat resistance, hardness. The glass that was used in this experiment was low alkaline glass (E Glass Bead, EGB731), as shown in Figure 3.6. This can be used together with glass fibre to improve dimensional stability. This is the one of the popular glass sphere among thermoplastic compound manufacturers in Japan. EGB731A was purchased from Potters-Ballotini Co., Ltd, Japan.

Figure 3.6: Glass bead (EGB731A)

3.1.9 Graphene nanoplatelets (GNPs)

Graphene nanoplatelets (GNPs) was chosen for the one of the candidates because it is an interesting filler that numerous studies revealed its addition into the polymer matrix could further improve the required mechanical and thermal properties. GNPs are nanoparticles consisting of short stacks of graphene sheets having a platelet shape. Actually, there are many various sized GNPs which have been added in polymers. Refer to several trusted researches, they used GNPs which was categorized as M grade [108, 179-181]. Particles have an average thickness of approximately 6 - 8 nanometers and a typical surface area of 120 to 150 m^2/g. The GNPs in this project is coded 900420 and it was purchased from Sigma-Aldrich Company LTD, United Kingdom (see Figure 3.7).

Figure 3.7: Graphene nanoplatelets (900420)

According to the selected reinforcing materials were mentioned earlier, the key properties of these fillers from various studies are shown in the Table 3.4.

Table 3.4: Key properties of selected reinforcing materials

Reinforcing materials	Key properties
Glass fibre	• High tensile and flexural modulus [59, 63-65] • Good corrosion resistance to almost all acids, alkalis, salts and organic solvents [4] • Good electrical insulation [4]
Carbon Fibre	• High tensile and flexural moduli [4, 71, 73-75] • High electrical conductivity, high thermal conductivity [4, 72, 74, 75] • Good corrosion resistance (apart from strong oxidants such as concentrated nitric acid, hypochlorite and dichromate oxidation) [4]
$CaCO_3$	• High tensile and flexural modulus [82-84, 87-89] • High stiffness and toughness [182]
Kaolin	• High tensile strength, flexural modulus and impact strength [94-96, 183] • Electrical, corrosion, and chemical resistance [94] • High abrasion resistance [94] • Flame retardancy [184]
Glass bead	• High tensile and flexural modulus [102, 104] • Good impact strength [101, 104] • Low shrinkage [185] • High heat distortion temperature [185] • Good dimensional stability [165] • High abrasion resistance, hardness [165] • high heat resistance [165]
GNPs	• Excellent thermal conductivity and electrical conductivity [107, 179, 186, 187] • High tensile modulus [107, 108, 113, 179, 186, 188-191] • High stiffness and strength, barrier resistance [107] • Flame retardancy [107]

3.2 Preparation of PP composites and sample specimens

3.2.1 PP composites with various loadings of fillers

Commercial grade PP containing 10 - 30 wt% of various fillers were processed in the Polylab twin-screw extruder (HAAKE, Germany), shown in Figure 3.8. The schematic of a typical extrusion machine and screw configurations are shown in Figure 3.9 and 3.10. The specification of twin screw extruder including main screw parameters is shown in Tables 3.5

and 3.6. PP and the filler were kept in closed containers in the storage room to prevent the moisture adsorption and they were dried again in a vacuum oven at 80 °C (as shown in Figure 3.11) over 15 hours before using compounding. PP resin and coupling agent were pre-mixed and fed into the main feed. Some fillers in powder form such as $CaCO_3$, kaolin, glass bead, GNPs, carbon fibre, were fed into the extruder by gravimetric feeder (Brabender Loss-in-Weight Feeder DDW-MD0-MT-0.5) with twin concave screw as shown in Figure 3.12. While, glass fibre composite, which is small rod form, was carefully pre-mixed manually before feeding it into the extruder.

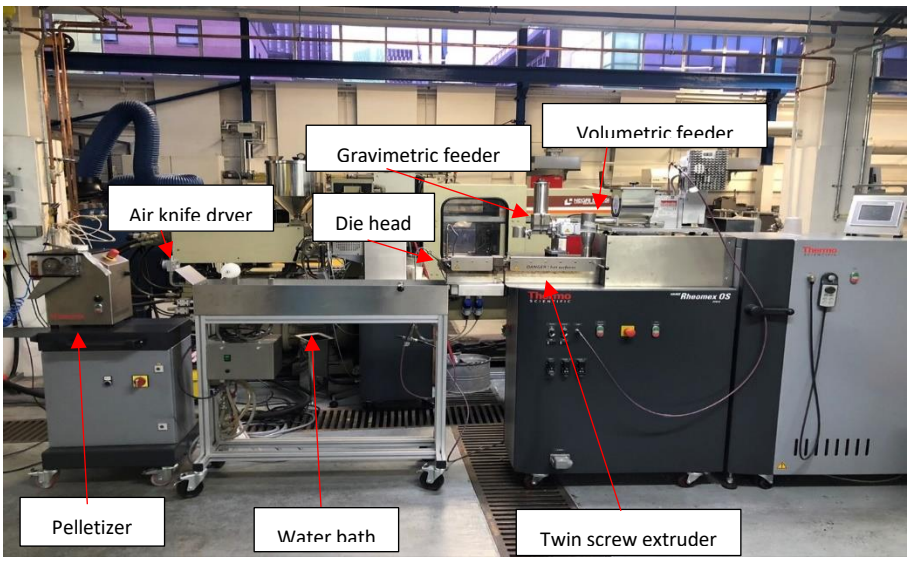

Figure 3.8: Haake Rheomax OS PTW16

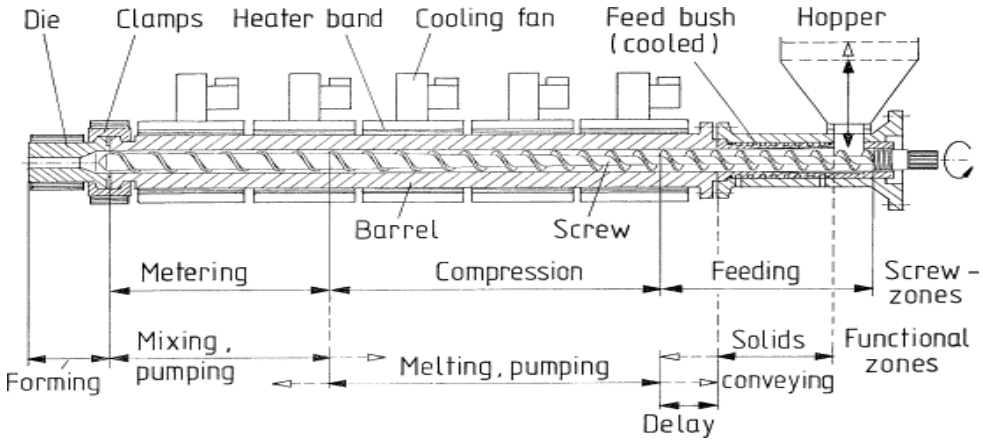

Figure 3.9: Schematic of a typical extrusion machine [192]

Table 3.5: Twin screw extruder specification

Item	Haake Rheomax OS PTW16
Screw Diameter	16 mm
L/D	40
Gear ratio	1 : 5.4
Rotation direction	Co-rotating
Max Screw speed	1100
Max temperature	350 °C
Max Pressure	100 bar
Max Torque	160 N.m
No. of extruder zone	10
Heating zone	9

Table 3.6: Main parameter of screws

Helix angle	Pitch	Diameter (D)	L/D
17.7°	16 mm	16 mm	40

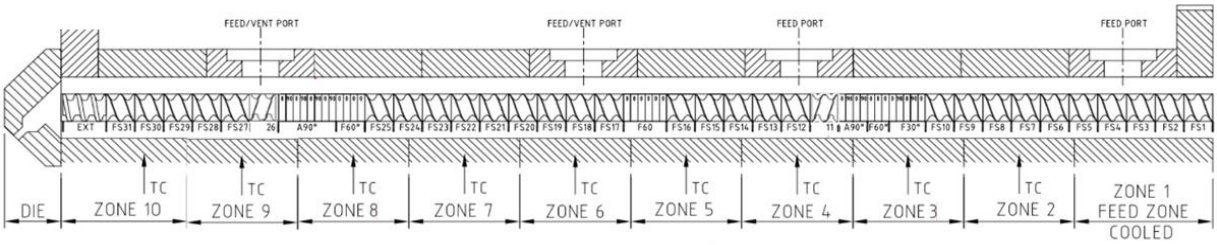

Figure 3.10: Screw configuration

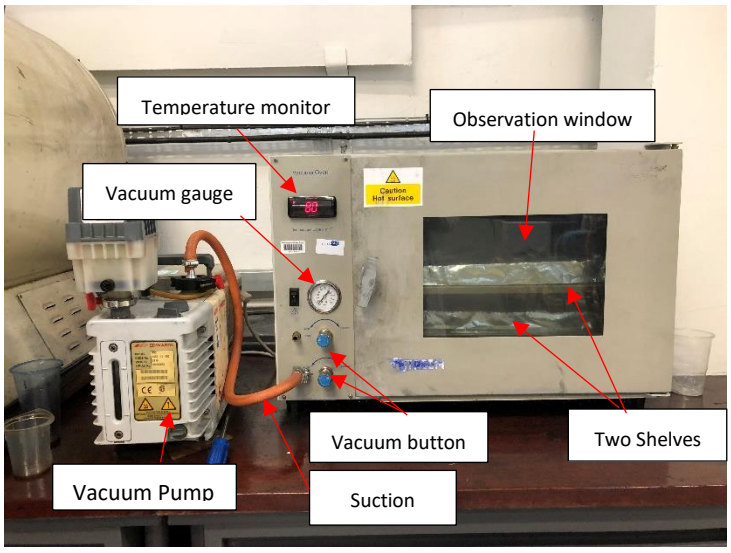

Figure 3.11: Vacuum oven

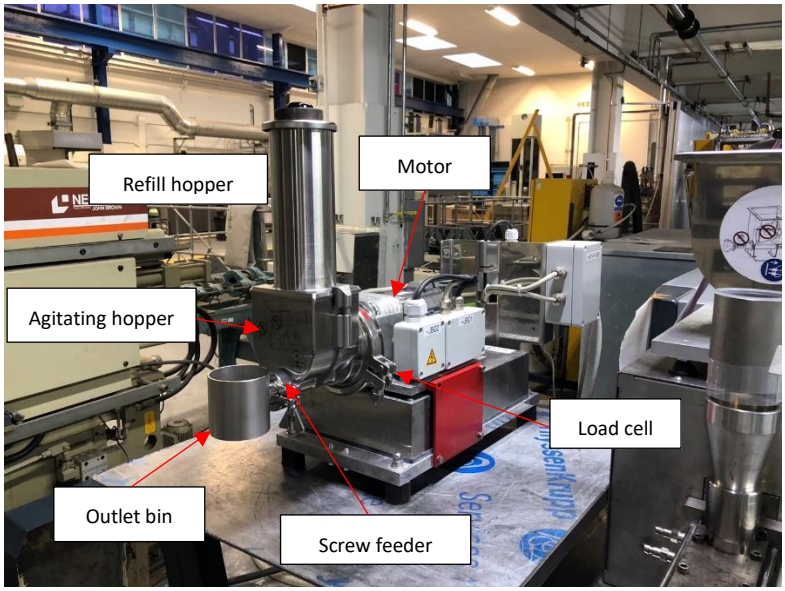

Figure 3.12: Gravimetric feeder (Brabender Loss-in-Weight Feeder DDW-MD0-MT-0.5)

The twin extruder contains ten zones of barrels, which has nine heating zones whereas the first zone was cooled. The screw configuration is shown in Figure 3.10. From the illustration, the first two zones are solid conveying or feed zone. These zones are designed mainly for conveying and preheat the polymer granules [193]. This zone has wider pitches of screw in order to fill more granules. The next zone is located at barrels no. 3 – 7. These zones have been called transition or melting or plasticating zone, where the polymer granules are melted and the resulting melt compressed. It has been shown in most extrusion applications that during melting the polymer particles are pressed together to form a contiguous solid bed which is pushed against the trailing flight flank [193]. From the seventh zone onwards they have been called metering or pumping zone. From the Figure 3.10, there are kneading blocks which are the important functional part of the co-rotating twin screw extruder. The melting process is generally carried out in the kneading block. Standard kneading blocks are characterized by the length, number of discs and the offset angle between the discs [194]. The screw channel is full of molten polymer which is pumped towards the die. The motion of the screw relative to the barrel induces a drag flow which, because of the geometry of the screw, has the net effect of pushing the polymer forward. This is resisted by the pressure gradient operating in the opposite direction, and the net melt flow rate through the metering zone is the sum of these two terms [193].

3.2.2 Formulations of composite systems

The formulations are the major elements which have to be considered for the whole project. The experiments in this study were separated into three sessions: screening experiments for selecting the best suited fillers for hybrid composites, determination of the best formulation of the neat PP based hybrid composites and recycled PP based hybrid composites.

For the first session, screening testing, this session investigated the most suitable filler from both fibre and particle families to be used in hybrid composite and further experiments. Neat PP based composites samples have been prepared by varying 10 - 30 wt% of various fillers which were glass fibre, carbon fibre, $CaCO_3$, glass bead, kaolin and GNPs. The designated composite and its composition are shown in Table 3.7. For the addition of coupling agent (PP-g-MA), the suitable content is 0.15 times of the total weight of filler content which were kaolin, glass bead, GNPs, glass fibre and carbon fibre. This ratio was recommended from the previous trusted study [174].

Table 3.7: Designation and composition of the PP and recycled –based composites samples

Samples	**Code**	**Resin** (wt%)	**Fillers** (wt%)	**Compatibilizer** (wt%)
Neat PP resin	PP Ref	100		
Recycled PP resin	rPP Ref	100		
Neat PP based composite				
with $CaCO_3$	PP/CC			
10 wt%	PP/CC10	90	10	
15 wt%	PP/CC15	85	15	
20 wt%	PP/CC20	80	20	
25 wt%	PP/CC25	75	25	
30 wt%	PP/CC30	70	30	
with Kaolin	PP/KL			
10 wt%	PP/KL10	88.5	10	1.5
20 wt%	PP/KL20	77	20	3
30 wt%	PP/KL30	65.5	30	4.5
with Glass bead	PP/GB			
10 wt%	PP/GB10	88.5	10	1.5
15 wt%	PP/GB15	82.75	15	2.25
20 wt%	PP/GB20	77	20	3
25 wt%	PP/GB25	71.25	25	3.75
30 wt%	PP/GB30	65.5	30	4.5
with GNPs	PP/GN			
10 wt%	PP/GN10	88.5	10	1.5
20 wt%	PP/GN20	77	20	3
30 wt%	PP/GN30	65.5	30	4.5

Table 3.7 (Continued): Designation and composition of the PP and recycled –based composites samples

Samples	**Code**	**Resin** (wt%)	**Fillers** (wt%)	**Compatibilizer** (wt%)
with Glass Fibre	PP/GF			
10 wt%	PP/GF10	88.5	10	1.5
15 wt%	PP/GF15	82.75	15	2.25
20 wt%	PP/GF20	77	20	3
25 wt%	PP/GF25	71.25	25	3.75
30 wt%	PP/GF30	65.5	30	4.5
with Carbon fibre	PP/CF			
10 wt%	PP/CF10	88.5	10	1.5
20 wt%	PP/CF20	77	20	3
30 wt%	PP/CF30	65.5	30	4.5

From the Table 3.7, the additional experiment with 15 wt% and 25 wt% were conducted for PP composites with $CaCO_3$, glass bead and glass fibre. This is because these experiments were conducted in order to recheck the trend of data whether there were some peak of data between filler contents (between 10 and 20 wt% and 20 and 30 wt%). While the other composites system had the clearly trend of data. The experimental results are described in Chapter 4 in topic 4.2.7.

The second session of experiments related to the investigation of the best formulation of selected candidates of fillers from both fibre and particle families. After the most suitable fillers were selected from the first section, formulations of hybrid composite were designed by using the Taguchi model with mixed level design as guidance. The investigated factors were content of selected fibrous and particle fillers. The number of levels for fibre and particle filler was 2 and 4 respectively. The experiments were designed with L8 mode and eight experiments and five further experiments for optimization were planned. The designated composites and their compositions are shown in Table 3.8.

Table 3.8: Designation and composition of the neat PP –based hybrid composites samples

Formulations	Code	Resin wt%	Fillers A wt%	Fillers B wt%	Compatibilizer wt%
Designed formulations from Taguchi					
• Hybrid Composite 1	HC1	X_1	A_1	B_1	C_1
• Hybrid Composite 2	HC2	X_2	A_2	B_2	C_2
• Hybrid Composite 3	HC3	X_3	A_3	B_3	C_3
• Hybrid Composite 4	HC4	X_4	A_4	B_4	C_4
• Hybrid Composite 5	HC5	X_5	A_5	B_5	C_5
• Hybrid Composite 6	HC6	X_6	A_6	B_6	C_6
• Hybrid Composite 7	HC7	X_7	A_7	B_7	C_7
• Hybrid Composite 8	HC8	X_8	A_8	B_8	C_8
Optimized formulations					
• Optimized hybrid Composite 1	HC9	X_9	A_9	B_9	C_9
• Optimized hybrid Composite 2	HC10	X_{10}	A_{10}	B_{10}	C_{10}
• Optimized hybrid Composite 3	HC11	X_{11}	A_{11}	B_{11}	C_{11}
• Optimized hybrid Composite 4	HC12	X_{12}	A_{12}	B_{12}	C_{12}
• Optimized hybrid Composite 5	HC13	X_{13}	A_{13}	B_{13}	C_{13}

The final session of experiments was the implementation of the best formulation from the second session to rPP. This experimental stage was designed to evaluate the most suitable rPP ratio of hybrid composites. These obtained rPP hybrid composites have to be comparable or superior to neat PP. The investigated factors were percentages by weight of rPP with five contents. The designation and the compositions of rPP based hybrid composite are shown in Table 3.9.

Table 3.9: Designation and composition of the rPP – based hybrid composites samples

Formulations	Code	Neat PP wt%	rPP wt%	Fillers A wt%	Fillers B wt%	Compatibilizer wt%
• rPP hybrid composite 1	rHC1	95	5	A_1	B_1	C_1
• rPP hybrid composite 2	rHC2	90	10	A_2	B_2	C_2
• rPP hybrid composite 3	rHC3	80	20	A_3	B_3	C_3
• rPP hybrid composite 4	rHC4	50	50	A_4	B_4	C_4
• rPP hybrid composite 5	rHC5	25	75	A_5	B_5	C_5
• rPP hybrid composite 6	rHC6	0	100	A_6	B_6	C_6

3.2.3 Processing conditions

The barrel temperature profile was set at the range of 180 – 210 °C with the screw speed of 70 rpm with 1.8 kg/hr for throughput. The temperature profile is in the Table 3.10 as follows.

Table 3.10: Temperature profile for PP composite compounding

Zone No.	Zone 1	Zone 2	Zone 3	Zone 4	Zone 5	Zone 6	Zone 7	Zone 8	Zone 9	Zone 10
Temperature (°C)	180	190	190	210	210	210	210	210	210	180

The obtained composites were extruded, cooled in water tank and air atmosphere and chopped into small pieces with 3 mm of diameter. Then, PP based composites were kept in a sealed sample bag to prevent moisture adsorption and were dried again in an oven at 80 °C for 4 hours before use in the preparation of sample specimens.

The procedure for the initial setting of the temperature profile is very important and affect composite performance since temperature profile is influential to mixing ability, and melting behaviour including dispersability. The temperature profile in Table 3.10 was set by the supported justifications. First, regarding the temperature of the feed zone, it is important that the plastic cannot melt in the feed zone (often externally cooled), otherwise bridging may occur or the grooved barrel may become clogged. In addition, it is the task of the feed zone to let the air escape from the inside of the extruder. Depending on the material being processed, this air may contain volatile components which could condense and contaminate the material if the temperatures in the feed zone are too cold [121]. For this study, the parameterization of the first zone behind the feed area was set at 180 °C. This setting has been used since the main task of the extruder is to melt the material by friction (dissipation). The set temperature should therefore be above the softening temperature or even above the crystalline melting temperature of the material [121].

In compounding process, there are rules of thumb for setting processing temperature. Generally for typical semi-crystalline materials, processing temperature should be set about 50°C – 75°C above the melting temperature [121, 195, 196]. Therefore, the processing temperature profile should be around 190 °C – 200 °C and the second and third zones of barrels have been set at 190°C in order to slightly increase the temperature to 200 °C for the following zones.

In this study, processing temperature profile of the fourth zone to ninth zone was set at the constant temperature of 210 ^{o}C since temperature need to be maintained at that certain point to obtain a uniform temperature profile.

For the last zone, the processing temperature was set as 180 ^{o}C, which was lower than from the previous zone. This is because there are various formulations of composites which were added with different filler loadings. These formulations require good mixing. The lower temperature, especially at the die, can encourage the generation of back pressure at the last zone before coming out through the die. Back pressure assists molten polymer steam flow back and improves mixing along the screw [197].

3.2.4 Specimen fabrication

Three types of composites specimens were prepared for testing mechanical properties: tensile, flexural and Izod impact testing. All these samples were prepared by injection moulding machines in the different dimensions.

For tensile testing, specimens were prepared by the Minijet injection moulding from HAAKE, Germany (as shown in Figure 3.13 into dumbbell shaped samples following ISO 527 standard (as shown in Figure 3.14). The process condition was obtained by fine tune the most suitable condition from starting with the melting temperature and tune the most suitable pressure and time to obtain full dumbbell shape with smooth surface and without bubbles and flash. The process condition are shown in the Table 3.11. The standard dimension of these samples are shown in Table 3.12. The main parts of the Minijet are cylinder, retaining pin, mould and injection piston. The injection piston transfers the pneumatic force to the melt inside the cylinder. The melt is forced through the injection nozzle to the mould [198].

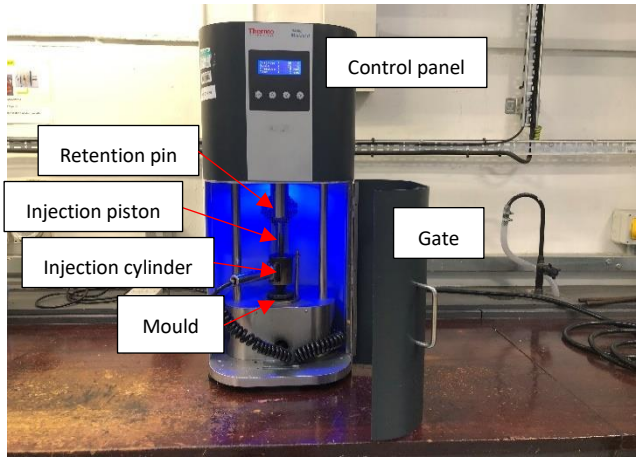

Figure 3.13: HAAKE Minijet injection moulding

Table 3.11: Processing condition parameter of Minijet

Barrel temperature (°C)	Mould temperature (°C)	Injection		Holding step	
		Pressure (bar)	Time (s)	Pressure (bar)	Time (s)
210	45	250	10	100	5

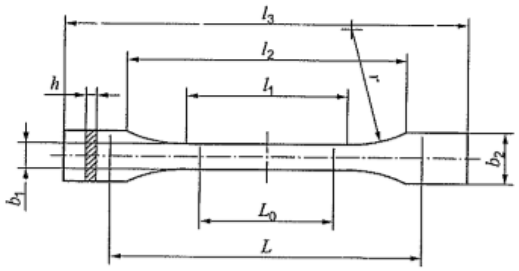

Figure 3.14: Specimen for tensile testing follow ISO 527 type 1BA [199]

Table 3.12: Dimension of type 1BA test specimen from ISO 527

	Specimen type	**1BA (mm.)**
l_3	Overall length	≥75
l_1	Length of narrow parallel-sided portion	30.0 ± 0.5
r	Radius	≥30
l_2	Distance between broad parallel-sided portions	58 ± 2
b_2	Width at ends	10 ± 0.5
b_1	Width at narrow portion	5 ± 0.5
H	Thickness	≥2
L_0	Gauge length	25 ± 0.5
L	Initial distance between grips	l_2 $^{+2}{}_{0}$

For the processing condition, the temperature of cylinder and mould were set at 210 °C and 45 °C, respectively. The molten composites were injected and flowed into the mould with the pressure of 250 bar in 10 seconds and then the pressure of machine was hold at 100 bar for 5 seconds to compensate the effect of shrinkage. The tensile specimens are shown in Figure 3.15. Before testing, the specimens had to be conditioned as in the standard ISO 291 for the material being tested. The preferred set of condition was maintained at 23°C and 50 % of relative humidity [200].

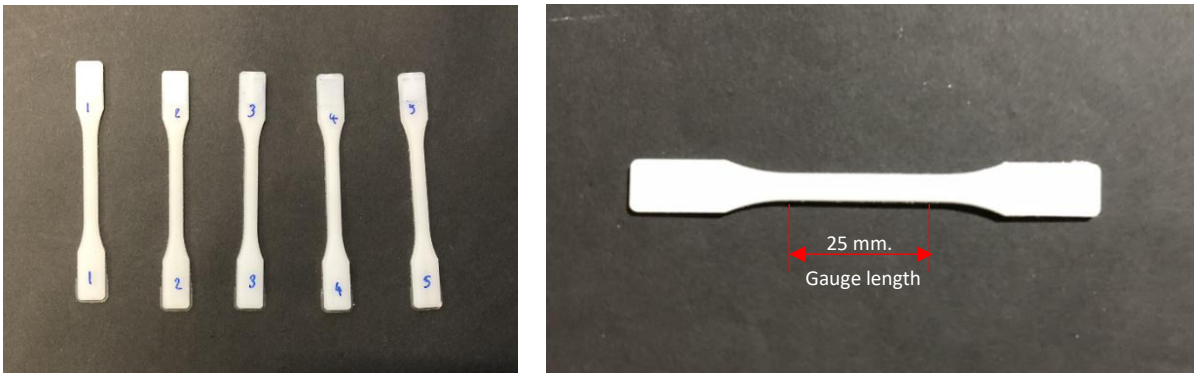

Figure 3.15: Injected specimen for tensile testing follow ISO 527 type 1BA [199]

In the case of specimens for flexural modulus and Izod impact testing these have to be referred to ISO 178 [201] and ISO 180 [202]. Specimens were cut into the standard dimension. The dimension, in millimetres, of the preferred test specimen are length 80 ± 2 mm, width 10 ± 0.2 mm, thickness 4.0 ± 0.2 mm.

Test specimens for Flexural and Izod impact testing were prepared by an injection moulder from Negri Bossi, Italy (Figure 3.16). The schematic of a typical injection moulding machine is shown in Figure 3.17. The process condition was chosen by fine tuning the most suitable for these composites by setting temperature in the range of melt temperature from compounding process and fine tune the injection pressure to obtain proper specimens without shrinkage, bubbles and flash. The process conditions are shown in Table 3.13. The test specimens have been prepared by the mould in Figure 3.18.

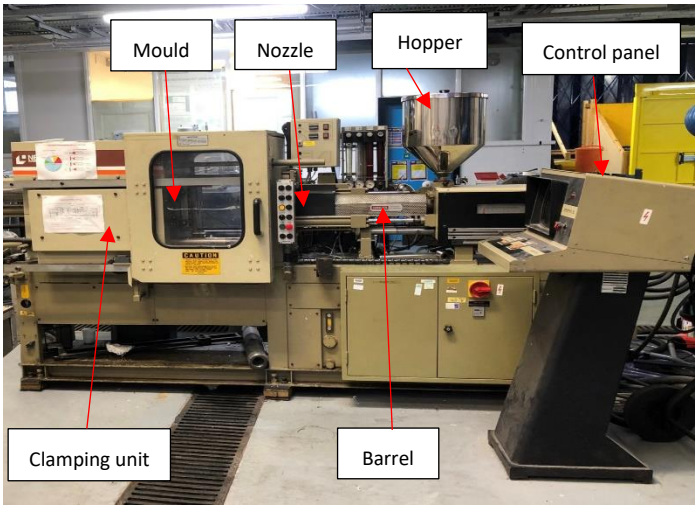

Figure 3.16: Injection moulding: Negri Bossi

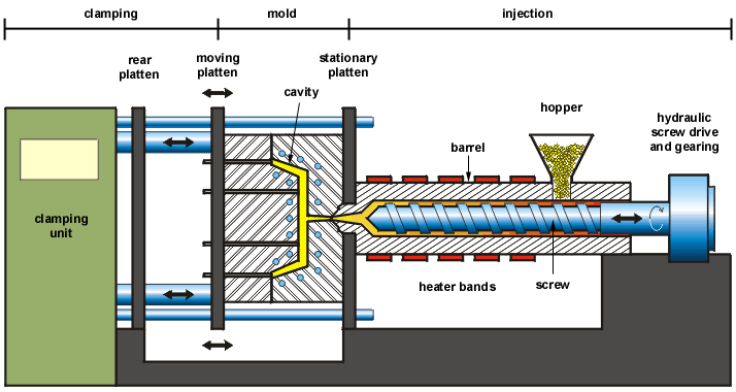

Figure 3.17: Schematic of a typical injection moulding machine [203]

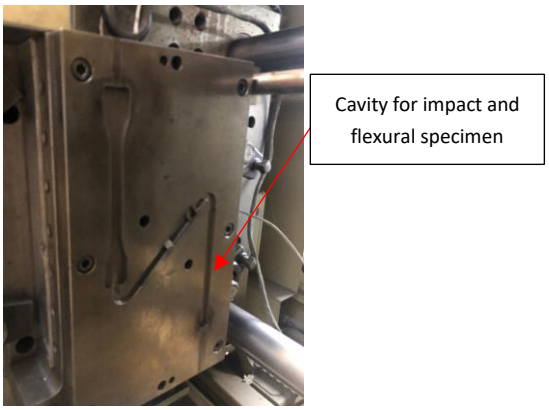

Figure 3.18: Mould for test specimens

The testing specimens for flexural modulus and Izod impact testing are shown in Figure 3.19 The specimens had to be conditioned as in the standard ISO 291 for the material being tested. The preferred set of condition was maintained at 23°C and 50 % of relative humidity [200].

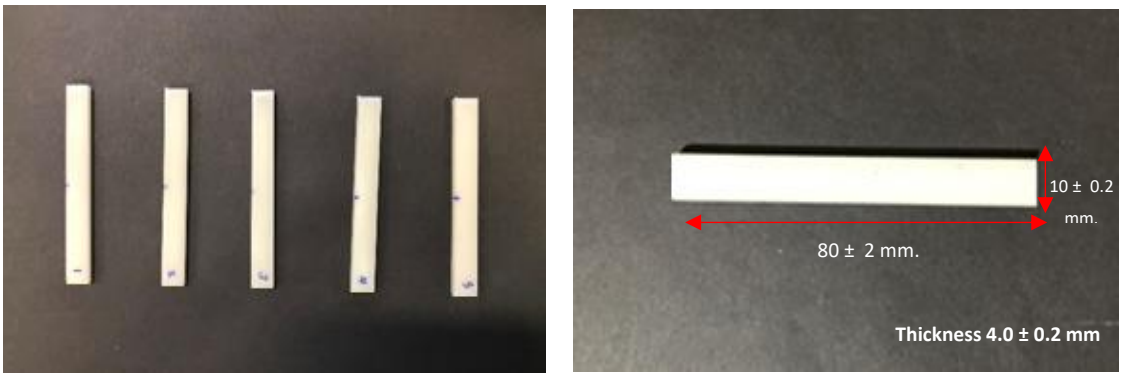

Figure 3.19: Testing specimens for flexural modulus from injection moulding (Negri Bossi)

Table 3.13: Processing conditions used for injection moulding with Negri Bossi

Barrel temperature (°C)	Injection Pressure (bar)	Holding step	
		Pressure (bar)	Time (s)
210 – 210 – 210 - 210	42	15	15

For Izod impact testing, the testing specimens had to be notched. The notch shall be located at the centre of the specimen. The specimens were notched by a notch maker, shown in Figure 3.20. Typically, the dimension and shape of notch shall be preferred type A, shown in Figure 3.21 [202]. The remaining width at the notch base has to be 8.0 ± 0.2 mm [202]. The testing specimens for flexural modulus and Izod impact testing are shown in the Figure 3.22. Before testing, the specimens had to be conditioned as in the standard ISO 291 for the material being tested. The preferred set of condition was maintained at 23°C and 50 % of relative humidity [200].

Figure 3.20: Notch maker

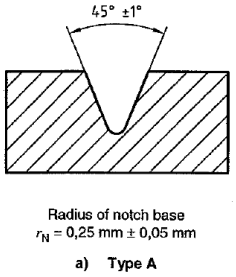

Figure 3.21: Notch dimension [202]

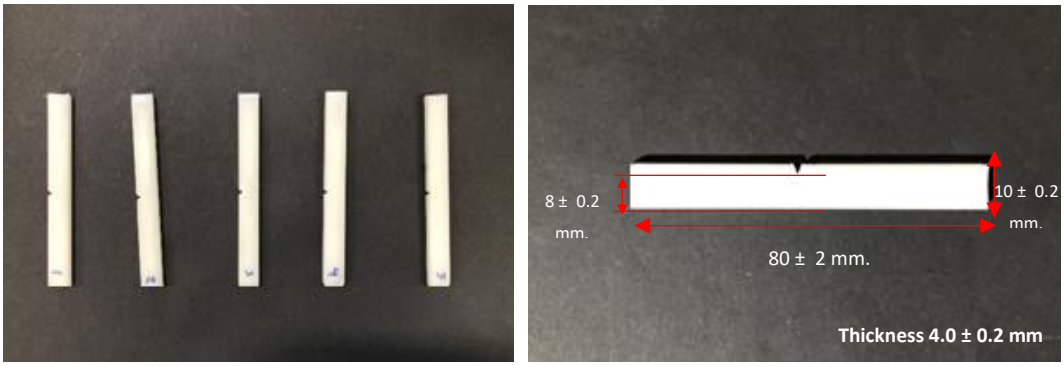

Figure 3.22: Notched testing specimens for Izod impact testing from injection moulding (Negri Bossi)

For rheology testing, the testing specimens had to be compressed by the compression moulding machine in the Figure 3.23. Compression moulding process was performed at a mould temperature of 210°C and mould pressure of 10 bar with pressing time of 4 min. After the material was compressed, the mould (see Figure 3.24) was opened and the samples were removed from the mould. Typically, sample Rheology testing is a disk with dimensions of

approximately 25 mm diameter and 1 mm in thickness. The dimension and shape shown in Figure 3.25.

Figure 3.23: Compression Moulding machine

Figure 3.24: Compression mould for rheology samples with a thickness of 1.00 ± 0.05 mm and a diameter of 25.00 ± 0.05 mm

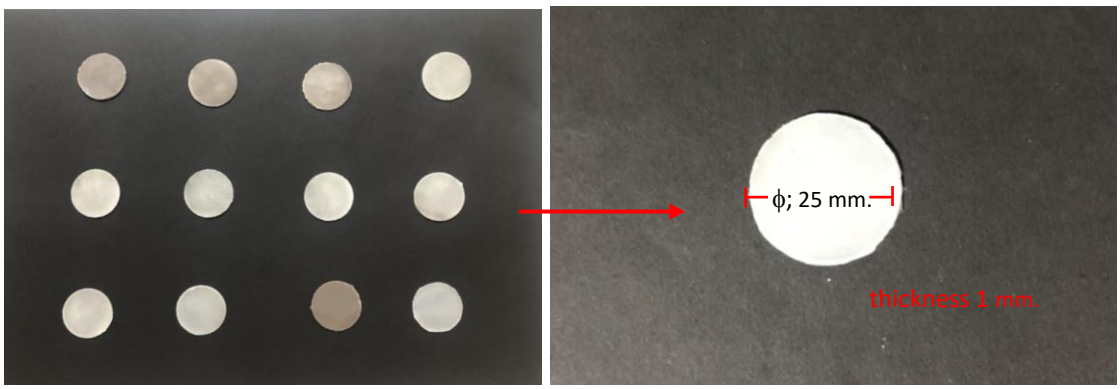

Figure 3.25: Compressed disc specimens for rheology testing with a thickness of 1.00 ± 0.05 mm and a diameter of 25.00 ± 0.05 mm

3.3 .Characterizations

3.3.1. Mechanical Properties

The composite and hybrid composite materials in this study have been investigated to be applied to various applications such as automotive and electrical appliance, etc. The suitable

final application should be considered from the composites properties such as tensile, flexural modulus and impact strength.

Tensile modulus this will be indicated the dimensional stability and the resistance of deformation. Tensile tests help determine the effectiveness and behavior of a material when a stretching force acts on it. Next properties is flexural modulus which is the important properties that can indicate the resistance to bending force during using. The last measured properties was also important is impact resistance can be indicated the toughness that takes into account both the strength and ductility of the composite materials [204].

3.3.1.1 Tensile testing

The tensile tests were performed according to ISO 527 [197] using the Instron 5984 model. The tensile properties known as tensile strength and elongation at break were recorded. The test specimen shall be conditioned in the controlled atmosphere is (23±2) ^{o}C and (50 ± 10) % R.H. The conditioning time is at least 16 hours [199]. The rate used was 50 mm/min with 1 kN load by Universal testing machine shown in the Figure 3.26. The thickness of the sample was measured using vernier callipers. Five specimens were tested and the average of the five best measurements was reported. All tests were done under room temperature.

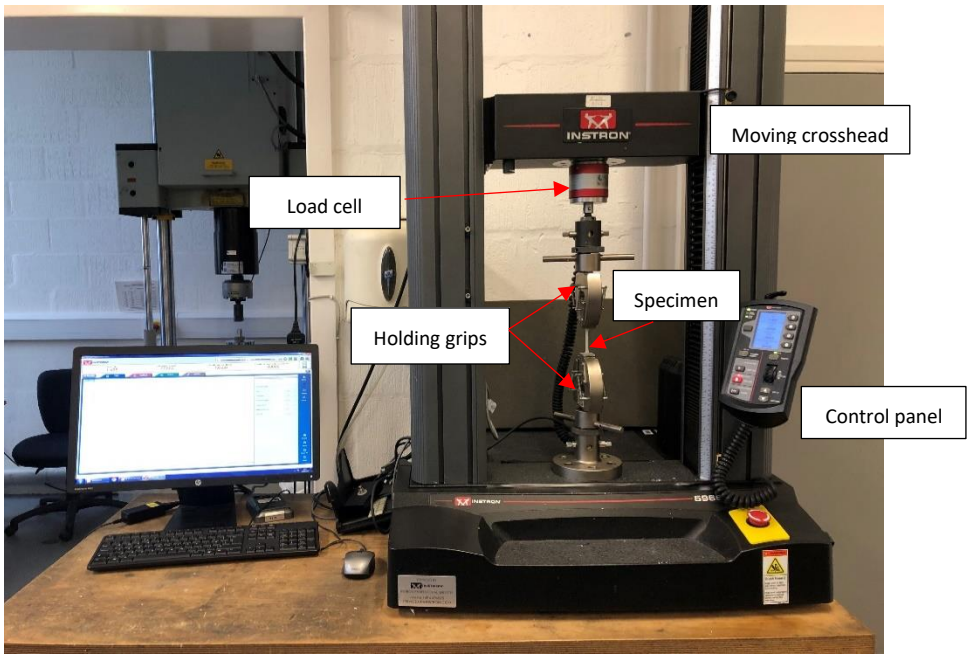

Figure 3.26: Tensile testing via Universal testing machine

Tensile properties have been evaluated by the calculations as follows,

Tensile stress (σ) was calculated by using the following equation 3.1

$$\sigma = \frac{F}{A} \qquad 3.1$$

Where σ is the stress value, expressed in megapascal (MPa), *F* is the measured force concerned, expressed in newton (N), *A* is the initial cross-sectional area of the specimen, expressed in square millimeter (mm^2)

Tensile strain (ε) was calculated by using the following equation 3.2

$$\varepsilon = \frac{\Delta L_0}{L_0} \qquad 3.2$$

Where ε is the strain value, expressed as a dimensionless ratio, or as a percentage, L_o is the gauge length of the test specimen, expressed in millimeter (mm), ΔL_o is the increase of the specimen length between the gauge marks, expressed in mm.

Tensile modulus (E_t) was calculated from slope of the stress/strain curve in the interval between strain 0.05% - 0.25%. It has been expressed in MPa or computing by using stress and strain value from the following equation 3.3

$$E_t = \frac{\sigma_2 - \sigma_1}{\varepsilon_2 - \varepsilon_1} \qquad 3.3$$

Where E_t is the tensile modulus, expressed in MPa σ_1 is the stress, expressed in MPa, measured at the strain value ε_1 is 0.0005 (0.05%), σ_2 is the stress, expressed in MPa, measured at the strain value ε_2 is 0.0025 (0.25%)

3.3.1.2 Flexural testing

The flexural tests were performed according to ISO 178 [201] using the Instron 5984 model which is shown in Figure 3.27.

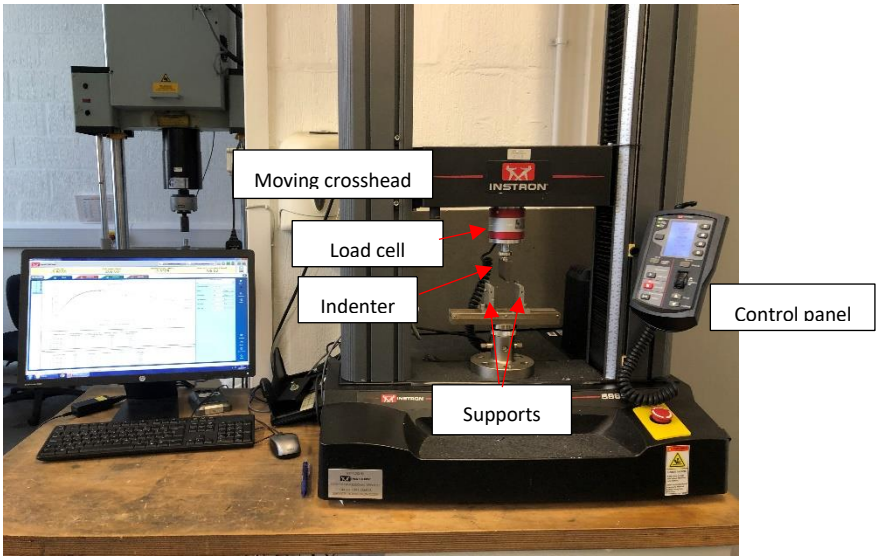

Figure 3.27: Flexural testing via Universal testing machine

The procedure used was test method 1 (three-point loading utilizing center loading) with a span width of 64 mm. The span width was calculated from the following equation 3.4:

$$L = (16 \pm 1)\bar{h} \qquad 3.4$$

Where L is the length of span, expressed in mm, $\bar{h}$ is average thickness of samples, expressed in mm.

The dimension of test specimens in millimetres was width 10 ± 0.2 mm, length 80 ± 2 mm and thickness 4 ± 0.2 mm. The crosshead rate used was 2 mm/min with 1 kN load. This test speed rate of 2 mm/min has been referred from ISO 178 which is the speed for the preferred test specimen. The test specimen shall be conditioned in the controlled atmosphere is (23 ± 2) ^{o}C and (50 ± 10) % Relative humidity. The flexural properties known as flexural strength and flexural modulus were recorded.

- **Flexural modulus**

To determine the flexural modulus, we calculate the deflections s_1 and s_2 corresponding to the given values of the flexural strain ε_{f1} = 0.0005 and ε_{f2} = 0.0025 using the following equation 3.5:

$$S_i = \frac{\varepsilon_{fi} L^2}{6h} \qquad (i = 1,2) \qquad 3.5$$

Where S_i is one of the deflections, in millimetres , $\varepsilon_{f\,i}$ is the corresponding flexural strain, whose values $\varepsilon_{f\,1}$ and $\varepsilon_{f\,2}$ are given above, L is the span, in mm, h is the thickness, in mm, of the specimen.

Calculate the flexural modulus E_f expressed in MPa, using the following equation 3.6:

$$E_f = \frac{\sigma_{f2} - \sigma_{f1}}{\varepsilon_{f2} - \varepsilon_{f1}} \qquad 3.6$$

Where σ_{f1} is the flexural stress, in MPa, measured at deflection s_1, σ_{f2} is the flexural stress, in MPa, measured at deflection s_2

The thickness of the sample was measured using Vernier calipers. Five specimens were tested and the average of the five best measurements were reported. All tests were done under room temperature.

3.3.1.3 Izod Impact Testing

For Izod notched impact strength testing, impact energy will be absorbed in breaking a notched specimen, referred to the original cross-sectional area of the specimen at the notch, with the pendulum striking the face containing the notch. The absorbed impact energy is expressed in kilojoules per square metre (kJ/m^2). The impact strength of the materials was carried out with pendulum energy of 11 J by using Instron Ceast 9050 in the Figure 3.28.

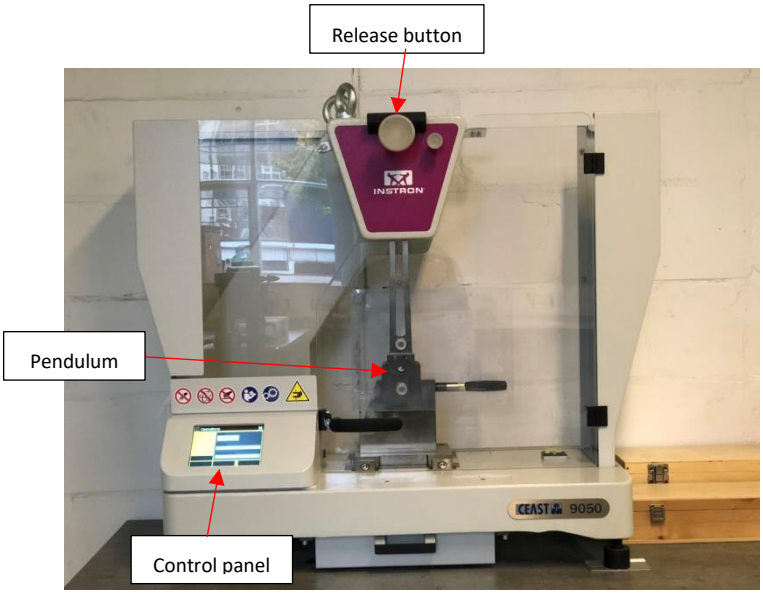

Figure 3.28: Izod Impact tester (Instron Ceast 9050)

All specimens had the following dimensions: 10 × 80 × 4 mm^3. Notched samples with a span length of 80 mm were mounted, according to ISO 180 [202]. For each kind of blend, five to ten specimens were tested and the average value is given. A set of 10 specimens shall be

tested. However, if the coefficient of variation (CV) (in equation 3.7) less than 5%, a minimum number of five test specimens is sufficient. All tests were done under room temperature.

$$\%\text{coefficient of variation} = \frac{\text{S. D.}}{\bar{x}} \times 100\% \qquad 3.7$$

Where S.D. is the standard deviation , $\bar{x}$ is the average of the dataset

3.3.2. Thermal Properties

Thermal property was required to be examined because the composite and hybrid composites have to be measured how physical properties of a sample change, along with temperature against time. DSC was chosen to be technic to determine thermal stability (Melting temperature (T_m), Crystallization temperature (T_c) including the degree of crystallization. This can indicate to processibility and process condition which will be used for compounding these composites. Moreover, it can examine the degree of crystallization which affect to the composite strength.

- **Differential Scanning Calorimetry (DSC)**

Differential scanning calorimeter (DSC) measurements were carried out using a DSC-60A Plus, manufactured by Shimadzu in Japan (see Figure 3.29). The samples were tested with heat, cool, heat mode. This is for eliminating the factor of heat history. The starting temperature was 40 ^oC and was raised to 200 ^oC with heating rate at 50 ^oC/min. Then it was cooled down to 40 ^oC under a nitrogen atmosphere at cooling rate of 10 ^oC/ min. Then, it was heated to 200 ^oC again with heating rate at 10 ^oC/min.

Figure 3.29: DSC-60A Plus

3.3.3. Morphological properties

The morphology of composite have to be investigated because it can indicate the composite structures, filler distribution including the interfacial adhesion between filler and polymer matrix. Therefore, the technic of scanning electron microscopy (SEM) was selected to use in this study to investigate the morphological properties in order to explain the phenomena and support the experimental results of each composite.

- **Scanning Electron Microscopy (SEM)**

SEM micrographs were obtained from TESCAN MIRA3 FEG-SEM in Figure 3.30. SEM was performed at 10.0 kV of acceleration voltage in vacuum atmosphere to investigate the surface morphology and dispersion of filler in Polypropylene matrix. The samples were prepared by from fracture areas of IZOD impact testing specimens on which 3 nm thickness of Gold-Palladium (Au/Pd) were applied by a Quorum Q150T ES which is a versatile sputter coater/turbo evaporator for preparing specimens for examination by SEM (see in the Figure 3.31).

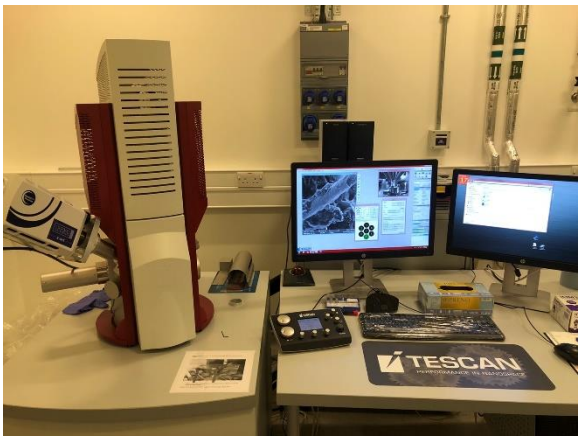

Figure 3.30: TESCAN MIRA3 FEG-SEM

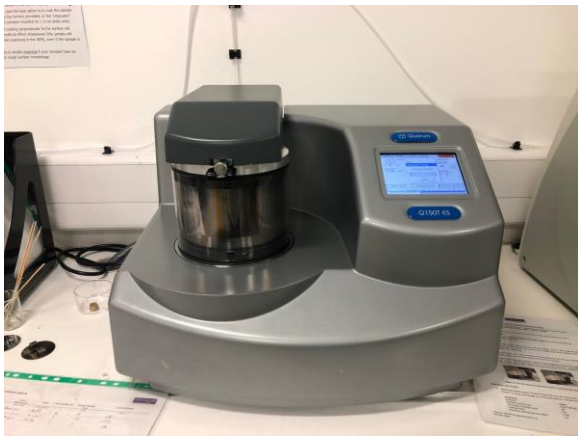

Figure 3.31: Quorum Q150T ES

3.3.4. Density

Density is the one of the important properties for composite parts which can indicate how heavy a composite material is. This can be considered whether it's suitable for manufacturing parts in any applications which may need lightweight properties ,etc. Density determinations are frequently performed by Archimedes' principle, which is also used with the density determination kit for the balances. This principle states that every solid body immersed in a

fluid apparently loses weight by an amount equal to that of the fluid it displaces [205]. The procedure for the density determination by Archimedes' principle depends on whether the density of solids or liquids has to be determined. Generally, density ρ is the quotient of the mass (*m*) and the volume (*V*), following equation 3.8

$$\rho = \frac{m}{V} \qquad 3.8$$

The international system of units specifies kg/m^3 as the unit of density. However, the unit g/cm^3 is better suited to lab purposes.

In this case determining the mass of a specimen of solid plastic was done in air. Then, the specimen is immersed in a liquid, its apparent mass upon immersion is determined, and its specific gravity (relative density) was calculated.

Fundamentally, the density of a solid is determined with the aid of a liquid whose density ρ, is known (water or ethanol are usually used as auxiliary liquids). The solid is weighed in air (A) and then in the auxiliary liquid (B). The density p can be calculated from the two weighing as follows equation 3.9.

$$\rho = \frac{A}{A-B}\,(\rho_o - \rho_L) + \rho_L \qquad 3.9$$

Where ρ is density of sample, in g/cm^3, *A* is sample weight in air , *B* is sample weight in the auxiliary liquid. ρ_o is density of the auxiliary liquid and ρ_L is the density of air (0.0012 g/cm^3). All testing specimens were extruded to get rid of the air bubbles and then they were cut into small rods. To determine the sample weight in the air, pieces of specimens have been weighted on the balance. While, the sample weight in the liquid has been conducted by putting the floating specimen (density less than 1 g/cm^3) on the basket in Figure 3.32 (b) while sinking specimens have to be put in the basket in Figure 3.32 (c). From both of sample weight in the air and in the liquid, we then calculated the density of specimen following equation 3.9. The determination of density has been conducted according to ASTM D792 [206].

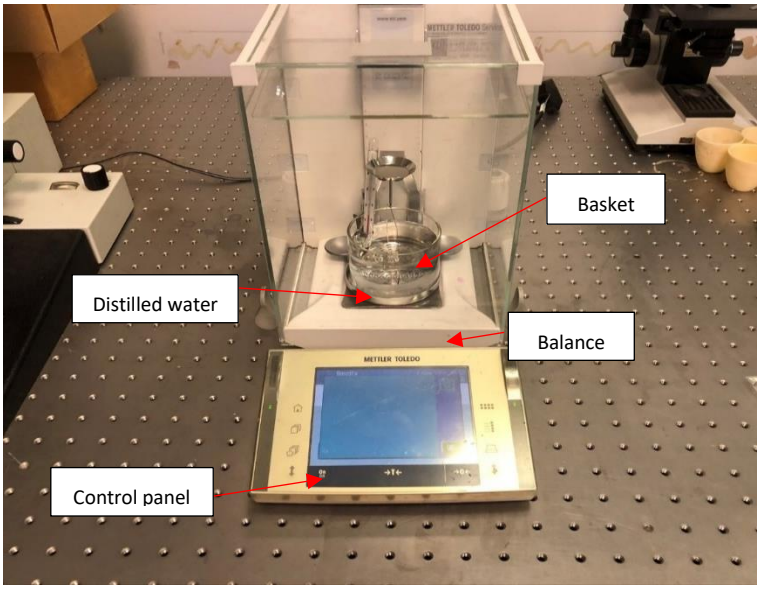

(a)

(b) (c)

Figure 3.32: (a) Density meter (b) basket for float specimen ($\rho < 1$) (c) basket for sink specimen ($\rho > 1$).

3.3.5 Melt flow index (MFI)

MFI is very important measurable property which can examine the flowability of the molten polymer. It is often used in the plastic industry in order to indicate the composite processibilty and quality control [207]. The flow characteristic of composites were determined with melt indexer according to ASTM D 1238-10 (Figure 3.33) [208]. Melt flow index was applied by using a 2.16 kg at 230 ^{o}C. The melt flow index is reported in gram per 10 minutes (g/10 min). At least five separate specimens have been tested for each formulation. The reported value has been from the average of these raw data.

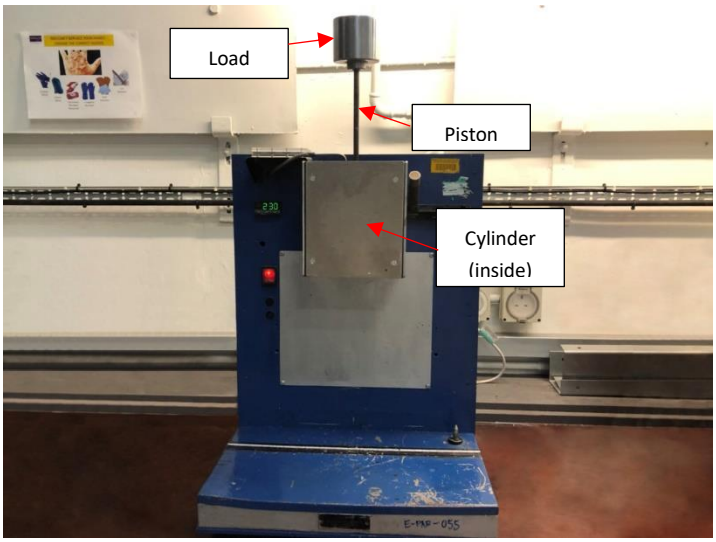

Figure 3.33: Melt flow indexer

3.3.6 Fourier Transform Infrared Spectroscopy (FTIR)

The presence of chemical functional groups of PP composites, PP hybrid composites and rPP hybrid composite due to the addition of various fillers was characterized by FTIR technique using attenuated total reflection or ATR mode (Figure 3.34). This technic was chosen to be analyzed in this study because it can indicate the chemical bonding that may be occurred from the addition of filler and compatibilizer. Moreover, the FTIR peaks were analyzed the chemical components including the chemical bonds from interfacial adhesion. The wavenumber in the analysis is in the range of 400 - 4000 cm^{-1}. The analysis was performed on the compressed film from the compression moulding machine.

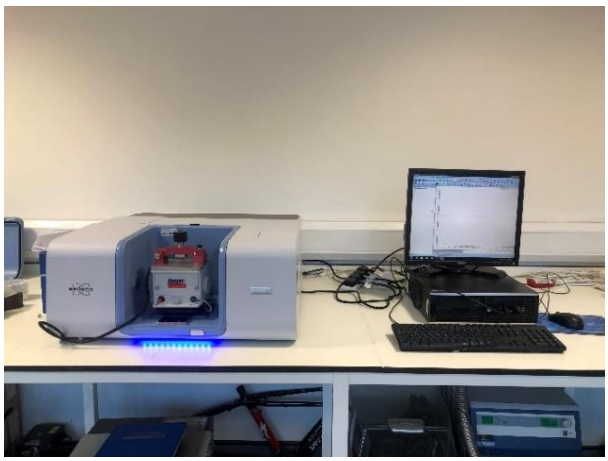

Figure 3.34: ATR FTIR spectrometer

3.3.7 Rheological measurements

Rheometer was selected to be used in this study in order to study the rheological bahaviour of composite and hybrid composites. This properties have to be investigated by comparison rheological bahaviour of composites from various types of fillers and filler content. This information can comprehend the flowability of each composite. The shear viscosity (η) of the PP composites were investigated from rotational rheometer (AR-G2 with Electrically Heated Plates) from TA instrument, USA, shown in Figure 3.35. The analysis was performed in a parallel plate rheometer on the disc specimens with a thickness of 1.00 ± 0.05 mm and a diameter of 25.00 ± 0.05 mm. Testing of the specimens were performed on both oscillation and flow mode using the rheometer. The measurement was also performed on steady shear flow mode which the shear rate was in the range of $0.1 - 10\ s^{-1}$ at 210°C to investigate the change of viscosity over the shear rates.

Figure 3.35: Rotational rheometer (AR-G2 with Electrically Heated Plates),TA instrument

The mentioned materials and methodologies would be applied in this study which aims to improve the performance of rPP to be comparable to neat PP via hybrid reinforcement systems. This project was separated into three stages of experiments which were discussed in the chapter 4, 5 and 6 as follows:

Chapter 4: Stage 1: Screening experiments for selecting the best suited fillers for hybrid composites

Chapter 5: Stage 2**:** Determination of the best formulation of neat PP based hybrid composite

Chapter 6: Stage 3: Recycled PP based hybrid composites

4. Screening experiments for selecting the best suited fillers for hybrid composites

To achieve the best possible performance of recycled PP hybrid composites, a comprehensive study will be carried out to investigate the effect of different families of fibres and filler types, as well as loading, by a number of screening tests. This chapter is focused to study the performance of candidate fillers from fibre and particle families with PP neat resin in various composites systems. These PP composites were evaluated by investigating various properties such as mechanical properties, thermal properties, rheological properties, density and MFI, morphological properties and spectroscopic properties. The experimental results were exhibited and summarized in radar charts to evaluate which candidates in each family could enhance the properties of PP and were selected as the suitable fillers for manufacturing hybrid composites discussed in chapter 5. The results obtained from these pre-screening experiments are presented as follows.

4.1 Compounding and properties of PP Composites

From the compounding of PP containing various fillers from fibre and particles families, the effect of these fillers on the processing and properties of PP was discussed in this section.

4.1.1 Compounding condition

Compounding process condition using a twin screw extruder is very important. It dictates the final mechanical performance of manufactured composites. Composites in this study were compounded by a Minilab co-rotating intermeshing twin-screw extruder (HAAKE, Germany). The screw diameter is 16 mm and the ratio of length to diameter (L/D) is 40. The maximum screw speed is 1100 rpm, maximum torque is 160 N.m and maximum pressure is 100 bar. Fillers in powder form such as calcium carbonate, kaolin, GNPs, milled carbon fibre were fed into the extruder by a gravimetric feeder (Brabender Loss-in-Weight Feeder, model DDW-MD0-MT-0.5) with twin concave screw at the feed zone (1st barrel zone). While, glass bead was fed into the extruder by a gravimetric feeder at the sixth barrel zone of extruder in order to minimize glass bead breakage [209-213]. While, raw materials in pellet or rod forms such as neat PP resins, compatibilizer (PP-g-MA), recycled PP and glass fibre were carefully manual pre-mixing before feeding into the extruder by a volumetric feeder. Since the accuracy of filler

content is very important and had to be controlled carefully, the calibration of volumetric and gravimetric feeder were required every single batch of the experiment in order to prevent and minimize the variation from feeders and different raw materials flowability.

Process condition of the extruder was established by tuning to get the best condition which can achieve the acceptable throughput and pellet properties. The barrel temperature profile was set at the range of 180 – 210 °C. The temperature profile for PP composites compounding is shown in the Table 4.1 as follows.

Table 4.1: Temperature profile for PP composite compounding

Zone No.	**Zone1** (FeedZone)	**Zone 2**	**Zone 3**	**Zone 4**	**Zone 5**	**Zone 6**	**Zone 7**	**Zone 8**	**Zone 9**	**Zone10** (Die)
Temperature (^oC)	180	190	190	210	210	210	210	210	210	180

The temperature profile of the extruder zones was established in the range of 180 - 210 ^oC which was set around 50 – 75 ^oC above the melting temperature (T_m) of semi-crystalline material [121, 195, 196]. This similar range of temperature profile were found in various PP-composite literatures [71, 84, 102, 214]. The screw speed using in this experiment, was 70 rpm with 1.8 kg/hr for throughput.

4.1.2 Sample preparations

For this study two different types of samples were prepared. Dumbbell shaped sample for tensile testing were prepared by the Minijet injection moulding from HAAKE, Germany as was explained in Section 3.2.4 The temperature of barrel and mould were set at 210 °C and 45 °C, respectively. The molten composites were injected and flowed into the mould with the pressure of 250 bars in 10 seconds and then the pressure of machine was hold at 100 bars for 5 seconds to compensate the effect of shrinkage. The processing conditions used are shown in the Table 4.2.

Table 4.2: Processing parameters used with Minijet for the preparation of tensile specimens

Barrel temperature	**Mould temperature**	**Injection step**		**Holding step**	
(^oC)	**(^oC)**	**Pressure (bar)**	**Time (s)**	**Pressure (bar)**	**Time (s)**
210	45	250	10	100	5

In case of the specimens for flexural and Izod impact testing following ISO178 [201] and ISO180 [202], specimens have to be prepared by injection moulding from Negri Bossi from

Italy was used for preparing the specimens for flexural and impact testing. The processing condition of injection moulding of Negri Bossi is shown in the Table 4.3.

Table 4.3: Processing condition parameter of Negri Bossi

Barrel temperature (°C)	Injection Pressure (bar)	Holding step	
		Pressure (bar)	Time (s)
210 – 210 – 210 - 210	42	15	15

4.2 Characterization of PP composites

The experiments in this section were focused on the study of reinforcing performances of candidate fillers from fibre and particle families with PP neat resin. These PP composites were promoted interfacial adhesion by the addition of compatibilizers and treated fillers see in the Table 3.7 in Chapter 3. PP-g-MA was added as coupling agents to PP/glass bead, PP/kaolin and PP/GNPs, PP/glass fibre and PP/carbon fibre composites while PP/$CaCO_3$ were prepared by the addition of coated with fatty acid was used as the filler for PP/$CaCO_3$ composite. This idea has been supported from various studies on polymer composites [52, 77, 78, 108, 155, 180, 185, 215-220]. The formulations of composites in this chapter were mentioned in Table 3.7 in Chapter 3.

To evaluate the performance of PP based composites from various fillers by various characterization techniques such as morphological analysis by SEM, spectroscopic properties by FTIR, rheology test, mechanical properties (tensile, flexural modulus and Izod impact strength), MFI, density and thermal properties were carried out.

4.2.1 Morphological properties

SEM is high solution imaging technique which is wildly used to investigate the microstructure of materials. This technique can be used to investigate filler dispersion, size of fillers in composites. The V-notched Izod impact-fractured surface of PP composites containing 10 wt% and 30 wt% were selected as the representatives of low and high filler content for each PP composites to investigate morphological properties in comparison with neat PP.

As shown in Figure 4.1 (a), the fractured surface of Izod impact specimen of unfilled PP was wavy and arranged regularly and perpendicular to the impact direction. This means that the crack propagated toward the cross section in wavy pattern until complete fracture of the specimen under the impact load. This phenomenon was supported from the earlier work by Liang et al. [102].

Figure 4.1(b), (c) and 4.2 (a),(b) showed the micrographs of the fracture surfaces of Izod sample of PP composites filled with 10 and 30 wt% of $CaCO_3$. From SEM image of the PP/$CaCO_3$ composite with 10 wt% in Figure 4.1 (b), it was obvious that the dispersion of $CaCO_3$ was relatively good, only a few agglomerates existed and the interfacial interaction between particles and matrix was strong. It can be seen highly dispersed particles and the strong interfacial interaction between nanoparticles and matrix [89]. While the SEM image of PP/$CaCO_3$ at 30 wt% in the red circled area in Figure 4.1 (c) shows many agglomerates which presented in the matrix composites. In the red circled area in Figure 4.2 (b), the crack of specimen occurred at the position of large agglomerates which acted as site of crack initiation. These led to brittle fracture because their large size and sharp edges. This result can be supported by Thio et al. [82].

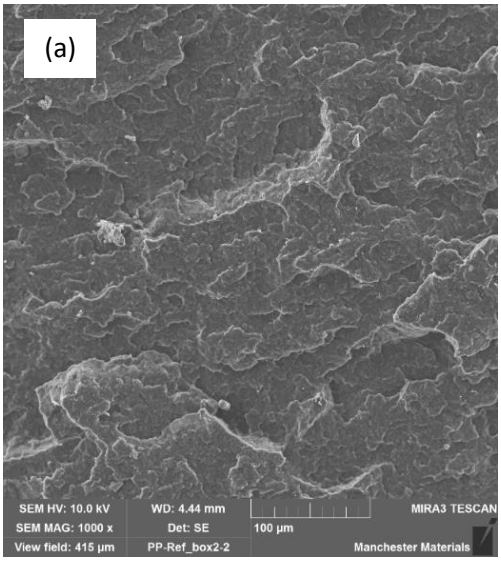

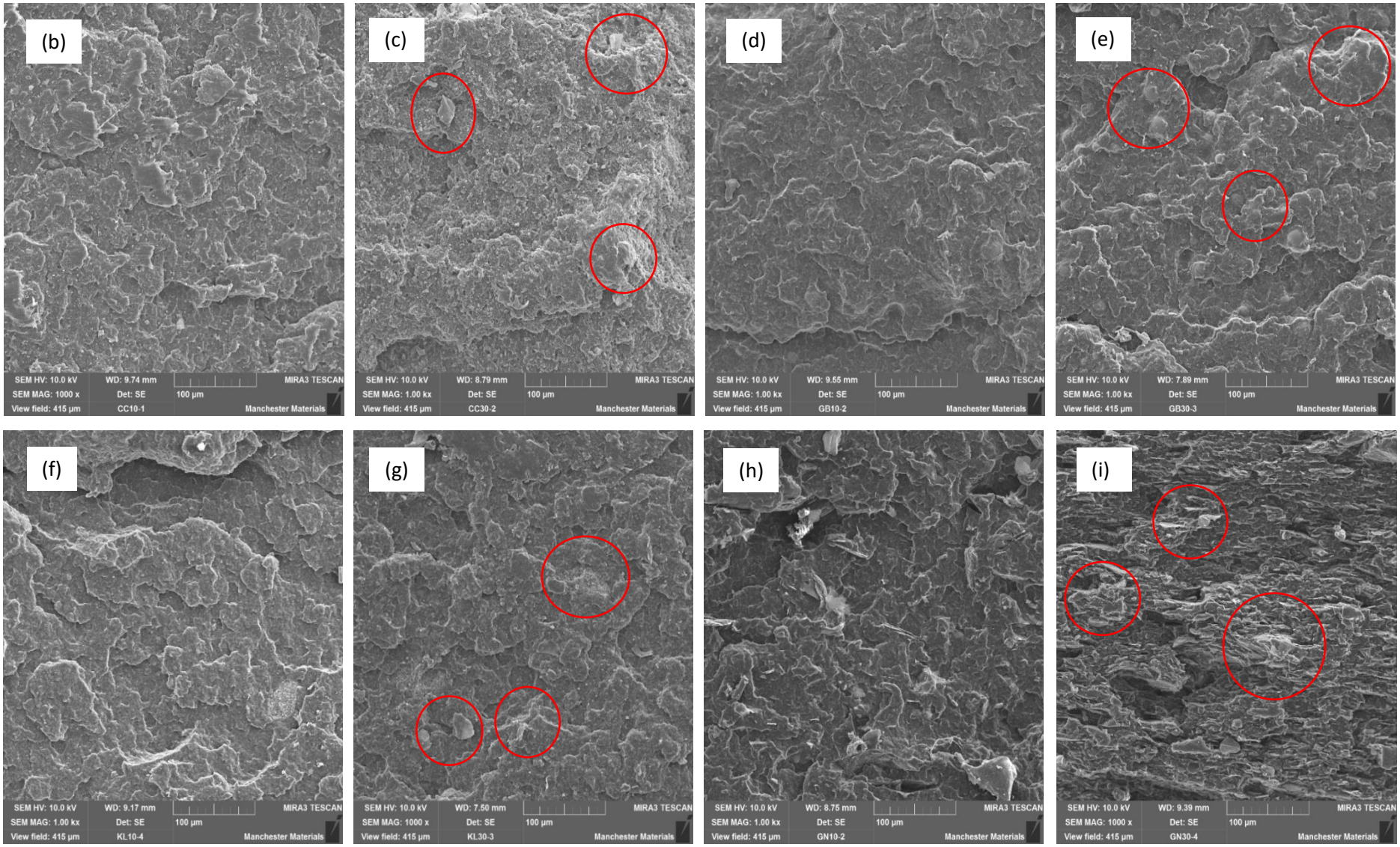

Figure 4.1: The SEM micrographs at 1000x of (a) neat PP (b) PP/CC10 (c) PP/CC30 (d) PP/GB10 (e) PP/GB30 (f) PP/KL10 (g) PP/KL30 (h) PP/GN10 (i) PP/GN30

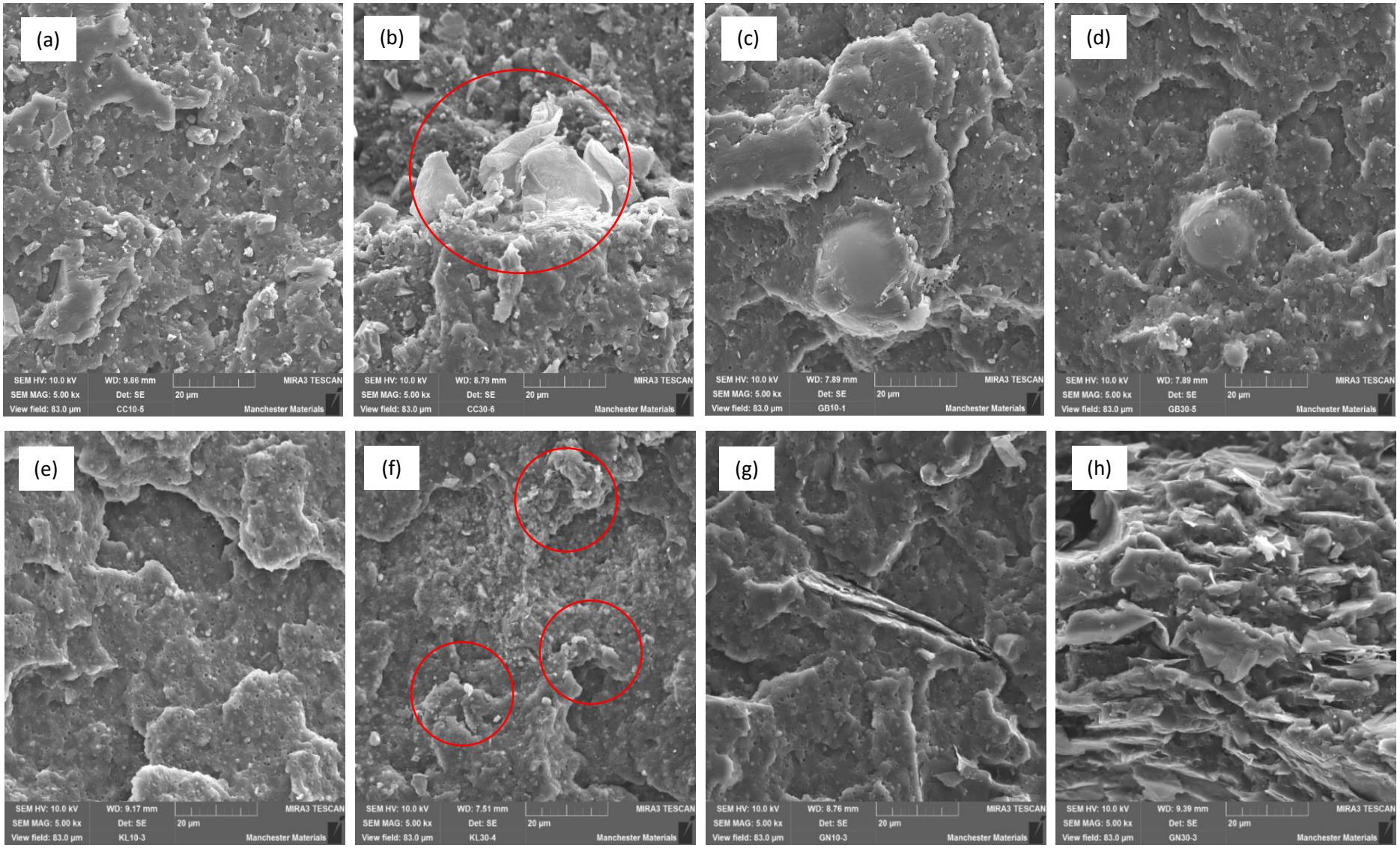

Figure 4.2: The SEM micrographs at 5000x of (a) PP/CC10 (b) PP/CC30 (c) PP/GB10 (d) PP/GB30 (e) PP/KL10 (f) PP/KL30 (g) PP/GN10 (h) PP/GN30

From the micrograph of PP/glass bead composite, it can be notable the adhesion between surface of glass beads and PP matrix. These can be indicated good interfacial adhesion from the incorporation of PP-g-MA. The impact load could be transferred effectively. For PP/glass bead 10 wt% in the Figure 4.1 (d), it can be seen that the dispersion of the glass beads in the PP matrix was not dense in the matrix and quite uniform. The fracture surface was not so smooth. However, it can be observed that there was a slight aggregation in PP/glass beads at 30 wt% which is shown in the red circled area in Figure 4.1 (e). This can be indicated the macroscopic stress cracks from the agglomerations in the Figure 4.2(d).

From the SEM images of PP/kaolin 10 wt% in Figure 4.1 (f), it can be observed that the homogenous dispersion of kaolin in the matrix. There was very few visible kaolin agglomeration. This led to good strength and rigidity of PP/kaolin composite. The surface was smooth which can be indicated the brittle fracture behaviour. Previous study by Ariffin et al. [96] reported similar results for this occurrence. Good dispersion can be achieved from the addition of PP-g-MA as compatibilizer. The coupling effect of PP-g-MA between filler and matrix led to the enhancement of adhesion between kaolin and PP. This can cause the higher modulus and strength. However, the red circled area in Figure 4.1 (g) exhibits the distribution of kaolin in the composite of PP/kaolin 30 wt% was quite not uniform. Some filler agglomerations were found in the micrograph in red circled areas in Figure 4.2 (f). This was possible that the agglomerations of kaolin with sharp corner are the point of stress concentration [95].

SEM micrograph in Figure 4.1 (h) which is fractured surface of PP/GNPs composite with 10 wt% GNPs shows that the dispersion of the GNPs in the matrix was quite uniform. The fractured surface was rough and the small agglomeration of GNPs was observed. However, the large agglomerations of GNPs was found in the SEM image in Figure 4.2 (h). The undispersed GNPs agglomerates were detected in the fractured area of PP/GNPs composite with 30 wt% GNPs which shows in the red circled area in Figure 4.1 (i) [113].

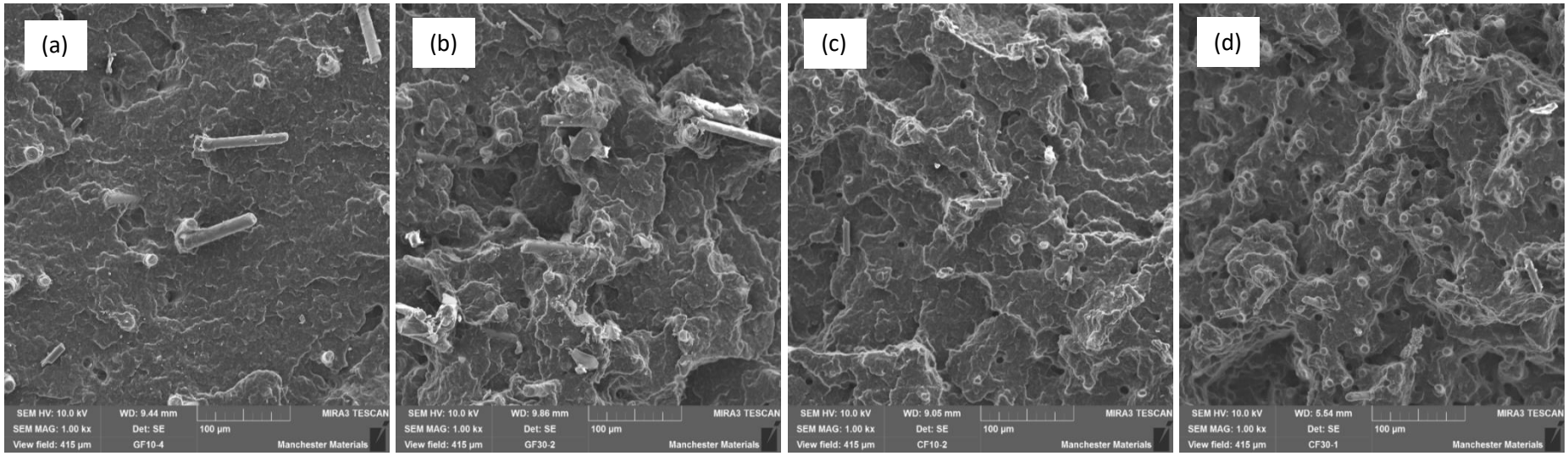

Figure 4.3: The SEM micrographs at 1000x of (a) PP/GF10 (b) PP/GF30 (c) PP/CF10 (d) PP/CF30

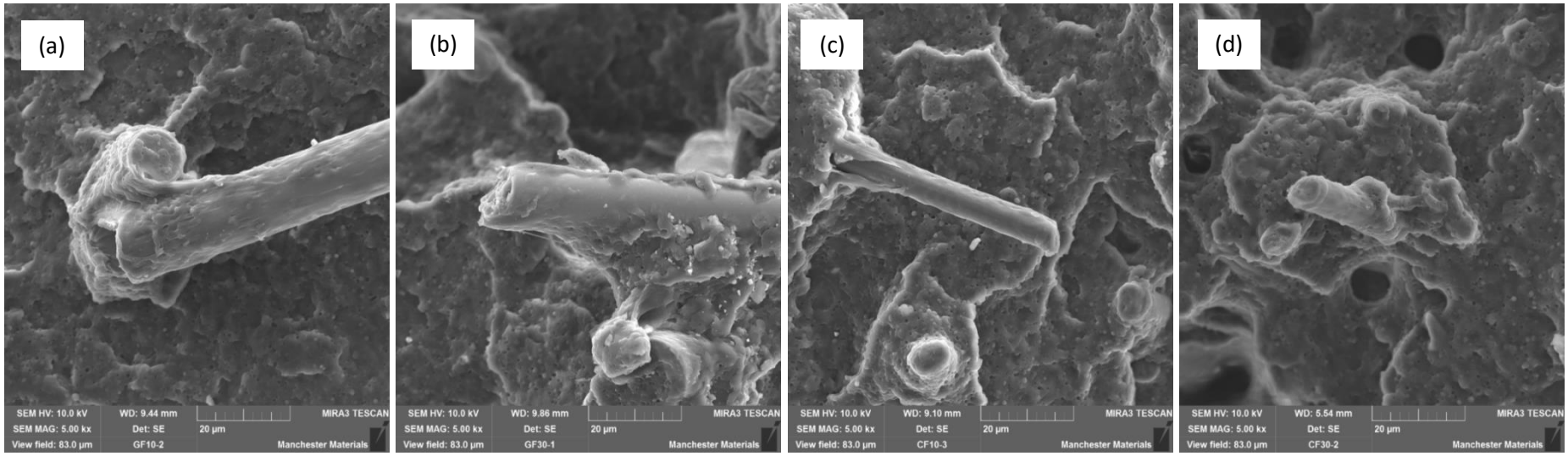

Figure 4.4: The SEM micrographs at 5000x of (a) PP/GF10 (b) PP/GF30 (c) PP/CF10 (d) PP/CF30

Regarding to SEM images in Figure 4.3 (a), (b) and 4.4 (a), (b), it can be found that the fractured glass fibre has rough surface from the surrounded polymer at the fibres. There is no visible splitting between the glass and the polymer. These can be indicated the strong adhesion between glass fibre and PP matrix from the compatibilizer (PP-g-MA) [63, 68]. The strong interfacial adhesion can be from the addition of glass fibres were treated with an amino silane coupling agent. The amino group could react with maleic anhydride groups and became grafted onto PP-g-MA chains to form chemical bonds. Meanwhile, the silane coupling agent also contained hydroxyl groups and could bond to the glass fibre [68]. At the surface of samples, the fibres were found which were evenly distributed on the composite matrix. Once the fracture of these fibres occurs, the fibres were broken into short fibres. This results can be supported with the previous literature by Etcheverry et al. [63].

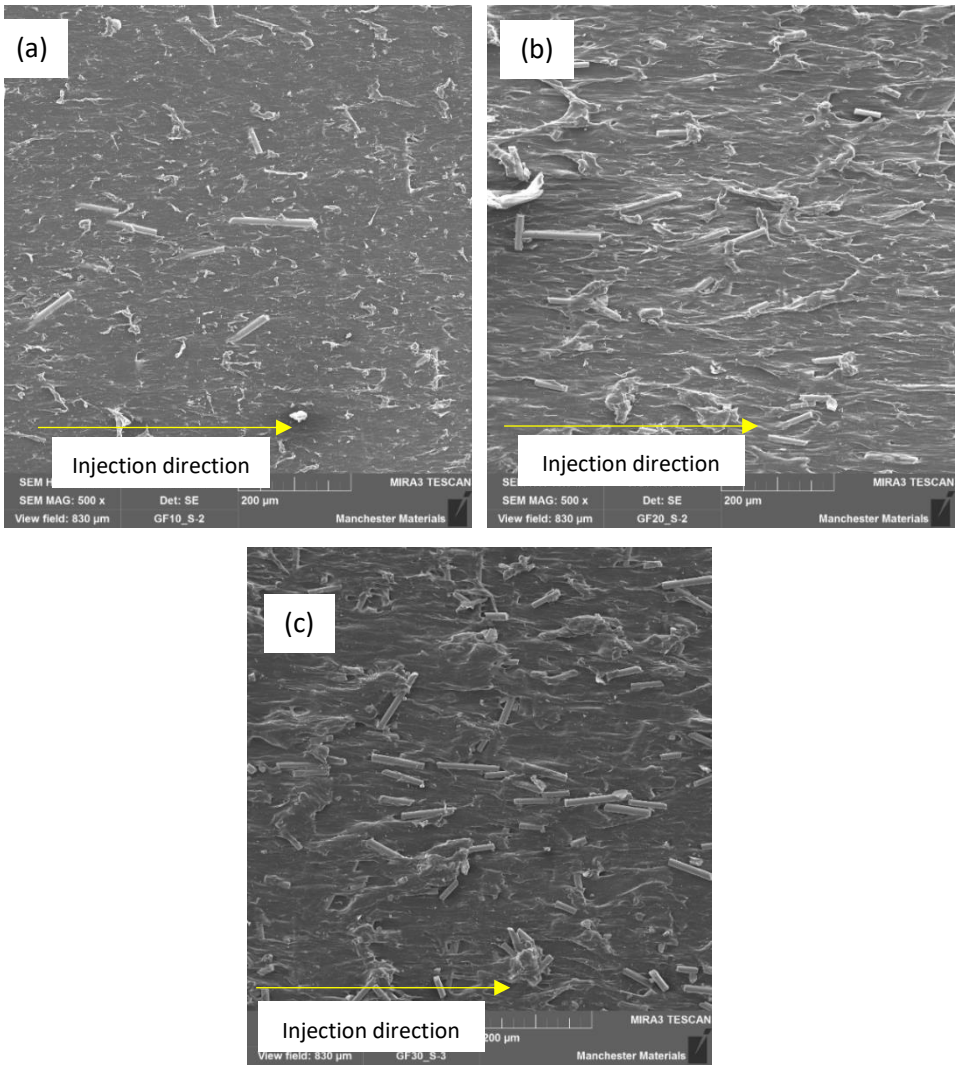

Figure 4.5: The SEM micrographs at 500x of the surface of injection moulding specimens of (a) PP/GF10 (b) PP/GF20 (c) PP/GF30

Furthermore, the surface of injection specimens of PP/glass fibre composites at 10 wt%, 20 wt% and 30 wt% were investigated. From the SEM images shown in Figure 4.3 (a),(b) and (c), it can be seen that the most of glass fibres were oriented in the direction of injection force. The distribution of glass fibre were quite good and the density of glass fibres in the polymer matrix depended on the fibre loading.

Figure 4.3 (c) and 4.4 (c) displays the polymer and composite fracture surfaces of PP/carbon fibre composites. These were observed the uniformly dispersion in the PP and no obvious agglomerations were found in PP filled with carbon fibre 10 wt%. Moreover, it can be see the polymer wrapped at the fibre which indicate a good adhesion. However, there are some pull-out carbon fibre which were found on the matrix of composite fractured surface for PP/carbon fibre 30 wt% composite in Figure 4.3 (d) and 4.4 (d). This can be attributed to the poor interfacial adhesion between carbon fibre and PP [73]. This defective areas attributed to carbon fibre debonding of the PP composites. Carbon fibres were distributed randomly at the higher carbon fibre loading and the number of voids distributed around the fibres and PP matrix. This phenomena was similar to the previous study by Pérez-Rocha et al. [71].

4.2.2 Spectroscopic property

To indicate the presence of fillers in the PP composites, infrared spectroscopy technique was used in order to identify each functional group by referring from the difference in vibrational energy absorption. These detected functional groups can indicate the existence of filler and chemical bonding in PP matrix.

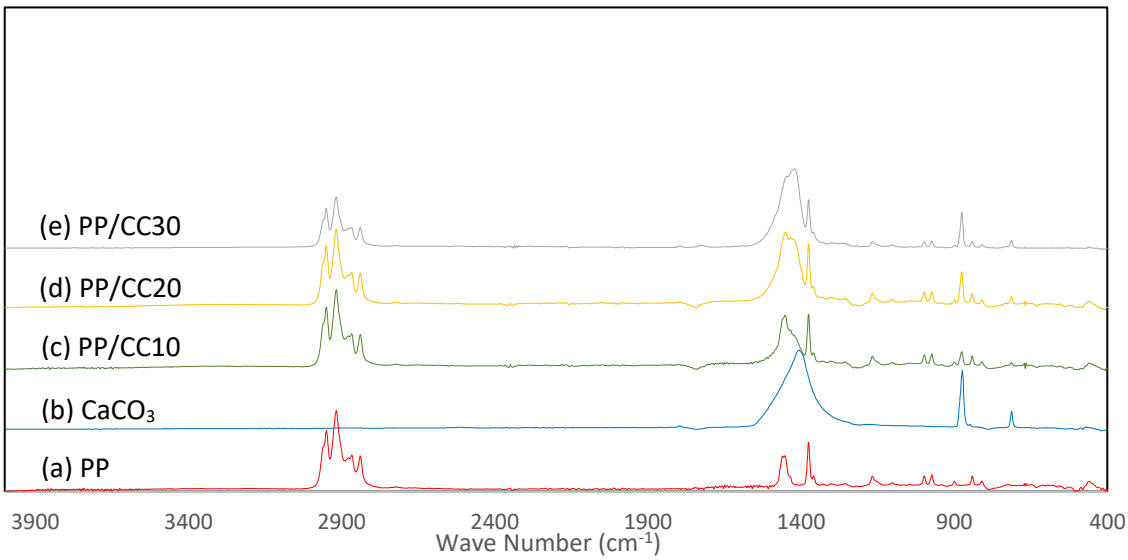

Figure 4.6: ATR-FTIR spectra of PP, $CaCO_3$ and PP/$CaCO_3$ composites

The IR spectra of PP, $CaCO_3$ and PP/$CaCO_3$ composites have been displayed in the Figure 4.6. The spectrum of $CaCO_3$ was appeared the characteristic absorption band at around 1,400 cm^{-1} and narrow band around 853 cm^{-1} which are characteristics of C-O stretching mode and bending mode of carbonate [221-223]. The spectra of the PP/$CaCO_3$ composites in Figure 4.6 (c), (d) and (e) displays the characteristic absorption bands around 1,420, 850 and 712 cm^{-1} could be indicated to vibrations of calcite structure in $CaCO_3$ [222]. In addition, the C-O stretching vibration band was more clearly seen at higher $CaCO_3$ content.

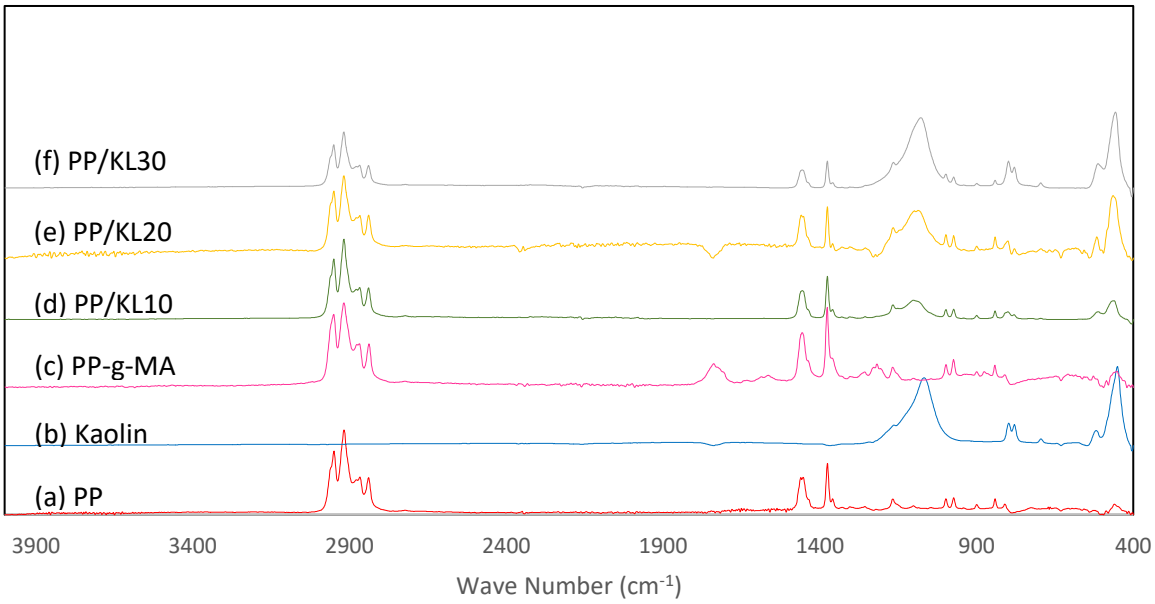

Figure 4.7: ATR-FTIR spectra of PP, kaolin, PP-g-MA, and PP/kaolin composites

In FTIR spectrum was shown in the Figure 4.7, it can be verified the presence of kaolin in PP/kaolin composites, the characteristic absorption bands of kaolin were identified. The peak around 1,030 – 1,070 cm^{-1} indicated the Si-O stretching vibration. The characteristic of Si-O groups can be identified from absorption band around 450 – 500 cm^{-1} [224]. Moreover, this peaks were more clearly seen at higher kaolin content. There are various peaks to indicate the characteristic of kaolin which are the absorption bands between 770 and 790 cm^{-1} corresponding to frequencies of Si-O-Al groups [224].

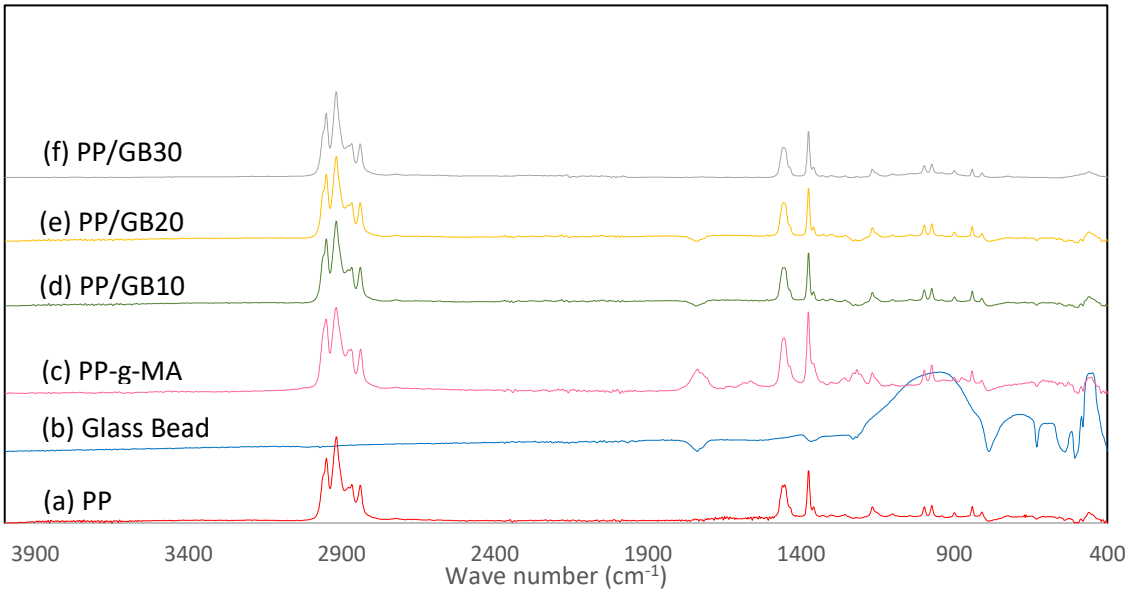

Figure 4.8: ATR-FTIR spectra of PP, Glass bead, PP-g-MA, and PP/glass bead composites

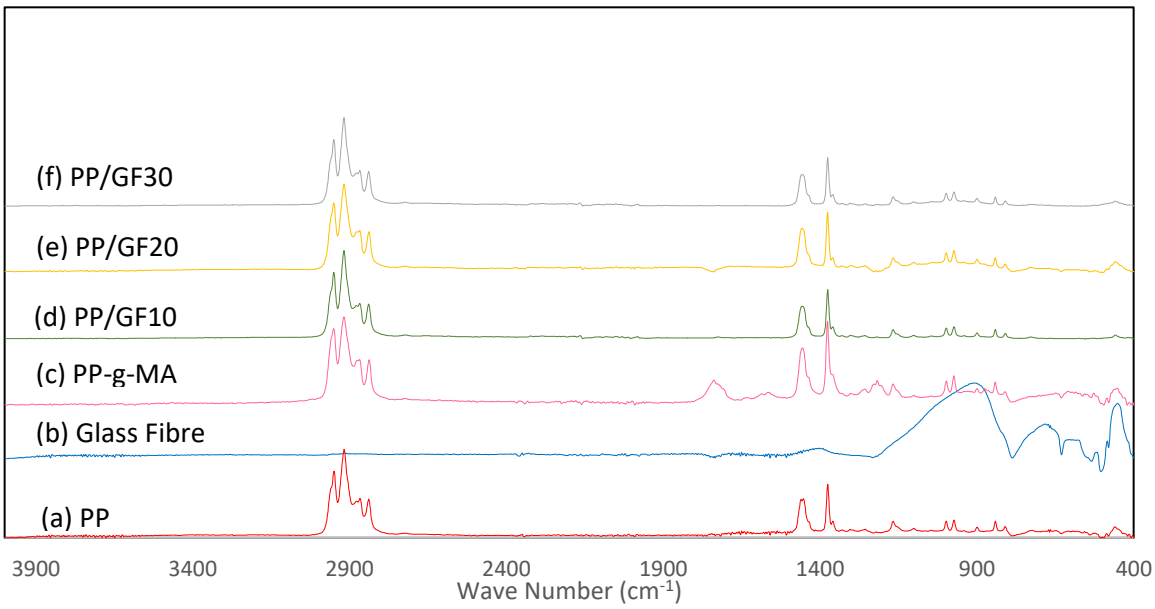

Figure 4.9: ATR-FTIR spectra of PP, Glass Fibre, PP-g-MA, and PP/glass fibre composites

Regarding to the one of limitations of ATR-FTIR technique is a relatively low sensitivity [225], so the FTIR spectrum of composites from Glass bead and glass fibre in the Figure 4.8 and 4.9 which have the similar structure has been unclearly identified. From the thorough consideration, it can be noticeable that the peak around 430 – 450 and 760 – 1200 cm^{-1} of PP/glass bead and PP/glass fibre composites in Figure 4.8 (d, e, f) and Figure 4.9 (d, e, f) are a bit boarder than neat PP. The peak around 430 – 450 cm^{-1} peaks are referred to (O-Si-O) bending vibrations mode, while peak around 760 – 1,200 cm^{-1} can be indicated to (Si-O)

asymmetric stretching and Si-O (in the SiO_4 tetrahedron) which are the structure of glass bead and glass fibre [226]. However, this technique may be not indicated clearly the existence of glass bead and glass fibre. SEM can be more suitable to analyze the structure and evaluate the presence of these fillers**.**

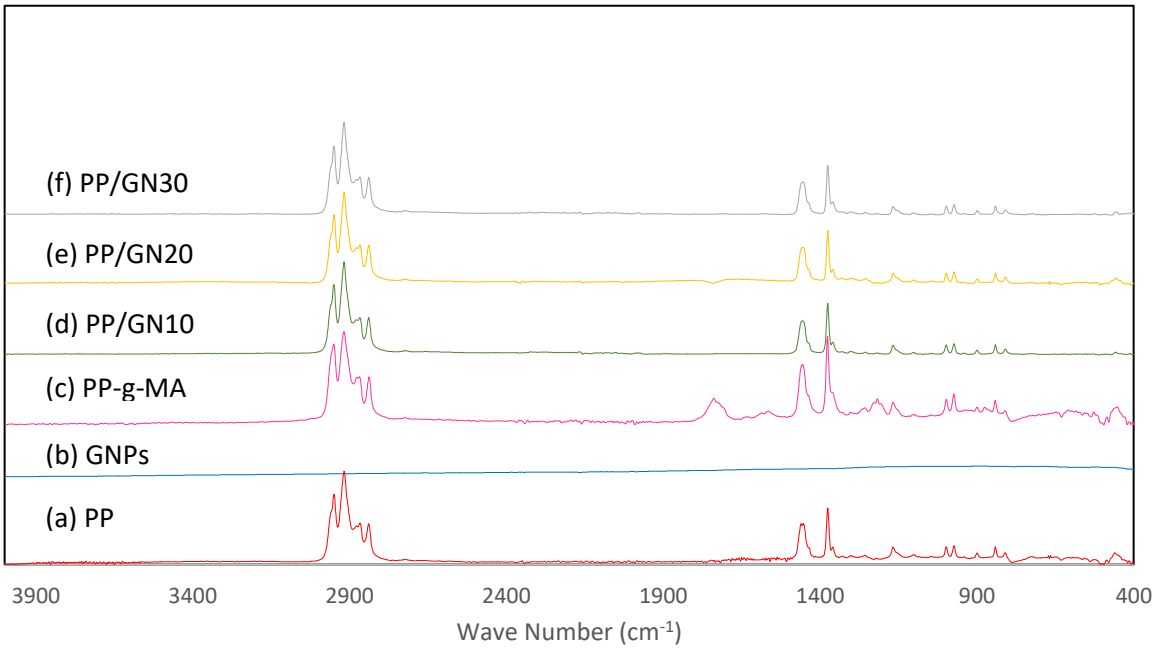

Figure 4.10: ATR-FTIR spectra of PP, GNPs, PP-g-MA, and PP/GNPs composites

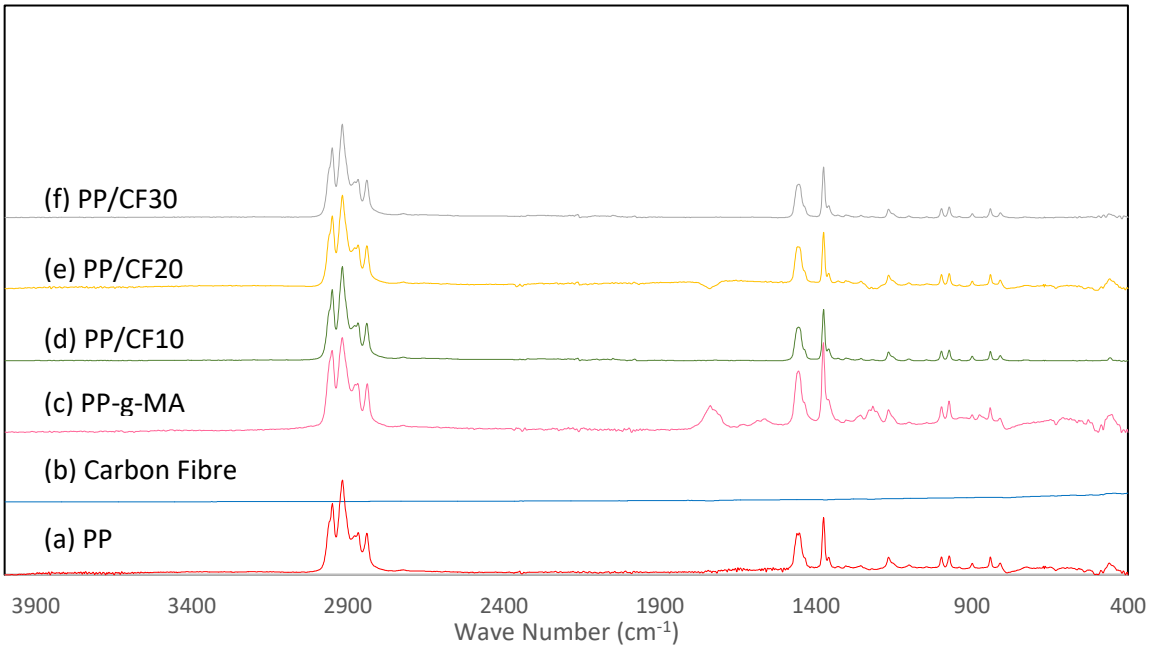

Figure 4.11: FTIR spectra of PP, carbon fibre, PP-g-MA, and PP/carbon fibre composites

From the ATR-FTIR spectra of PP/GNPs in Figure 4.10, there is no visible peaks were appeared in the spectrum of GNPs powder in Figure 4.10(b) indicating the absence of any functional groups. This supported the findings of the studies of Geng et al., Inuwa et al. and Patole et al. [180, 227, 228]. The result can be confirmed the purity of GNPs which has been used in this study. Moreover, it can be also seen that there are very few functional groups present in the FTIR spectra of carbon fibre in Figure 4.11(b). This is due to the very high absorbance of carbon fibre products which was supported by the investigation of Li et al. [229].

From the ATR-FTIR spectra of PP composites were mentioned, the important chemical functional groups are shown in the Table 4.4.

Table 4.4: Wavenumber and assignment of the major IR band of PP composites

Wave number (cm^{-1})	Major functional group
430 – 450	O-Si-O bending vibrations mode [224, 226]
450 – 500	Si-O groups [224]
712, 874 and 1420	vibrations of calcite [222]
760 – 1200	Si-O asymmetric stretching Si-O in the SiO_4 tetrahedron [226]
770 and 790	Si-O-Al groups [224]
853 – 873	C-O bending mode of carbonate [221, 222]
1030 – 1070	Si-O stretching vibration [224]
1400 – 1453	C-O stretching mode of carbonate [221, 222]

4.2.4 Rheological behaviour

From the shear viscosity curve that was obtained from rotational rheometer, the samples of PP based composites were selected for rheology analysis on steady shear flow mode which the shear rate was in range of 0.1 – 10 s^{-1} at 210 ^{o}C to investigate the change of viscosity over the shear rates. In this stage, PP composites from glass bead, kaolin and glass fibre were selected to conduct the rheology analysis. The viscosity curve are shown in the Figure 4.12.

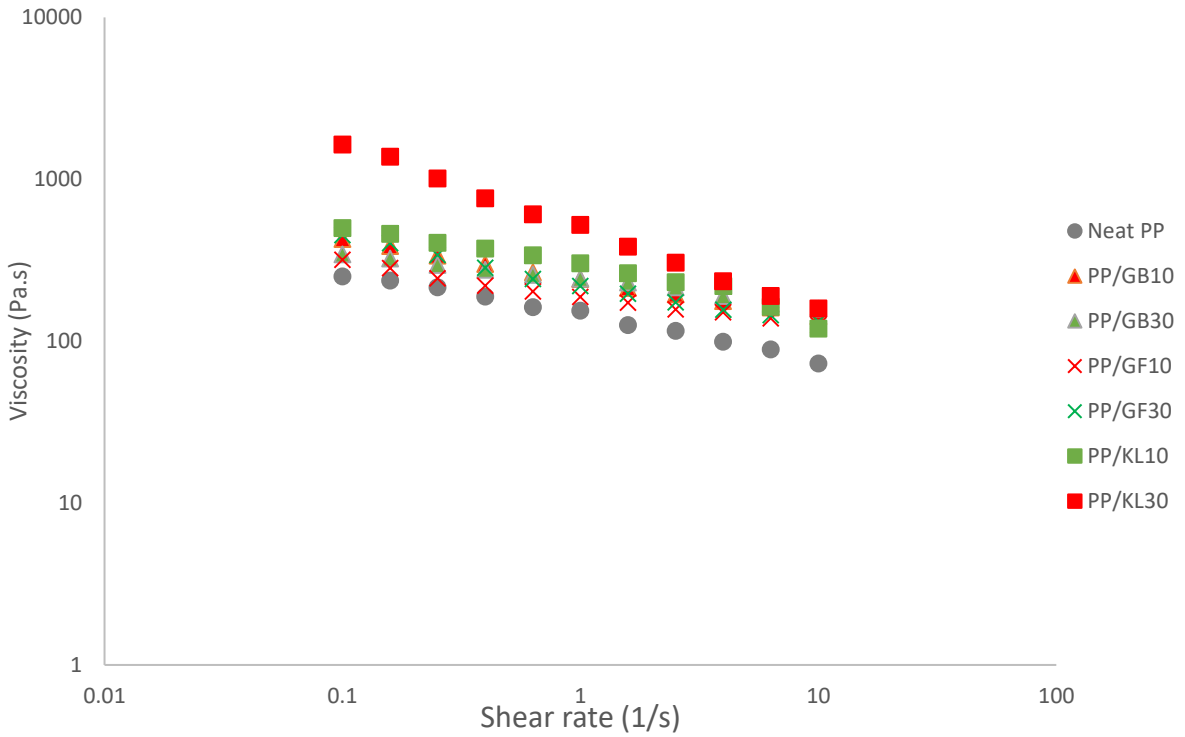

Figure 4.12: Viscosity curves of neat PP, PP composites with 10 wt% and 30 wt% of glass bead, kaolin and glass fibre

From the Figure 4.12, it can be seen that the viscosity of all samples from neat PP and PP composites decreased as the shear rate increases. This can be further noted that the shear thinning behaviour of the materials [230]. All of selected PP composites were more viscous than neat PP due to the incorporation of fillers. For PP/glass fibre composites, it can be seen that composites at 30 wt% of glass fibre had higher viscosity than 10 wt% due to the restriction of the polymer chain motion by the entanglements of glass fibres obstruct polymer chain mobility [231, 232]. The results for these polymers show similarities in the same trends with PP/kaolin composite. The viscosity of PP/kaolin increased with the addition of higher kaolin content [233, 234]. As the kaolin loading increased, the PP chain mobility were affected by the overloading of kaolin particles in the system which perturb the normal flow and hinder the mobility of chain segments in melt flow, consequently increasing the value of the apparent viscosity [233]. In case of PP/glass bead composite, it can be observed that the viscosity of PP/glass bead did not drop as much as PP/glass fibre and kaolin composite due to the morphology of glass bead which is sphere and did not affect to flowability of polymer molten steam [230, 235].

4.2.5 Melt flow index

MFI is measurement which determine how well the materials flows in a certain temperature and shear rate. It can be considered as an indicator of the flowability of the thermoplastic materials. In thermoplastic industry, MFI is an important parameter that is widely used to characterize the flow property of resins due to its easy measurement [230]. The MFI value was obtained follow ASTM D 1238-10 standard. MFI was generally applied by using a 2.16 kg at 230 ^{o}C for PP. The MFI is reported in gram per 10 minutes (g/10 min) [48]. The MFI of neat PP, extruded PP (ext-PP) and PP bases composites are shown in Figure 4.13, Table C.1 in Appendix C.

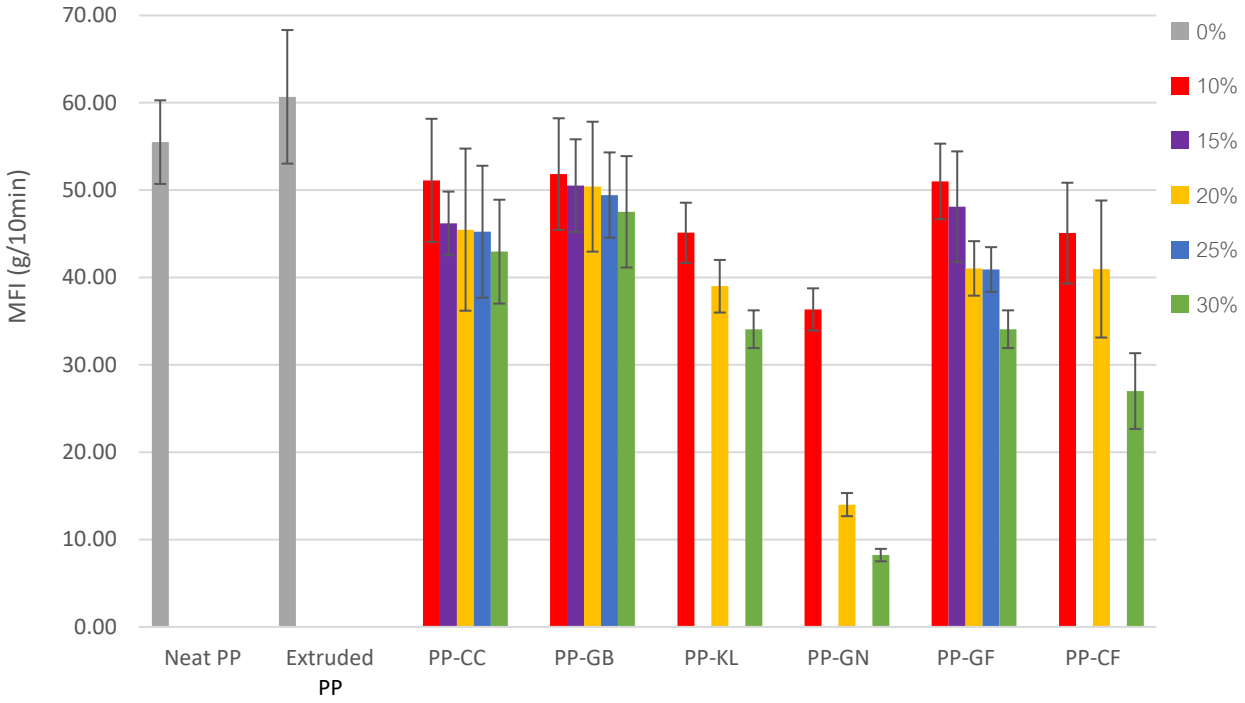

Figure 4.13: Measured MFI of neat PP, extruded PP and PP based composites

The neat PP grade P739ET from SCG chemicals was selected to use in this study due to its high MFI which is 55.5 g/10 min. This allows it to achieve good flow characteristics and shorter cycle time which is suitable for injection moulding application. From the Figure 4.13, it can be observed that MFI of extruded PP which was from neat PP increased from 55.5 g/10min to 60.7 g/10 min. The change indicated a decrease of viscosity and molecular weight of neat PP [50]. The result indicates that PP structure can be destroyed due to chain scissions mechanisms of PP, caused by a thermo mechanical degradation during extrusion process [50, 236-242]. This degradation can reduce the mass average molecular weight. Entanglements

and intermolecular interactions decrease with decreasing chain length and molecular weight, increasing the mobility of the polymer chains and their ability to slide past each other. The decrease in forces between the chains could be seen in the increase of MFI and resulting the polymer viscosity decreases [48, 50, 161].

The addition of fillers leads to a subsequent decrease in MFI. For the measurement of MFI of PP based composites, it can be seen that the MFI value decrease when increasing filler content. That means the viscosity of PP composites increased as results of high content of the filler. This result supports evidence from previous observations [152, 232, 237, 243]. This is because the incorporation of rigid fillers to limit the molecular mobility or agglomerations hinders melt flow of PP and increase the viscosity of PP composites at the melt stage. Furthermore, it can be seen that PP/GNPs had a huge drop when increasing GNPs content due to significant agglomeration from the large aspect ratio of GNPs, which reduced lubricating capability and increased viscosity [181, 243, 244]. On the other hand, the MFI values of PP/glass bead composite were changed slightly which can be supported by the previous research [230]. This is due to the spherical shape of glass bead which act like tiny ball bearing. This can lubricate the overall composite flow or viscosity characteristics at the higher fibre loading [235].

4.2.6 Thermal stability

The differential scanning calorimetry (DSC) thermograms of the samples of neat PP and composite at 30 wt% of fillers were selected as the representatives of each composites shown in the Appendix C. The values of crystallization temperature (T_c), the melting temperature (T_m), melting transition enthalpy (ΔH_m) and crystallization enthalpy (ΔH_c) were calculated from the DSC curves. The results are summarized in Table 4.5.

Table 4.5: DSC-determined thermal characteristics of PP composites

Sample	T_c (°C)	ΔH_c(J/g)	T_m (°C)	ΔH_m(J/g)
Neat PP	113.9	93.9	163.0	78.3
PP/CC30	116.2	68.8	161.3	48.6
PP/GB30	118.7	69.4	162.7	57.9
PP/KL30	122.3	69.4	164.9	58.9
PP/GN30	126.1	78.2	163.2	69.9
PP/GF30	116.4	65.2	161.8	42.6
PP/CF30	120.0	72.7	161.0	60.5

As seen from the Table 4.5, there was no significant difference in the melting temperature (T_m) of neat PP and PP composites. $CaCO_3$, glass bead, kaolin, GNPs, glass fibre and carbon fibre PP composites. This can be implied that fillers in composites have no significant effect to melting temperature of materials. However, the consideration of the peak crystallization temperatures (T_c) during the cooling scan were shown in the Table 4.4. This can be shown that the crystallization exotherm of PP composites were higher than neat PP. The crystallization temperature of PP increased by 2.3°C, 4.8 °C , 8.4 °C, 12.2 °C, 2.5 °C and 6.1 °C with 30 wt% of PP/$CaCO_3$, PP/glass bead, PP/kaolin, PP/GNPs, PP/glass fibre and PP/carbon fibre composites, respectively. This shows the significant increasing T_c of PP composites from kaolin, glass bead, GNPs and carbon fibre. This is because these fillers can act as nucleating agent and induce crystallization at higher temperature than virgin PP [73, 147, 152]. This is because GNPs with large aspect ratio can easier hinders polymer chain mobility which can limit the formation of crystal. It can decelerate the crystallization of PP [108].

4.2.7 Mechanical properties

4.2.7.1 Tensile properties

The results of tensile strength at yield, tensile strength at break and tensile modulus were tested follow ISO 527 [199]. At least five specimens from each formulation were tested. Normally, tensile test is used to determine how materials will behave under tension load and the results of tensile properties have been shown in the Figure 4.12. Tensile data are also shown Table C.2 in Appendix C.

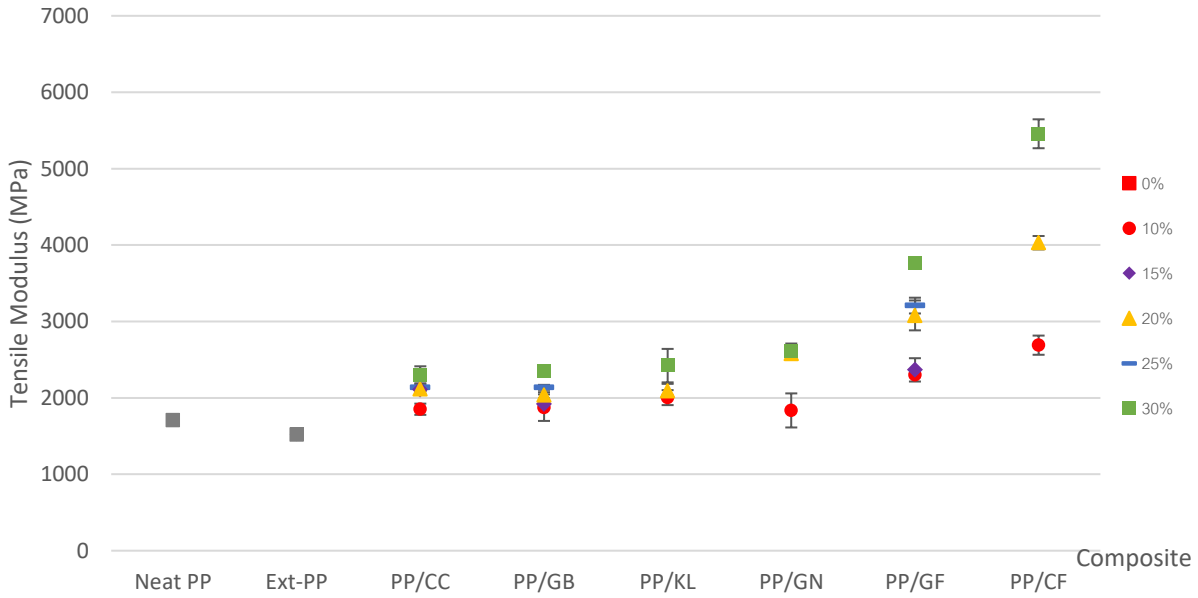

Figure 4.14: Tensile modulus of neat PP, extruded PP and PP based composites

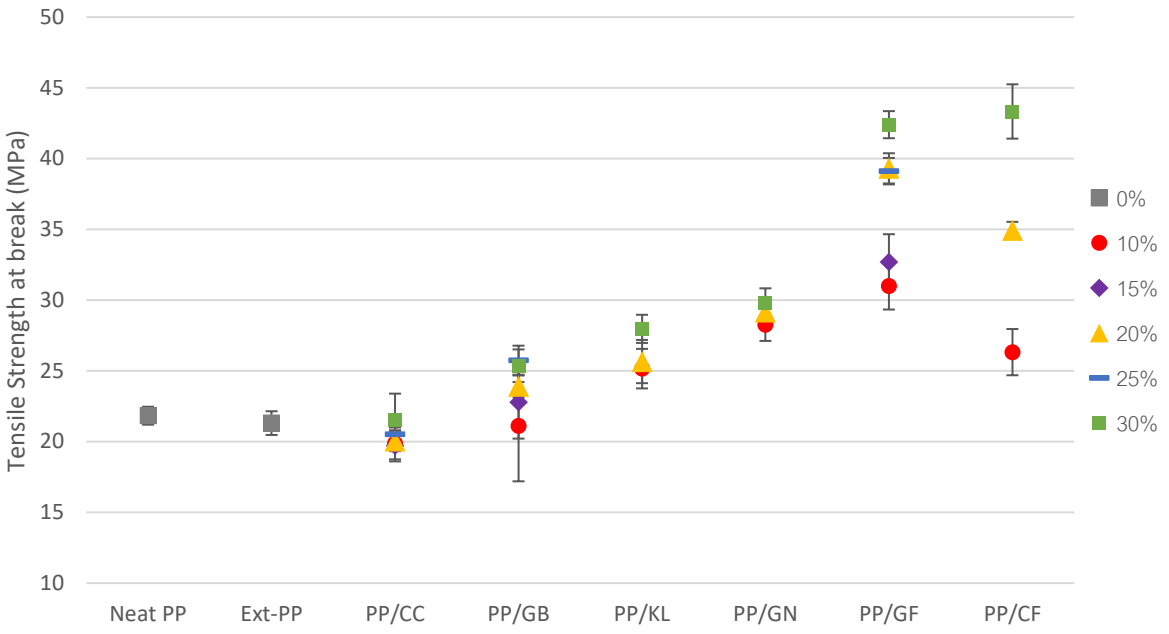

Figure 4.15: Tensile strength at break of neat PP, extruded PP and PP based composites

From the Figure 4.14 and 4.15 represent the tensile modulus and tensile strength at break of PP composites with different amount of fillers. It can be seen that the tensile modulus of neat PP (P739ET) was higher almost 10 % compared to extruded PP. The main reason of the reduction of the modulus is the polymer chain scission from thermal degradation in process. It led to the decrease of the entanglement of the molecular network and intermolecular interactions between the crystalline phase and the amorphous phase which contribute to the decrease of the lamellae thickness. This result is also supported by the previous literatures [50, 237, 238, 245].

From particle family, composites from the addition of $CaCO_3$, glass bead, kaolin and GNPs have been evaluated. The common problem that frequently found is poor interfacial adhesion between the filler surface and the matrix. It is another factor that affects tensile modulus. In case of kaolin added polymer composites, the characteristic of kaolin which has highly polar hydrophilic surfaces, whereas the polymer (such as PP, PE, etc) are non-polar and hydrophobic. This is quite difficult to achieve uniform dispersion of filler. The poor interaction between filler and polymer matrix has strong tendency of large agglomeration which can influence to the mechanical of finished materials [216]. From this limitation of the poor interfacial adhesion between filler and polymer matrix, the addition PP-g-MA as the compatibiliser has been applied in this research to promote the interfacial adhesion between

polymer matrix and some fillers in this project. This is due to the formation of covalent linkages and hydrogen bonds between the maleic anhydride and the functional groups on fillers [216]. There are a number of similar investigations on better mechanical properties of composited adding PP-g-MA have been reported in many literatures [52, 77, 78, 108, 155, 180, 185, 215-220]. However, PP-g-MA may be not the most suitable adhesion promoter for $CaCO_3$. This is because PP-g-MA can react well with some chemical functional group of fillers which very few contain in structure of $CaCO_3$ [216]. However, the coated $CaCO_3$ particles has been implemented to improve interfacial adhesion between $CaCO_3$ and polymer matrix. Ground $CaCO_3$, coated with fatty acid was selected to be used in this study. Generally the one of fatty acid modifiers that has been used wildly is stearic acid. It is coated on the $CaCO_3$ powder surface because it contains a nonpolar long-chain hydrocarbon group, which can facilitate nonpolar modification effects and compatible with non-polar polymer [220]. This idea has been supported from various studies on $CaCO_3$ added polymer composites [178, 218-220].

It can be seen that all of PP composites had higher tensile strength at break and tensile modulus comparing to extruded neat PP. The improvement in modulus is commonly due to the overall reason of the rigidness of fillers in PP matrix such as $CaCO_3$, kaolin and glass bead which are the minerals that are naturally more rigid than PP. There are many observations that can support these results. $CaCO_3$, glass bead and kaolin particles are inherently stiff and rigid. The incorporation of these fillers can influence the stiffness of the whole bulk of composite by restrict the mobility of polymer molecule [95, 216, 246, 247]. From the Figure 4.14, it can be seen that the tensile modulus of these three fillers were quite similar in the same filler loading. However, the results of tensile strength at break showed a little increase in tensile stress at break when increasing $CaCO_3$ loading. It was described in the literature that tensile strength of PP/$CaCO_3$ composite depended on both interfacial strength and surface contact area [84]. The effect of interfacial adhesion from fatty acid coating on $CaCO_3$ may be not as strong as the covalent bonding from PP-g-MA like PP composites from glass bead, kaolin and GNPs [216, 220].

Furthermore, it is quite obvious that PP/GNPs composite had the highest improvement in tensile modulus in high loading (20-30 wt%). The addition of only 10 wt% of GNPs results in an increase of the tensile modulus and the tensile strength at break of about 18 and 21%, respectively, as compared with that of extruded neat PP values. As the loading of GNPs

increases to 30 wt%, the tensile modulus and tensile strength at break of PP/GNPs composites showed significantly increase of about 68% and 27%, respectively. This great improvement of tensile properties was a result of high mechanical strength and a large aspect ratio as well as strong interfacial interaction between GNPs and PP matrix which led to better interfacial stress transfer efficiency and restricts the movement of the polymer chains. Moreover, the existence of PP-g-MA as compatibilizer caused the enhancement of ability to wetting of the surface between the polymer matrix and GNPs. This can promote the improvement of tensile strength of composites. These results also supported the previous literatures [68, 110, 248]. Considering between glass fibre and carbon fibre, increasing fillers content from 10 - 30 wt% increased the tensile strength at break of PP composite. The tensile modulus of composites were improved comparing to extruded neat PP. From Figure 4.14, it is notable that tensile modulus of carbon fibre was higher than glass fibre. The addition of 10 wt% of carbon fibre resulted in an increase of the tensile modulus and the tensile strength at break of about 73% and 12%, respectively as compared with that of extruded neat PP. As the loading of carbon fibre increases to 30 wt%, the tensile modulus and tensile strength at break of PP/GNPs composites showed drastically increase of about 250% and 85%, respectively.

From these results, it can be analyzed by referring to interfacial bonding and stress transfer along fillers. As the consideration at fibre properties, the carbon fibre has higher modulus than glass fibre [249, 250]. Normally, the interfacial bonding between fibres and PP matrix is weak. This is mainly because there are less reactive groups on the carbon fibres, which can improve the fibre/matrix interfacial adhesion. To breakthrough this limitation, the addition of compatiblizer has been applied for these experiment especially in fibre family. The presence of PP-g-MA can improve the interfacial adhesion between PP and fibre, resulting in a further improvement in tensile. This can be seen in the rough surface of fracture composite specimens in Figure 4.2. The interfacial adhesion is essential to transfer stresses from the matrix to the fibre under tensile loading [68]. The phenomenon had been proved in the previous researches [62, 63, 68, 77, 78]. Furthermore, the stresses during mechanical testing are not high enough to cause the fibre failure after matrix fractures. For this reason, fibres were pulled out from the matrix instead of fracture [153].

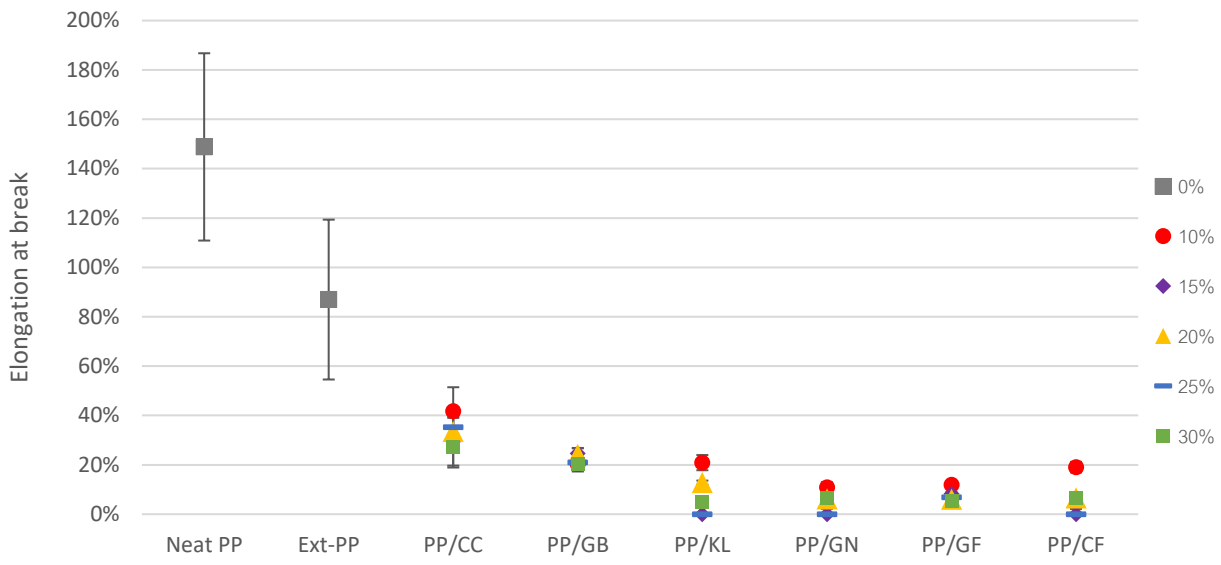

Figure 4.16: Elongation at break of neat PP, extruded PP and PP based composites

From the Figure 4.16, elongation at break of neat PP, extruded PP and PP based composites have been shown. Comparing the neat PP to extruded neat PP, elongation decreased almost 47% after extrusion. This is because the length of polymer chains were reduced due to chain scission from thermal degradation in process. It facilitated the disentanglement of polymer chain and decrease the number of intermolecular interactions between the crystalline phase and the amorphous phase. As a result, elongation at break was reduced [237, 245].

The percentage of elongation at break of PP composites from $CaCO_3$, kaolin and GNPs were dramatically dropped compare to extruded PP and neat PP. Generally in the particulate filler, the decrease in elongation was also an effect of the increment of the stiffness and rigidity of composites by the incorporation of rigid fillers. These rigid particles limited the movement of the PP macromolecule chains and weakening the ability to cope with external forces, resulting in an increase in the brittleness of the composites [95, 216]. Moreover, the agglomerations of these fillers in high concentration acted as stress concentrators and obstruct the ability for stretching of polymer matrix [95, 216].

However, it can be notified that increasing fillers content from 10 – 30 wt%, the elongation at break of composite declined significantly, except PP composite in glass bead system. It was found that increasing fillers content from 10 - 30 wt% the elongated percentage of PP/glass bead composite did not significantly change. They still maintained at around 20% due to the

regular spherical and uniform shape of the glass beads does not influence the elongation significantly [251].

For the PP composites from the fibre family, there are similarities of the reduction of elongation at break when the fibre loading increased from 10 wt% to 30 wt% for both of glass and carbon fibre, This is because the rigid fibres hinder the movement of polymer chains so the chains cannot move freely. The elongation at break was reduced with increasing fibre content [78, 165].

4.2.7.2 Flexural properties

Flexural testing for polymer and composites is the measurement to assess the ability of a material to resist deformation under bending load. The results of flexural strength and flexural modulus are shown in Figure 4.17, Table C.3 in Appendix C. The testing specimens were conducted the bending testing follow ISO 178 [201].

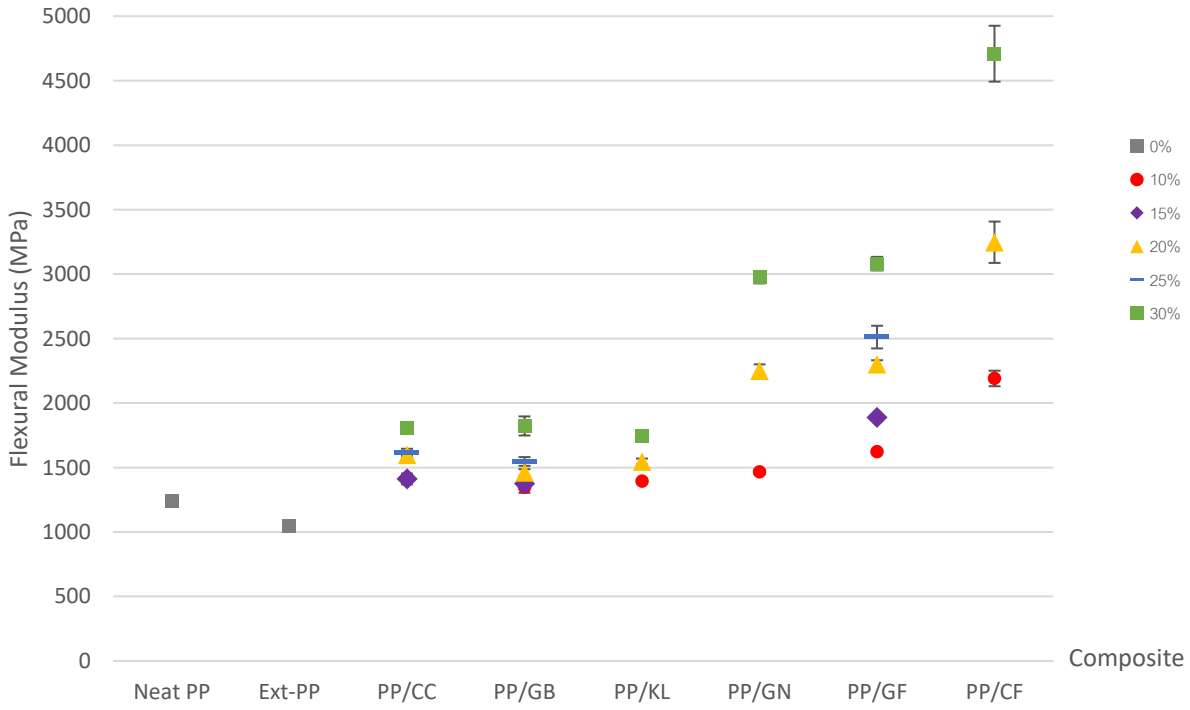

Figure 4.17: Flexural Modulus of neat PP, extruded PP and PP based composites

Refer to information from the Figure 4.17, flexural modulus of neat PP (P739ET) was higher a bit compared to extruded PP (around 2%). Moreover, it was found that increasing fillers content from 10 - 30 wt% increased the flexural modulus of every composites from 14% to

284% comparing to extruded neat PP. These measured flexural modulus were closely related and it is expected that the trend of tensile testing. Both of them should be the similar but the magnitude was probably different. This is due to the differences of deformation mode (three-point bending in flexural testing and vs. failure under extension in tensile), shape and dimensions of the samples (flex bars vs. dog-bone shape samples) [252].

For the particle reinforced composites, it was observed the improvement of flexural modulus from PP composites with $CaCO_3$, kaolin and glass beads which are the reinforced materials from natural minerals which are more rigid than PP [96, 98, 104, 151]. These particles can enhance rigidity of composites comparing to extruded neat PP. The improvement of these three fillers were in the same range which were 14 – 50% increment when increasing filler content from 10 wt% to 30 wt%. These improvement of flexural modulus can indicate the strong interfacial adhesion between fillers and the matrix.

Furthermore, it was obvious notable that the PP/GNPs composites has the best enhancement of flexural modulus comparing to PP composites in particle reinforced fillers. This is due to the small particle size with more surface area of 120 to 150 m^2/g. High surface area can promote the adhesion between filler and polymer matrix and increase the rigidity of composite [215, 252].

Considering between glass fibre and carbon fibre, the flexural modulus of composites were raised when increasing filler content [73, 77, 253]. Flexural modulus of carbon fibre was much higher than glass fibre because carbon fibre has higher modulus over glass fibre inherently [249, 250]. Moreover, the average size of carbon fibre (100 micron) is much smaller than glass fibre (4000 micron) which was mentioned in Table 3.2 in Chapter 3. The added fibres with good adhesion with polymer matrix (in Figure 4.2) act as the load carrier where stress can be transferred from the polymer matrix which can lead to stress distribution within the composite [73, 155].

From the results of tensile and flexural moduli, it can be found that the addition of rigid fillers to polymer matrix can positively influence to tensile and flexural properties including stiffness of composites. However, these properties can be improved better by using small particles with uniform distribution and dispersion. This is because small particles have more surface area to adhere strongly to polymer matrix which can lead to strong reinforcing effect. However, the problem can occur with very fine particles since they can adhere strongly to each other and form agglomerations. These can lead to the initiation of failure sites. The using

of coupling agent and surface treatment can assist to reduce particle-particle interaction and prevent the formation of agglomerated structures [165].

4.2.7.3 Izod impact properties

The testing specimens were conducted the impact testing follow ISO 180 [202]. Izod impact testing is one of methods to determine the toughness of materials by measuring energy required to propagate a crack rapidly. Izod impact test normally only involves the plane directly ahead of the notch tip where in a material with very low level of plastic response, the fracture becomes unstable. Whereas, tensile test is the slower test eventually probes the whole gauge volume of the specimen. Moreover, the presence of the notch can impose velocity much higher which results in a large value of local strain rate in the Izod impact testing experiment. The magnitude is larger than that in the tensile test. Therefore, it is not surprising that the two toughness measurements present quite different trends [82].

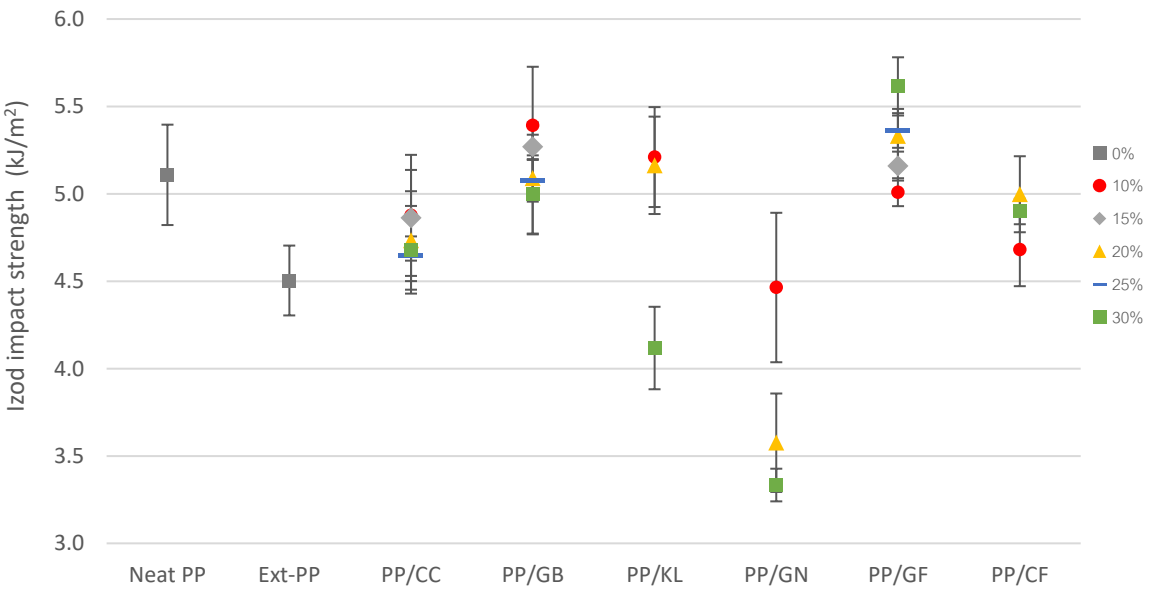

Figure 4.18: Izod impact strength of neat PP, extruded PP and PP- based composites

According to information from the Figure 4.18 and Table C.4 in Appendix C, Izod impact strength of neat PP (P739ET) was higher compared to extruded neat PP resin around 10%. The extruded neat PP had lower impact strength comparing to neat PP since the thermal aging from extrusion induced lower molecular weight that was attributed to chain scission

mechanism. The increment of processing cycles had reduced the resistance towards impact according to previous researches [159, 161, 236, 239, 242, 254].

For the particles family, it was found that PP filled $CaCO_3$ composite especially in lower content had better impact resistance than extruded neat PP since the good dispersion of $CaCO_3$ particles in the polymer matrix [89]. However, the impact strength of PP polymer decreased with the increasing the content of $CaCO_3$ varying from 10 wt% to 30 wt% since $CaCO_3$ has high surface energy which were easy to agglomerate in higher content. The agglomerates were easy to debond from the matrix. The primary role of these agglomerates was to trigger brittle fracture and can be weak point of composite when they were applied impact load [82]. This phenomenon can be used for describing the impact results with PP/kaolin composites. The impact strength of PP/kaolin was reduced when increasing kaolin content from 10 wt% to 30 wt%. The impact strength of PP/kaolin at 30 wt% dramatically dropped from 20 wt% from 5.16 kJ/m^2 to 4.12 kJ/m^2. This was because kaolin is inorganic rigid particle with high surface energy when it was mixed with hydrophobic like PP, the agglomeration of kaolin was so serious [100]. Not only, the addition of these rigid particles limited the movement of the PP macromolecule chains, weakening the ability to cope with external forces, resulting in an increase in the brittleness but this agglomeration can also create many crack initiations and stress-concentration sites. These can become weak point of composites which were very sensitive to impact stresses and cause detrimental effects on the impact properties of the composite [92]. Furthermore, the interfacial adhesion of kaolin particles and PP matrix is small, which becomes the weak point of composite materials. Although PP-g-MA was added as the coupling agent but the high shear from extruder has to be much required to reduce the size of agglomeration especially for high filler content.

For the experimental results from the set of PP/glass bead composites which were varied glass bead content from 10 wt% to 30 wt%. All of average impact strength of these PP/glass bead had higher impact strength than extruded neat PP. The impact strength decreased when increased the filler content. This is because these glass beads play a role in inducing crazes and blocking the propagation of crack to improve toughness of composite [104, 166]. A number of crazes of matrix surround the well-adhered glass beads can absorb the impact deformation energy [104]. This phenomenon occurred well on low glass bead content which the dispersion and distribution of glass beads in the matrix was uniform with good interfacial adhesion between glass bead and PP matrix in the Figure 4.2(c). On the other hand, there

were more void were generated in the matrix of high glass bead content in the Figure 4.2(d). This can lead to glass beads de-bond from the matrix and increase damage in the matrix [104, 105]. Although the increasing filler content can improve toughness due to large energy absorption by good adhesion glass bead but creation of a large number of micro-cavities and poor dispersion of glass beads in the polymer matrix could not be compensated [104, 105, 166]. Another reasons that supported the worse impact resistance in high filler concentration is inter-particle spacing between adjacent particles become shorter when glass bead content increased. This can restrict the amount of plastic deformation generated in the matrix ligament and also reducing the fracture toughness of these composites [105].

Regarding to Figure 4.18, it can be seen the addition of GNPs did not improve the impact strength of PP composite. The impact strength of PP/GNPs composites reduced when increasing GNPs content [107]. The further increasing of GNPs content from 10 wt% to 20 wt% and 30 wt% had a negative impact on the mechanical performance, i.e. 3.58 kJ/m^2 and 3.33 kJ/m^2 reduced as compared to 10 wt% GNPs filled composite which is 4.46 kJ/m^2. This deterioration in impact strength was considered to be due to the aggregation and orientation of GNPs which can be observed from the SEM image in Figure 4.2 (h). Another point has to be addressed is the characteristic of GNPs which has very low bulk density 0.0215 g/cm^3 as shown in the Table 3.3. This can be implied that the addition of GNPs in high concentration, the much higher volume of GNPs had to be added. The presence of large volume of GNPs can improves the rigidity but can cause the immobilization of the macromolecular chains and contributed increasing the brittleness and reduced impact strength of PP-based matrix [186].

Considering fibre family between glass fibre and carbon fibre, the impact strength of PP composites improve when adding glass and carbon fibre. For the PP/glass fibre composite, the results of the study indicates that the impact strength improve comparing to extruded neat PP when increasing the glass fibre concentration. The impact strength of the highest glass fibre content in the study which was 30 wt% was 5.61 kJ/m^2 which was 25% increasing compare to extruded neat PP. These results reflect those of some literatures [214, 255] which also found that impact strength improve when increasing fibre content. This is due to the property of high-strength fibres can be transferred stress from polymer matrix [63, 68]. The glass fibres were well adhered with polymer matrix which was the effect of added PP-g-MA that acted as coupling agent supporting by SEM images Figure 4.5. This also accords with our earlier observations [63, 68, 152, 214, 215] which showed that both higher amount of glass

fibres and the better interface bonding between glass fibre and PP matrix can caused ease-of-stress transmission from the weak matrix to strong fibres before the fracture occurs [68, 161]. The dissipation of impact energy can originate more at the more fibre inclusion [214, 256]. Furthermore, the presence of well adhered glass fibres could act as barrier to crack propagation which can promote impediment of crack propagation and also prevent the fibre pullout [63]. In this case, the propagation of crack needs more energy to break and allow the crack grow through the fissure path tortuosity which occurred from a greater amount of bonded fibre fragments [63].

In the case of PP/carbon fibre composites, it can be the impact strength slightly increased when increasing the carbon fibre content from 10 wt% to 20 wt% and maintain and slightly dropped when increase to 30 wt%. It cannot be seen the significantly reinforced effect at the addition of carbon fibre of 10 wt%, the impact strength was similar to extruded neat PP. However, when increasing the carbon fibre content to 20 wt%, impact strength increases considerably due to the reinforcement of the carbon fibres in polypropylene and reached the highest at 5 kJ/m^2. This can be attributed to the highly ordered structure of atoms in carbon fibre and the cohesion between the matrix and the fibre. This result can support the previous study that was investigated by Kumar D. T. et al. [77]. However, it can be visible the downward trend of impact strength when increasing content to 30 wt%. The impact strength slightly reduced to 4.9 kJ/m^2. The reduction of this properties with the addition of carbon fibre at high content could have been by restriction of the chain mobility of polymer molecules since molecules cannot move freely. This is due to this rigid filler and the creation of stress region concentrations at the ends of fibres is another reason for crack formation in the matrix around the carbon fibres. This required less energy to initiate the cracking propagation and the resulting microcracks propagated, therefore reducing the resistance to impact [71, 78]. These results corroborate the findings of previous literatures which claimed that when the critical level of extent of cracking across the weakest section, the surrounding fibres and matrix can no longer support the increasing load, the failure of the specimen occurs in the weakest region [128, 250, 257].

4.2.8 Density

Density is the one of the important composite properties. This can be determined a property of composite that is relative to the object's mass and volume. In the plastic industry, density

is used to determine indirectly to the mass of manufacturing part. Maintaining low density composites is essential for automotive applications, as any weight reduction serves to improve fuel efficiency, etc [244].

The Table 4.6 shows the measured density of neat PP, recycled PP, extruded neat and recycled PP and PP bases composites.

Table 4.6: Measured density of PP based composites

Composites	Density (g/cm^3)	SD
Neat PP	0.910	0.014
Extruded PP	0.910	0.014
PP/CC10	0.940	0.022
PP/CC15	0.975	0.019
PP/CC20	1.053	0.027
PP/CC25	1.073	0.059
PP/CC30	1.117	0.011
PP/GB10	0.943	0.004
PP/GB15	0.969	0.005
PP/GB20	1.023	0.008
PP/GB25	1.057	0.003
PP/GB30	1.146	0.042
PP/KL10	0.943	0.024
PP/KL20	1.017	0.013
PP/KL30	1.078	0.022
PP/GN10	0.932	0.010
PP/GN20	0.988	0.010
PP/GN30	0.995	0.027
PP/GF10	0.934	0.022
PP/GF15	0.967	0.016
PP/GF20	1.008	0.003
PP/GF25	1.037	0.008
PP/GF30	1.075	0.023
PP/CF10	0.955	0.011
PP/CF20	0.972	0.028
PP/CF30	1.031	0.022

The neat PP (P739ET) has a density around 0.91 and 0.94 g/cm^3 respectively. This PP was chosen as base resin for PP composite by adding six fillers from particle and fibre family. The density of these fillers that were obtained from suppliers are shown in the Table 4.7.

Table 4.7: Density of fillers for neat PP based composites

Composites	Density (g/cm^3)
Particulate fillers	
Calcium Carbonate ($CaCO_3$)	2.70
Glass Bead	2.60
Kaolin	2.60
Graphene Nanoplatelets (GNPs)	1.90
Fibrous fillers	
Glass fibre	2.60
Carbon fibre	1.55

Regarding to measured density of PP composites in Table 4.6, it is obvious to see that every PP composites had higher density comparing to neat PP. Density increased when increasing filler content. As seen in Table 4.6 the measured density of PP, recycled PP and all PP-composites which had content lower than 20 wt% were below 1 g/cm^3. In comparison, the PP composites from $CaCO_3$, glass bead, kaolin and glass fibre had the value of density in the same range due to the density of each filler were so similar in 2.6-2.7 g/cm^3. These fillers are denser than GNPs and carbon fibre which had density 1.9 and 1.55 g/cm^3. The addition of $CaCO_3$, glass bead, kaolin and glass fibre in PP matrix resulted in composites with highest density at 30 wt% in the range of 1.075 – 1.146 g/cm^3 which denser than PP/GNPs and PP/carbon fibre. Thus, substitution of fillers with GNPs, carbon fibre has the potential for weight reduction of manufactured parts.

4.3. Screening process for selecting the best suited fillers

4.3.1 Filler selection procedure

Screening stage is one of the most important procedures of the experimental plan of this study. The candidates of filler both from fibrous and particles had to be selected as the best candidates for using in the hybrid composite. This process was so complicated since there were a lot of factors that had to be considered such as mechanical properties, composite cost, etc. For these reasons, process of selection including criteria have been clarified by the considerations as follows.

4.3.1.1 The percentage of improvement

The percentage of improvement is one of important indicators that can evaluate the performance of composites. These percentages were calculated by comparing to properties of neat PP which was set as the references. The percentages were calculated by the equation 4.1 as follows,

$$\text{The percentage of change} = \left(\frac{\left(Composite's\ results - \ neat\ PP's\ result\right)}{neat\ PP's\ result}\right) \times 100\% \quad 4.1$$

The percentages of change of mechanical properties of PP based composites were tabulated in the Table C.5 in Appendix C. These neat PP based composites were evaluated mechanical properties such as tensile modulus, flexural modulus and Izod impact testing. Then, these information were tabulated and compared to mechanical properties of extruded PP. The performances of composited were calculated as percentage of change compare to properties neat PP. To verify the impact of filler performance on application, the involved mechanical properties has to be considered carefully for materials selection. In order to give a clear example, the washing tab has been used as the model application for this filler selection process.

Good washing tubs require impact resistance because the washing tub has to resist and stabilize during washing cycles. This generates a massive about of vibration [258]. However, another property has to be concern should be flexural modulus. This is because washing tub has to resist to bending force during washing cycle. The last measured properties was also important is tensile modulus this will be indicated the dimensional stability and the resistance of deformation. Therefore, the mechanical properties were selected for consideration were Impact strength, flexural modulus and tensile modulus.

4.3.1.2 Composite Costs (for raw materials)

Composite cost is the one of the important factors in plastic industries. Therefore, it has been considered as one aspects for screening test. Composite costs was calculated from cost of fillers and PP resin by the ratio in composite. They were calculated in GBP per one kilogram of composite. Firstly, the price of reinforcing fillers are shown in the Table 4.8.

Table 4.8: The price of reinforcing fillers

Reinforcing fillers	Price per kg (GBP/kg)
PP resin (P739ET)	1.7
$CaCO_3$ (OMYACARB-2T)	0.1
Glass Bead (EGB731)	2.3
Kaolin (SILFIT Z 91)	1.3
Graphene nanoplatelets (900420)	516
Glass fibre (CS331)	0.85
Milled carbon fibre (FP-MCF-2)	58.14
Coupling agent (Polybond3200)	2.3

Refer to the materials cost in the Table 4.8, the estimated composite cost for each composites from each formulations has been shown in the Table 4.9.

Table 4.9: Composite formulation costs

Composites	Composite cost (GBP/kg composite)
Neat PP	1.70
PP/CC10	1.54
PP/CC15	1.46
PP/CC20	1.38
PP/CC25	1.30
PP/CC30	1.22
PP/GB10	1.77
PP/GB15	1.81
PP/GB20	1.84
PP/GB25	1.88
PP/GB30	1.91
PP/KL10	1.67
PP/KL20	1.64
PP/KL30	1.61
PP/GN10	53.14
PP/GN20	104.42
PP/GN30	154.8
PP/GF10	1.62
PP/GF15	1.59
PP/GF20	1.55
PP/GF25	1.51
PP/GF30	1.47
PP/CF10	7.35
PP/CF20	13.01
PP/CF30	18.66

4.3.1.3 Composite performance rating

The selection procedure of the candidates of filler both from fibrous and particles for best candidates for using in the hybrid composite. This process was so complicated since there were a lot of aspects had to be considered such as mechanical properties, composite cost, etc. Not only the mechanical properties, composite cost were important to consider but other properties have to be concerned such as MFI, Density and process complication. As we also knew that MFI can indicate how well the materials flows. It is an important parameter that is widely used to characterize the flow property of resins due to its easy measurement [230]. For density is another important properties can be related to the weight of manufacturing part [244]. The percentage of improvement used a scale of (-5) to 5 to rank each percentage in a mechanical properties. Zero (0) means the properties of neat PP. Negative value represents lower values of each properties comparing to neat PP. On the other hand, the positive number means higher value of each properties comparing to neat PP. For each step of ranking number represents the percentage of change from neat PP. The definition of rating for each properties were shown in the Table C.6 – C.8 in the Appendix C.

Moreover, the composite rating were calculated and also show in the Table C.9 in Appendix C. These information were used to develop the radar charts by comparing the properties in the aspects of mechanical properties (tensile Modulus, flexural Modulus and Izod impact strength), MFI, density, composite cost including process complicity. The information was compared to the information set of neat PP. The radar charts were showed in the Figure 4.19 – 4.24. Each composite has been rated by calculating in the form of number with decimal for the exact rating and differentiate each composite. These calculated rating numbers are shown in the Table C.9 in the Appendix C.

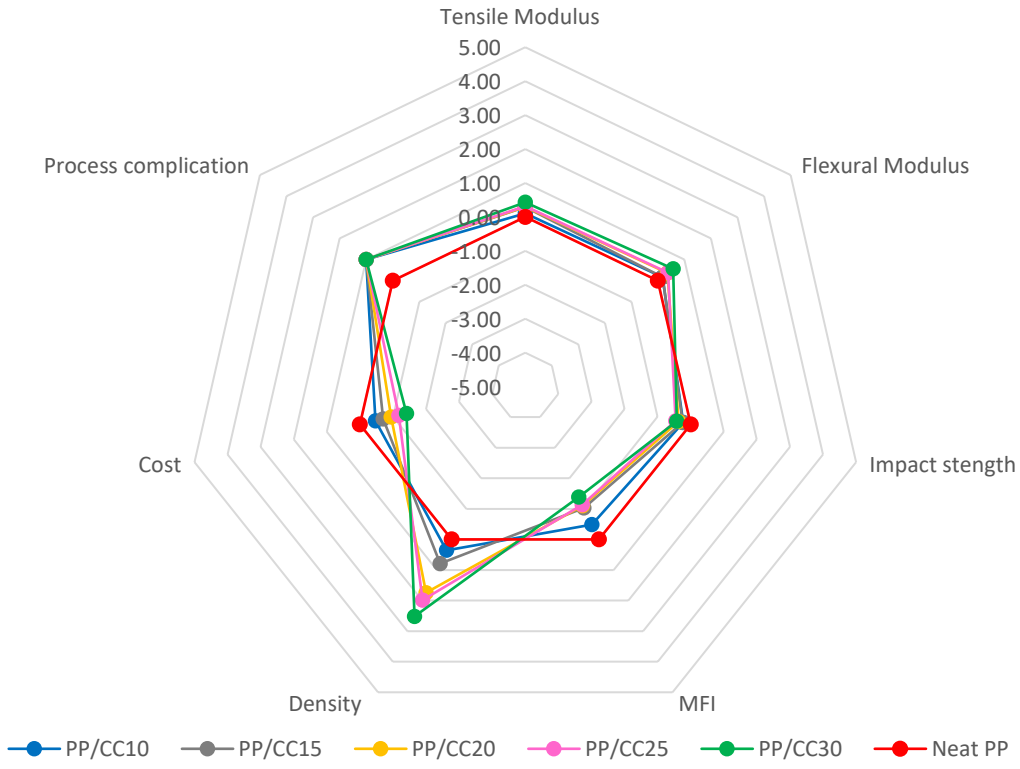

Figure 4.19: Radar chart compares neat PP and PP/$CaCO_3$ composites

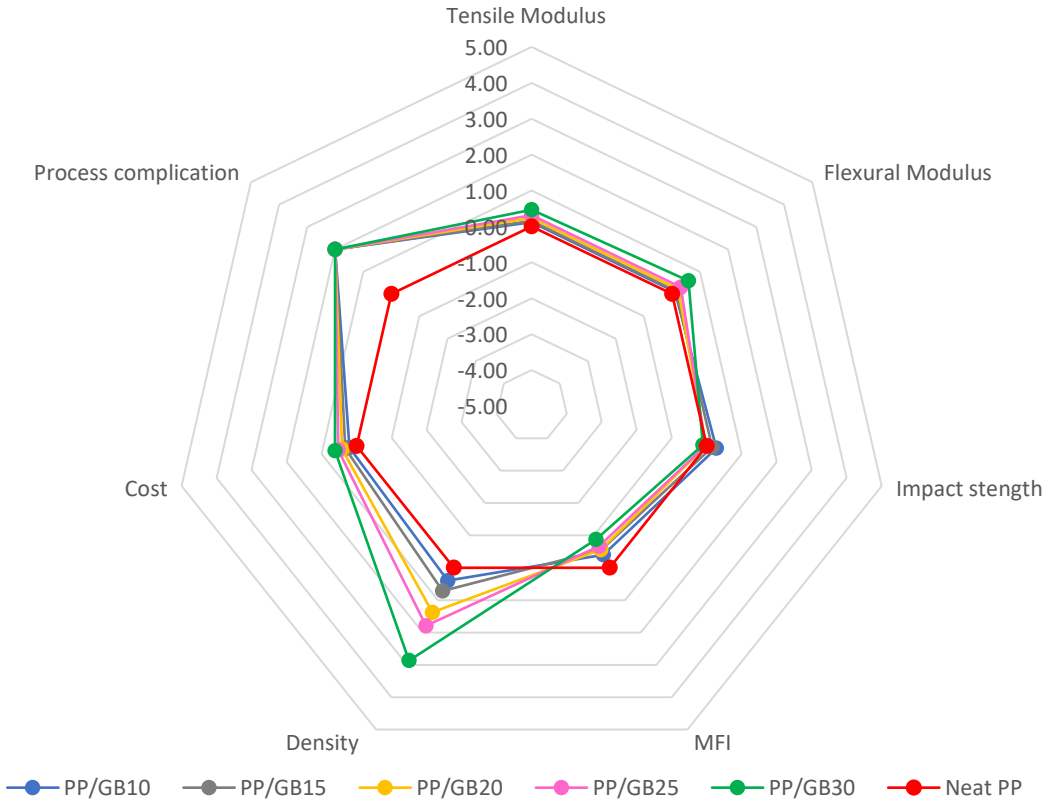

Figure 4.20: Radar chart compares neat PP and PP/glass bead composites

Figure 4.21: Radar chart compares neat PP and PP/kaolin composites

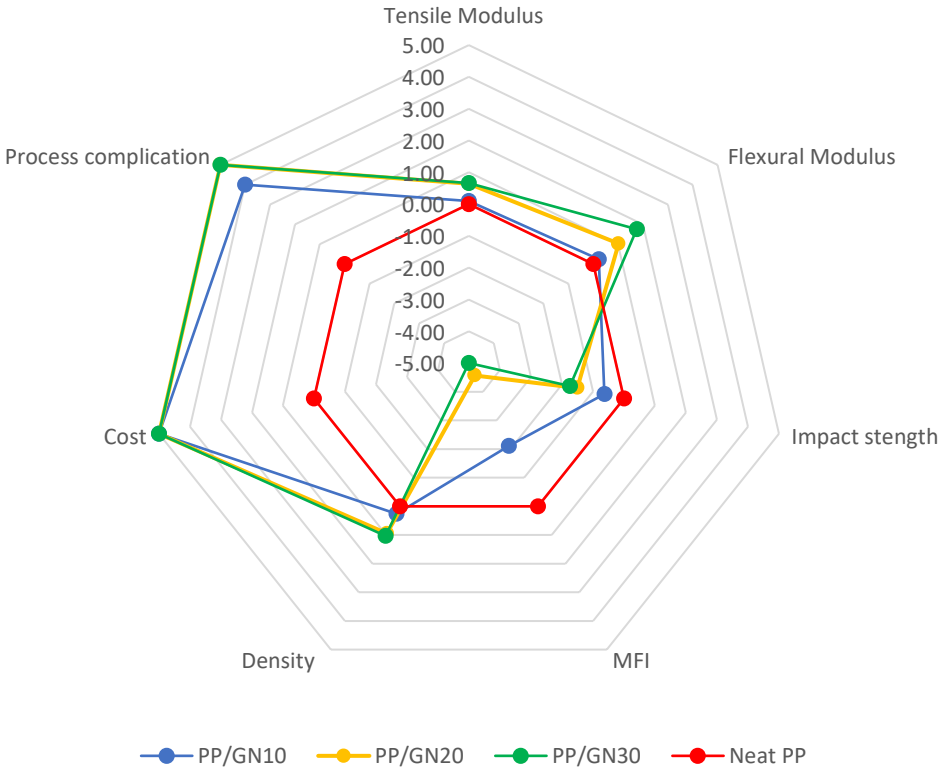

Figure 4.22: Radar chart compares neat PP and PP/GNPs composites

Figure 4.23: Radar chart compares neat PP and PP/glass fibre composites

Figure 4.24: Radar chart compares neat PP and PP/carbon fibre composites

For particle family, if they were considered from the improvement of mechanical properties, it can be seen that although PP/GNPs had the great improvement for tensile and flexural properties but impact strength were so poor with much more complicated manufacturing process and much more expensive. Therefore, GNPs were cut off for the candidate for the next session. While, PP/$CaCO_3$ composite, it seems PP/$CaCO_3$ could be the good candidate but the impact strength were worse than neat PP. Moreover, it can be seen that PP based composites from glass bead and kaolin could be selected as the suitable candidates from particles family. This is because, PP based composite of glass bead and kaolin had the improvement for all of mechanical properties. The performance of PP/glass bead and PP/kaolin composite were compared the radar chart in the Figure 4.25.

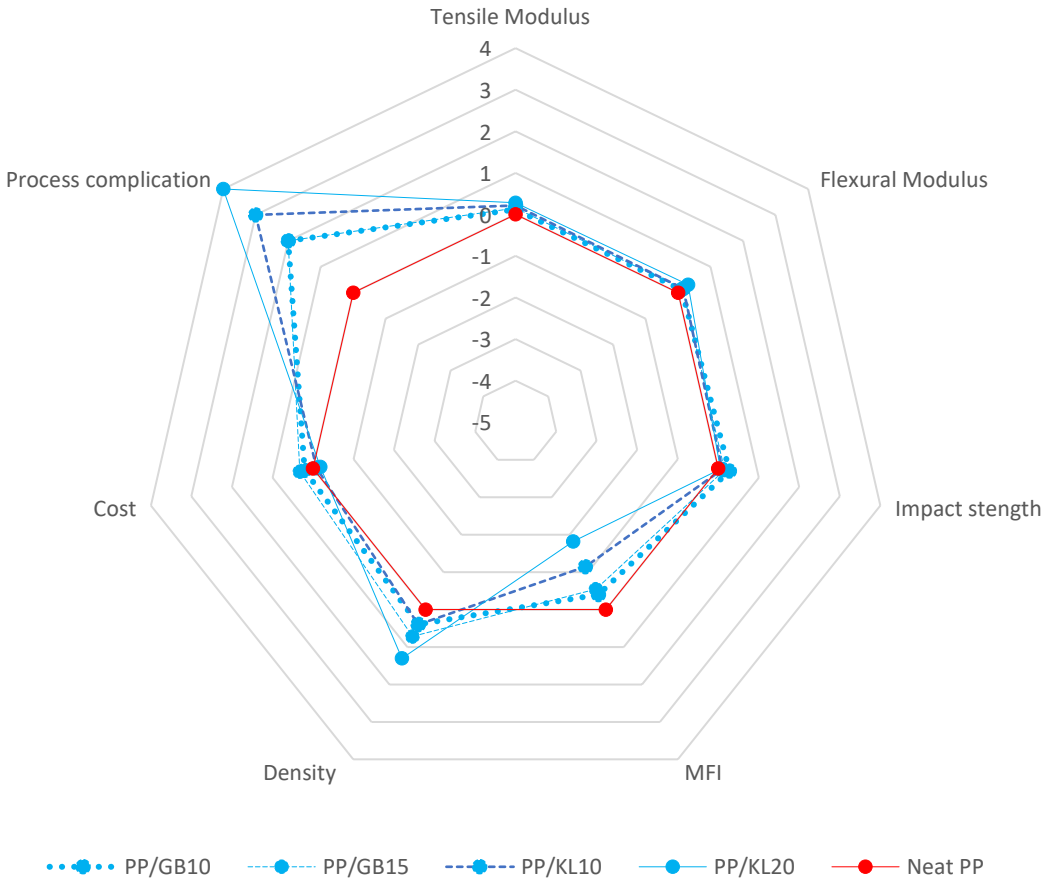

Figure 4.25: Radar chart compares neat PP and potential candidates of PP composites from particulate family

However, PP/glass bead composites had better overall mechanical properties than PP/kaolin. All of mechanical properties have been improved. Another points have to be addressed is the difficulty of production process. From the radar chart, it can be seen that the production of

PP/kaolin has been more complex than composite from glass bead. Therefore, the most suitable fillers from particle family is *The Glass Bead.*

For the fibrous family, PP based composites from glass fibre and carbon fibre with loading from 10 – 30 % by weight have been evaluated. It can be seen that although the PP/carbon fibre had the larger improvement for tensile and flexural modulus than PP/glass bead composite but impact properties of composites from carbon fibre were dropped comparing to neat PP. Furthermore, the composite cost of PP/carbon fibre was much more expensive than PP/glass fibre. However, the PP/glass fibre composites have improved performances for all of mechanical properties (tensile strength, flexural modulus and impact strength) and had lower composite cost than PP/carbon fibre. The performance of PP/glass fibre composites which provided their all of mechanical properties improved compare to neat PP are shown in the radar charts in Figure 4.26. Due to these information, it can be considered that the most suitable fillers from fibre family is *The Glass fibre.*

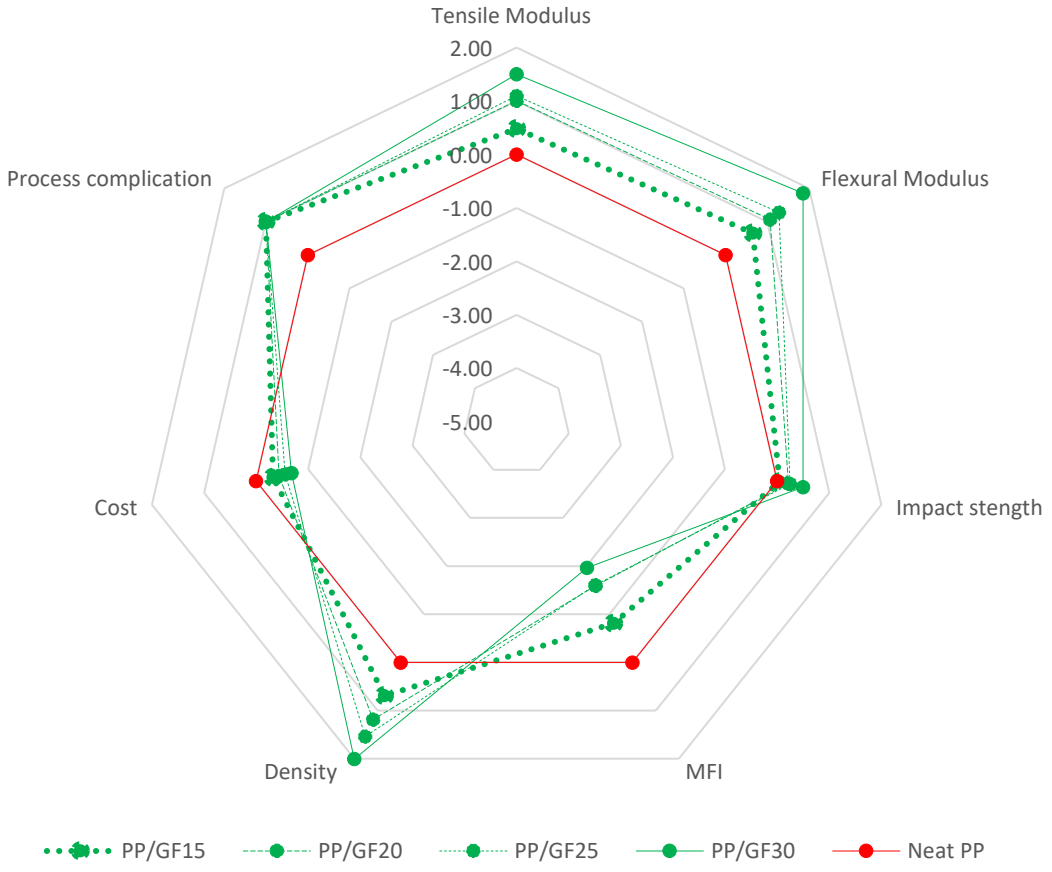

Figure 4.26: Radar chart compares neat PP and potential candidates of PP composites from fibrous family

4.4 Conclusion

The experiments in Chapter 4 were designed in order to evaluate the reinforcing performances of candidate fillers from fibre and particle families with neat PP resin in various composites systems by screening test. The candidates from particles family were $CaCO_3$, kaolin, glass bead and GNPs while glass fibre and carbon fibre were the candidate from fibre family. The best processing conditions for neat PP based composites were evaluated. While, the performance of neat PP based composites from various fillers by investigating mechanical properties, thermal properties, rheological properties, density, MFI, the presence of chemical functional groups fracture mode by FTIR including composite structure by SEM. The most suitable fillers were considered in terms of the percentage of properties improvement, composite cost and processibility.

- Firstly, the effect of filler types and loading on mechanical and thermal properties of neat PP composite systems were investigated as a reference result. The filler content were varied from 10 – 30 wt.%. In terms of the mechanical properties, it was found that increasing of the filler content from 10 - 30 wt.%.
- For particle family, PP/glass bead composites had best overall mechanical properties among the rest.
- All of mechanical properties have been improved and can be processed easier than others. Mechanical properties of PP/glass bead such as tensile, flexural modulus and Izod impact strength showed improvements by 37%, 47% and 6%, respectively compared to neat PP. These PP/glass bead composites were improved with a simple compounding process and with an acceptable cost (1.77 – 1.91 GBP/kg of composite).
- However, although PP/GNPs had the great improvement for tensile and flexural properties but impact strength were so poor with much more complicated manufacturing process and much more expensive in the range of 53 – 154 GBP/kg while the cost of other composites are in the range of 1.2 – 18 GBP/kg. Therefore, GNPs was not considered as the suitable candidate.
- PP/$CaCO_3$ composite, it seems PP/$CaCO_3$ could be the good candidate but the impact strength were worse than neat PP which were less than neat PP about 5 – 9%.

- PP/kaolin had good overall mechanical performance but the production of PP/kaolin has been more complex than composite from glass bead. Therefore, the most suitable fillers from particle family is *The Glass Bead.*
- For the fibrous family, PP/carbon fibre was not selected due to its worse impact strength, which was less than 2 – 8% compared to neat PP and also being more expensive than PP/glass fibre as well.
- The incorporation of glass fibre could promote the impact strength up from 4% to 10% compared to neat PP by increasing the glass fibre content from 20 to 30 wt%. Therefore, the most suitable fillers from fibre family was the Glass Fibre.

Regarding to the findings from the experiments in Chapter 4, glass bead and glass fibre were selected as the filler to be combined as hybrid composite for the next chapter.

5. Determination of the best formulation of neat PP based hybrid composite

In Chapter 4, the performance PP composites with various fillers from particulate and fibrous families were evaluated. The most suitable fillers from each family were selected to combine as the hybrid composites. Therefore, the experimental results and discussions relating to the experiments to determine the best formulation of neat PP based hybrid composite is presented in Chapter 5.

From the experimental results presented in Chapter 4, the suitable fillers have been selected by evaluating various aspects such as:

- The composite performance by evaluating the improvement of mechanical properties (tensile modulus, flexural modulus and Izod impact strength) of hybrid composites
- The ease of processibility by evaluating the MFI of hybrid composites
- The weight of manufactured parts by determining density of the hybrid composites
- The hybrid composite material cost

To compare the performances of composite in every aspects, the radar charts were created to oversee the overall performance of the composites from particular and fibrous families. From radar charts presented in Figures 4.25 – 4.26 in Chapter 4, the most suitable filler from particle family is “glass bead” while “glass fibre” was selected as the best candidate from the fibrous family. The neat PP based hybrid composites by glass bead and glass fibre were prepared in order to find out the most suitable formulations for applying in recycled PP based hybrid composites in the next chapter.

5.1 Target of experiment

The PP based hybrid composites by glass bead and glass fibre were prepared in order to evaluate the composite performance of recycled PP (MOPLEN QCP300P Ivory) in the next chapter. The purpose of experiment is to improve recycled PP based composite to comparable to neat PP. In order to setting target, the properties of extruded recycled PP were evaluated and show in Table 5.1.

Table 5.1: Average mechanical properties (tensile modulus, flexural modulus and Izod impact strength) of neat PP, extruded rPP

Composites	Tensile Modulus (MPa)	Flexural Modulus (MPa)	Izod impact strength (kJ/m^2)
Neat PP	1708.6 ± 38.9	1240.3 ± 30.4	5.11 ± 0.29
Extruded recycled PP	1478.1 ± 69.1	1042.2 ± 10.2	4.34 ± 0.17
% Difference	-13%	-16%	-15%

From Table 5.1, the target of the percentage of improvement of the most suitable formulation of the combination of glass bead and glass fibre should improve these three mechanical properties at least 16%. Not only the improvement of the mechanical properties was considered as one of the criteria for the suitable formulation but there were more aspects had to be also considered such as the ease of processibility by evaluating MFI, the composite cost including the composite density, which reflects to the dimension stability and weight of manufactured parts.

Commercially, the melt flow index of resins of PP/glass fibre composite for injection moulding process is not less than 10 g/10min, which shown in the datasheets in Appendix B. Therefore, this MFI value was set as target for hybrid composites, which had to be not less than 10g/10min. In term of density, the target value was set from the several PP/glass fibre resins that have been commercially used in market in the injection molding application. Typically the glass fibre reinforced PP resin should not be more than 1.300 g/cm^3 (as shown in Appendix B). Lastly, the cost of hybrid composites should not more than neat PP resin (P739ET), which is about 1.7 GBP/kg. Therefore, the target values that were set as the criteria in order to select the best combination between glass bead and glass fibre are shown in Table 5.2 as follows.

Table 5.2: Target for selecting the hybrid composites

Criteria	Target
The improvement of mechanical properties (Tensile modulus, flexural modulus and Izod impact strength)	> 16%
Melt flow index	>10g/10min
Density	<1.300 g/cm^3
Composite cost	<1.7 GBP/kg

The experimental results were rated and summarized as radar charts. The obtained results from neat PP based hybrid composites were considered by comparing each property follow

the priority follow tables, which started with mechanical properties, MFI, density and composite cost.

5.2 Design of experiments

To investigate the most suitable combination between glass beads and glass fibres, the proper design of experiments is very important. Prior to the design of experiment were figured out by applying Taguchi method as guidance, the suitable range of both glass bead and glass fibre contents had to be considered by referring results in the previous chapter in Figure 5.1, 5.2 and 5.3.

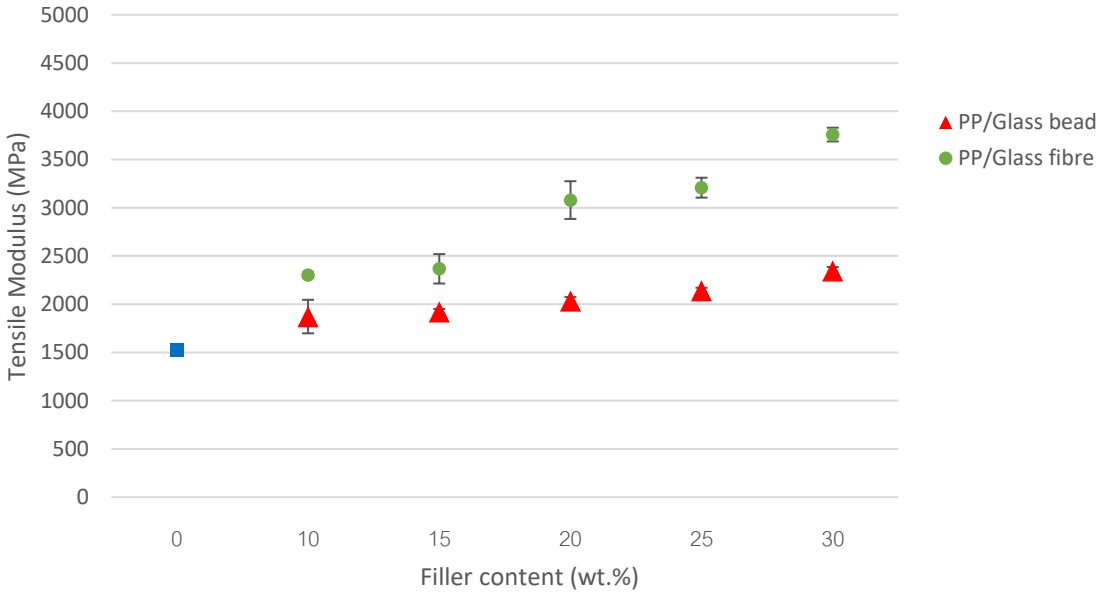

Figure 5.1: Tensile modulus of PP/glass bead and PP/glass fibre composites

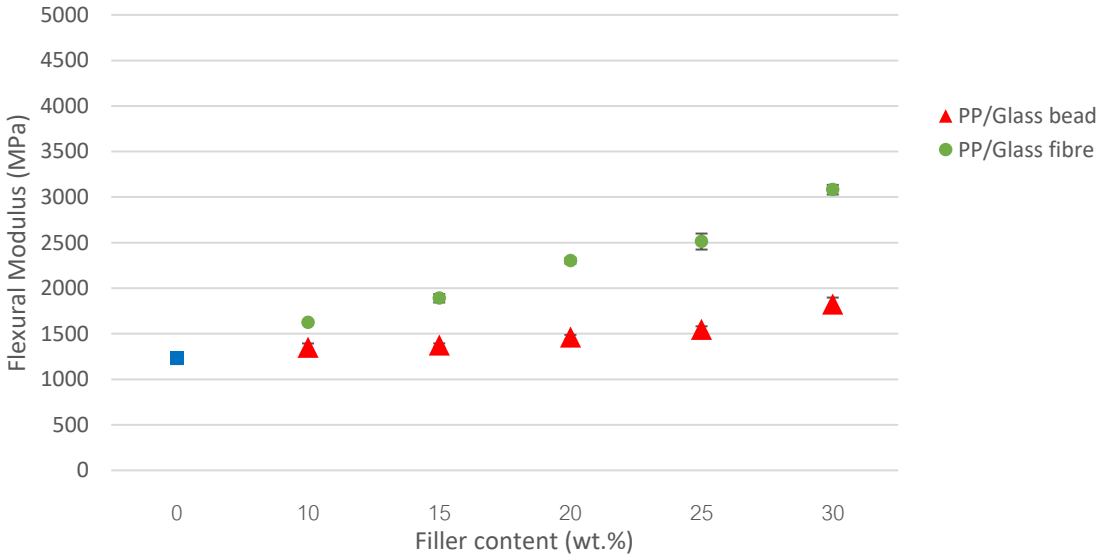

Figure 5.2: Flexural modulus of PP/glass bead and PP/glass fibre composites

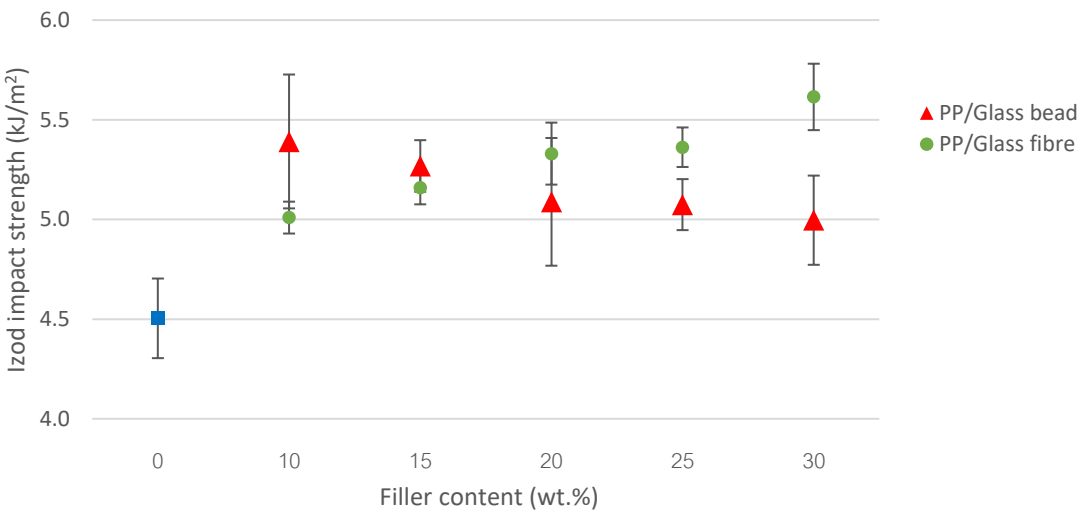

Figure 5.3: Izod impact strength of PP/glass bead and PP/glass fibre composites

From Figure 5.1 and 5.2, it can be obviously seen that the tensile and flexural modulus increased with increasing the loading of glass bead and glass fibre. These phenomena were discussed in Chapter 4 and also supported by various earlier literatures [46, 55, 218 - 219]. However, it can be notable in Figure 5.3 that the impact strength of PP/glass fibre increased with increasing glass fibre content while it was dropped when increasing glass bead content. This observation also supported by the literature by Yang et al. [75]. They investigated the mechanical properties by varying the glass bead content. The results showed that the elastic modulus has increased until critical concentration and then decreased [75]. In order to investigate the critical concentration of glass bead, the experiment at 1,2 and 5 wt% were conducted additionally. The results of Izod impact testing of the additional experiments are shown in Figure 5.4.

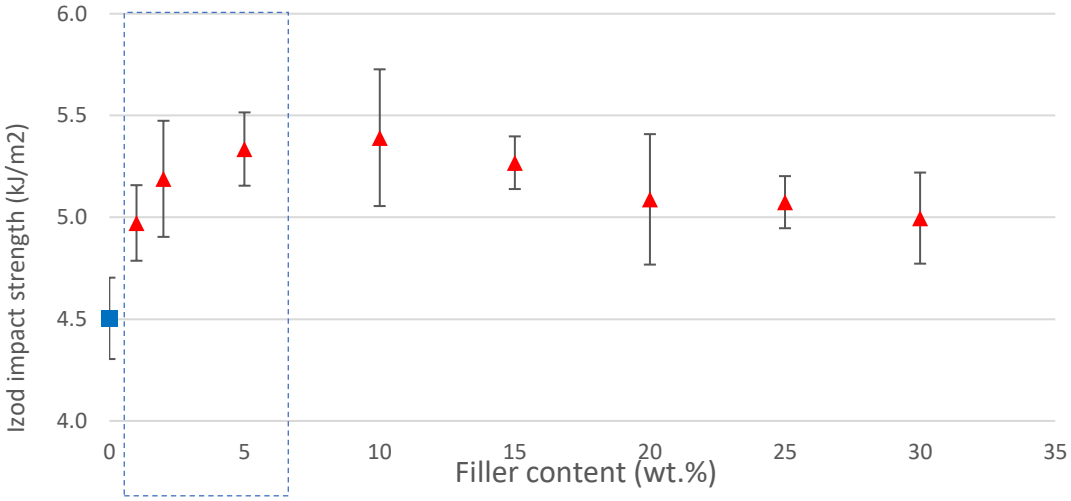

Figure 5.4: Izod impact strength of PP/glass bead composites from 0 to 30 wt%

From Figure 5.4, it can be found that the impact strength of the PP/glass bead composites first increased with increasing glass bead content up to 10 wt%, thereafter, it decreased. The similar results were observed by the previous study from Yang et al. [101]. This was because of the interaction between the glass bead and the matrix was really good. The defects from the agglomerations in the composites increased obviously in the case of higher filler content due to particle-particle interaction become stronger with increasing particle content [165]. Therefore, the low range from 1 to 10 wt% were chosen to be varied for hybrid composite in this chapter.

The design of experiments (DOE) is a highly effective tool to analyze the influence of process parameters on hybrid composite performance [259]. The experimental trials were designed by referring guidance from Taguchi techniques using Minitab 18 software. Taguchi's method tests a pair of factors and gives optimum results, thereby saving a number of experiments, cost and time [259-262].

In this study, the content of glass bead and glass fibre were selected as parameters. A mixed design Taguchi method was applied based on the L8 with eight experimental units, but with four factors at four levels and two levels as the guidance. The experiments were conducted using the different factors and levels of variables shown in Table 5.3 [263].

Table 5.3: Factors and levels of parameters were used for the hybrid composites

Selected filler from particle family	Filler Content (wt%)	Selected filler from fibre family	Filler Content (wt%)
Glass bead	1 2 5 10	Glass fibre	10, 30

Factors were chosen to go into this design based on the selected filler from Chapter 4, which were glass bead and glass fibre. Each filler was tested at two and four levels. Glass fibre was tested at two levels, which were 10 wt% representing low glass fibre content and 30 wt% representing high glass fibre content. The four loadings of glass bead were based on the range finding tests, which showed in Figure 5.4. This included a range of low loading to critical content that should have the highest impact strength. The range covered from 1 to 10 wt%. Moreover, PP-g-MA was incorporated in these formulations with the 0.15-fold of total filler

content [174]. The designed experimental run using L8 from Taguchi method are shown in Table 5.4.

Table 5.4: Glass bead and glass fibre contents in experimental trials using L8 from Taguchi method

Experiment number	Glass bead Content (wt%)	Glass fibre Content (wt%.)
HC1	1	10
HC2	1	30
HC3	2	10
HC4	2	30
HC5	5	10
HC6	5	30
HC7	10	10
HC8	10	30

5.3 Compounding condition

For composites manufacturing, PP hybrid composite with various percentage of glass bead, glass fibre and PP-g-MA, were mixed in a co - rotating twin screw extruder (Haake Rheomax OS PTW16) at a screw speed of 70 rpm with throughput of 1.8 kg/hr. The temperature profiles were 180/190/190/210/210/210/210/210/210/180 °C, which are the same conditions was mentioned in Table 4.1 in Chapter4. Glass bead in powder was fed into the extruder by a gravimetric feeder in the barrel at the sixth barrel zone of extruder in order to minimize glass bead breakage [209-213]. The schematic is shown in Figure 5.5. While, raw materials in pellet or rod forms such as neat PP resins, compatibilizer (PP-g-MA) and glass fibre were carefully manual pre-mixing before feeding into the extruder by a volumetric feeder.

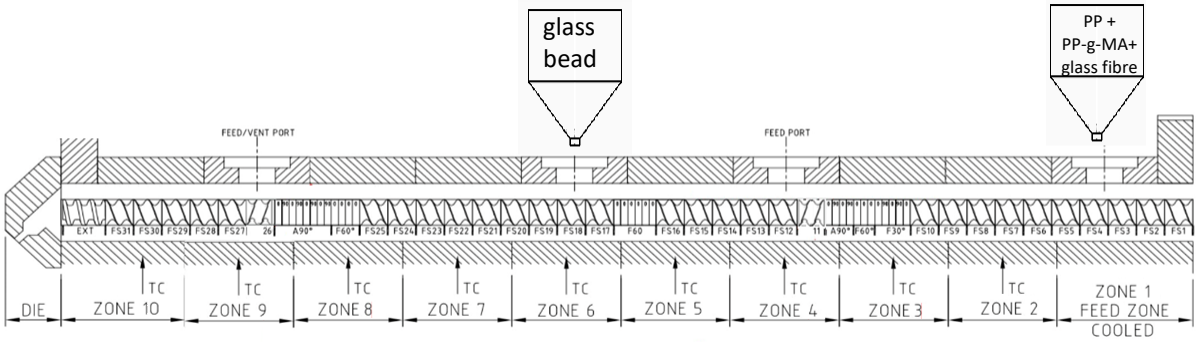

Figure 5.5: Schematic of a twin screw extrusion machine for PP/glass bead/glass fibre hybrid composite

5.4 Characterization of PP composites

To evaluate the performance of neat PP based hybrid composites, glass bead and glass fibre were investigated by various characterization techniques. Preliminarily, the mechanical properties (tensile modulus, flexural modulus, and Izod impact strength), MFI, density were investigated as the critical properties to evaluate overall propertied of hybrid composites.

5.4.1 Mechanical properties

According to target of the experiment in Chapter 5, which evaluate the improvement of mechanical properties in term of tensile modulus, flexural modulus and Izod impact strength. Therefore these three properties will be discussed in this chapter, the other properties are shown in the Appendix D.

5.4.1.1 Tensile modulus

The effect of total filler content (wt%) on tensile modulus of extruded PP and PP based hybrid composites are shown in Figure 5.6 and 5.7. The experimental raw data of tensile modulus have been shown in Table D.1 in Appendix D.

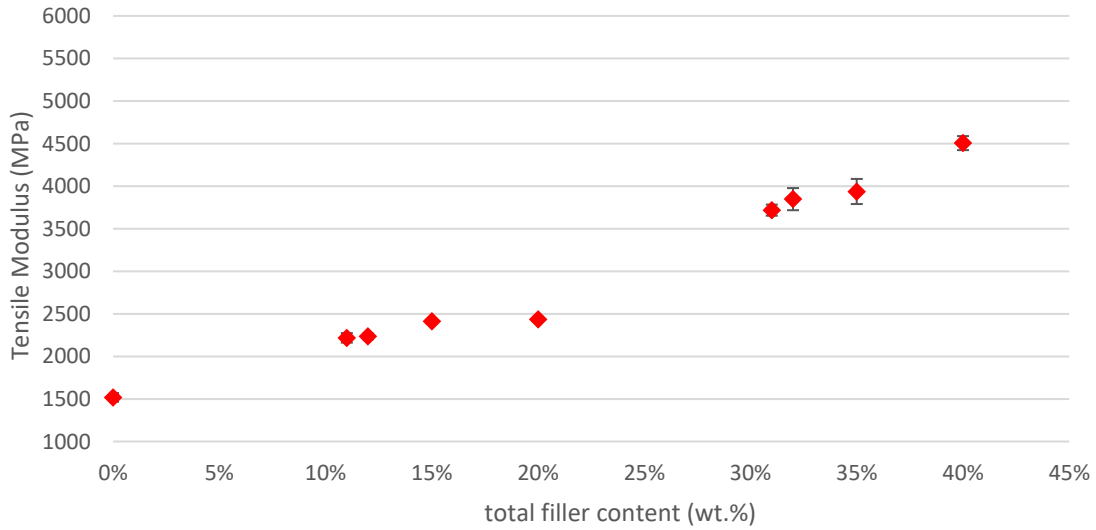

Figure 5.6: Tensile modulus of extruded PP and neat PP based hybrid composites versus the percentage of total filler content (%)

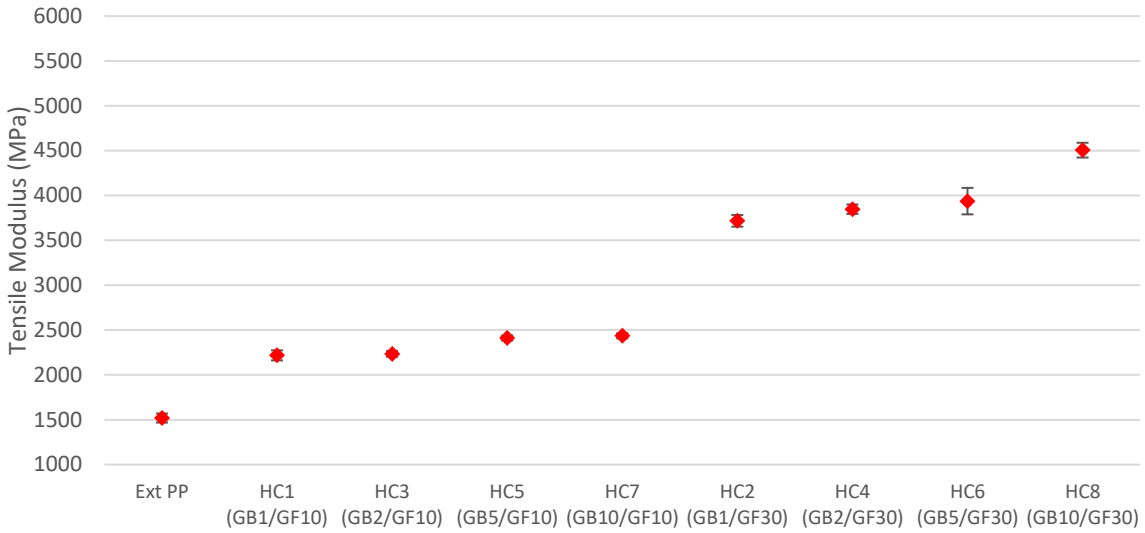

Figure 5.7: Tensile modulus of extruded PP and neat PP based hybrid composites

From Figure 5.6, it can be observed that tensile modulus of PP/glass bead/glass fibre hybrid composite increased with increasing the total concentration of fillers in the system. This similar behaviour was also reported earlier in the literature data by Hashemi et al. [264]. The enhancement in modulus was due to the overall reason of the rigidness of glass beads and glass fibres with the well-bonded with PP matrix. There are several observations that can support these results [165, 246]. The incorporation of glass beads and glass fibre can influence the stiffness of the whole bulk of composite by restrict the mobility of polymer molecule [165, 246].

In case of the tensile modulus of hybrid composites are shown in Figure 5.7, it can be notable that the hybrid composites were grouped into the group of hybrid composites with 10 wt% and varied glass bead content from 1,2,5 and 10 wt% and group of hybrid composites with 30 wt% with the same range of glass bead content. In case of the hybrid composites of PP with aminosilane-treated glass bead and glass fibre at any constant glass fibre concentration, increasing glass bead content showed the significantly improved tensile modulus. It can be observed that incorporation of treated glass bead and glass fibres led to the substantial increment of modulus. The maximum tensile modulus was achieved in HC8, which was incorporated with 10 wt% of glass bead and 30 wt% of glass fibre. This was about 250% greater as compared to that of referent PP, which was much higher than that of matrix polymer's modulus. This indicated the existence of good interfacial adhesion of the glass fibre reinforcement with the addition of PP-g-MA, consequently resulting in an efficient

reinforcement mechanism [209]. The increasing total fillers content can reduce the interparticle distance of filler, the interfacial interactions between the glass fibre and glass bead between the matrix polymer with both components can play an important role in maximizing the mechanical strength behaviour of PP composites reinforced with hybrid fibrous-particulate reinforcement. These well-adhered fillers can promote the stress transfer from the matrix with less occurrence of microspheres and fibre-polymer interfacial de-bonding from the matrix polymer and the coalescence into bigger cracks, which can cause the failure of material. This result can be supported by the earlier literatures by Carvalho et al [209].

5.4.1.2 Flexural modulus

The effect of total filler content (wt%) on flexural modulus of extruded PP and PP based hybrid composites are shown in Figures 5.8 and 5.9. The experimental raw data of flexural modulus have been shown in Table D.2 in the Appendix D.

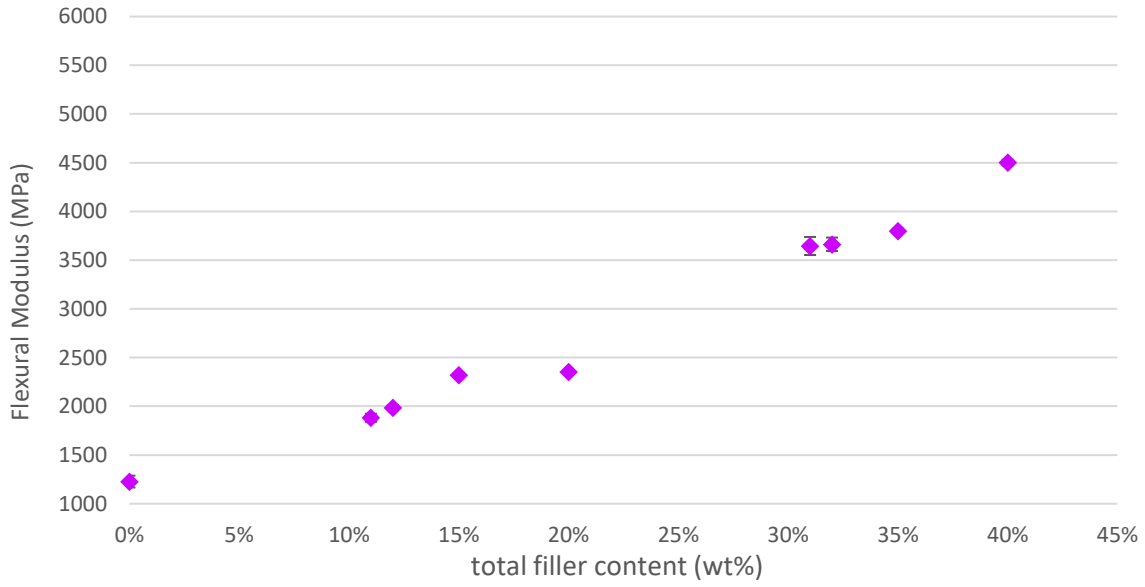

Figure 5.8: Flexural modulus of extruded PP and neat PP based hybrid composites versus the percentage of total filler content (%)

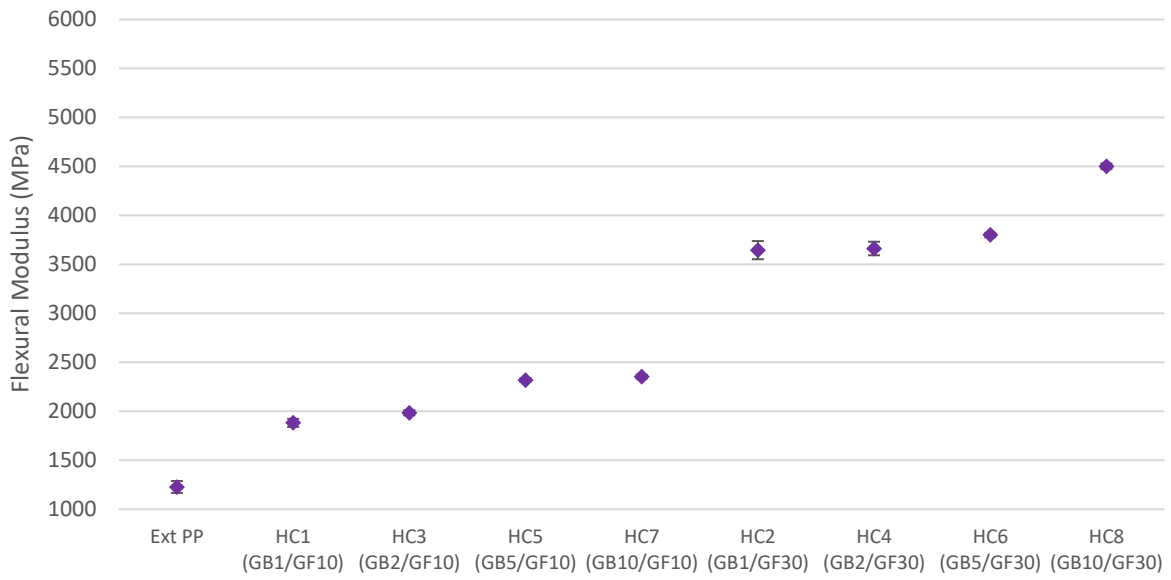

Figure 5.9: Flexural modulus of extruded PP and neat PP based hybrid composites

From Figures 5.8 and 5.9, it can be observed that the trend of flexural modulus was similar to tensile modulus but probably different magnitude. This is due to the differences of deformation mode (three-point bending in flexural testing versus under extension in tensile), shape and dimensions of the samples (flexural testing bars versus dog-bone shape samples), etc [252, 265]. The increasing total fillers content by the addition of glass bead in PP composites with constant concentration of glass fibre led to an increase of the flexural modulus of every composite from 53% to 267% comparing to extruded neat PP. It can be seen that flexural modulus elevated significantly by increasing total filler content. The greatest flexural modulus is achieved in HC8, which is hybrid composite with 10 wt% of glass bead and 30 wt% of glass fibre. The flexural modulus was 267% superior when compared to extruded neat PP. This was due to the good adhesion between matrix and rigid fillers from the addition of PP-g-MA as compatibilizer, which can assist to reduce particle-particle interaction and prevent the formation of agglomerated structures [165]. This can limit the polymer chains movement and subsequently raises the rigidity. The incorporation of glass bead and glass fibres, which are rigid fillers marginally increased the flexural modulus. This results can be supported by similar literature by Carvalho et al. and Parhizkar, et al [209, 266]. Moreover, the increase of filler content, the glass fibre-glass bead interparticle distance was reduced in this system with increasing total volume content of hybrid reinforcement. The interfacial interactions between the high aspect ratio glass fibre and low aspect ratio glass

bead filler particles played an important role in maximizing the mechanical strength behaviour of PP composites reinforced with hybrid fibrous-particulate reinforcement. This results can be supported by the earlier study by Carvalho et al [209].

5.4.1.3 Izod Impact properties

The Izod impact strength of extruded PP and PP based hybrid composites in various total filler content (wt%) are shown in Figures 5.10 and 5.11. The raw data of Izod impact strength have been shown in Table D.3 in the Appendix D.

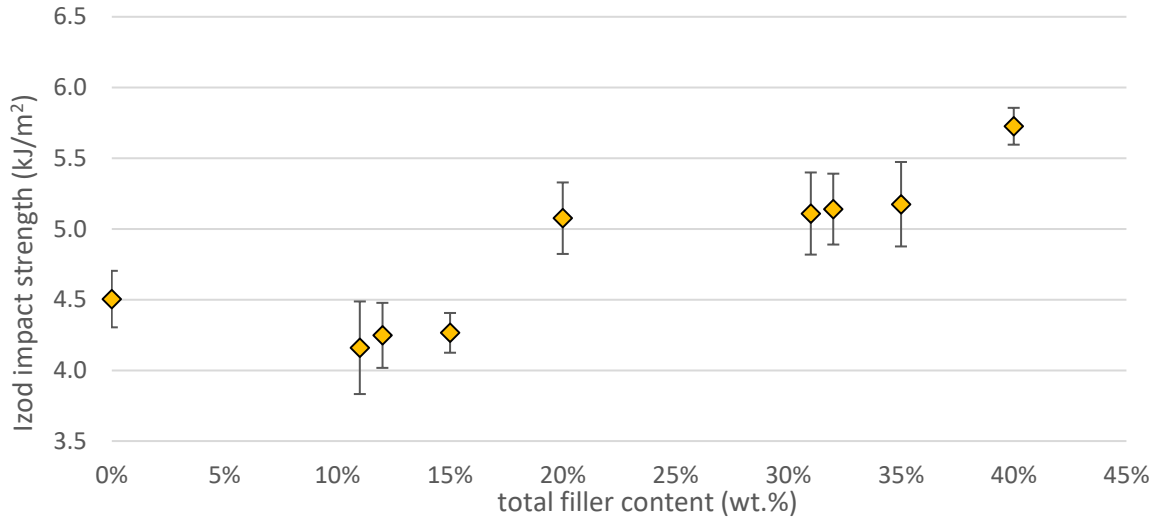

Figure 5.10: Izod impact strength of extruded PP and neat PP based hybrid composites versus the percentage of total filler content (%)

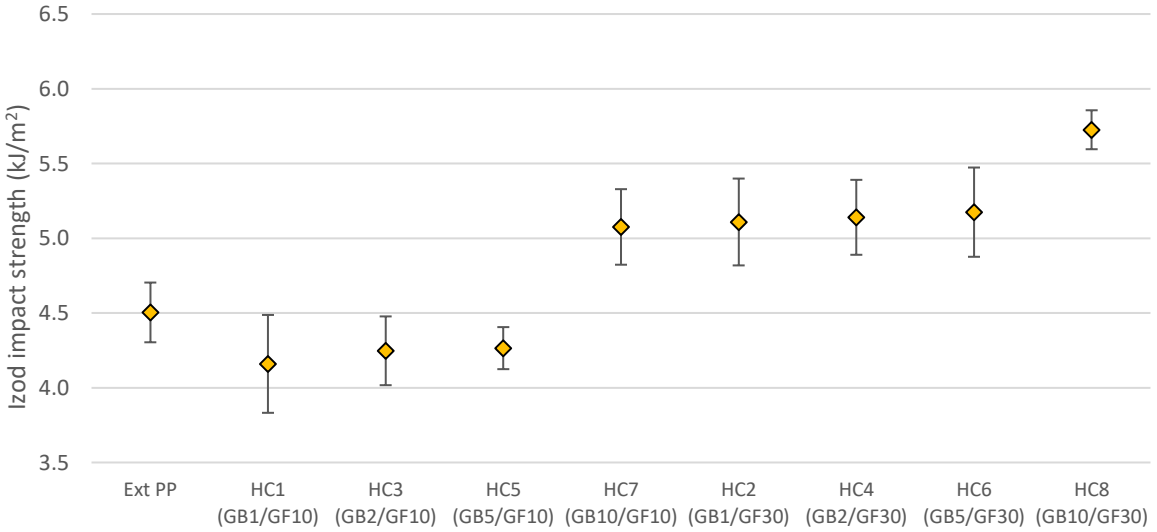

Figure 5.11: Izod impact strength of extruded PP and neat PP based hybrid composites

From Figures 5.10 and 5.11, it can be observed that the Izod impact strength of PP/glass bead/glass fibre hybrid composite increased with increasing total filler content. However, the hybridization of PP with glass beads and glass fibres reduced impact strength to a level, which was lower than extruded neat PP. This similar behaviour was also reported earlier in the literature by Hashemi et al [267]. However, the toughening effect from these fillers were insignificant in the case of low filler contents because of the small interaction between the filler and the matrix from the quite small number of fillers [102]. These particles may obstruct the stress transfer efficiency at the fibre-polymer interface [209]. Moreover, the possible reasons from Carvalho et al. [209] can be supported that the factor of the interparticle distance between glass bead and glass fibre in the polymer matrix was high in the low total filler content. This affected to the hybrid fibrous-particulate reinforcement [209].

However, it can be seen that the impact strength of hybrid composites in the high filler content, which contained 30 wt% of glass fibre and 1, 2, 5 and 10 wt% were improved with increasing total filler content. In the high content of total filler concentration, the interparticle distance of filler was reduced. These well adhered fillers can promote the stress transfer from the matrix with less occurrence of microspheres and fibre-polymer interfacial debonding [209]. Not only, the effective stress transfer of well-adhere glass fibres from the matrix, the addition of glass beads showed the positive effect. The presence of particles could also dissipate impact energy by pinning and bowing mechanisms [236, 266]. There are many studies [236, 266, 268-281] supported that the incorporation of rigid glass beads can increase the impact strength or toughness by increasing the crack resistance mainly through a crack-pinning mechanism [236, 271, 277, 279, 280]. The crack-pinning mechanism or crack deflection becomes the dominant mechanism of toughening [271]. It had been proposed earlier by Lange [273] and has since been modified and extended by Evans [281] and Green et al [272]. This may be a further energy absorption mechanism [275].

Basically, the pinning mechanism can be described by various literatures [269, 271, 272, 275, 277, 279, 280]. In the particulate composite system, the crack front moves to intersect the impenetrable obstacles, which may be the rigid and well-bonded particles. These particles can impede cracks by pinning down the crack and so cause the crack front to bow out between the particles acting as anchors in Figure 5.12 (a). These rigid filler particles create the obstruction to the propagation of the crack front and cause an increase in toughness by bowing out the crack front between the particles resulting in many secondary cracks as

elliptical shape at breakaway. Afterwards, both cracks grow around the fillers and these bifurcated crack propagation connect again later, with the delayed central crack. In systems where the obstacles or fillers are weaker, the particle or the particle-matrix interface may fail before the crack-bowing process is complete. In this case the glass beads with well-adhesion played a role in hindering the propagation of the crack [275]. The crack pinning is shown in Figure 5.12 (a) and (b). Work by Zotti et al. [276], supported that increasing the filler weight percent, crack pinning and crack deflection became the predominant failure modes [276].

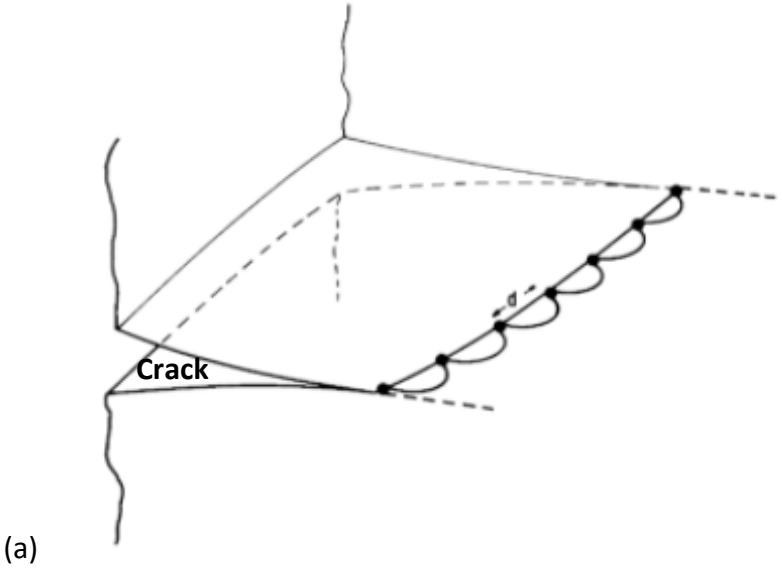

(a)

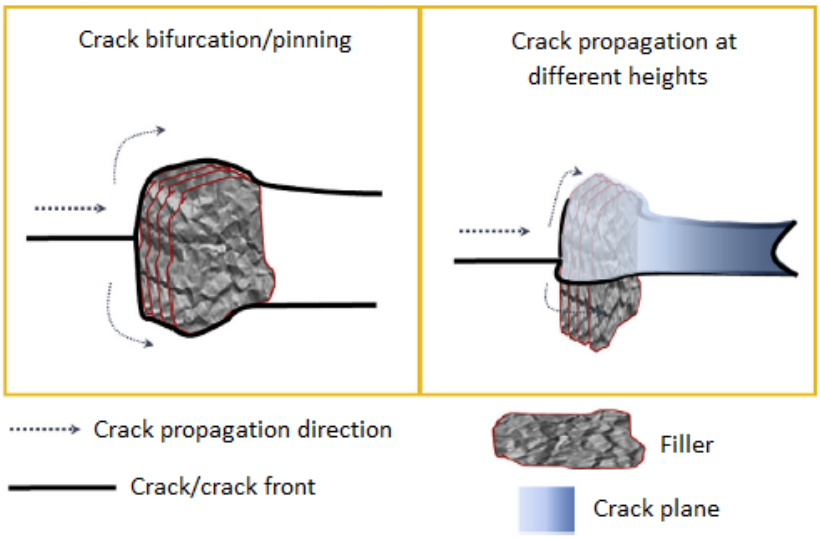

(b)

Figure 5.12: Schematics of (a) the interaction of the crack front. The straight line illustrates the crack front prior to the application of stress. The bowed position illustrates its configuration prior to breakaway and fracture [273] (b) diagram indicating the observed failure mechanism (white dotted line arrow indicate crack propagation direction) [269]

Moreover, another interesting idea was proposed by Spanoudakis et al. [270]. They described that the maximum stresses should be in the matrix above and below the poles of the particles in the particulate composites with well-bonded rigid particles. This means that propagating cracks will be attracted to the poles of the particles rather than their equators as shown in Figure 5.13.

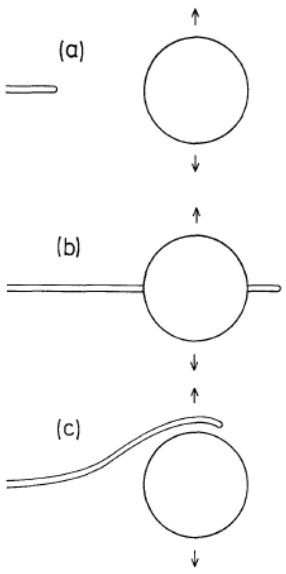

Figure 5.13: Schematic illustration of the path of a crack around a particle in a composite under stress. (a) Crack approaching particle. (b) Crack moving around equator or poorly-bonded particle. (c) Crack attracted to poles of well-bonded particle [270]

Regarding to the experimental results of mechanical properties of tensile, flexural modulus and Izod impact strength, it can be observed that these properties were improved with increasing the total filler contents. This is due to the synergistic effect from the addition of both of rigid fillers, which were glass bead and glass fibre can increase the rigidity of the hybrid composite [165, 236, 266, 280]. Moreover, the one of the important factors is the good interfacial adhesion between fillers and PP matrix from the incorporation of PP-g-MA as the compatibilizer, this can promote the well-adhered fillers, which can transfer stress from matrix more effectively [63, 68, 209]. The applications of 30 wt% glass fibres and 10 wt% of glass into neat PP (HC8) could be noticeably elevated the tensile and flexural moduli including Izod impact strength. The greatest tensile, flexural moduli and Izod impact strength were found to be in HC8 respectively. These properties were observed in HC8 when compared to pure PP. It displayed greater tensile, flexural modulus and impact strength compare to extruded neat PP, were 197%, 267% and 27% larger respectively.

5.4.2 Melt flow index

The measured melt flow index of neat PP and PP based hybrid composites are shown in Figure 5.14 and also are shown in Table D.4 in the Appendix D.

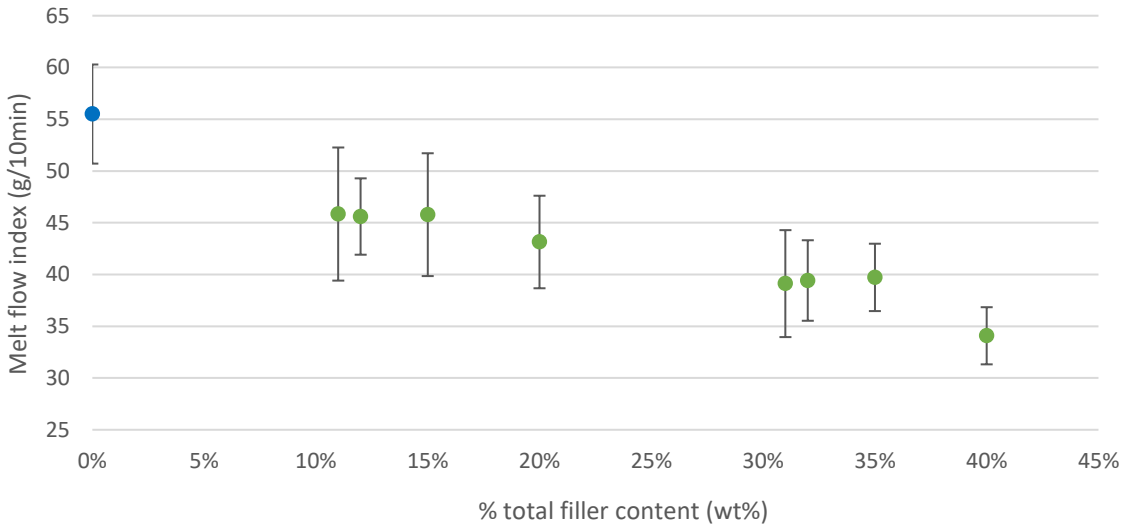

Figure 5.14: Melt flow index of neat PP and PP based hybrid composites versus the percentage of total filler content (%)

From Figure 5.14, it can be observed that MFI of all of hybrid composites decreased from neat PP, which is 55.5 g/10min. The change indicated an increase of viscosity of hybrid composite. This is because the incorporation of glass bead and glass fibre which are rigid filler to limit the molecular mobility and hinders melt flow of PP and increase the viscosity of PP composites at the melt stage [231].

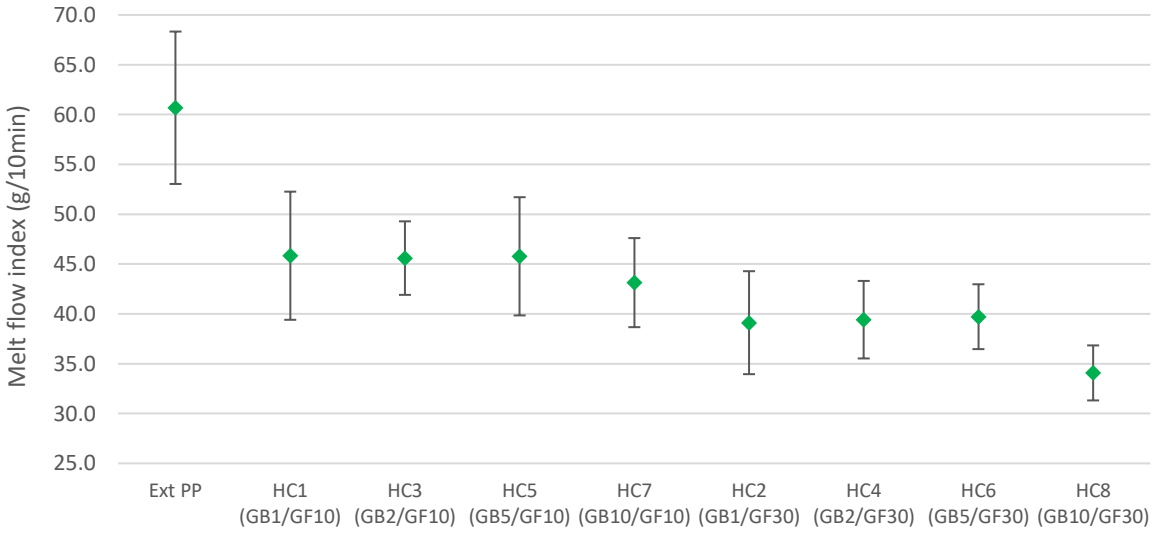

Figure 5.15: Melt flow index of extruded PP and PP based hybrid composites

From Figure 5.15, it can be seen that the values of average melt flow index of hybrid composites were separated into two groups, which relied on the content of glass fibre. The hybrid composites from 10 wt% of glass fibre with different glass bead contents from 1, 2 and 5 wt% had melt flow index in the range of 43 – 45 g/10 min. Meanwhile another group of hybrid composites with 30 wt% glass fibre and various glass bead content from 34 – 39 g/10min. It can be found that glass fibre influenced the viscosity of composite greater than glass bead by the natural properties of the filler itself [141]. The MFI of hybrid composites with 30 wt% of glass fibre were lower than hybrid composite with 10 wt% since the restriction of chain mobility due to this rigid fibre [231]. However, the MFI values of hybrid composites in the same content of glass fibre changed slightly. This is due to the spherical shape of glass bead, which act like tiny ball bearing. This can lubricate the overall composite flow or viscosity characteristics at the higher fibre loading. This can be supported by Milewski [235].

5.4.3 Density

The measured density of extruded PP and hybrid composites are shown in Figure 5.16 and in Table D.5 in the Appendix D .

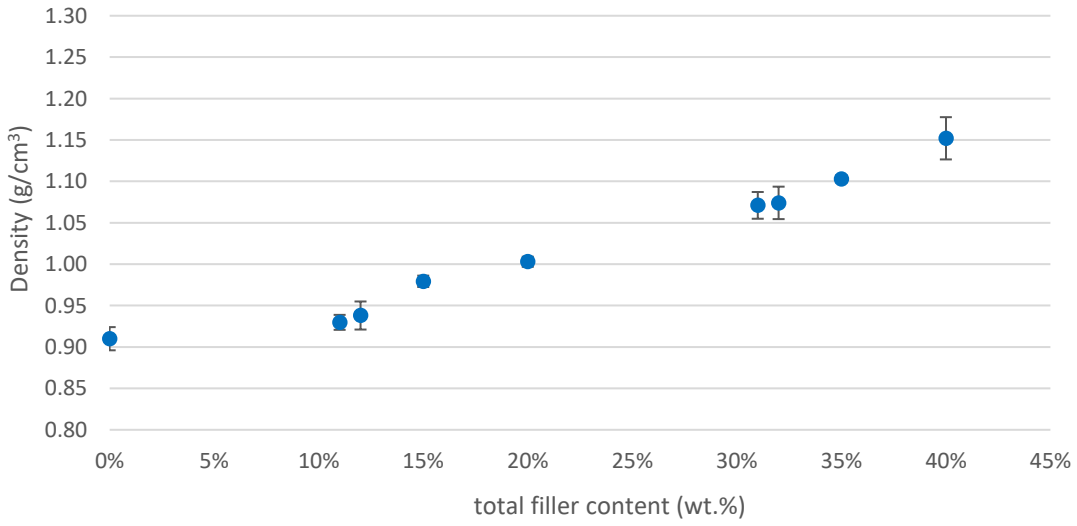

Figure 5.16: Density of extruded PP and neat PP based hybrid composites versus total content (%)

Figure 5.16 shows the effect of total content on the density of hybrid composite materials. It is obviously seen that the density of hybrid composites increased with the increase in total filler content. The density of hybrid composite was higher than 1 g/cm^3 at the higher 20% filler content, whereas it reached the value of 1.152 g/cm^3 at the total filler content of

40 wt%. Information of hybrid composites in Figure 5.15 reports that the increase was arisen linearly from the increasing total filler content in the composites. This is due to glass fibre and glass bead have the similar density (2.6 g/cm^3) as shown in Tables 4.12.

5.4.4 Composite cost (for raw materials)

The raw materials cost of hybrid composites were calculated from fillers and polymer based resin. They were calculated in GBP per one kilogram of composite are shown in Table 5.5.

Table 5.5: Composite formulation costs

Composites	Composite cost (GBP/kg)
Neat PP	1.70
HC1 (PP/GB1/GF10)	1.63
HC2 (PP/GB1/GF30)	1.48
HC3 (PP/GB2/GF10)	1.64
HC4 (PP/GB2/GF30)	1.49
HC5 (PP/GB5/GF10)	1.66
HC6 (PP/GB5/GF30)	1.51
HC7 (PP/GB10/GF10)	1.70
HC8 (PP/GB10/GF30)	1.54

From Table 5.5, it can be seen that all of the hybrid composites were not more expensive than neat PP. This is because the glass fibre and glass bead were cheaper than neat PP resin. The more added filler content contributed to the cheaper composite cost. However, the hybrid composite were added higher ratio of glass bead such as HC1, HC3, HC5 and HC7 were more expensive. This is due to the price of glass bead (EG731) was more expensive than glass fibre (CS331), which are 2.3 and 0.85 GBP/kg regarding to Table 4.7. The most expensive hybrid composite was HC7, which was added 10 wt%of glass bead and 10 wt% of glass fibre. The HC7's composite cost was 1.7 GBP/kg, which equivalent to neat PP.

5.5 Evaluation of hybrid composite performance

Regarding to targets for the selection of the most suitable hybrid composite, the criteria has been mentioned in Table 5.2.

For the evaluation, the measured experimental results of eight hybrid composites, which were designed by the guideline from Taguchi L8 were tabulated in Table 5.11.

Table 5.6: The percentage of change of PP composites

Composites	Tensile Modulus (MPa)	% Diff	Flexural Modulus (MPa)	% Diff	Impact strength (kJ/m^2)	% Diff
Extruded PP	1518.94		1227.3		4.50	
HC1 (GB1/GF10)	2217.84	46%	1881.9	53%	4.16	-8%
HC2 (GB1/GF30)	3718.06	145%	3645.4	197%	5.11	13%
HC3 (GB2/GF10)	2234.57	47%	1985.2	62%	4.25	-6%
HC4 (GB2/GF30)	3847.41	153%	3662.2	198%	5.14	14%
HC5 (GB5/GF10)	2411.42	59%	2319.3	89%	4.27	-5%
HC6 (GB5/GF30)	3937.41	159%	3800.2	210%	5.17	15%
HC7 (GB10/GF10)	2435.81	60%	2353.3	92%	5.08	13%
HC8 (GB10/GF30)	4505.76	197%	4501.5	267%	5.73	27%

The overall improvements of mechanical properties, MFI, density and composite costs were rated follow the rating definition, which has been mentioned in Table C.6 – C.8 in Appendix C**.** These calculated rating values in the range of -5 to 5 by establishing the value of extruded PP as reference. The rating of PP based hybrid composites are shown in Table D.6 in Appendix D. The positive rated values mean the higher values comparing to extruded PP while negative values represent lower values of each properties. Furthermore, the experimental results were rated and summarized as radar charts in Figure 5.17.

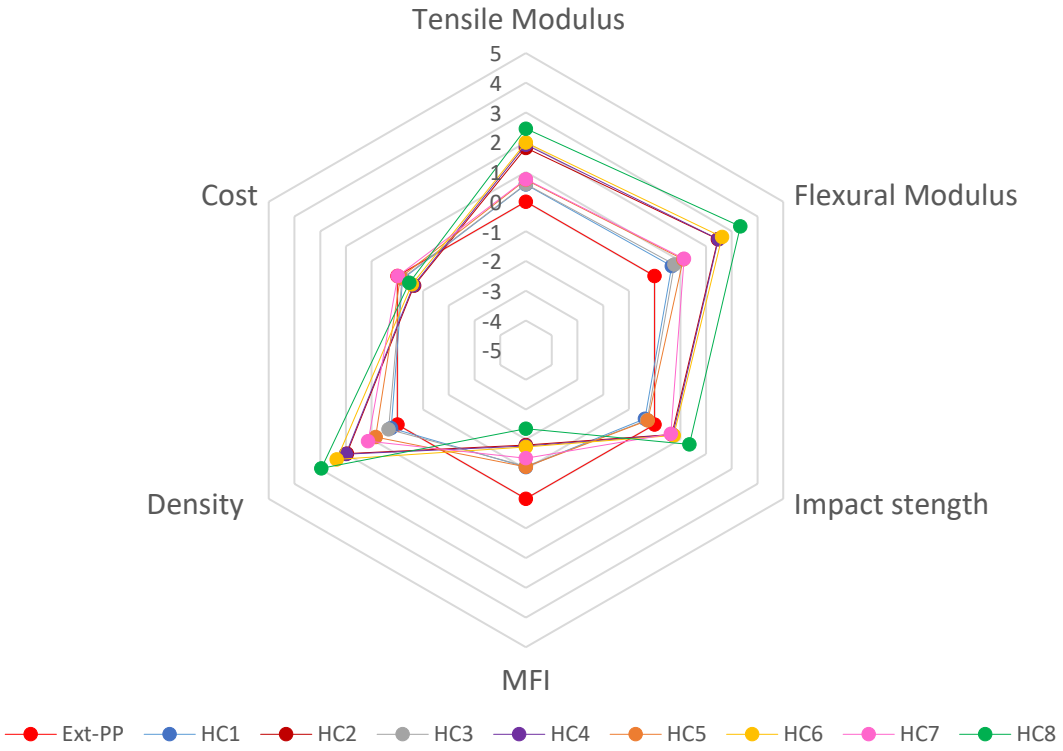

Figure 5.17: Radar chart compares extruded PP and PP based hybrid composites

From the radar chart in Figure 5.17, it can be seen that HC8, PP hybrid composites with 10 wt% of glass bead and 30 wt% of glass fibre was considered as the most suitable formulation among all of hybrid composite formulations. This is due to the superior mechanical properties e.g. tensile, flexural modulus and Izod impact strength, cheaper cost according to the supported information as mentioned earlier. Moreover, the density and melt flow index were acceptable at 1.152 g/cm^3 and 34.1 g/10min, which was not higher than 1.3 g/cm^3 and not less than 10g/10min, which were set as the criteria for density and MFI.

From the preliminary evaluation of the performance of hybrid composites, it can be observed that there were some rooms of further improvements in term of density and melt flow index. The additional experiments was investigated for the further improvements in term of mechanical properties with the acceptable range of density, which will be affected to the dimension stability, weight of manufactured part and MFI, which affects to processability.

The additional experiments were established based on trends of mechanical properties, which increased with increasing total filler content in Figures 5.6, 5.8 and 5.10. The additional experimental setting was studied by starting at the formulation of HC8 with 10 wt% of glass bead and 30 wt% of glass fibre. These experiments were formulated to investigate the effect of ratio of glass bead content in hybrid composites with the constant glass fibre content at 30 wt% in the further glass bead amounts and effect of glass fibre content in hybrid composites. The additional experiments were shown in Table 5.7.

Table 5.7: Additional experimental runs for further evaluation.

Experiment number	Glass bead Content (%wt.)	Glass fibre Content (%wt.)
HC9	7.5	30
HC10	15	30
HC11	20	30
HC12	15	35
HC13	10	40
PP/GF40	0	40
PP/GF50	0	50

From Table 5.7, HC9 was designed to investigate the gap between HC6 and HC8, which contained 5 wt% and 10 wt% of glass bead and confirm the properties of hybrid composites and carried out the exact trend of composites. HC10 and HC11 were designed to follow the hybrid composites' properties with the increasing glass bead content. To investigate the

effect of glass fibre content of hybrid composite, HC12 and HC13 were designed to indicate the effect of hybrid composite on increased glass fibre content. The properties of HC13 were compared to H7 and HC8, which contained different glass fibre content at the constant glass bead content at 10 wt%. Not only the properties of hybrid composites were characterized, the PP/glass fibre composite with 40 wt% and 50 wt% were prepared in order to compare with hybrid composites. The properties of hybrid composites were discussed as followed.

5.5.1 Mechanical properties

5.5.1.1 Tensile modulus

The experimental results of tensile modulus from these additional experiments are shown in Figure 5.18 and also in Table D.7 in Appendix D.

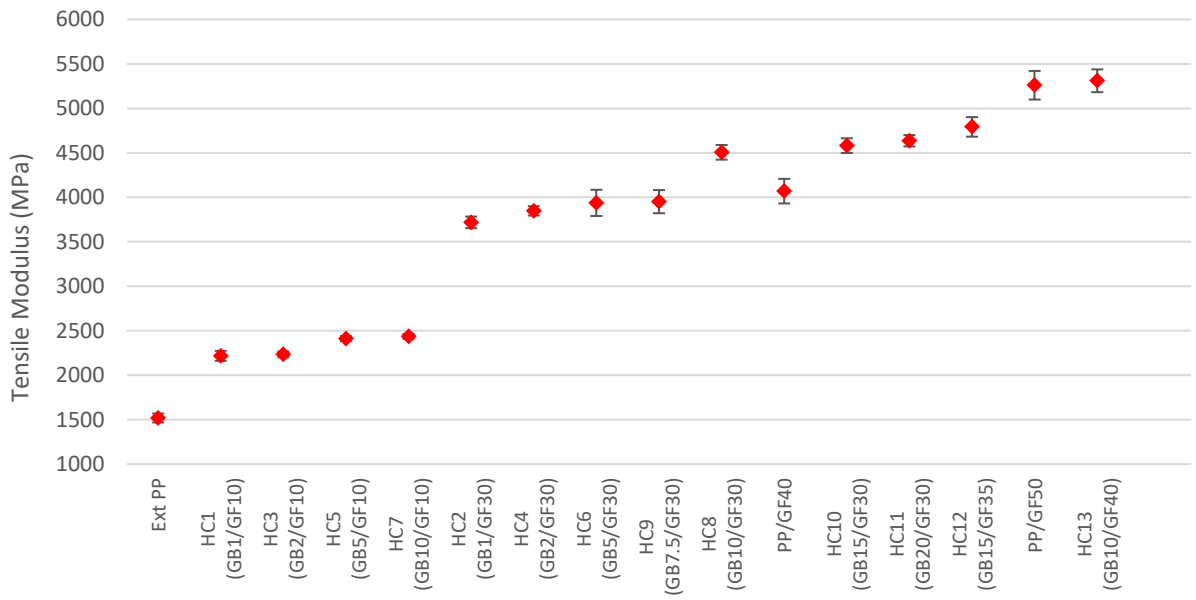

Figure 5.18: Tensile modulus of extruded PP, PP based composite and hybrid composites in different percentage by weight of glass bead and glass fibre (%).

From Figure 5.18, it can be observed that tensile modulus of PP/glass bead/glass fibre hybrid composite increased with the total concentration of filler in the system. This similar behaviour was also reported earlier in the literature data [264]. The enhancement in modulus was due to the overall reason of the rigidness of treated glass beads and treated glass fibres with the well-bonded with PP matrix influence the stiffness of the whole bulk of composite by restrict the mobility of polymer molecule [165, 246]. In case of the tensile modulus of hybrid composites of HC11, HC12 and HC13, which were incorporated with 50 wt% of total filler, the

tensile modulus were decreased with increasing ratio of glass bead content. It can be seen that average tensile modulus of HC11 was 4,636.1 MPa, which was the lowest comparing to HC12 and HC13, which had average tensile modulus as 4,791.8 and 5,310.4 MPa respectively. The ratio of glass bead in HC11 was 0.4 of the total filler content while the glass bead ratio of HC12 and HC13 were 0.3 and 0.2 respectively. The mechanical performance of hybrid composite with aminosilane-treated 40 wt% of glass fibre and 10 wt% of glass bead indicated that tensile modulus were improved comparing to PP/glass fibre of equivalent glass fibre content at 50 wt%. On the other hand, the tensile property of this same total content of HC11 and HC12 showed the decrease in tensile modulus with increasing glass bead content [209]. It can be found that the tensile modulus of the hybrid composites is a function of the relative concentration of glass fibre in the total reinforcement concentration. This finding was supported by the previous work by Morelli et al. [282] In this case, it can be noted that the glass fibre mainly affected to performance of hybrid composite since glass fibre can more effectively enhance the stiffness than particles. This similar effect can be referred to the previous reports [134, 283, 284].

5.5.1.2 Flexural modulus

The experimental results of flexural modulus from the additional experiments are shown in Figure 5.19 and also in Table D.8 in the Appendix D.

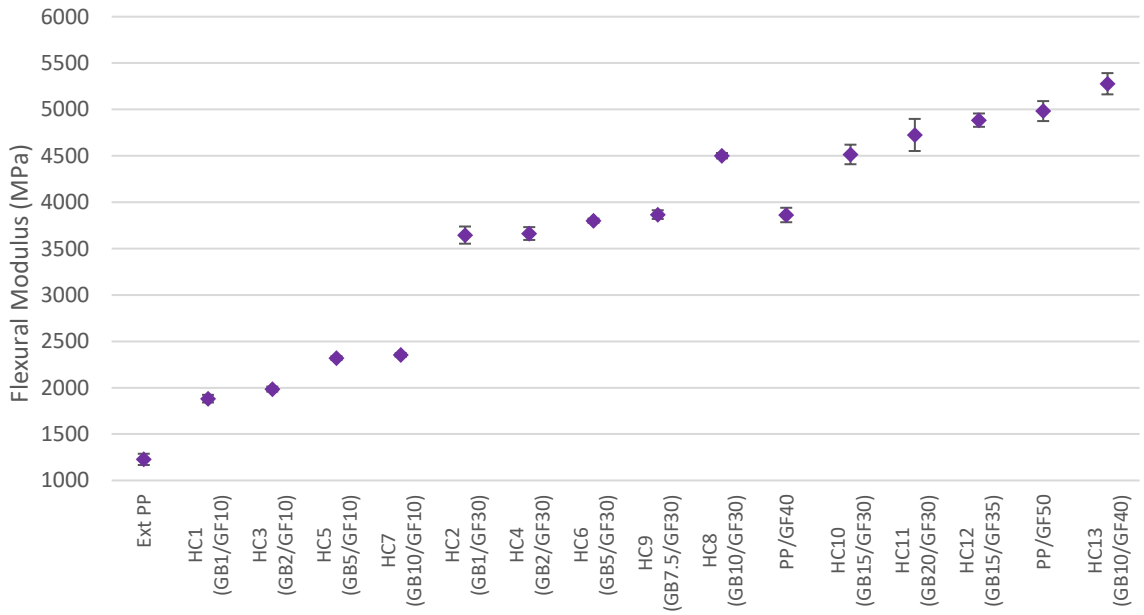

Figure 5.19: Flexural modulus of extruded PP, PP based composite and hybrid composites in different percentage by weight of glass bead and glass fibre (%)

The trend was observed in flexural tests resembled the tensile testing as shown in Figure 5.19. Utilizing 40 wt% of glass fibre and 10 wt% of glass bead for HC13 enhanced flexural modulus to 5,277.1 MPa. While, the flexural modulus of HC11 and HC12 were 4,724.7 and 4,884.7 MPa respectively, which were less than PP/glass fibre composite with the same total filler content. However, the flexural modulus of HC13 was improved by 6% from PP/50 wt% of glass fibre. The reinforcing effect of glass bead and glass fibre was clearly demonstrated in the flexural modulus of composites. The modulus of the hybrid glass bead and glass fibre was higher than the PP composite with glass fibre, which the same total filler content. It can be observed the properties of PP/GF40 versus HC8 and PP/GF50 versus HC13. Therefore, it could be indicated that a positive synergistic effect was managed between glass fibre and glass bead in stiffness. These flexural properties enhancement was more pronounced in the hybrid composites of suitable ratio of glass bead and glass fibre. This phenomenon can be described with the similar explanation as mentioned in the tensile properties.

5.5.1.3 Izod impact properties

The experimental results of Izod impact strength from the additional experiments are shown Figure 5.20 and also in Table D.9 in the Appendix D.

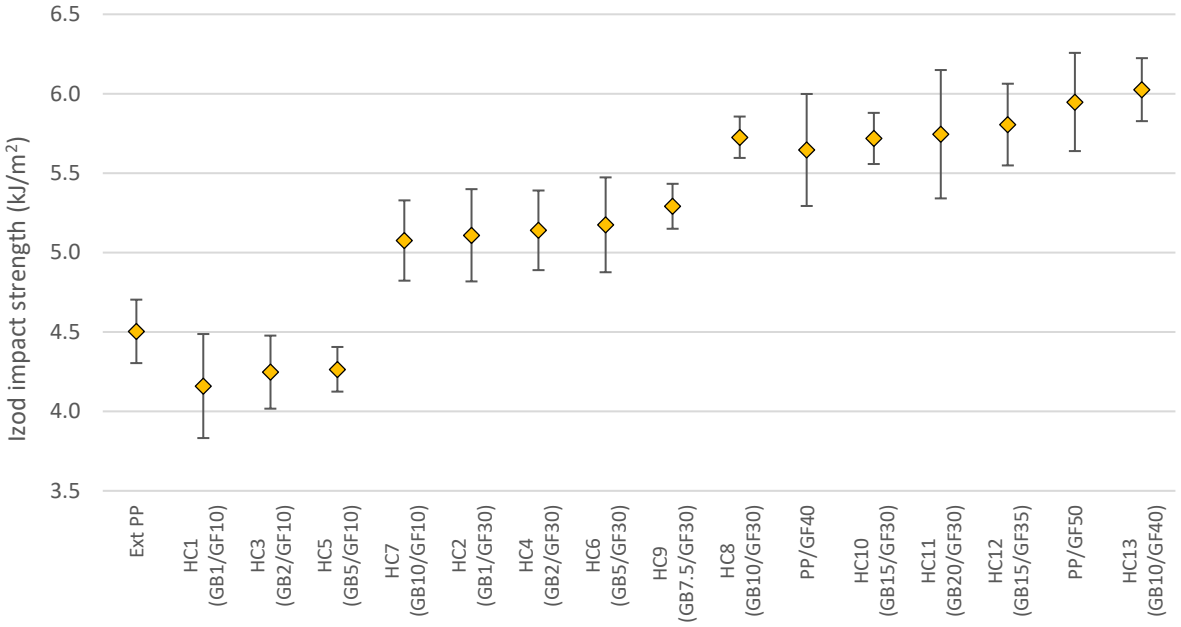

Figure 5.20: The Izod impact strength of extruded PP, PP based composite and hybrid composites in different percentage by weight of glass bead and glass fibre (%)

From Figure 5.20, the Izod impact strength of hybrid composite increased with increasing total filler content. This trend relied to the experimental results from Izod impact strength of hybrid composites, which was discussed earlier in the topic 5.3.5.3. The presence of particles in the optimum content could also dissipate impact energy by pinning and bowing mechanisms, which was supported by many literatures [236, 266, 268-281] and was discussed earlier. As can be seen from Figure 5.20, HC13 had the highest Izod impact strength comparing to HC11 and HC12, which contained 50 wt% of total glass fillers. The ratio of glass bead content in HC13, which was less than HC11 and HC12 in high total filler content can influence to higher Izod impact strength of HC13. This result can be supported by the similar findings [267, 285]. Moreover, it is quite clear to consider the information in Figure 5.4, it is presented that the impact strength of the PP/glass bead composites first increased with increasing glass bead content up to 10 wt%, thereafter, it decreased. This is because too high glass bead content caused the accumulation or agglomerate phenomenon of the filler in the matrix, which can be generated easily because of bad dispersion when the particle concentration is quite high. This will lead to a decrease in the impact strength. This phenomenon can be supported by the previous investigation [102, 267]. Moreover, these agglomerations can obstruct the stress transfer mechanism of glass fibre in hybrid composite. However, it can be noticed a bit better average impact strength for hybrid composite comparing to PP/glass fibre composites in the same total content in PP/GF40 versus HC8, PP/GF50 versus HC13. In this case, the hybridization synergistic effect was quite not so advantageous. This is due to the high aspect ratio glass fibre mainly affected to performance of hybrid composite since glass fibre can more effectively enhance the toughness than the pinning effect from glass bead, which had lower aspect ratio [209, 236].

5.5.2 Morphological properties

The fractographs of neat PP hybrid composites were commonly studied using SEM to observe the V-notched Izod impact-fractured surface of the hybrid composites. Some specimens of hybrid composites were selected by considering the neat PP hybrid composites filled with 30 wt% of glass fibre and different glass bead contents from 1-20 wt% and sample from hybrid composites with 40 wt% of glass fibre and 10 wt% of glass bead, which was the highest mechanical performance in this study. The micrographs of these samples are shown in Figure 5.21.

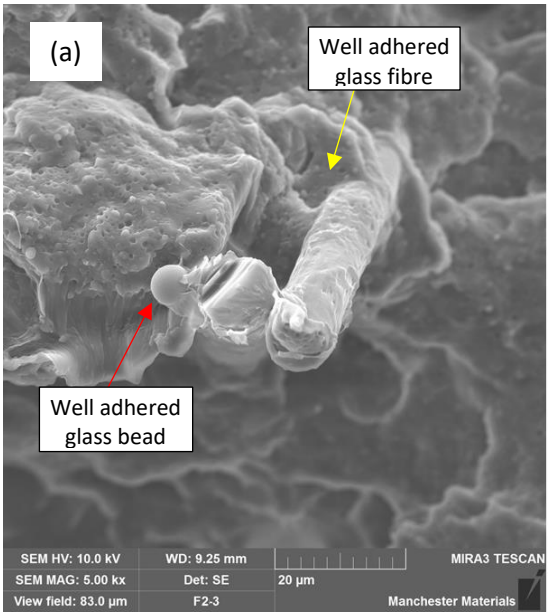
(a)
Well adhered glass fibre
Well adhered glass bead
SEM HV: 10.0 kV
WD: 9.25 mm
MIRA3 TESCAN
SEM MAG: 5.00 kx
Det: SE
20 µm
View field: 83.0 µm
F2-3
Manchester Materials

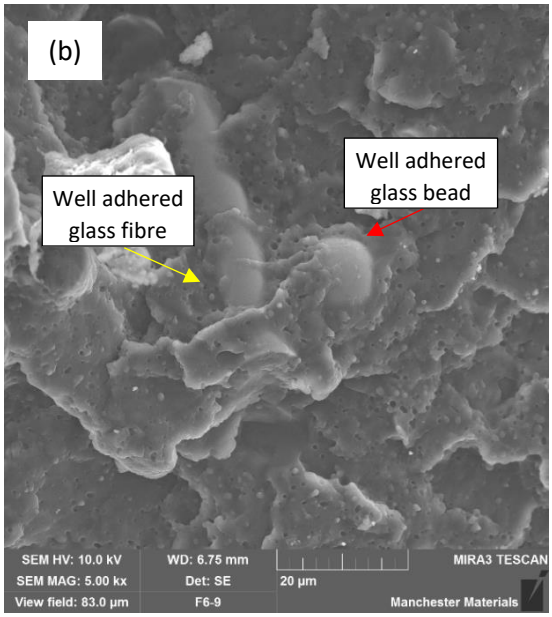
(b)
Well adhered glass bead
Well adhered glass fibre
SEM HV: 10.0 kV
WD: 6.75 mm
MIRA3 TESCAN
SEM MAG: 5.00 kx
Det: SE
20 µm
View field: 83.0 µm
F6-9
Manchester Materials

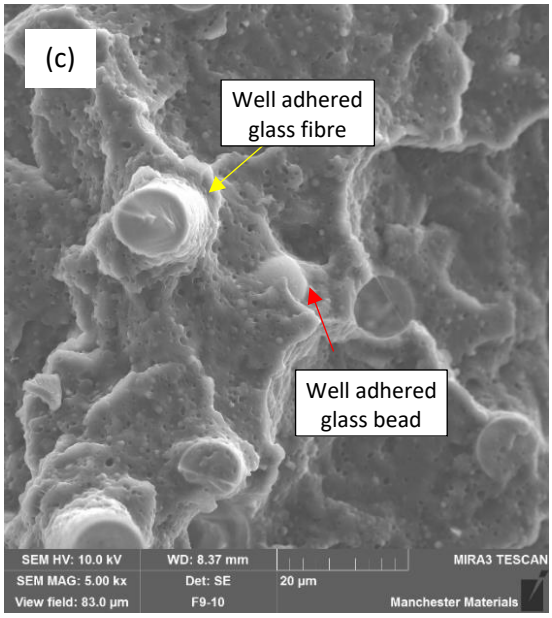
(c)
Well adhered glass fibre
Well adhered glass bead
SEM HV: 10.0 kV
WD: 8.37 mm
MIRA3 TESCAN
SEM MAG: 5.00 kx
Det: SE
20 µm
View field: 83.0 µm
F9-10
Manchester Materials

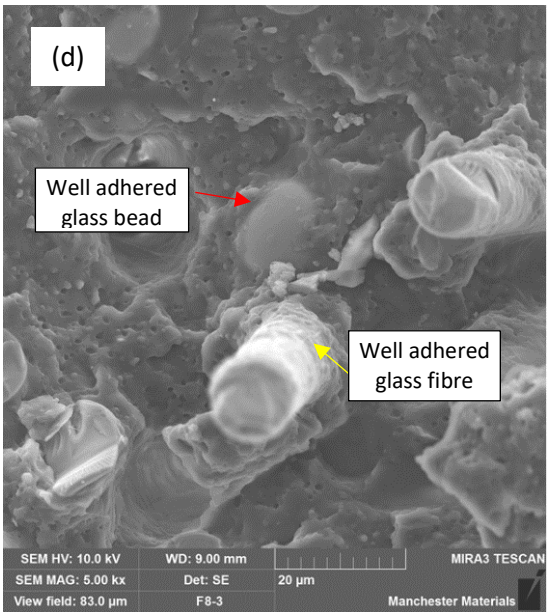
(d)
Well adhered glass bead
Well adhered glass fibre
SEM HV: 10.0 kV
WD: 9.00 mm
MIRA3 TESCAN
SEM MAG: 5.00 kx
Det: SE
20 µm
View field: 83.0 µm
F8-3
Manchester Materials

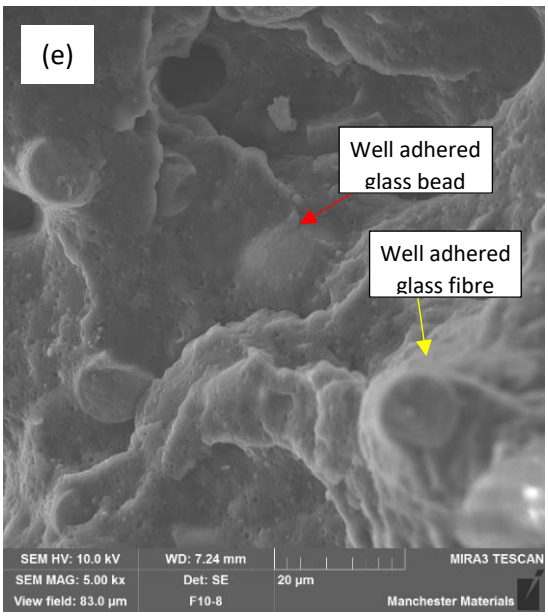
(e)
Well adhered glass bead
Well adhered glass fibre
SEM HV: 10.0 kV
WD: 7.24 mm
MIRA3 TESCAN
SEM MAG: 5.00 kx
Det: SE
20 µm
View field: 83.0 µm
F10-8
Manchester Materials

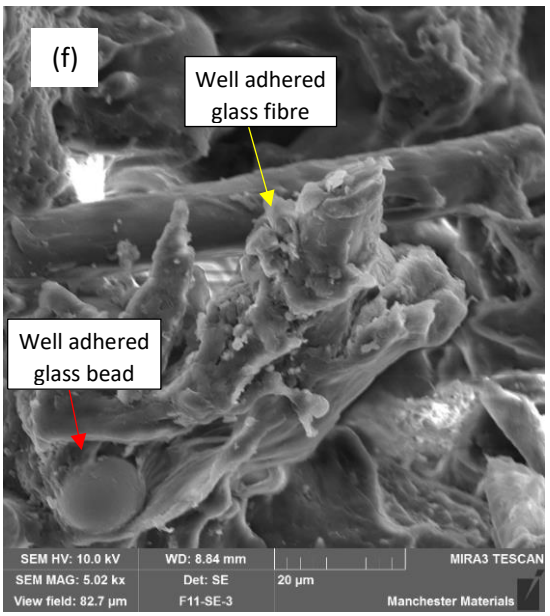
(f)
Well adhered glass fibre
Well adhered glass bead
SEM HV: 10.0 kV
WD: 8.84 mm
MIRA3 TESCAN
SEM MAG: 5.02 kx
Det: SE
20 µm
View field: 82.7 µm
F11-SE-3
Manchester Materials

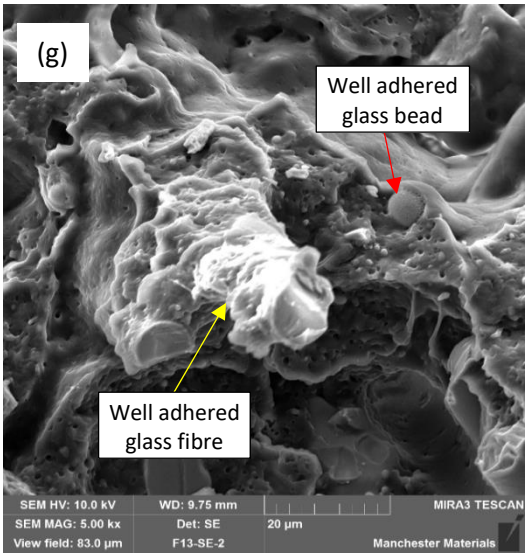

Figure 5.21: The micrographs of the fracture surfaces of Izod sample at 5000x of PP hybrid composites with 30 wt% of glass fibre and different glass bead contents (a) 1 wt% (b) 5 wt% (c) 7.5 wt% (d) 10 wt% (e) 15 wt% (f) 20 wt% (g) PP hybrid composites with glass bead 10 wt% and glass fibre 40 wt% at 5000x

As shown in Figure 5.21, it can be found that the fractured surface of PP hybrid composite from Izod impact specimen had rough surface from the surrounded polymer mass at the fibres. There is no visible splitting between the glass and the polymer. The very good better polymer matrix wetting of glass fibres in the composite with aminosilane-treated glass bead and glass fibre could be observed. These can be indicated the strong adhesion between glass bead, glass fibre and PP matrix from the compatibilizer (PP-g-MA) [63, 68]. PP-g-MA was added in each formulation with 0.15 time of total filler concentration [174]. The strong interfacial adhesion was observed. PP Hybrid composites containing aminosilane-treated glass bead and glass fibre, the interfacial compatibilization reaction occurs through strong amide and imide covalent bonds between amine ($-NH_2$) and maleic anhydride (-MA) co-reactive functional groups, which is considered to be of higher reactivity according to Orr et al. [286, 287]. Thus, the chemical interfacial compatibilization between the maleic anhydride functionalized PP compatibilizer present in PP matrix and the aminosilane-treated glass bead and glass fibre had greater efficiency in promoting the verified strong PP polymer-glass filler interfacial adhesion [209]. It is clear that in PP hybrid composites containing 30 wt% of treated glass fibre and various treated glass bead content with 0.15-fold of PP-g-MA addition [174]. It is possible to increase in the strength and toughness from the mechanical improvement, which were mentioned earlier. These enhancement in the strength and toughness of hybrid PP composite with the use of compatibilizer can be explained based on the more secured

anchoring of the treated filler to PP matrix. It can be seen the ligaments that were created in the interfacial regions between PP matrix and treated glass fibre and glass bead. These ligaments played the role of anchor, which improve the interfacial adhesion between the treated fillers and PP matrix. This led to significant improvement in the strength and toughness of the resulting composite. This phenomenon can be supported by the similar investigation by Patankar et al [288].

According to the overall mechanical properties, which were mentioned earlier, HC13, the hybrid composite with 40 wt% of glass fibre and 10 wt% of glass bead was the highest mechanical in terms of tensile, flexural moduli and Izod impact strength. Therefore, this sample was selected to analyze SEM at the inner matrix plain to investigate fibre and bead orientation. The micrograph of the inner plain of HC13 is shown in Figure 5.22.

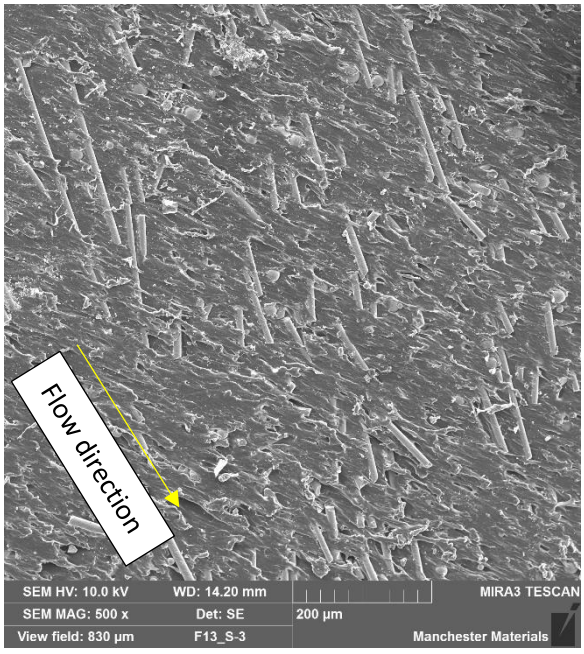

Figure 5.22: The micrographs of the inner surface of PP hybrid composites filled with 30 wt% of glass fibre and 10 wt% of glass bead contents at 500x

Figure 5.22 shows the inner surface of PP hybrid composites filled with 30 wt% of glass fibre and 10 wt% of glass bead contents at 500x, which was prepared by injection molding. It was subjected to morphological characterization. SEM with low magnification was used to determine the dispersion and orientation of the filler inside the PP matrix. It can be observed that most of glass fibres in the matrix were aligned in the flow direction in similar injection molded samples. This scenario was similar to previous work by Abdelwahab et al. and Gomez-

Monterde et al. [283, 289]. This observation was associated with the enhancement of stress distribution and influence high values in mechanical properties such as tensile and flexural test [283].

5.5.3 Spectroscopic properties

To indicate the presence of fillers in the neat PP hybrid composites, infrared spectroscopy technique was used in order to identify each functional group by referring from the difference in vibrational energy absorption. These detected functional groups can indicate the existence of filler and chemical bonding in PP matrix.

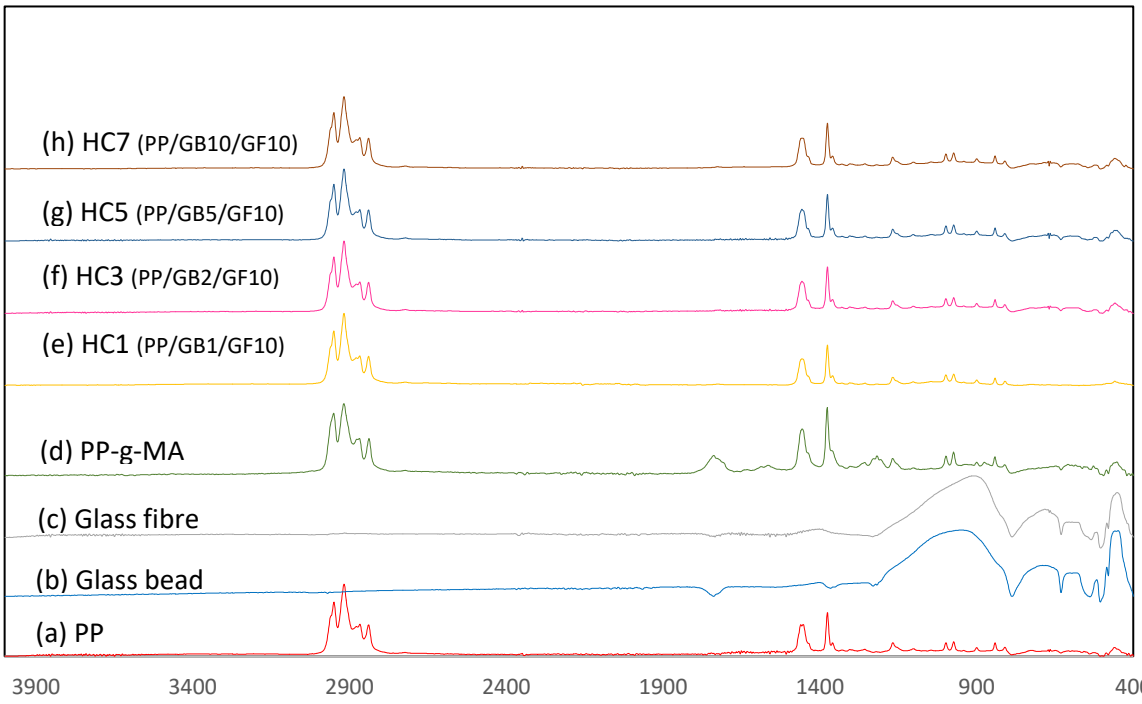

Figure 5.23: ATR-FTIR spectra of neat PP, glass bead, glass fibre, PP-g-MA and neat PP based hybrid composite (e) HC2, (f) HC4, (g) HC6, (h) HC8, (i) HC10, (j) HC11, (k) HC12 and (l)HC13

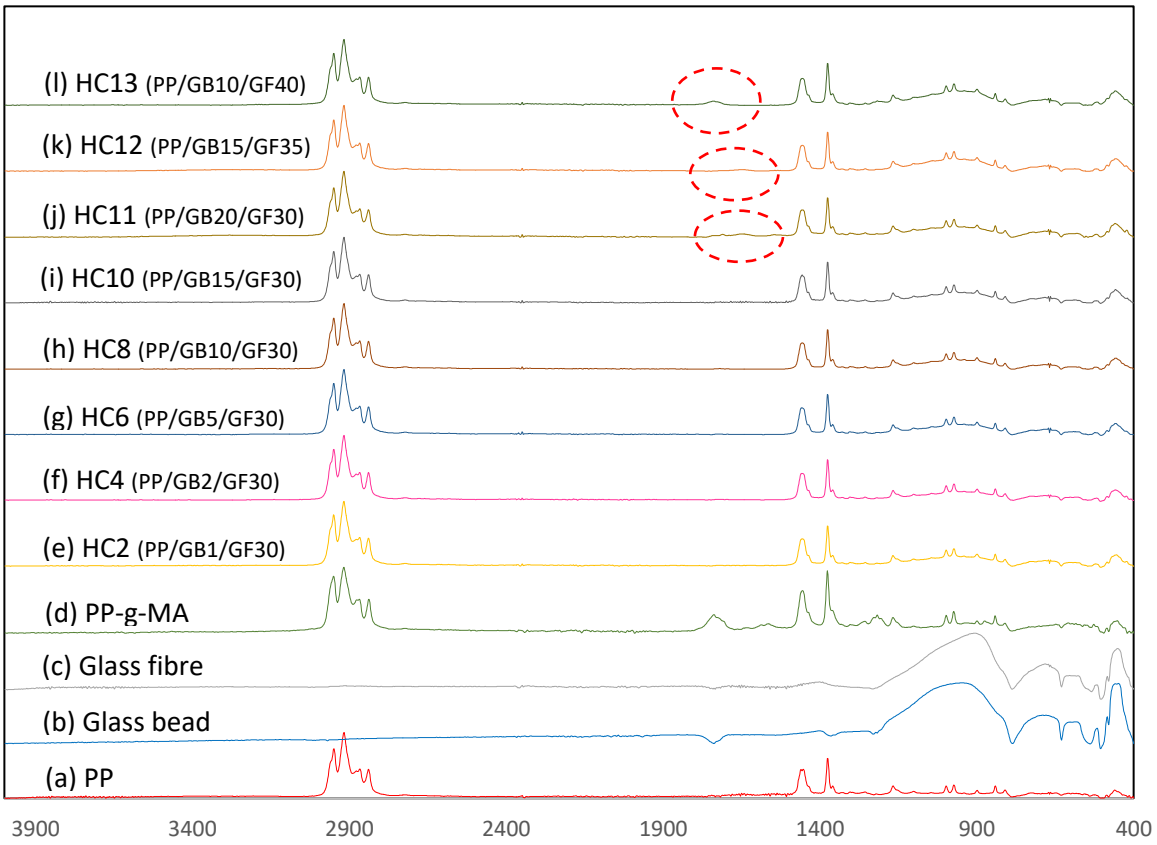

Figure 5.24: ATR-FTIR spectra of neat PP, glass bead, glass fibre, PP-g-MA and neat PP based hybrid composite (e) HC2, (f) HC4, (g) HC6, (h) HC8, (i) HC10, (j) HC11, (k) HC12 and (l)HC13

From the FTIR spectrum of glass bead and glass fibre, which are shown in Figure 5.23 (b,c) and 5.24 (b,c), it is obvious that both of filler have the similar structure It can be noticeable that the board peaks around 450 – 470 and 900 – 1,100 cm^{-1} of glass bead and glass fibre in Figure 5.23 (b,c) and 5.24 (b,c). The peak around 450 – 470 cm^{-1} peaks are referred to (O-Si-O) bending vibrations mode, while peak around 760 – 1,200 cm^{-1} can be indicated to (Si-O) asymmetric stretching and Si-O (in the SiO_4 tetrahedron), which are the structure of glass bead and glass fibre [226].

In order to identify the presence of glass bead and glass fibre by ATR-FTIR, it may be not indicated clearly the existence of glass bead and glass fibre in Figure 5.17 (e, f, g, h), which show ATR-FTIR spectra of neat PP, glass bead, glass fibre, PP-g-MA and neat PP based hybrid composite filled glass fibre 10 wt% and various glass bead content from 1,2,5 and 10 wt%. It can be unclearly seen the peak around 450–470 cm^{-1} are referred to (O-Si-O) bending vibrations mode and very low board peak around 900 – 1,100 cm^{-1} can be indicated to (Si-O) asymmetric stretching and Si-O (in the SiO_4 tetrahedron). It can be observed that the height

of peaks increased with increasing filler content. Moreover, the peak of Maleic Anhydride in PP-g-MA was shown around 1,650 – 1,850 cm^{-1}, which is referred to carbonyl frequency range of the anhydride [290], in Figure 5.17 (d) and 5.18(d). The peak of Maleic Anhydrid around 1,650 -1,850 cm^{-1} cannot be visible since the total concentration of Maleic Anhydride in the hybrid composites were very low (0.017 – 0.03 wt%). Therefore, this peak cannot be detected regarding to the one of limitations of ATR-FTIR technique is a relatively low sensitivity [225]. However, ATR-FTIR spectra of hybrid composites with higher total filler content, which had total filler concentration more than 45 wt% such as HC11, HC12 and HC13, show very small peaks around 450 – 470 cm^{-1}. This peak indicated to (O-Si-O) bending vibrations mode and board peak around 900 – 1,100 cm^{-1} referred to (Si-O) asymmetric stretching and Si-O (in the SiO_4 tetrahedron). The height of peaks were higher due to higher total PP-g-MA content in hybrid composites, which were about 0.075 wt%. These Maleic Anhydride peaks can be indicated the adhesion between fillers and PP matrix.

From the ATR-FTIR spectra of PP composites were mentioned, the important chemical functional groups are shown in the Table 5.8.

Table 5.8: Wavenumber and assignment of the major IR band of PP hybrid composites

Wave number (cm^{-1})	**Major functional group**
450 – 470	O-Si-O bending vibrations mode [226]
900 – 1,100	Si-O asymmetric stretching Si-O in the SiO_4 tetrahedron [226]
1,650 -1,850	C=O symmetric stretching of carbonyl frequency range of the anhydride [290]

5.5.4 Rheological behaviour

From the shear viscosity curve that was obtained from rotational rheometer in Figure 5.25. The samples of PP based hybrid composites were selected for rheology analysis at on steady shear flow mode, which the shear rate was in range of 0.1 – 10 s^{-1} at 210 ^{o}C to investigate the change of viscosity over the shear rates.

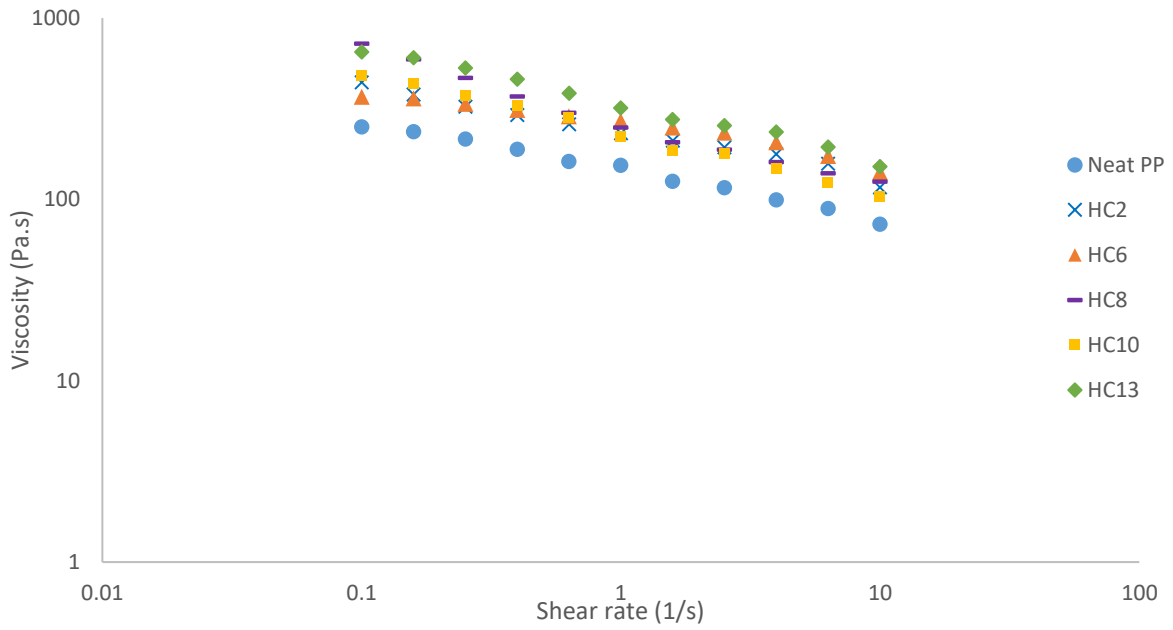

Figure 5.25: Viscosity curves of neat PP, PP hybrid composite with 30 wt% of glass fibre and different glass bead content at 1,5,10 and 15 wt% and PP hybrid composite with 40 wt% of glass fibre and 10 wt% of glass bead.

From Figure 5.25, it can be seen that the viscosity of all samples from neat PP and PP hybrid composites decreased as the shear rate increases. This can be further noted that the shear thinning behaviour of the materials [230]. All of selected PP composites were more viscous than neat PP due to the entanglements of glass fibres with the synergy of glass bead that obstruct polymer chain mobility [231]. The results for these polymers show similarities in the same trends at higher shear rate but the viscosity was lower due to high shear rate [230, 235]. Furthermore, it can be seen that HC13 had the highest viscosity due to it contained 40 wt% of glass fibre and had highest total filler content. The high content of glass fibre can restrict the polymer chain motion by the entanglements of glass fibres obstruct polymer chain mobility [231, 232].

From the viscosity curves, it can be observed that the viscosity was influenced by the interaction between glass beads and molten polymer. At low filler contents of glass bead at 1 and 5 wt% in HC2 and HC6, the viscosity was slightly higher than HC8 and HC10, which contained higher glass bead at 10 and 15 wt%. This is because at lower glass bead content, interaction between surface of glass beads and molten polymer played a significant role to decreases the flowability, resulting in the increase of the viscosity. Meanwhile, the slippage between glass beads was the dominating effect at higher filler content and resulting in the decrease of the viscosity. This observation was considered at the higher shear rate (higher

than 1 s^{-1}), this is due to the variation of the viscosity in relative low shear rate was more significant than at higher shear rate. This finding had similar trend compared to the previous study from Yang et al [230].

5.5.5 Melt flow index

The melt flow index of additional hybrid composites are shown in Figure 5.26 and their raw data were exhibited in Table D.10 in Appendix D.

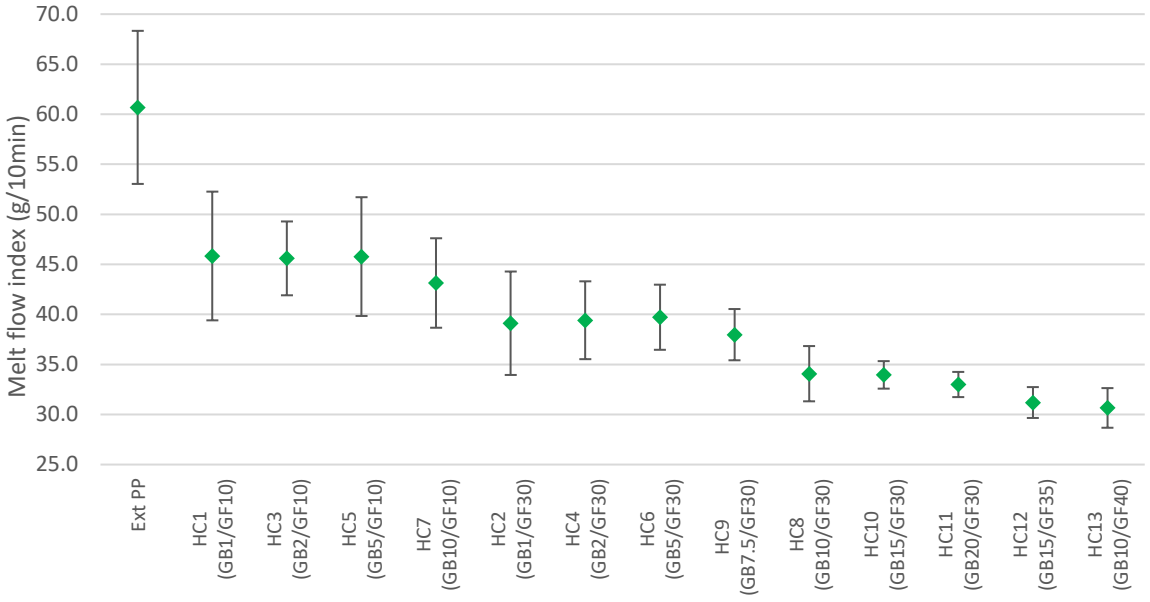

Figure 5.26: Melt flow index of neat PP and PP based hybrid composites

From Figure 5.26, it can be observed that average MFI of of HC11, HC12 and HC13 which are hybrid composite with 50 wt% of total content were similar, which in the range of 30.24 – 31.50 g/10min. This is due to the spherical shape of glass bead, which can lubricate and maintain the overall composite flow or viscosity characteristics [235]. Figure 5.26 shows all of average MFI of hybrid composites. It is obvious to see that MFI of hybrid composites decreased with the inclusion of filler. The change indicated an increase of viscosity of hybrid composite. This is because the incorporation of glass bead and glass fibre, which are rigid filler to limit the molecular mobility and hinders melt flow of PP and increase the viscosity of PP composites at the melt stage [231]. However, the incorporation of glass bead played important role to maintain melt viscosity due to the spherical shape [235].

5.5.6 Thermal stability

The DSC thermograms of the samples of neat PP and the neat PP based hybrid composites are shown in Table 5.8 and Figure D.1 – D.6 in Appendix D. The samples were selected from all of neat PP based hybrid composites by grouping into group of hybrid composite with glass fibre content at 30 wt% varying glass bead content at 1,5,10 and 15 wt% (HC2, HC6 HC8 and HC10) and the group of hybrid composite with glass bead content at 10 wt% varying glass fibre content at 10,30 and 40 wt% (HC2, HC6 HC8 and HC10). The values of crystallization temperature (T_c), the melting temperature (T_m), melting transition enthalpy (ΔH_m) and crystallization enthalpy (ΔH_c) were calculated from the DSC curves, and the results are summarized in Table 5.8. Furthermore, the percentage of the crystallinity of samples (X_c) was calculated using Equation 5.1:

$$X_c\ (\%) = \frac{\Delta H_m}{\Delta H_o \times w} \times 100 \qquad 5.1$$

in which w means weight fraction of PP, ΔH_m for melting enthalpy and ΔH_o for theoretical melting enthalpy of the 100% crystalline PP, which is 209 J/g [56].

Table 5.9: DSC-determined thermal characteristics of PP composites

Samples	T_c (°C)	ΔH_c(J/g)	T_m (°C)	ΔH_m(J/g)	X_c (%)
Neat PP	113.89	93.85	162.99	78.30	37.5
Hybrid composites (Fix glass fibre at 30 wt%)					
HC2 (PP/GB1/GF30)	114.8	68.6	160.8	55.3	38.3
HC6 (PP/GB5/GF30)	116.1	63.7	160.7	53.9	39.7
HC8 (PP/GB10/GF30)	115.1	64.4	159.5	61.8	49.3
HC10 (PP/GB15/GF30)	114.4	48.3	162.3	42.1	36.6
Hybrid composites (Fix glass bead at 10 wt%)					
HC7 (PP/GB10/GF10)	115.2	84.3	159.2	68.7	41.1
HC8 (PP/GB10/GF30)	115.1	64.4	159.5	61.8	49.3
HC13 (PP/GB10/GF40)	114.9	55.3	159.6	47.9	45.8

From Table 5.9, it is observed that neat PP based hybrid composites had the crystallization temperature higher than neat PP. This means that the initial of crystallization get a bit delayed about 1 – 2 °C when compared with neat PP. This is shown that the incorporation of glass beads and glass fibre has promoted the nucleating effect in the PP. The heterogeneous inclusion of glass bead and glass fibre in PP enhances crystallization with the formation of

spherulites, and the presence of glass bead and glass fibre increased the nucleation acts as an excellent nucleating agent in PP [148, 291].

From Table 5.9, it is notable that the percentage of crystallinity of hybrid composites from two groups showed a trend of first increasing and then decreasing with increasing the filler content. For the group of hybrid composites with 10 wt% of glass bead, it can be seen that X_c reached a maximum value at 49.3% at 30 wt% of glass fibre, then X_c dropped at the higher glass fibre content of 40 wt%. This trend occurred to another group with 30 wt% of glass fibre, X_c increased with increasing glass bead content at 10 wt%, then X_c reduced with increasing to 15 wt%. This is because a small amount of glass bead and glass fibre could act as the nucleating agent in the system. This promoted the heterogeneous nucleation of PP and causing the improvement of crystallinity. However, when higher filler content, the crystallinity decreased since the presence of filler obstruct the polymer chain diffusion towards the growth of spherulites of PP from expanding in all direction. This caused a decrease in crystallinity [292, 293]. This results can be supported by works of Wang et al. and Frihi et al. [292, 293]. Furthermore, Frihi et al. also reported some hypothesis to support this phenomenon. They explained that the increasing number of growing crystallites due to the particle-promoted nucleation results in an increase of crystallite impingements that necessarily generate an increasing amount of clusters of constrained molten chains unable to crystallize [292]. Furthermore, the melting temperature of hybrid composites were a bit less than neat PP. There was the report from Rasana et al. supported that it may be from the heterogeneous inclusion of glass bead and glass fibre in composite. This reduces the melting temperature of hybrid composite, which indicates the formation of imperfect PP crystals with the inclusion of fillers [148].

5.5.7 Density

The measured density of neat PP and hybrid composites are shown in Figure 5.26 and Table D.11 in Appendix D.

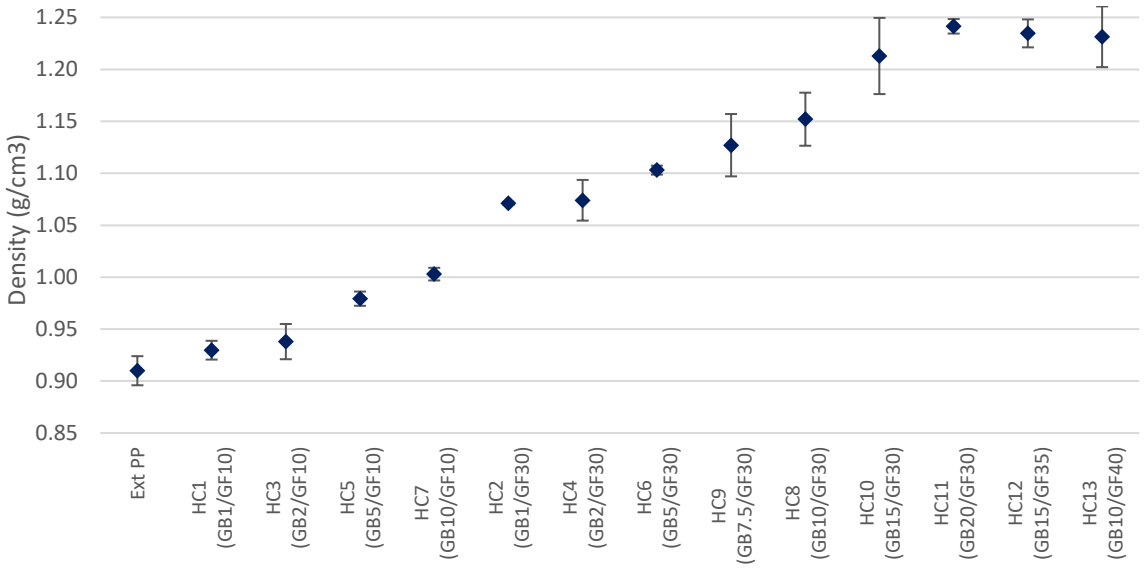

Figure 5.27: Density of extruded PP and neat PP based hybrid composites versus glass bead and glass fibre content (%)

Figure 5.27 shows density of additional hybrid composites. The density of HC9, HC10 and HC11, which were prepared with 30 wt% of glass fibre and glass bead content at 7.5, 15 and 20 wt% can fit the trend of density of the previous set of experiment, which was mentioned in Figure 5.16. It is obviously seen that the density linearly increased with the increase in total filler content. However, the consideration of the density of HC11, HC12 and HC13, which are hybrid composite with 50 wt% of total content but the different ratio of glass bead and glass fibre was observed. It was found that density of these three hybrid composites were quite similar in the range. This is due to glass fibre and glass bead have the similar density (2.6 g/cm^3) as shown in Tables 4.12.

5.5.8 Composite cost (for raw materials)

The cost of hybrid composites from the additional experiments were calculated from fillers and polymer based resin. They were calculated in GBP per one kilogram of composite are shown in Table 5.10.

Table 5.10: Hybrid composite costs from additional experiments

Composites	Composite cost (GBP/kg)
HC9 (PP/GB7.5/GF30)	1.53
HC10 (PP/GB15/GF30)	1.58
HC11 (PP/GB20/GF30)	1.61
HC12 (PP/GB15/GF35)	1.54
HC13 (PP/GB10/GF40)	1.47

From Table 5.10, it can be seen that all of the hybrid composites were cheaper than neat PP, which was about 1.7 GBP per kg. However, it can be seen that HC11 was the most expensive comparing to HC12 and HC13, which were the hybrid composites with 50 wt% of total content. This is because HC11 was higher ratio of glass bead, the more expensive filler than HC12 and HC13.

5.6 Evaluation of the performance hybrid composites

Regarding to targets for selection the most suitable hybrid composite, the criteria has been mentioned in Table 5.2. For the evaluation, the measured experimental results of all of hybrid composites (HC1-HC13), which were tabulated in Table 5.11.

Table 5.11: The average experimental results and composite costs of hybrid composites and extruded PP

Composites	Tensile Modulus		Flexural Modulus		Izod Impact strength		MFI	Density	Cost
	MPa	% Diff	MPa	% Diff	kJ/m^2	% Diff	g/10 min	g/cm^3	GBP /kg
Extruded PP	1518.9		1227.3		4.50		60.7	0.910	1.70
HC1 (GB1/GF10)	2217.8	46%	1881.9	53%	4.16	-8%	45.8	0.930	1.63
HC2 (GB1/GF30)	3718.1	145%	3645.4	197%	5.11	13%	39.1	1.071	1.48
HC3 (GB2/GF10)	2234.6	47%	1985.2	62%	4.25	-6%	45.6	0.938	1.64
HC4 (GB2/GF30)	3847.4	153%	3662.2	198%	5.14	14%	39.4	1.074	1.49
HC5 (GB5/GF10)	2411.4	59%	2319.3	89%	4.27	-5%	45.8	0.979	1.66
HC6 (GB5/GF30)	3937.4	159%	3800.2	210%	5.17	15%	39.7	1.103	1.51
HC7 (GB10/GF10)	2435.8	60%	2353.3	92%	5.08	13%	43.1	1.003	1.70
HC8 (GB10/GF30)	4505.8	197%	4501.5	267%	5.73	27%	35.3	1.152	1.54
HC9 (GB7.5/GF30)	3951.3	160%	3866.2	215%	5.29	17%	38.0	1.127	1.53
HC10 (GB15/GF30)	4581.1	202%	4514.7	268%	5.72	27%	33.4	1.213	1.58
HC11 (GB20/GF30)	4636.1	205%	4724.7	285%	5.75	28%	33.0	1.241	1.61
HC12 (GB15/GF35)	4791.8	215%	4884.7	298%	5.81	29%	31.2	1.235	1.54
HC13 (GB10/GF40)	5310.4	250%	5277.1	330%	6.03	34%	30.7	1.231	1.47

According to information in Table 5.11, the consideration of the most suitable formulation was concerned to the percentage of improvement of mechanical properties, melt flow index, density and composite costs by the target, which are showed in Table 5.2. From the preliminary consideration, the potential candidates of hybrid composites, which their all properties passed target are HC8, HC9, HC10, HC11, HC12 and HC13. These hybrid composites will be rated and with rating definition, which has been mentioned in Table C.6 – C.8 in

Appendix C**.** The rated experimental results are shown in Table D.12 in Appendix D and summarized as radar charts in Figure 5.28.

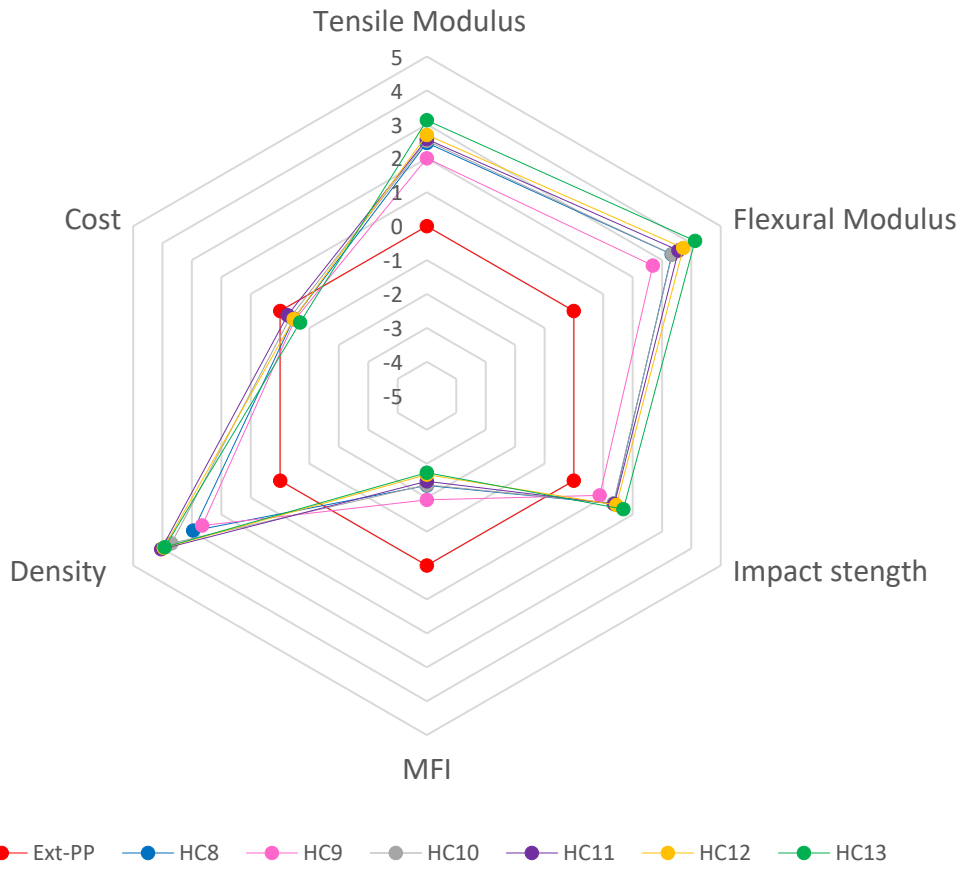

Figure 5.28: Radar chart compares extruded PP and PP based hybrid composites

From the radar chart in Figure 5.28, it can be seen that HC13, PP hybrid composites with 10 wt% of glass bead and 40 wt% of glass fibre was the most suitable formulation among all of hybrid composite formulations. This is due to the superior mechanical properties e.g. tensile, flexural modulus and Izod impact strength with the 250%, 330% and 34% improvement respectively compare to extruded PP. Moreover, cost of HC13 was also cheaper due to the combination of fillers, which cheaper than neat PP. The density and melt flow index were acceptable at 1.231 g/cm^3 and 30.7 g/10min, which was not higher than 1.3 g/cm^3 and not less than 10g/10min, which were the typical value of PP/Glass fibre composite for injection moulding application in the current market.

5.7 Conclusion

In Chapter 5, the best performing fillers from each family which were glass fibre and glass bead were used to manufacture hybrid composite systems. These hybrid composite systems were investigated on neat PP resin. Then, thirteen sets of experimental trials were carried out by varying the ratios of glass bead and glass fibre combinations which were designed by Taguchi model as guidance and also further five combinations were designed in the optimization phase. Based on the experimental results, it can be concluded that PP hybrid composites with 10 wt% of glass bead and 40 wt% of glass fibre and 7.5 wt% of PP-g-MA (HC13) was the most suitable formulation among all of hybrid composite formulations tested. This is considering their superior mechanical properties e.g. tensile, flexural modulus and Izod impact strength with 211%, 325% and 18% improvement respectively compared to the neat PP. Moreover, the raw materials cost of HC13 was also cheaper due to the combination of fillers, which was 14% cheaper than neat PP. The density and melt flow index were at 1.231 g/cm^3 and 30.7 g/10min, which was not higher than 1.3 g/cm^3 and not less than 10g/10min, which were the typical value of PP/glass fibre composite for injection moulding application in the current market. However, the properties of HC13 compares to neat PP are shown in Table 5.12.

Table 5.12: The average experimental results and composite costs of HC13 and Neat PP

	Tensile Modulus		**Flexural Modulus**		**Izod Impact strength**		**MFI**		**Density**		**Cost**	
	MPa	% Diff	MPa	% Diff	kJ/m^2	% Diff	g/10 min	% Diff	g/cm^3	% Diff	GBP/kg	% Diff
Neat PP	1708.6		1240.3		5.11		55.5		0.910		1.70	
HC13 (GB10/GF40)	5310.4	211%	5277.1	325%	6.03	18%	30.7	-45%	1.231	35%	1.47	-14%

From the thorough evaluation of the performance of hybrid composites, it can be surprisingly observed that HC13, the neat PP hybrid composite with 10 wt% of glass bead and 40 wt% of glass fibre and 7.5 wt% of PP-g-MA was considered as the most suitable formulation. This is because all of mechanical properties of HC13 were improved compared to neat PP. This formulation would be applied in the rPP hybrid composite to observe how well it can improve the properties of rPP. The effect of rPP mixing ratio on the rPP hybrid composites' performance would be varied and investigated in the next chapter.

6. Recycled PP based hybrid composites

In Chapter 5, the performance of hybrid composites with glass bead and glass fibre in various formulations was evaluated. Based on the results presented in Chapter 4, the most suitable hybrid composite formulations selected to be applied for rPP based composites were the PP composites with 10 wt% of glass bead, 40 wt% of glass fibre and 7.5 wt% of PP-g-MA (HC13). The formulation of HC13 was further studied by replacing neat PP by rPP in this chapter.

6.1 Target of the experiment

The PP based hybrid composites with 10 wt% of glass bead, 40 wt% of glass fibre and 7.5 wt% of PP-g-MA were applied with rPP composites. The effect of blending ratio between recycled and neat PP to composite performance were investigated. The recycled hybrid composites were evaluated by investigating the mechanical properties (such as tensile, flexural, impact testing), thermal properties, rheological properties, density, morphological properties and spectroscopic properties by FTIR.

The rPP resin used in this chapter was MOPLEN QCP300P Ivory from LyondellBasell Industries, USA. It contains at least 99 % of recycled material from pre-sorted municipal plastic waste. This rPP resin was designed for compounding and injection molding process. The purpose of this experiment was to improve rPP based composites to be comparable to neat PP. Therefore, the targets values for the properties of rPP hybrid composite were referred to the properties of neat PP and the acceptable values of density and MFI that were mentioned in Tables 5.1 and 5.2 in Chapter 5. Due to these hybrid composites being prepared by the same formulation, the hybrid composite cost was not considered as one of the criteria. However, the target will be focused on the investigation of the highest blending ratio of rPP in composites that can maintain acceptable composite performance. The targets, which were considered as criteria to select the most suitable blending ratio of rPP. The targets were set by comparing each property to neat PP, which are shown in the Table 6.1.

Table 6.1: Targets for selecting the rPP based hybrid composites

Criteria	Target
Mechanical properties	
• Tensile modulus	1708.6 MPa
• Flexural modulus	1240.3 MPa
• Izod impact strength	5.11 kJ/m^2
Melt flow index	>10 g/10min
Density	<1.300 g/cm^3

The experimental results were rated and summarized as radar charts. The obtained results from rPP based hybrid composites were rated by comparing each property to neat PP. In case of the mechanical properties of all rPP hybrid composites are not comparable to neat PP, the optimization of formulation and methodology will be further investigated.

6.2 Design of experiments

In this study, the blending ratios between rPP and neat PP were varied to investigate the effect of rPP content in hybrid composites on composite performance. The experiments were conducted using different ratios of rPP in percentage by weight, which were 5, 10, 20, 50, 75 and 100 wt%. Every formulation of rPP hybrid composites were compounded with the addition of 10 wt% of glass bead, 40 wt% of glass fibre and 7.5 wt% of PP-g-MA. These rPP hybrid composites were prepared with the same processing conditions that were mentioned in section 5.3 in Chapter 5. The compositions of rPP hybrid composites are shown in Table 6.2.

Table 6.2: Compositions used to manufacture rPP hybrid composites

Experiment no.	Neat PP (wt%)	rPP (wt%)	Glass bead (wt%)	Glass fibre (wt%)	PP-g-MA (wt%)
rHC1	95	5	10	40	7.5
rHC2	90	10			
rHC3	80	20			
rHC4	50	50			
rHC5	25	75			
rHC6	0	100			

6.3 Compounding conditions

For manufacturing, the rPP hybrid composites were extruded in a co-rotating twin screw extruder (Haake Rheomax OS PTW16) at a screw speed of 70 rpm with 1.8 kg/hr

for optimum throughput, which was not over 80% of torque limit of extruder. The temperature profiles were 180/190/190/210/210/210/210/ 210/210/180 °C, which are the same conditions was mentioned in the Table 4.1 in Chapter4. Glass bead in powder form was fed into the extruder by a gravimetric feeder in the barrel at the sixth barrel zone of the extruder, in order to minimize glass bubble breakage [209-213]. Meanwhile, raw materials in pellet or rod forms such as neat PP resins, rPP resins, compatibilizer (PP-g-MA) and glass fibre, were carefully and manually pre-mixed before feeding into the extruder by a volumetric feeder. The schematic is shown in Figure 6.1.

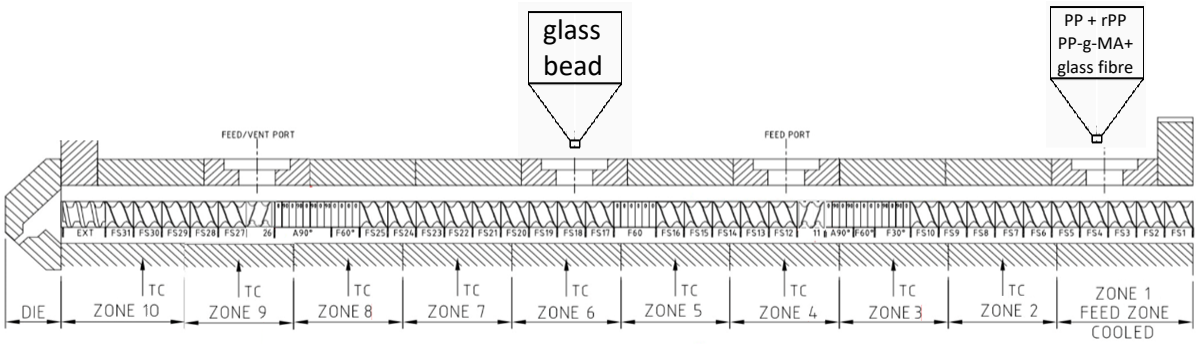

Figure 6.1: Schematic of a twin screw extrusion machine for PP/glass bead/glass fibre hybrid composite

6.4 Characterization of PP composites

To evaluate the performance of rPP based hybrid composites from glass bead and glass fibre with the PP-g-MA as compatibilizer were investigated by various characterization techniques. The mechanical properties, melt flow index, and density, were investigated as the critical properties to evaluate the overall performance of hybrid composites.

6.4.1 Mechanical properties

Mechanical properties were evaluated in terms of tensile modulus, flexural modulus and Izod impact strength. The raw data of these mechanical properties were exhibited in Appendix E.

6.4.1.1 Tensile modulus

The measured tensile modulus of rPP/glass bead/glass fibre composites with PP-g-MA in various percentages of rPP were displayed in the Figure 6.2 and Table E.1 in Appendix E.

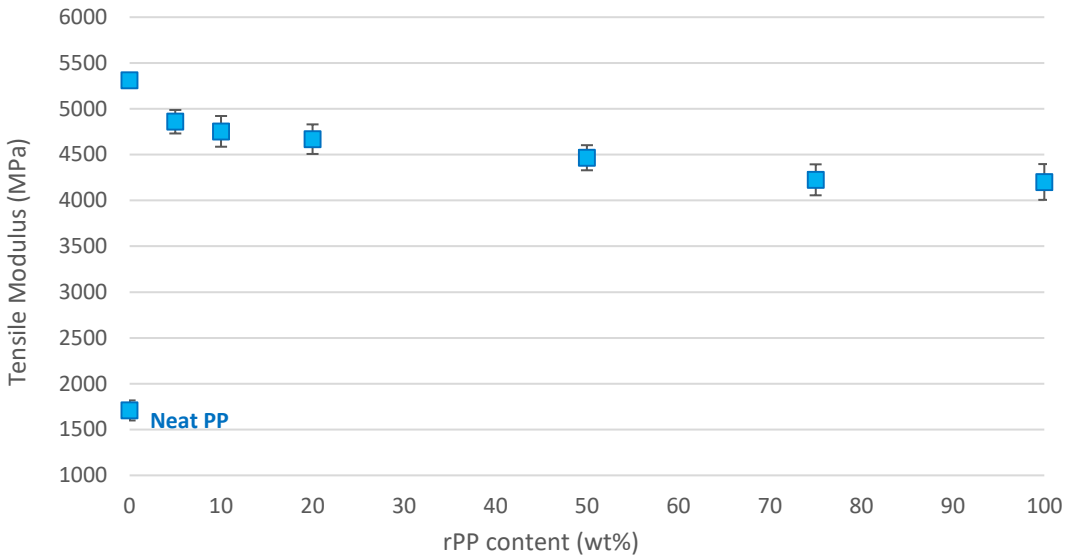

Figure 6.2: Tensile modulus of rPP hybrid composites with different percentages of rPP content (%)

From Figure 6.1, it is observed that all of the rPP hybrid composites had superior tensile modulus comparing to neat PP. This is due to the reinforcing effect from glass bead and glass fibre with the good interfacial adhesion between fillers and matrix from the addition of PP-g-MA, as was discussed in Chapter 5. However, it can be found that the addition of small amount of rPP, which were 5 and 10 wt% caused only a slight change of tensile modulus. This behaviour can be attributed to a minimal effect of thermal degradation towards the mechanical properties of rPP. However, a significant decrease can be observed with the increasing of blending ratio of rPP to more than 10 wt% in this hybrid composite. The increase in mixing ratio of rPP in blended rPP hybrid composites resulted in the reduction of tensile modulus. As the amount of rPP was increased over 75 wt%, the tensile modulus of rPP hybrid composites decreased more than 20% comparing to PP based composite with the same formulation. This is because the portion of low molecular weight species in the partially degraded material in the rPP was increased according to the amount of increasing rPP. The thermal degradation from the reprocessing of PP material can cause the breakage of polymer chain, in the phenomenon known as chain scission. This phenomenon has shortened the chain within the polymer and resulted in a reduction of molecular weight, leading to the worsening of mechanical performance [154, 167, 168].

Moreover, there is another factor that influences this reduction of tensile modulus, which is contamination in the rPP resin. Work by Jmal et al. [151] reported that contaminants and additives have an important impact on mechanical properties of composites. There were

complicated components in the rPP resin, because it can be constituted by a mix of grades, which are not completely miscible or absorb low molecular weight compounds. This may result in a lack of adhesion at the phase boundaries, which is one of the main reasons for the brittleness of recycled plastics and reduction in mechanical properties [151, 173]. The increasing mixing ratio of rPP can also enhance the occurrence of contamination. This led to deteriorating tensile properties. Similar results were attained by the previous work from Karaagac et al [172].

6.4.1.2 Flexural modulus

The measured flexural modulus of rPP/glass bead/glass fibre composites with PP-g-MA in various percentages of rPP are displayed in the Figure 6.3 and Table E.2 in Appendix E.

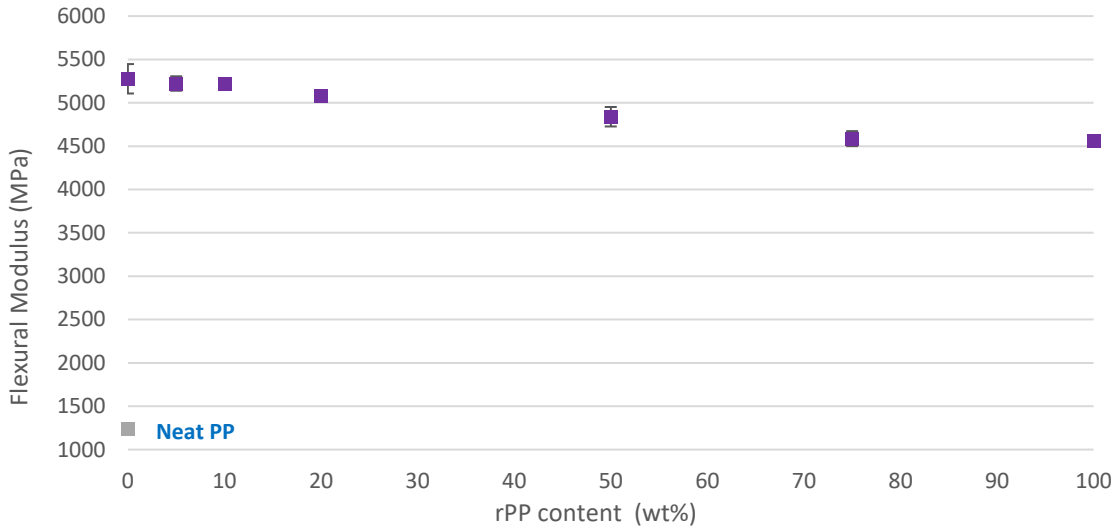

Figure 6.3: Flexural modulus of rPP hybrid composites with different percentages of rPP content (%)

From Figure 6.3, it can be observed that the flexural modulus tend to decrease with the increase of mixing ratio of rPP. This behaviour was similar to tensile modulus but of a different magnitude. The flexural modulus of the rPP hybrid composites was practically unchanged by adding rPP less than 10 wt%. The Figure 6.3 shows a small reduction with respect to the virgin sample. According to the finding, blending with small amount, less than 20 wt% of rPP was acceptable and did not seriously deteriorate its mechanical properties due to thermal degradation [154, 167]. However, the flexural modulus was decreased when increasing mixing ratio of rPP over 20 wt%. Flexural modulus was decreased about 4% at the ratio of rPP at 20 wt%, and achieved a minimum value with a 13% decrease at 100 wt%, compared to

virgin PP based hybrid composite (HC13). This behaviour was due to a decrease in molecular weight during re-processing of material because of the polymer chain deterioration [154, 161].

However, compared to tensile modulus, it can be observed that the flexural modulus was almost unaffected. The flexural modulus slightly dropped only 1% by small amount of rPP, less than 10 wt%, while the flexural modulus decreased by 14% at 100 wt% of rPP, but it was considerably less than for the tensile modulus. This observation can be explained from the difference of deformation mode between tensile and flexural properties [167, 252]. Since these specimens were prepared by injection moulding, this causes some fibre orientation of in the flow direction, especially on the skin of specimen where the temperature decreases more rapidly than in the core. This phenomenon would lead to a flexural stiffening of the structure since this property is more affected by the degree of orientation in the surface layers of the specimens than in the core ones [167].

6.4.1.3 Izod impact properties

The Izod impact strength of rPP/glass bead/glass fibre composites with PP-g-MA in various percentages of rPP are displayed in the Figure 6.4 and Table E.3 in Appendix E.

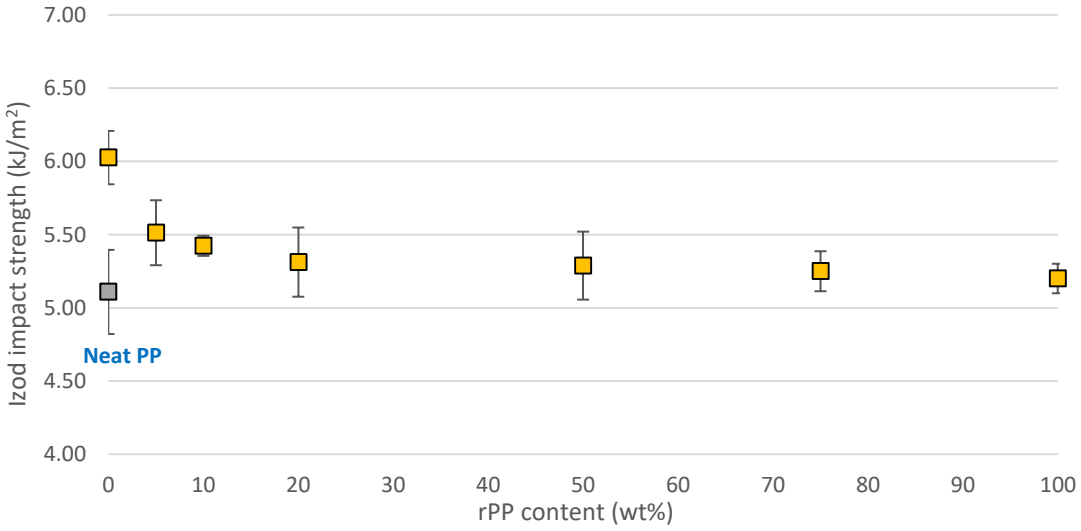

Figure 6.4: Izod impact strength of rPP hybrid composites with different percentages of rPP content (%)

From Figure 6.4 it is apparent that the Izod impact strength decreased significantly with the addition of rPP. The impact strength dropped 9% by addition of 5 wt% of rPP, and achieved the minimum value at 14% at 100 wt% of rPP. The decrease of impact strength can be

described in a similar manner as other properties, which were correlated with the thermal degradation and shear rate [167, 169]. Moreover, the impact strength decreases with increasing the amount of contamination [172]. The presence of contaminations such as labels, glue, printing, product residue, mix of polymer grades, low molecular weight compounds can deteriorate the impact strength by the various species, which may not be completely miscible or absorb low molecular weight compounds [172, 173].

6.4.2 Melt flow index

The measurement of melt flow index of neat PP and PP based hybrid composites follows the ASTM D 1238-10 standard [208]. These results are shown in the Figure 6.5 and Table E.4 in Appendix E.

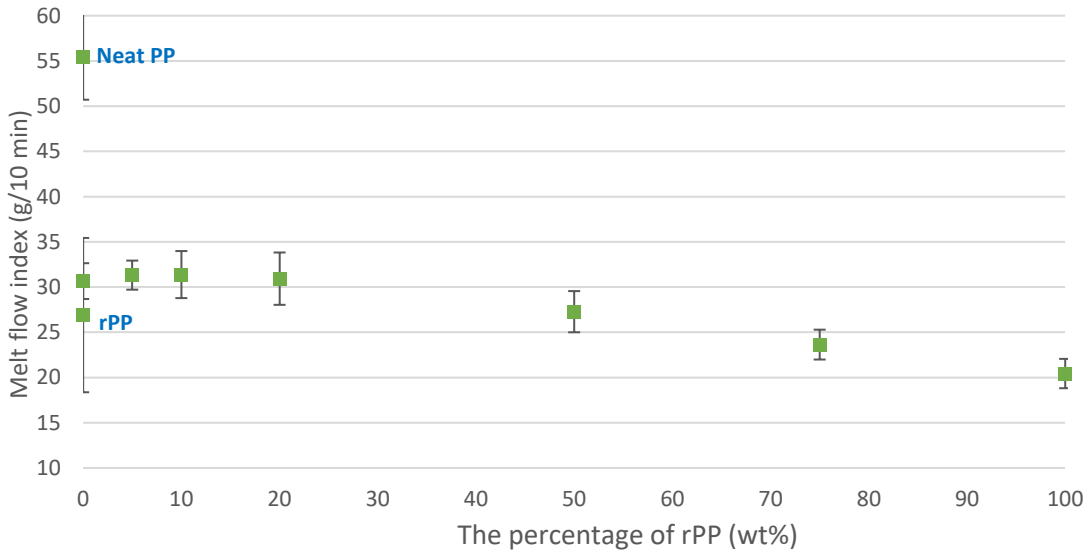

Figure 6.5: Melt flow index of rPP hybrid composites with different percentages of rPP content (%)

From Figure 6.5, it can be observed that MFI of all of rPP hybrid composites decreased in comparison to rPP resin, which was 26.9 g/10min. The change indicates an increase of viscosity of hybrid composite. This is because the incorporation of glass bead and glass fibre, which are rigid fillers, limits molecular mobility and hinders melt flow of PP, and therefore increases the viscosity of PP composites at the melt stage [231]. Moreover, MFI decreased as the amount of rPP in the mixing ratio was increased. This is due to the MFI of rPP being lower than that of neat PP resin, which is 55.5 g/10min. Moreover, the reduction in MFI may be due

to contaminants in the rPP resin, which increased with increasing the mixing ratio of rPP. Similar results were also obtained by Shan Tai et al. [171].

6.4.3 Density

The measured melt flow index of neat PP, and PP bases hybrid composites are shown in the Figure 6.6 and Table E.5 in Appendix E.

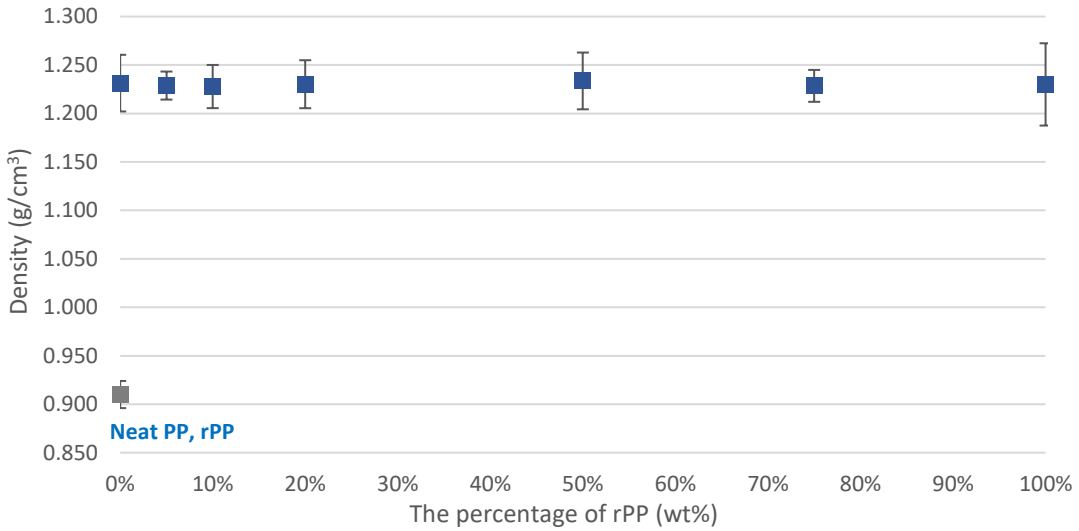

Figure 6.6: Density of rPP hybrid composites with different percentages of rPP content (%).

Figure 6.6 shows the effect of total content of glass bead and glass fibre on the density of hybrid composite materials. It is seen that the density of rPP hybrid composites were in the same range of HC13, which was a PP hybrid composite. This is because the density of neat PP (P739ET), which was used as based resin for HC13 was quite similar to the density of rPP based resin (MOPLEN QCP300P Ivory) for rPP hybrid composites. The density of rPP hybrid composites were in the range of 1.128 – 1.134 g/cm^3. However, it can be observed that the hybrid composite with 100% of rPP had a quite wide range of variation in density, as seen in its error bar. Such a variation is due to the properties of the rPP resin, which may be from various sources and quite not consistent.

6.4.4 Morphological properties

Samples of rPP hybrid composites with 5, 50 and 100 wt% of rPP were selected for SEM analysis. These composites were compounded by adding 10 wt% of glass bead and 40 wt% of glass fibre. The micrographs of these samples are shown in Figure 6.7.

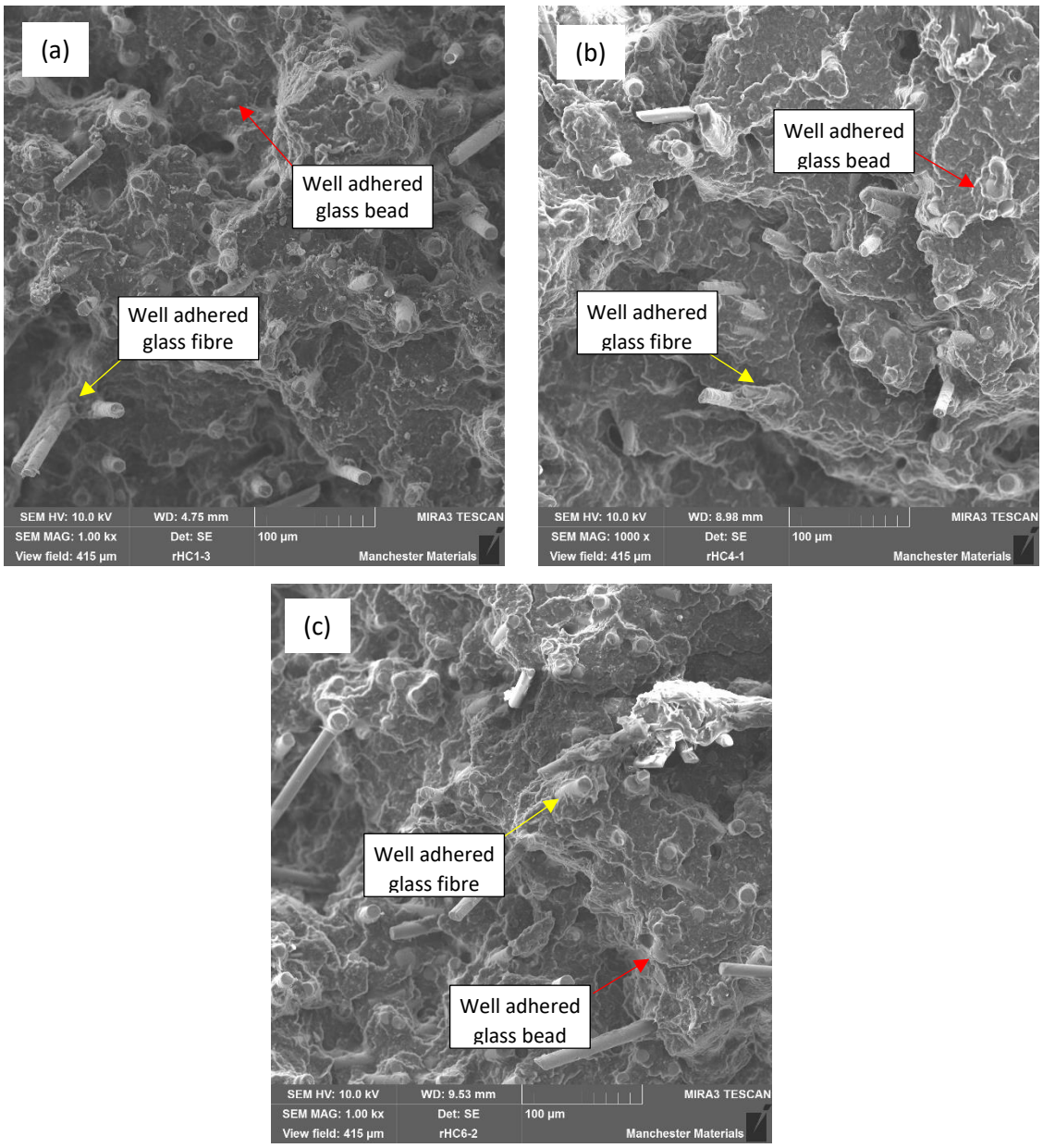

Figure 6.7: The micrographs of the fracture surfaces of Izod sample at 1000x of rPP hybrid composites filled with 10 wt% of glass bead, 40 wt% of glass fibre, 7.5 wt% of PP-g-MA and different ratio of rPP content (a) 5 wt% (b) 50 wt% (c) 100 wt%.

From the fractographs of rPP hybrid composites in Figure 6.7, it can be observed the good interaction between glass bead-polymer matrix and glass fibre-polymer matrix. This is due to the rough surface on the glass fibre and the surrounded polymer mass at the glass beads. There is no visible splitting between the glass and the polymer. These are from aminosilane-treated glass bead and glass fibre, which were reacted to PP-g-MA [63, 68, 286-288]. However, Figure 6.6 suggested that there was no significant morphological difference at the

interface of composites made with the virgin PP and the addition of rPP. There is no visible phase separation between neat PP and rPP.

6.4.5 Rheological behaviour

Figure 6.8 shows the shear viscosity curve that was obtained from rotational rheometer. The samples of PP and rPP based hybrid composites were selected for rheological analysis on steady shear flow mode, with shear rate in the range of 0.1 – 10 s^{-1} at 210 ^{o}C, to investigate the change of viscosity over the shear rate.

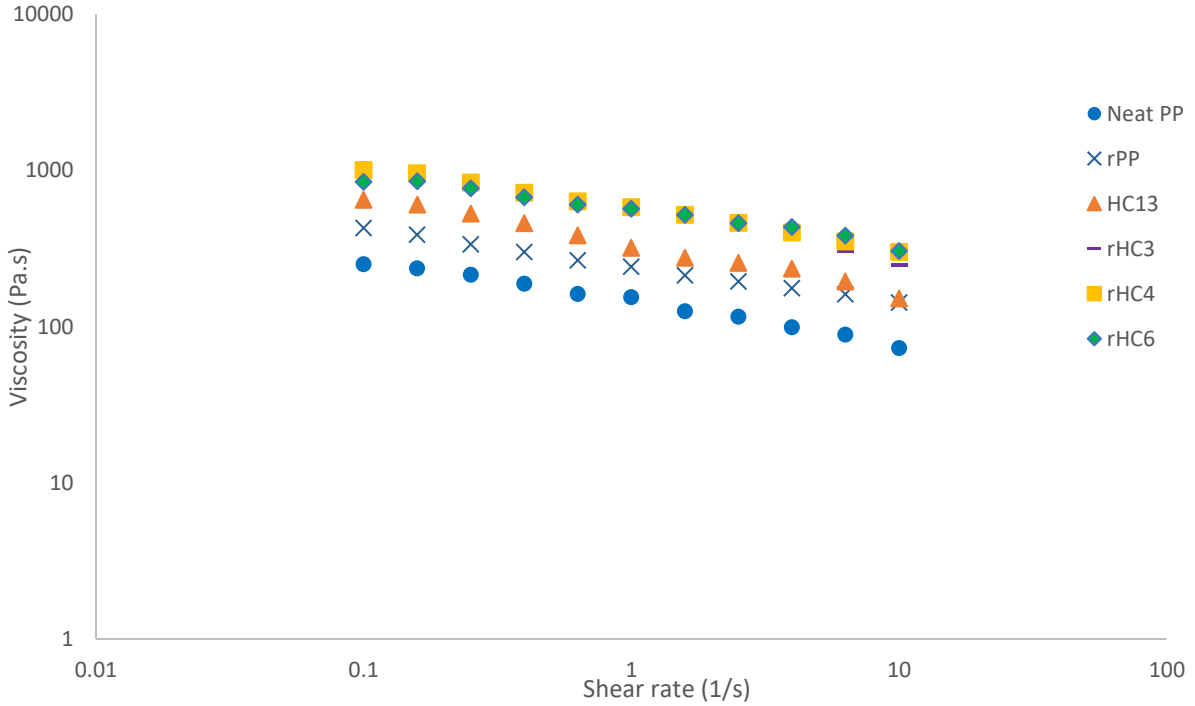

Figure 6.8: Viscosity curves of neat PP, PP and rPP composite with 10 wt% of glass bead and 40 wt% of glass fibre with different rPP content at 0, 20, 50 and 100 wt%.

From Figure 6.8, it can be seen that the viscosity of all the rPP composites decreased as the shear rate increases. This is an indication that the shear thinning behaviour is affected by the reprocessing [50]. Moreover, all composites had higher viscosity than neat PP due to the entanglements of glass fibres with the synergy of glass bead that obstruct polymer chain mobility [231]. The results for all these polymers show similar trends, with lower viscosity due to high shear rate [230].

This viscosity curves also exhibited that the viscosity of the rPP (plotted data with x-marker) was higher than that of the neat PP (plotted data with ●-marker). The viscosity of the rPP

resin affected directly the final viscosity of the rPP hybrid composites [171]. The increase of portion of more viscous rPP resin contributed to higher viscosity of the rPP hybrid composites.

6.4.6 Thermal stability

The DSC samples of rPP resin and rPP based hybrid composites with different ratio of rPP from 5 wt% to 100 wt% were analyzed. The values of T_c, T_m, ΔH_m, ΔH_c and the percentage of crystallinity were calculated from the DSC curves and tabulated in Table 6.3. DSC thermograms are shown in Appendix E.

Table 6.3: DSC-determined thermal characteristics of rPP hybrid composites.

Samples	T_c (°C)	ΔH_c(J/g)	T_m (°C)	ΔH_m(J/g)	X_c (%)
Neat PP	113.9	93.9	163.0	78.3	37.5
rPP	120.9	91.4	159.7	63.6	30.7
HC13 (100:1)*	114.9	55.3	159.6	47.9	45.8
rHC1 (95:5)*	119.7	57.9	160.3	50.4	48.2
rHC3 (80:20)*	120.4	44.8	160.0	37.6	36.0
rHC4 (50:50)*	120.3	37.2	159.6	32.3	30.9
rHC5 (25:75)*	120.8	49.5	159.0	43.7	41.8
rHC6 (0:100)*	120.1	50.2	158.8	36.5	35.0

** Ratio between neat PP: rPP*

The results of DSC are summarized in Table 6.3. Remarkably, the crystallization temperature of rPP hybrid composites in rPP/neat PP blends shifted to higher temperature, relative to the crystallization temperature of rPP, and remained almost constant in all blend rPP hybrid composites. Meanwhile, the melting temperature of rPP hybrid composites shifted to lower temperature, relative to the melting temperature of rPP, with increasing of blending ratio of rPP. Regarding the crystallization degree of rPP hybrid composites, these decreased with increasing ratio of rPP content. This can be related to the effect of contaminants and additives in rPP, which can reduce the mobility of polymer chains that affect to crystallinity induction. Similar results were also obtained by a study reported by Jmal et al. [151]. However, it can be observed the raise of the total crystallinity of rPP relative to that of neat PP blends, which appeared when the blend contained 75 wt % of rPP. This could be related to the deviation in crystallization behaviour of the rPP resin due to inconsistent properties of rPP. This finding has a similar trend compared to a previous study by Aumnate et al. [294].

6.5 Evaluation of the performance of hybrid composites

In regard to the targets in selecting the most suitable rPP hybrid composite, the criteria was mentioned in the Table 6.1. A summary of the experimental results of rPP hybrid composites discussed above are presented in Table 6.4

Table 6.4: The percentage of change of rPP composites.

Composites	Tensile Modulus			Flexural Modulus			Izod Impact strength			MFI	Density
	MPa	% Diff from		MPa	% Diff from		kJ/m^2	% Diff from		g/10min	g/cm^3
		Neat PP	HC13		Neat PP	HC13		Neat PP	HC13		
Neat PP	1708.6			1240.3			5.11			55.5	0.91
HC13	5310.4	211		5277.1	325		6.03	18		30.7	1.231
rHC1 (95:5)*	4859.2	184	-8	5222.6	321	-1	5.51	8	-9	31.3	1.229
rHC2 (90:10)*	4753.9	178	-10	5221.3	321	-1	5.42	6	-10	31.4	1.225
rHC3 (80:20)*	4668.9	173	-12	5084.0	310	-4	5.31	4	-12	30.9	1.230
rHC4 (50:50)*	4466.2	161	-16	4839.3	290	-8	5.29	4	-12	27.3	1.234
rHC5 (25:75)*	4225.2	147	-20	4586.7	270	-13	5.25	3	-13	23.6	1.229
rHC6 (0:100)*	4201.8	146	-21	4557.6	267	-14	5.20	2	-14	20.4	1.230

** Ratio between neat PP: rPP*

From Table 6.4, it can be found that the mechanical properties (tensile modulus, flexural modulus and Izod impact strength) decreased with increasing rPP mixing ratio, due to the effect from higher portion of low molecular weight polymer from thermal degradation and contamination, as discussed earlier. However, the reinforced effect from hybrid composites between glass bead and glass fibre, according to the proposed formulation from Chapter 5 (10 wt% of glass bead, 40wt% of glass fibre and 7.5 wt% of PP-g-MA), can improve the mechanical properties of rPP to be better than those of neat PP.

The percentage of change of mechanical properties, MFI and density compared to neat PP were rated following the definition mentioned in the Table D8 - D10 in Appendix**.** Positive rated values for each property mean higher values comparing to extruded PP, while negative values represent lower values compared to PP. Furthermore, the rated raw data were shown in Table E.6 in Appendix E. The radar charts of these properties are exhibited in the Figure 6.9.

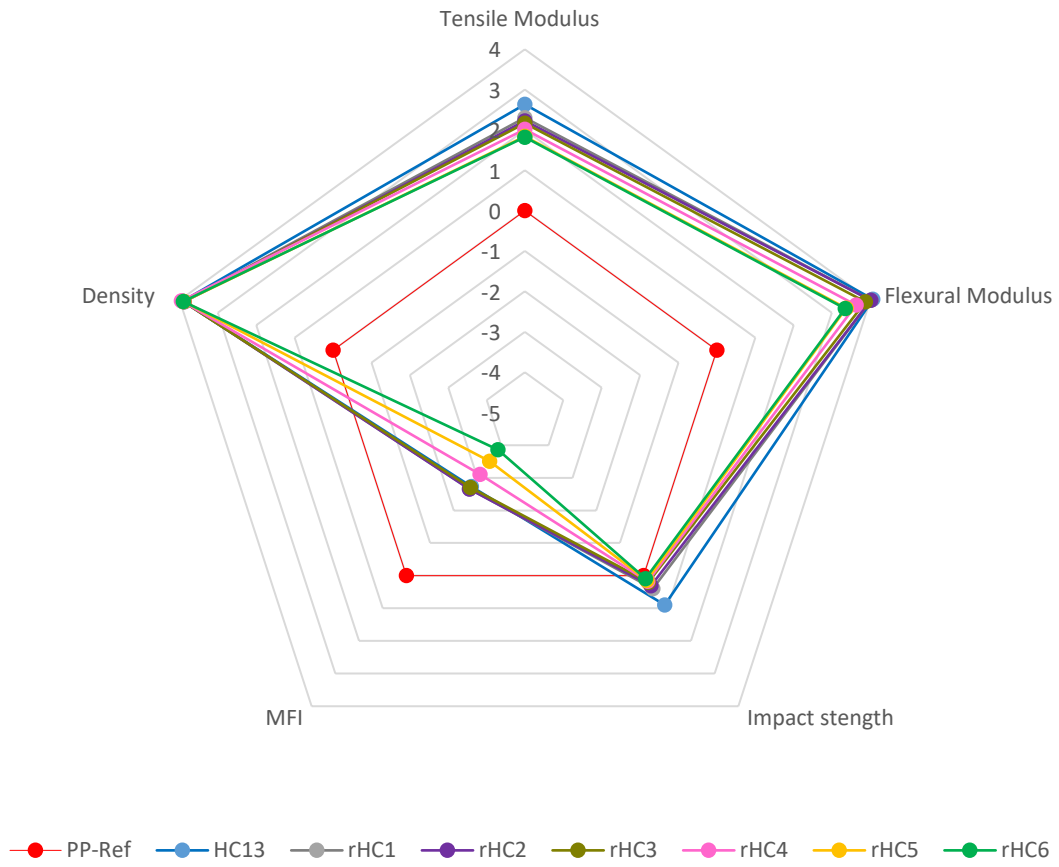

Figure 6.9: Radar chart to compare neat PP and rPP based hybrid composites**.**

From the radar chart in Figure 6.9, it can be seen that the hybrid composite system of 10 wt% of glass bead and 40 wt% of glass fibre with PP-g-MA (HC13) can improve mechanical properties of rPP to be comparable to those of neat PP. In a composite with reinforcing particulate fibres, significant improvements were achieved upon the flexural, tensile modulus and impact strength. The density of these rPP hybrid composite were not changed significantly due to the similar density of rPP and neat PP. Density of these rPP composites were also in the acceptable range (less than 1.3 g/cm^3). Comparing to neat PP and PP hybrid composite (HC13), rPP hybrid composites had lower MFI, but these overall properties of rPP hybrid composites were acceptable following the criteria in the Table 6.1. The rPP hybrid composite with 100% of rPP provided a quite low MFI of 20 g/10min, but it was acceptable if compared with PP/glass fibre resin in the market, which in the range of 3 – 10 g/10min. In conclusion, the implementation of the formulation of HC13 by replacing neat PP with rPP could be effective since the performance of rPP was developed according to the set targets in Table 6.1.

6.6 Conclusion

At the final stage of the project, the selected combination of glass fibre and glass bead reinforcements (HC13) was used to manufacture recycled PP based composites. Composites were manufactured by varying the percentage of recycled PP up to six levels (5, 10, 20, 50, 75 and 100 wt%) in order to investigate the mechanical properties. It can be found that the increase in mixing ratio of rPP in blended rPP hybrid composites resulted in the reduction of tensile, flexural modulus and Izod impact strength. However, the addition of small amount of rPP, which were less than 10 wt% caused only a slight change of tensile and flexural modulus. Significant decrease can be observed with the increasing of blending ratio of rPP to more than 10 wt% in this hybrid composite. While, it is apparent that the Izod impact strength decreased significantly with the addition of rPP. The impact strength dropped 9% by addition of 5 wt% of rPP, and achieved the minimum value at 14% at 100 wt% of rPP.

In conclusion, the implementation of the formulation HC13, which was 10 wt% of glass bead and 40 wt% of glass fibre with PP-g-MA, by replacing neat PP with rPP, could be effective since the performance of rPP was demonstrated to be comparable to that of neat PP in term of the tensile, flexural modulus and impact strength. Here, it should be noted that the incorporation of rPP of up to 20 wt% can be considered as the optimum mixing ratio to maintain the MFI to be in the similar value (30.93 g/10min) to that of neat PP based composites (30.66 g/10min), and also to maintain superior mechanical properties over neat PP.

7. Conclusions and recommendations for further works

This study aimed to explore potential methodologies that can improve the performance of recycled PP (rPP) to be comparable to neat PP, which can be used in potential applications via hybrid reinforcement systems. From the key learnings from number of literatures, this present work were developed by adapting methods overcome the knowledge gaps and limitations. The novelty of this research was created by considering processibility and composite cost, the suitable compatibilizer dosage and the maximum filler content and maximum ratio of recycled PP to obtain the acceptable range to the composite in the market. The research finding and recommendations can be stated:

7.1 Significant research findings

To achieve the aims and objectives of this study, the experiments were carried out in three stages.

7.1.1 Screening experiments for selecting the best suited fillers for hybrid composites

Firstly, to achieve the suitable fillers for rPP hybrid composites, a comprehensive study was carried out to investigate the effects of different types and loadings of fillers, by a number of screening experiments. The reinforcing performance of various candidate fillers was evaluated, from the fibre family, including glass fibre and carbon fibre, while representatives from the particle family were $CaCO_3$, kaolin, glass bead and GNPs, with PP neat resin in various composites systems. These PP composites exhibited enhanced interfacial adhesion by the treated fillers and the addition of compatibilizers. From the experimental works, the following specific conclusions can be drawn:

- All PP composites had higher tensile and flexural modulus comparing to the neat PP, due to the overall rigidness of fillers in the PP matrix with good interfacial adhesion. These increased with increasing the filler content to from 10 to 30 wt%.
- The increasing filler content in the range 10 to 30wt%, the elongation at break were decreased except for the PP/glass bead system that did not significantly change the elongation behaviour.
- The impact strength of PP composites with $CaCO_3$, kaolin and GNPs decreased with increasing the filler content, since these fillers formed agglomerate at higher content.
- For PP/glass bead, it can be found that the impact strength first increased with increasing glass bead content up from 1 to 10 wt%, thereafter, it decreased with

increasing up to 50 wt%. This was because agglomerations in composites increased due to particle-particle interaction become stronger with increasing particle content.

- Adding glass fibre can improve impact strength due to the effective stress transfer.
- The presence of strong interfacial adhesion of fillers in the composites by SEM images. There was no visible split between filler from both of neat PP and rPP matrix. Moreover, good dispersion of fillers in low filler content were notable while the presence of larger agglomerations with increasing the filler content.
- MFI decreased in the range of 15 to 77% with increasing the filler content from 10 to 30 wt%., except for the MFI of PP/glass bead composites that only changed slightly, which less than 5% reduction from 10 to 30wt%.
- The filler selection process were proceeded by evaluating in terms of improvements of the mechanical properties, processability and cost. For the particle family, it was observed that:
    - GNPs were not suitable due to poor impact strength, complicated manufacturing process and being much more expensive.
    - PP/$CaCO_3$ composite was not suitable due to the worse impact strength, which were less than neat PP about 5 to 9%.
    - The PP/kaolin had worse impact strength and more complicated compounding process than PP/glass bead so PP/kaolin was not chosen as suitable candidate.
    - PP/glass bead composites had the best overall mechanical properties. Tensile, flexural modulus and Izod impact strength were better with the maximum improvement at 37%, 47% and 6% respectively than neat PP. These PP/glass bead composites were manufactured with the simple compounding process and with an acceptable cost. Therefore, the most suitable fillers from particle family was *Glass Bead.*
- For the fibrous family, it was found that:
    - PP/carbon fibre was not selected due to worse impact properties, which less than 2 to 8% comparing to neat PP and being more expensive than glass fibre.
    - The incorporation of glass fibre can promote impact strength up from 4% to 10% improvement comparing to neat PP with increasing glass fibre content

from 20 to 30 wt%. Therefore, the most suitable fillers from fibre family was *Glass fibre.*

7.1.2 Determining the best formulation of neat PP based hybrid composites

The suitable fillers were selected by the screening test which are glass bead and glass fibre. These filler were investigated to improve performance of PP by combining as hybrid composite. With the hybrid composites, the glass bead were varied at 1 to 20 wt%, while the glass fibre was varied from 10 to 40 wt%. Based on the experimental results, the following specific conclusions can be stated:

- The tensile and flexural modulus and impact strength of PP/glass bead/glass fibre hybrid composite with PP-g-MA with increasing the total filler concentration from 10 to 50 wt%. A positive synergistic effect of the incorporation glass fibre and glass bead promoted stiffness of hybrid composites. Moreover, the presence of particles could also dissipate impact energy and inhibited crack propagation by pinning mechanisms.
- In the cases of tensile and flexural modulus of hybrid composites with the same total filler, the moduli were decreased with increasing ratio of glass bead content because glass fibre can more effectively enhance the stiffness than particles.
- Based on the experimental results, it can be concluded that PP hybrid composites with 10 wt% of glass bead and 40 wt% of glass fibre and 7.5 wt% of PP-g-MA (HC13) was the most suitable formulation among all of hybrid composite formulations. This is considering their superior mechanical properties e.g. tensile, flexural modulus and Izod impact strength with the 250%, 330% and 34% improvement respectively compare to extruded PP.
- Composite cost of HC13 was also cheaper due to the combination of fillers, which 14% cheaper than neat PP.
- The density and melt flow index were acceptable at 1.231 g/cm^3 and 30.7 g/10min, which was not higher typical values (1.3 g/cm^3 and 10g/10min) of PP/glass fibre composite for injection moulding application in the current market.

7.1.3. Recycled PP based hybrid composites

The most suitable hybrid composite formulation which was selected to be applied for rPP based composite was the PP composites with 10 wt% of glass bead, 40 wt% of glass fibre and

7.5 wt% of PP-g-MA (HC13). This formulation was further studied by replacing neat PP with rPP. The target was to improve the performance of rPP to be comparable to neat PP and hence to increase the use of rPP by prompting the circular economy. The mixing ratio of rPP to neat PP was varied from 5 to 100 wt% of rPP to investigate the rPP hybrid composites, with the same processing conditions as for the earlier experiments.

- All of the rPP hybrid composites had superior tensile, flexural modulus and impact strength in comparison to neat PP.
- A significant decrease of flexural and tensile modulus can be observed with increasing of the blending ratio of rPP to 20 wt% to 100 wt%, the flexural and tensile modulus decreased 4 to 14% and 12 to 21% respectively. This is due to the higher portion of low molecular weight species and impurities.
- MFI of all of rPP hybrid composites decreased with increasing mixing ratio of rPP. This is attributed to the lower MFI of rPP and impurities in rPP resins.
- In conclusion, the implementation of the formulation of HC13 by replacing neat PP with rPP, could be effective since the performance of rPP was demonstrated to be comparable to that of neat PP.
- The incorporation of rPP of up to 20 wt% can be considered as the optimum mixing ratio to maintain the MFI to be in the similar value to that of neat PP based composites (30.7g/10min), and also to maintain superior mechanical properties over neat PP.

7.2 Recommendations for further works

Due to the Covid-19 pandemic, there were restrictions that obstructed the experimental work plan. Some experimental tasks had to be carefully selected, to be carried out as much as possible according to the limited duration of lab work under the Covid-19 circumstances. Based on the experimental findings, the following recommendations can be made for extending the work in future.

7.2.1 Evaluating further aspects of rPP hybrid composites

The experimental results in Chapter 6 can be augmented by investigation of further aspects that can improve the performances of rPP hybrid composites, such as effect of screw

configurations, processing conditions, additive content and different rPP sources. These properties have been expected to influence to performance of rPP hybrid composites.

7.2.2 Improvements to the properties of hybrid composites

Related to the experimental results from the mechanical properties, there was some room for improvements with regard to the impact strength and MFI. It was found that the impact strength of hybrid composites exhibited the least improvement in comparison to tensile and flexural moduli. Here, the effect of impact modifiers, filler types and content can be explored.

7.2.3 Optimization of the scalability to the commercial scale

In order to commercially implement the formulations and concept of this study, the effect of extruder size (i.e, the difference between the lab and commercial scale extruders or compounding devices) shall be further studied. Different machine size might give different mixing behaviours and resulting composite properties.

7.2.4 Evaluating aspects of fibre length of PP/glass fibre and PP/carbon fibre in comparison

The further experiments should be investigated in order to compare the performance of the PP/glass fibre and PP/carbon fibre composites with the same range of the fibre length. These experiments will be gained more comprehension of composite performances under the fibre length control.

7.2.5 Further investigate other polymer composite systems

The findings from this project can be expanded by applying to other polymer composite systems especially polyolefin such as Polyethylene (PE), etc. These experiments can be the guidelines for improve the recycled polymers and apply to high-end applications such automotive, electrical appliance, etc.

References

[1] R. R. Nagavally, "Composite materials-history, types, fabrication techniques, advantages, and applications," *Int J Mech Prod Eng,* vol. 5, no. 9, pp. 82-7, 2017.

[2] D. Nwabunma and T. Kyu, *Polyolefin composites*. John Wiley & Sons, 2008.

[3] S. Thomas *et al.*, "Composite Materials," in *Ullmann's Encyclopedia of Industrial Chemistry*, pp. 1-44.

[4] R.-M. Wang, S.-R. Zheng, and Y. G. Zheng, *Polymer matrix composites and technology*. Elsevier, 2011.

[5] D. K. Rajak, D. D. Pagar, R. Kumar, and C. I. Pruncu, "Recent progress of reinforcement materials: A comprehensive overview of composite materials," *Journal of Materials Research and Technology,* vol. 8, no. 6, pp. 6354-6374, 2019.

[6] S. M. Sapuan, "Chapter 3 - Composite Materials," in *Composite Materials*, S. M. Sapuan Ed. Boston: Butterworth-Heinemann, 2017, pp. 57-93.

[7] İ. H. Hacıalioğlu. "A Review of the Global Composites Market and Turkish Composites Market " https://www.reinforcer.com/en/author/default/General-Secretary-Kompozit-Sanayicileri-Dernegi/61/350/0 (accessed 08/03/2021, 2021).

[8] "Global Composites Market Research Report 2020." QY Research. https://www.marketstudyreport.com/reports/global-composites-market-research-report-2020?gclid=Cj0KCQjwiYL3BRDVARIsAF9E4GfxI88nIPoDYSknRwQx9UCkkR8lYzvkJWUHDlZqjaEyrGk-wGzay1YaAnmVEALw_wcB (accessed 08/03/2021, 2021).

[9] L. Martinez. "Thermoset and Thermoplastic Composites." https://www.instron.com/en/our-company/press-room/blog/2014/april/thermoset-and-thermoplastic-composites-what-is-the-difference (accessed 2021 August, 1, 2021).

[10] T. Johnson. "Thermoplastic vs. Thermoset Resins." https://www.thoughtco.com/thermoplastic-vs-thermoset-resins-820405 (accessed 2021, Auguest 1, 2021).

[11] Q. T. Shubhra, A. Alam, and M. Quaiyyum, "Mechanical properties of polypropylene composites: A review," *Journal of thermoplastic composite materials,* vol. 26, no. 3, pp. 362-391, 2013.

[12] V. K. Thakur, M. K. Thakur, and A. Pappu, *Hybrid Polymer Composite Materials: Applications*. Elsevier Science, 2017.

[13] B. Wassener. "Raising Awareness of Plastic Waste." https://www.nytimes.com/2011/08/15/business/energy-environment/raising-awareness-of-plastic-waste.html (accessed 08/05/2020, 2020).

[14] V. K. Thakur, M. K. Thakur, and A. Pappu, *Hybrid Polymer Composite Materials: Properties and Characterisation*. Elsevier Science, 2017.

[15] H. B. Vinay, H. Govindaraju, and P. Banakar, "Experimental study on mechanical properties of polymer based hybrid composite," *Materials Today: Proceedings,* vol. 4, no. 10, pp. 10904-10912, 2017.

[16] V. Arumugaprabu, T. J. Ko, M. Uthayakumar, and R. D. Joel Johnson, "11 - Failure analysis in hybrid composites prepared using industrial wastes," in *Failure Analysis in Biocomposites, Fibre-Reinforced Composites and Hybrid Composites*, M. Jawaid, M. Thariq, and N. Saba Eds.: Woodhead Publishing, 2019, pp. 229-244.

[17] M. Jawaid, M. Thariq, and N. Saba, *Structural Health Monitoring of Biocomposites, Fibre-Reinforced Composites and Hybrid Composites*. Elsevier Science, 2018.

[18] C. T. Herakovich, *Mechanics of fibrous composites*. New York: Wiley (in English), 1998.

[19] B. Alemour, O. Badran, and M. Hassan, "A Review of Using Conductive Composite Materials in Solving Lightening Strike and Ice Accumulation Problems in Aviation," *Journal of Aerospace Technology and Management,* vol. 11, 03/01 2019, doi: 10.5028/jatm.v11.1022.

[20] "A350 Family Shaping the future of air travel." https://www.airbus.com/aircraft/passenger-aircraft/a350xwb-family.html (accessed 08/03/2021, 2021).

[21] S. M. Kiran Pulidindi. "Aerospace Composites Market Size " https://www.gminsights.com/industry-analysis/aerospace-composites-market (accessed 08/05/2020, 2020).
[22] (2019) 2019 state of industry report. *CompositesThe Official Magazine of the American Composites Manufacturers Association Manufacturing*. 34.
[23] G. Marsh, "Next step for automotive materials," *Materials Today,* vol. 6, no. 4, pp. 36-43, 2003/04/01/ 2003, doi: https://doi.org/10.1016/S1369-7021(03)00429-2.
[24] M. Balasubramanian, *Composite materials and processing*. CRC press, 2013.
[25] A. P. Mouritz, E. Gellert, P. Burchill, and K. Challis, "Review of advanced composite structures for naval ships and submarines," *Composite Structures,* vol. 53, no. 1, pp. 21-42, 2001/07/01/ 2001, doi: https://doi.org/10.1016/S0263-8223(00)00175-6.
[26] V. McConnell, "Application of Composites in Sporting Goods," *Comprehensive Composite Materials,* vol. 6, pp. 787-809, 12/31 2000, doi: 10.1016/B0-08-042993-9/00194-7.
[27] T. Wautelet, *The Concept of Circular Economy: its Origins and its Evolution*. 2018.
[28] O. Franklin-Wallis. "Plastic recycling is a myth': what really happens to your rubbish?" https://www.theguardian.com/environment/2019/aug/17/plastic-recycling-myth-what-really-happens-your-rubbish (accessed.
[29] "How Environment-Friendly Life Science Labs Are Minimizing Plastic Waste." https://www.genfollower.com/life-science-labs-minimizing-plastic-waste/ (accessed 08/03/2021, 2021).
[30] "The Amount of Plastic Waste Worldwide." http://environment.cenn.org/waste-management/publications/amount-plastic-waste-worldwide/ (accessed 10/05/2020, 2020).
[31] R. Geyer, J. Jambeck, and K. Law, "Production, use, and fate of all plastics ever made," *Science Advances,* vol. 3, p. e1700782, 07/01 2017, doi: 10.1126/sciadv.1700782.
[32] "Global plastics industry - Statistics & Facts." Ian Tiseo. https://www.statista.com/topics/5266/plastics-industry/ (accessed 23/03/2021, 2021).
[33] N. Singh, D. Hui, R. Singh, I. P. S. Ahuja, L. Feo, and F. Fraternali, "Recycling of plastic solid waste: A state of art review and future applications," *Composites Part B: Engineering,* vol. 115, pp. 409-422, 2017/04/15/ 2017, doi: https://doi.org/10.1016/j.compositesb.2016.09.013.
[34] R. Turner, C. Kelly, R. Fox, and B. Hopkins, "Re-Formative Polymer Composites from Plastic Waste: Novel Infrastructural Product Application," *Recycling,* vol. 3, p. 54, 11/23 2018, doi: 10.3390/recycling3040054.
[35] E. L. US, B. Irving, T. Martinsen, and K. Mareckova, "EMISSIONS FROM WASTE INCINERATION," 2019.
[36] M. Macklin. "Is it Really Worth the Convenience? 6 Ways Plastic is Harming Animals, the Planet and Us." https://www.onegreenplanet.org/environment/how-plastic-is-harming-animals-the-planet-and-us/ (accessed 5/10/2019, 2019).
[37] S. Lerner. "WASTE ONLY How the Plastics Industry Is Fighting to Keep Polluting the World." https://theintercept.com/2019/07/20/plastics-industry-plastic-recycling/ (accessed 04/05/2020, 2020).
[38] "Production of plastics worldwide from 1950 to 2019 " https://www.statista.com/statistics/282732/global-production-of-plastics-since-1950/ (accessed 05/01/2021, 2021).
[39] C.-S. Jeannie Evers. "Great Pacific Garbage Patch." https://www.nationalgeographic.org/encyclopedia/great-pacific-garbage-patch/ (accessed.
[40] E. Van Eygen, D. Laner, and J. Fellner, "Circular economy of plastic packaging: Current practice and perspectives in Austria," (in eng), *Waste Manag,* vol. 72, pp. 55-64, Feb 2018, doi: 10.1016/j.wasman.2017.11.040.
[41] "2019 Plastic Recycling Trends." https://industrytoday.com/2019-plastic-recycling-trends/ (accessed 20/05/2020, 2020).

[42] J. Poulakis, P. Varelidis, and C. Papaspyrides, "Recycling of polypropylene-based composites," *Advances in Polymer Technology: Journal of the Polymer Processing Institute,* vol. 16, no. 4, pp. 313-322, 1997.
[43] J. Korhonen, A. Honkasalo, and J. Seppälä, "Circular economy: the concept and its limitations," *Ecological economics,* vol. 143, pp. 37-46, 2018.
[44] Z. Yuan, J. Bi, and Y. Moriguchi, "The Circular Economy: A New Development Strategy in China," *Journal of Industrial Ecology,* vol. 10, pp. 4-8, 02/08 2008, doi: 10.1162/108819806775545321.
[45] P. R. Europe. "CIRCULAR ECONOMY." https://www.plasticsrecyclers.eu/circular-economy (accessed 20/05/2020, 2020).
[46] "RECYCLING IS IN A SERIOUS CRISIS. So let's fix it, shall we?" https://www.recycleacrossamerica.org/recycling-facts (accessed 10/10/2020, 2020).
[47] "Recycling Basics." https://www.epa.gov/recycle/recycling-basics (accessed 10/10/2020, 2020).
[48] D. Weckström, "Changes in mechanical properties of recycled polypropylene," Plastic Technology, Arcada-University of Applied Sciences, 2008. [Online]. Available: https://core.ac.uk/download/pdf/38057135.pdf
[49] H. Jmal *et al.*, "Influence of the grade on the variability of the mechanical properties of polypropylene waste," *Waste Management,* vol. 75, 02/01 2018, doi: 10.1016/j.wasman.2018.02.006.
[50] C. Spicker, N. Rudolph, I. Kühnert, and C. Aumnate, "The use of rheological behavior to monitor the processing and service life properties of recycled polypropylene," *Food Packaging and Shelf Life,* vol. 19, pp. 174-183, 2019.
[51] "Global amount of macro- and microplastics lost to the environment by type 2018." Ian Tiseo. https://www.statista.com/statistics/1016824/macro-microplastics-lost-to-environment-by-type/ (accessed.
[52] D. Mekap and S. Palsule, "Secondary Fiber / Recycled Polypropylene Composites," *Asian Journal of Research in Chemistry,* vol. 5, p. 655, 05/07 2012.
[53] C. Rogueda-Berriet, N. Bahlouli, D. Pessey, and Y. Rémond, "Mechanical behavior of recycled polypropylene composites under tensile, bending, and creep loading: experimental and modeling," *Journal of engineering materials and technology,* vol. 133, no. 3, 2011.
[54] D. G. Papageorgiou, I. A. Kinloch, and R. J. Young, "Hybrid multifunctional graphene/glass-fibre polypropylene composites," *Composites Science and Technology,* vol. 137, pp. 44-51, 2016.
[55] J. Hartikainen *et al.*, "Polypropylene hybrid composites reinforced with long glass fibres and particulate filler," *Composites Science and Technology,* vol. 65, no. 2, pp. 257-267, 2005.
[56] F. A. Ghasemi, I. Ghasemi, S. Menbari, M. Ayaz, and A. Ashori, "Optimization of mechanical properties of polypropylene/talc/graphene composites using response surface methodology," *Polymer Testing,* vol. 53, pp. 283-292, 2016.
[57] S. Zaferani, "Introduction of polymer-based nanocomposites," 2018, pp. 1-25.
[58] L. F. Miranda, L. H. Silveira, S. Leonardo, and A. Munhoz, "Irradiation of a Polypropilene-Glass Fiber Composite," *Advances in Science and Technology,* vol. 71, pp. 138-144, 10/01 2010, doi: 10.4028/www.scientific.net/AST.71.138.
[59] S. M. Zebarjad, R. Bagheri, S. Seyed Reihani, and M. Forunchi, "Investigation of deformation mechanism in polypropylene/glass fiber composite," *Journal of applied polymer science,* vol. 87, no. 13, pp. 2171-2176, 2003.
[60] C. Eberhardt, A. Clarke, M. Vincent, T. Giroud, and S. Flouret, "Fibre-orientation measurements in short-glass-fibre composites—II: A quantitative error estimate of the 2d image analysis technique," *Composites Science and Technology,* vol. 61, no. 13, pp. 1961-1974, 2001.
[61] C. C. Wang, Y. Y. Zhao, H. Y. Ge, and R. S. Qian, "Enhanced mechanical and thermal properties of short carbon fiber reinforced polypropylene composites by graphene oxide," *Polymer Composites,* vol. 39, no. 2, pp. 405-413, 2018.

[62] G. Jannerfeldt, R. Törnqvist, N. Rambert, L. Boogh, and J.-A. E. Månson, "Matrix modification for improved reinforcement effectiveness in polypropylene/glass fibre composites," *Applied Composite Materials,* vol. 8, no. 5, pp. 327-341, 2001.
[63] M. Etcheverry and S. E. Barbosa, "Glass fiber reinforced polypropylene mechanical properties enhancement by adhesion improvement," *Materials,* vol. 5, no. 6, pp. 1084-1113, 2012.
[64] S.-Y. Fu and B. Lauke, "Effects of fiber length and fiber orientation distributions on the tensile strength of short-fiber-reinforced polymers," *Composites Science and Technology,* vol. 56, no. 10, pp. 1179-1190, 1996.
[65] M. Carling and J. Williams, "Fiber length distribution effects on the fracture of short-fiber composites," *Polymer composites,* vol. 11, no. 6, pp. 307-313, 1990.
[66] F. Ramsteiner and R. Theysohn, "Tensile and impact strengths of unidirectional, short fibre-reinforced thermoplastics," *Composites,* vol. 10, no. 2, pp. 111-119, 1979.
[67] V. Gupta, R. Mittal, P. Sharma, G. Mennig, and J. Wolters, "Some studies on glass fiber-reinforced polypropylene. Part II: Mechanical properties and their dependence on fiber length, interfacial adhesion, and fiber dispersion," *Polymer composites,* vol. 10, no. 1, pp. 16-27, 1989.
[68] M. Chen, C. Wan, Y. Zhang, and Y. Zhang, "Fibre orientation and mechanical properties of short glass fibre reinforced PP composites," *Polymers and Polymer Composites,* vol. 13, no. 3, pp. 253-262, 2005.
[69] V. Gupta, R. Mittal, P. Sharma, G. Mennig, and J. Wolters, "Some studies on glass fiber-reinforced polypropylene. Part I: Reduction in fiber length during processing," *Polymer composites,* vol. 10, no. 1, pp. 8-15, 1989.
[70] B. Lauke, B. Schultrich, and W. Pompe, "THEORETICAL CONSIDERATIONS O TOUGHNESS OF SHORT-FIBR-REINFORCD THRMOPLASTICS," *Polymer-Plastics Technology and Engineering,* vol. 29, no. 7-8, pp. 607-806, 1990.
[71] D. Pérez-Rocha, A. Morales-Cepeda, F. Navarro-Pardo, T. Lozano-Ramírez, and P. G. Lafleur, "Carbon fiber composites of pure polypropylene and maleated polypropylene blends obtained from injection and compression moulding," *International Journal of Polymer Science,* vol. 2015, 2015.
[72] H. Yılmaz, Y. Imai, K. Nagata, K. Sato, and Y. Hotta, "Localized thermal analysis of carbon fiber-reinforced polypropylene composites," *Polymer composites,* vol. 33, no. 10, pp. 1764-1769, 2012.
[73] L. Altay *et al.*, "Manufacturing of recycled carbon fiber reinforced polypropylene composites by high speed thermo-kinetic mixing for lightweight applications," *Polymer Composites,* vol. 39, no. 10, pp. 3656-3665, 2018.
[74] Y. Xiaochun, Y. Youhua, F. Yanhong, Z. Guizhen, and W. Jinsong, "Preparation and characterization of carbon fiber/polypropylene composites via a tri-screw in-line compounding and injection molding," *Advances in Polymer Technology,* vol. 37, no. 8, pp. 3861-3872, 2018.
[75] C.-L. Huang, C.-W. Lou, C.-F. Liu, C.-H. Huang, X.-M. Song, and J.-H. Lin, "Polypropylene/graphene and polypropylene/carbon fiber conductive composites: mechanical, crystallization and electromagnetic properties," *Applied Sciences,* vol. 5, no. 4, pp. 1196-1210, 2015.
[76] G. Pritchard, *Plastics additives: an AZ reference*. Springer Science & Business Media, 2012.
[77] A. Dt, K. Prasad, and P. Rao, "Study of Mechanical Properties of Carbon Fiber Reinforced Polypropylene," *International Journal of Engineering Research and,* vol. V4, 10/26 2015, doi: 10.17577/IJERTV4IS100500.
[78] N. G. Karsli and A. Aytac, "Effects of maleated polypropylene on the morphology, thermal and mechanical properties of short carbon fiber reinforced polypropylene composites," *Materials & Design,* vol. 32, no. 7, pp. 4069-4073, 2011.
[79] H.-I. Kim, W. Han, W.-K. Choi, S.-J. Park, K.-H. An, and B.-J. Kim, "Effects of maleic anhydride content on mechanical properties of carbon fibers-reinforced maleic anhydride-grafted-poly-propylene matrix composites," *Carbon letters,* vol. 20, pp. 39-46, 2016.

[80] G. Staab, *Laminar composites*. Butterworth-Heinemann, 2015.
[81] P. Withers, "Elastic and thermoelastic properties of brittle matrix composites," 2016.
[82] Y. Thio, A. Argon, R. Cohen, and M. Weinberg, "Toughening of isotactic polypropylene with CaCO3 particles," *Polymer,* vol. 43, no. 13, pp. 3661-3674, 2002.
[83] K. Mitsuishi, S. Ueno, and K. Kameyama, "Crystallization behavior of polypropylene filled with calcium carbonate of various shape," *Die Angewandte Makromolekulare Chemie: Applied Macromolecular Chemistry and Physics,* vol. 215, no. 1, pp. 11-24, 1994.
[84] D. Eiras and L. A. Pessan, "Mechanical properties of polypropylene/calcium carbonate nanocomposites," *Materials Research,* vol. 12, no. 4, pp. 517-522, 2009.
[85] K. Palanikumar, R. AshokGandhi, B. Raghunath, and V. Jayaseelan, "Role of Calcium Carbonate (CaCO3) in improving wear resistance of Polypropylene (PP) components used in automobiles," *Materials Today: Proceedings,* vol. 16, pp. 1363-1371, 2019.
[86] T. Dai Lam, T. V. Hoang, D. T. Quang, and J. S. Kim, "Effect of nanosized and surface-modified precipitated calcium carbonate on properties of CaCO3/polypropylene nanocomposites," *Materials Science and Engineering: A,* vol. 501, no. 1-2, pp. 87-93, 2009.
[87] T. Thenepalli, A. Y. Jun, C. Han, C. Ramakrishna, and J. W. Ahn, "A strategy of precipitated calcium carbonate (CaCO 3) fillers for enhancing the mechanical properties of polypropylene polymers," *Korean Journal of Chemical Engineering,* vol. 32, no. 6, pp. 1009-1022, 2015.
[88] Y. Leong, M. A. Bakar, Z. M. Ishak, and A. Ariffin, "Characterization of talc/calcium carbonate filled polypropylene hybrid composites weathered in a natural environment," *Polymer Degradation and Stability,* vol. 83, no. 3, pp. 411-422, 2004.
[89] K. Yang, Q. Yang, G. Li, Y. Sun, and D. Feng, "Morphology and mechanical properties of polypropylene/calcium carbonate nanocomposites," *Materials letters,* vol. 60, no. 6, pp. 805-809, 2006.
[90] C.-M. Chan, J. Wu, J.-X. Li, and Y.-K. Cheung, "Polypropylene/calcium carbonate nanocomposites," *polymer,* vol. 43, no. 10, pp. 2981-2992, 2002.
[91] Y. Lin, H. Chen, C.-M. Chan, and J. Wu, "High impact toughness polypropylene/CaCO3 nanocomposites and the toughening mechanism," *Macromolecules,* vol. 41, no. 23, pp. 9204-9213, 2008.
[92] Y. Leong, M. Abu Bakar, Z. M. Ishak, A. Ariffin, and B. Pukanszky, "Comparison of the mechanical properties and interfacial interactions between talc, kaolin, and calcium carbonate filled polypropylene composites," *Journal of Applied Polymer Science,* vol. 91, no. 5, pp. 3315-3326, 2004.
[93] M. C. Rocha, A. H. Silva, F. M. Coutinho, and A. L. N. Silva, "Study of composites based on polypropylene and calcium carbonate by experimental design," *Polymer Testing,* vol. 24, no. 8, pp. 1049-1053, 2005.
[94] J. Duca, "Kaolin," *Functional Fillers for Plastics,* pp. 221-239, 2005.
[95] S. Maiti and B. Lopez, "Tensile properties of polypropylene/kaolin composites," *Journal of applied polymer science,* vol. 44, no. 2, pp. 353-360, 1992.
[96] A. Ariffin, A. Mansor, S. Jikan, and Z. Mohd. Ishak, "Mechanical, morphological, and thermal properties of polypropylene/kaolin composite. Part I. The effects of surface-treated kaolin and processing enhancement," *Journal of applied polymer science,* vol. 108, no. 6, pp. 3901-3916, 2008.
[97] N. A. Rahim, Z. Ariff, A. Ariffin, and S. Jikan, "Study on effect of filler loading on the flow and swelling behaviors of polypropylene-kaolin composites using single-screw extruder," *Journal of Applied Polymer Science,* vol. 119, no. 1, pp. 73-83, 2011.
[98] A. Helmy, E. Ferreiro, and S. De Bussetti, "The surface energy of kaolinite," *Colloid and Polymer Science,* vol. 283, no. 2, pp. 225-228, 2004.
[99] E. Chibowski and K. Terpilowski, "Surface free energy of polypropylene and polycarbonate solidifying at different solid surfaces," *Applied surface science,* vol. 256, no. 5, pp. 1573-1581, 2009.

[100] J. Yao, H. Zhu, Y. Qi, M. Guo, Q. Hu, and L. Gao, "Tough and Reinforced Polypropylene/Kaolin Composites using Modified Kaolin," in *IOP Conference Series: Materials Science and Engineering*, 2018, vol. 359, no. 1: IOP Publishing, p. 012034.
[101] K. Yang, Q. Yang, G. Li, J. Kuang, and Z. Jiang, "Mechanical properties and morphologies of polypropylene with different sizes of glass bead particles," *Polymer composites,* vol. 29, no. 9, pp. 992-997, 2008.
[102] J. Liang and C. Wu, "Effects of the glass bead content and the surface treatment on the mechanical properties of polypropylene composites," *Journal of applied polymer science,* vol. 123, no. 5, pp. 3054-3063, 2012.
[103] K. W. Kwok, Z. Gao, C. Choy, and X. Zhu, "Stiffness and toughness of polypropylene/glass bead composites," *Polymer composites,* vol. 24, no. 1, pp. 53-59, 2003.
[104] J. Liang and R. Li, "Mechanical properties and morphology of glass bead–filled polypropylene composites," *Polymer composites,* vol. 19, no. 6, pp. 698-703, 1998.
[105] C. P. Tsui, C. Y. Tang, and T. Lee, "Strain damage and fracture properties of glass bead filled polypropylene," in *European Structural Integrity Society*, vol. 27: Elsevier, 2000, pp. 395-406.
[106] J.-Z. Liang, "Estimation of thermal conductivity for polypropylene/hollow glass bead composites," *Composites Part B: Engineering,* vol. 56, pp. 431-434, 2014.
[107] R. Sengupta, M. Bhattacharya, S. Bandyopadhyay, and A. K. Bhowmick, "A review on the mechanical and electrical properties of graphite and modified graphite reinforced polymer composites," *Progress in polymer science,* vol. 36, no. 5, pp. 638-670, 2011.
[108] M. A. Al-Saleh *et al.*, "Polypropylene/graphene nanocomposites: Effects of GNP loading and compatibilizers on the mechanical and thermal properties," *Materials,* vol. 12, no. 23, p. 3924, 2019.
[109] J.-Z. Liang, "Effects of tension rates and filler size on tensile properties of polypropylene/graphene nano-platelets composites," *Composites Part B: Engineering,* vol. 167, pp. 241-249, 2019.
[110] M. El Achaby, F. E. Arrakhiz, S. Vaudreuil, A. el Kacem Qaiss, M. Bousmina, and O. Fassi-Fehri, "Mechanical, thermal, and rheological properties of graphene-based polypropylene nanocomposites prepared by melt mixing," *Polymer composites,* vol. 33, no. 5, pp. 733-744, 2012.
[111] Z. Xu *et al.*, "Relationship between the structure and thermal properties of polypropylene/graphene nanoplatelets composites for different platelet-sizes," *Composites Science and Technology,* vol. 183, p. 107826, 2019.
[112] T. Gopakumar and D. Pagé, "Polypropylene/graphite nanocomposites by thermo-kinetic mixing," *Polymer Engineering & Science,* vol. 44, no. 6, pp. 1162-1169, 2004.
[113] S. He, J. Zhang, X. Xiao, Y. Lai, A. Chen, and Z. Zhang, "Study on the morphology development and dispersion mechanism of polypropylene/graphene nanoplatelets composites for different shear field," *Composites Science and Technology,* vol. 153, pp. 209-221, 2017.
[114] M. Mistretta, L. Botta, A. Vinci, M. Ceraulo, and F. La Mantia, "Photo-oxidation of polypropylene/graphene nanoplatelets composites," *Polymer Degradation and Stability,* vol. 160, pp. 35-43, 2019.
[115] M. R. Jamir, M. S. Majid, and A. Khasri, "Natural lightweight hybrid composites for aircraft structural applications," in *Sustainable composites for aerospace applications*: Elsevier, 2018, pp. 155-170.
[116] D. G. Baird and D. I. Collias, *Polymer processing: principles and design*. John Wiley & Sons, 2014.
[117] C. Rauwendaal, *Polymer extrusion*. Carl Hanser Verlag GmbH Co KG, 2014.
[118] S. H. Bumm, J. L. White, and A. I. Isayev, "Glass fiber breakup in corotating twin screw extruder: Simulation and experiment," *Polymer composites,* vol. 33, no. 12, pp. 2147-2158, 2012.
[119] B. M. Lekube, B. Purgleitner, K. Renner, and C. Burgstaller, "Influence of screw configuration and processing temperature on the properties of short glass fiber reinforced polypropylene composites," *Polymer Engineering & Science,* vol. 59, no. 8, pp. 1552-1559, 2019.

[120] "Temperature Control Systems and Electric Heaters." https://www.process-heating.com/articles/90598-the-importance-of-temperature-control-in-plastic-injection-molding (accessed 20/10/2020, 2020).
[121] SHS_Extrusion_Training. "How to set up optimal extrusion barrel temperatures." SHS_Extrusion_Training. https://www.extrusion-training.de/en/wie-erkenne-ich-das-perfekte-extruder-temperaturprofil/ (accessed 20/10/2020, 2020).
[122] B. Krause, P. Pötschke, and L. Häußler, "Influence of small scale melt mixing conditions on electrical resistivity of carbon nanotube-polyamide composites," *Composites Science and Technology,* vol. 69, no. 10, pp. 1505-1515, 2009.
[123] T. Villmow, P. Pötschke, S. Pegel, L. Häussler, and B. Kretzschmar, "Influence of twin-screw extrusion conditions on the dispersion of multi-walled carbon nanotubes in a poly (lactic acid) matrix," *Polymer,* vol. 49, no. 16, pp. 3500-3509, 2008.
[124] G. O. Lim, K. T. Min, and G. H. Kim, "Effect of cooling rate on the surface resistivity of polymer/multi-walled carbon nanotube nanocomposites," *Polymer Engineering & Science,* vol. 50, no. 2, pp. 290-294, 2010.
[125] Y. Li and H. Shimizu, "High-shear processing induced homogenous dispersion of pristine multiwalled carbon nanotubes in a thermoplastic elastomer," *Polymer,* vol. 48, no. 8, pp. 2203-2207, 2007.
[126] T. Villmow, B. Kretzschmar, and P. Pötschke, "Influence of screw configuration, residence time, and specific mechanical energy in twin-screw extrusion of polycaprolactone/multi-walled carbon nanotube composites," *Composites Science and Technology,* vol. 70, no. 14, pp. 2045-2055, 2010.
[127] A. Isayev, "Kinetic Model of Glass Fiber Breakup in Corotating Twin Screw Extruder," 2012.
[128] G. Ozkoc, G. Bayram, and E. Bayramli, "Short glass fiber reinforced ABS and ABS/PA6 composites: processing and characterization," *Polymer composites,* vol. 26, no. 6, pp. 745-755, 2005.
[129] K. M. Cantor, "Analyzing extruder energy consumption," *SPE ANTEC technical papers,* vol. 2, pp. 1300-1306, 2010.
[130] P. Pötschke, A. R. Bhattacharyya, and A. Janke, "Carbon nanotube-filled polycarbonate composites produced by melt mixing and their use in blends with polyethylene," *Carbon,* vol. 42, no. 5-6, pp. 965-969, 2004.
[131] G. S. Ezat, A. L. Kelly, M. Youseffi, and P. D. Coates, "Effect of screw configuration on the dispersion and properties of polypropylene/multiwalled carbon nanotube composite," *Polymer Composites,* vol. 40, no. 11, pp. 4196-4204, 2019.
[132] N. L. Feng, S. D. Malingam, and S. Irulappasamy, "Bolted joint behavior of hybrid composites," in *failure analysis in biocomposites, fibre-reinforced composites and hybrid composites*: Elsevier, 2019, pp. 79-95.
[133] M. M. Thwe and K. Liao, "Durability of bamboo-glass fiber reinforced polymer matrix hybrid composites," *Composites science and technology,* vol. 63, no. 3-4, pp. 375-387, 2003.
[134] S.-Y. Fu, G. Xu, and Y.-W. Mai, "On the elastic modulus of hybrid particle/short-fiber/polymer composites," *Composites Part B: Engineering,* vol. 33, no. 4, pp. 291-299, 2002.
[135] M. N. Fazita, H. A. Khalil, T. M. Wai, E. Rosamah, and N. S. Aprilia, "Hybrid bast fiber reinforced thermoset composites," in *Hybrid Polymer Composite Materials*: Elsevier, 2017, pp. 203-234.
[136] N. Saba, M. Jawaid, M. T. H. Sultan, and O. Alothman, "Hybrid multifunctional composites—recent applications," *Hybrid Polymer Composite Materials,* pp. 151-167, 2017.
[137] M. Asim, M. Jawaid, N. Saba, M. Nasir, and M. T. H. Sultan, "Processing of hybrid polymer composites—a review," *Hybrid polymer composite materials,* pp. 1-22, 2017.
[138] V. Arumugaprabu, T. J. Ko, M. Uthayakumar, and R. D. J. Johnson, "Failure analysis in hybrid composites prepared using industrial wastes," in *Failure Analysis in Biocomposites, Fibre-Reinforced Composites and Hybrid Composites*: Elsevier, 2019, pp. 229-244.
[139] V. P. Mcconnell, "Application of composites in sporting goods," 2000.

[140] B. Alemour, O. Badran, and M. R. Hassan, "A review of using conductive composite materials in solving lightening strike and ice accumulation problems in aviation," *Journal of Aerospace Technology and Management,* vol. 11, 2019.
[141] M. A. Bakar, Y. Leong, A. Ariffin, and Z. M. Ishak, "Mechanical, flow, and morphological properties of talc-and kaolin-filled polypropylene hybrid composites," *Journal of Applied Polymer Science,* vol. 104, no. 1, pp. 434-441, 2007.
[142] M. İnal, S. Sahin, and Y. Sahin, "Optimization of the Young's Modulus of Low Flow Polypropylene Talc/Colemanite Hybrid Composite Materials with Artificial Neural Networks," *IFAC-PapersOnLine,* vol. 51, no. 30, pp. 277-281, 2018.
[143] X. Yan, Y. Yang, and H. Hamada, "Tensile properties of glass fiber reinforced polypropylene composite and its carbon fiber hybrid composite fabricated by direct fiber feeding injection molding process," *Polymer Composites,* vol. 39, no. 10, pp. 3564-3574, 2018.
[144] M. A. Khan, J. Ganster, and H.-P. Fink, "Hybrid composites of jute and man-made cellulose fibers with polypropylene by injection moulding," *Composites Part A: Applied Science and Manufacturing,* vol. 40, no. 6-7, pp. 846-851, 2009.
[145] R. Gogoi, G. Manik, and B. Arun, "High specific strength hybrid polypropylene composites using carbon fibre and hollow glass microspheres: Development, characterization and comparison with empirical models," *Composites Part B: Engineering,* vol. 173, p. 106875, 2019.
[146] J. Himani and J. Purnima, "Development of glass fiber, wollastonite reinforced polypropylene hybrid composite: Mechanical properties and morphology," *Materials Science and Engineering: A,* vol. 527, no. 7-8, pp. 1946-1951, 2010.
[147] S. Jacob, K. Suma, J. M. Mendaz, A. George, and K. George, "Modification of polypropylene/glass fiber composites with nanosilica," in *Macromolecular symposia*, 2009, vol. 277, no. 1: Wiley Online Library, pp. 138-143.
[148] R. Nanoth and K. Jayanarayanan, "Polypropylene/short glass fiber/nanosilica hybrid composites: evaluation of morphology, mechanical, thermal, and transport properties," *Polymer Bulletin,* vol. 75, 06/01 2018, doi: 10.1007/s00289-017-2173-1.
[149] M. A. AlMaadeed, R. Kahraman, P. N. Khanam, and N. Madi, "Date palm wood flour/glass fibre reinforced hybrid composites of recycled polypropylene: Mechanical and thermal properties," *Materials & Design,* vol. 42, pp. 289-294, 2012.
[150] I. O. Oladele, I. O. Ibrahim, A. D. Akinwekomi, and S. I. Talabi, "Effect of mercerization on the mechanical and thermal response of hybrid bagasse fiber/CaCO3 reinforced polypropylene composites," *Polymer Testing,* vol. 76, pp. 192-198, 2019.
[151] H. Jmal *et al.*, "Influence of the grade on the variability of the mechanical properties of polypropylene waste," *Waste Management,* vol. 75, pp. 160-173, 2018.
[152] U. Soy, F. Findik, and S. Yetgin, "Fabrication and mechanical properties of glass fiber/Talc/CaCO 3 filled recycled PP composites," *Am J Appl Sci,* vol. 14, no. 9, pp. 878-885, 2017.
[153] M. Rokbi, A. Khaldoune, M. Sanjay, P. Senthamaraikannan, A. Ati, and S. Siengchin, "Effect of processing parameters on tensile properties of recycled polypropylene based composites reinforced with Jute fabrics," *International Journal of Lightweight Materials and Manufacture,* vol. 3, no. 2, pp. 144-149, 2020.
[154] K. M. Hyie, S. Budin, N. Martinus, Z. Salleh, and N. R. N. M. Masdek, "Tensile and flexural investigation on polypropylene recycling," in *Journal of Physics: Conference Series*, 2019, vol. 1174, no. 1: IOP Publishing, p. 012005.
[155] M. Szpieg, "Development and characteristics of a fully recycled CF/PP composite," Luleå tekniska universitet, 2011.
[156] K. Darshan, K. Naveen, and H. Rasmi, "Mechanical and thermal behaviour of a recycle polypropylene using fillers as an additives," *Int J Sci Eng Technol Res,* vol. 3, pp. 2532-2535, 2014.
[157] M. Al-Maadeed, Y. M. Shabana, and P. N. Khanam, "Processing, characterization and modeling of recycled polypropylene/glass fibre/wood flour composites," *Materials & Design,* vol. 58, pp. 374-380, 2014.

[158] T. Li, C. Ng, and R. Li, "Impact behavior of sawdust/recycled–PP composites," *Journal of Applied Polymer Science,* vol. 81, no. 6, pp. 1420-1428, 2001.
[159] M. H. Othman, "Recycled Polypropylene-Nanoclay Composites–Mechanical Properties," 2020.
[160] F. Gu, P. Hall, and N. Miles, "Development of composites based on recycled polypropylene for injection moulding automobile parts using hierarchical clustering analysis and principal component estimate," *Journal of Cleaner Production,* vol. 137, pp. 632-643, 2016.
[161] K. Wang, F. Addiego, N. Bahlouli, S. Ahzi, Y. Rémond, and V. Toniazzo, "Impact response of recycled polypropylene-based composites under a wide range of temperature: effect of filler content and recycling," *Composites Science and Technology,* vol. 95, pp. 89-99, 2014.
[162] Y. Zheng, F. Gu, Y. Ren, P. Hall, and N. J. Miles, "Improving mechanical properties of recycled polypropylene-based composites using Taguchi and ANOVA techniques," *Procedia CIRP,* vol. 61, pp. 287-292, 2017.
[163] F. J. H. T. V. Ramos, R. H. M. Reis, I. Grafova, A. Grafov, and S. N. Monteiro, "Eco-friendly recycled polypropylene matrix composites incorporated with geopolymer concrete waste particles," *Journal of Materials Research and Technology,* vol. 9, no. 3, pp. 3084-3090, 2020.
[164] V. Bogataj, P. Fajs, M. Omahen, C. Peñalva, A. Henttonen, and M. Cop, "Utilization of recycled polypropylene, cellulose and newsprint fibres for production of green composites," 2019.
[165] A. Sjögren, "Failure behaviour of polypropylene/glass bead composites," Luleå tekniska universitet, 1995.
[166] J.-Z. Liang and R. Li, "Brittle–ductile transition in polypropylene filled with glass beads," *Polymer,* vol. 40, no. 11, pp. 3191-3195, 1999.
[167] R. Scaffaro, L. Botta, and G. Di Benedetto, "Physical properties of virgin-recycled ABS blends: Effect of post-consumer content and of reprocessing cycles," *European Polymer Journal,* vol. 48, no. 3, pp. 637-648, 2012.
[168] M. M. Raj, H. V. Patel, L. M. Raj, and N. K. Patel, "Studies on mechanical properties of recycled polypropylene blended with virgin polypropylene," *International Journal of Science Innovations Today,* vol. 2, no. 3, pp. 194-203, 2013.
[169] L. G. Barbosa, M. Piaia, and G. H. Ceni, "Analysis of impact and tensile properties of recycled polypropylene," *International Journal of Materials Engineering,* vol. 7, no. 6, pp. 117-120, 2017.
[170] K. Ragaert, L. Delva, and K. Van Geem, "Mechanical and chemical recycling of solid plastic waste," *Waste Management,* vol. 69, pp. 24-58, 2017.
[171] H.-S. Tai and J.-L. Yeh, "Evaluation and verification of the virgin–recycled mixing ratio of polypropylene plastic," *Journal of the Chinese Institute of Engineers,* vol. 41, no. 1, pp. 69-75, 2018.
[172] E. Karaagac, T. Koch, and V.-M. Archodoulaki, "The effect of PP contamination in recycled high-density polyethylene (rPE-HD) from post-consumer bottle waste and their compatibilization with olefin block copolymer (OBC)," *Waste Management,* vol. 119, pp. 285-294, 2021.
[173] L. Scelsi *et al.*, "A review on composite materials based on recycled thermoplastics and glass fibres," *Plastics, rubber and composites,* vol. 40, no. 1, pp. 1-10, 2011.
[174] J. S., "Correlation properties and morphology of PP and glass fibre composites," Internal Report, 2019.
[175] "Global glass fiber market worth US$14.27 billion by 2019." https://www.materialstoday.com/composite-industry/news/global-glass-fiber-market-worth-us1427-billion/ (accessed 14/03/2020, 2020).
[176] X. Dai and P. Bates, "Mechanical properties of vibration welded short-and long-glass-fiber-reinforced polypropylene," *Composites Part A: Applied Science and Manufacturing,* vol. 39, no. 7, pp. 1159-1166, 2008.
[177] "Calcium Carbonate Market: Paper Industry Continues to Offer Lucrative Opportunities." https://www.transparencymarketresearch.com/calcium-carbonate-market.html (accessed 03/12/2020, 2020).

[178] P. Mantilaka, H. M. T. G. Pitawala, D. G. G. P. Karunaratne, and R. Rajapakse, *STEARIC ACID-COATED CALCIUM CARBONATE NANOCRYSTALLITES FROM DOLOMITE*. 2014.
[179] J. A. King, D. R. Klimek, I. Miskioglu, and G. M. Odegard, "Mechanical properties of graphene nanoplatelet/epoxy composites," *Journal of applied polymer science,* vol. 128, no. 6, pp. 4217-4223, 2013.
[180] I. M. Inuwa, A. Hassan, S. A. Samsudin, M. H. Mohamad Kassim, and M. Jawaid, "Mechanical and thermal properties of exfoliated graphite nanoplatelets reinforced polyethylene terephthalate/polypropylene composites," *Polymer Composites,* vol. 35, no. 10, pp. 2029-2035, 2014.
[181] C. I. Idumah and A. Hassan, "Characterization and preparation of conductive exfoliated graphene nanoplatelets kenaf fibre hybrid polypropylene composites," *Synthetic Metals,* vol. 212, pp. 91-104, 2016.
[182] G. Wypych and G. Wypych, "Fillers–Origin, Chemical Composition, Properties, and Morphology," *Handbook of Fillers (Fourth Edition), Chem Tec Publishing,* pp. 13-266, 2016.
[183] M. Tawfik, N. Ahmed, and A. Ward, "Characterization of kaolin-filled polymer composites," 07/15 2018, doi: 10.2417/spepro.004978.
[184] S. Zhang *et al.*, "Effects of kaolin on the thermal stability and flame retardancy of polypropylene composite," *Polymers for advanced technologies,* vol. 25, no. 9, pp. 912-919, 2014.
[185] B. Yalcin *et al.*, "3M Glass Bubbles iM16K for Reinforced Thermoplastics," *Technical Paper, issued Oct,* 2016.
[186] R. S. Chen, M. F. H. Mohd Ruf, D. Shahdan, and S. Ahmad, "Enhanced mechanical and thermal properties of electrically conductive TPNR/GNP nanocomposites assisted with ultrasonication," *PloS one,* vol. 14, no. 9, p. e0222662, 2019.
[187] Y.-S. Jun, J. G. Um, G. Jiang, G. Lui, and A. Yu, "Ultra-large sized graphene nano-platelets (GnPs) incorporated polypropylene (PP)/GnPs composites engineered by melt compounding and its thermal, mechanical, and electrical properties," *Composites Part B: Engineering,* vol. 133, pp. 218-225, 2018.
[188] S. Ansari and E. P. Giannelis, "Functionalized graphene sheet—Poly (vinylidene fluoride) conductive nanocomposites," *Journal of Polymer Science Part B: Polymer Physics,* vol. 47, no. 9, pp. 888-897, 2009.
[189] T. Ramanathan *et al.*, "Functionalized graphene sheets for polymer nanocomposites," *Nature nanotechnology,* vol. 3, no. 6, pp. 327-331, 2008.
[190] A. Ashori, S. Menbari, and R. Bahrami, "Mechanical and thermo-mechanical properties of short carbon fiber reinforced polypropylene composites using exfoliated graphene nanoplatelets coating," *Journal of Industrial and Engineering Chemistry,* vol. 38, pp. 37-42, 2016.
[191] M. A. Tofighy and T. Mohammadi, "Barrier, diffusion, and transport properties of rubber nanocomposites containing carbon nanofillers," in *Carbon-Based Nanofiller and Their Rubber Nanocomposites*: Elsevier, 2019, pp. 253-285.
[192] E. Grünschloss, "Polymer Single Screw Extrusion: Modeling," 2001.
[193] P. T. D. "EXTRUSION PLASTICS." https://www.thermopedia.com/content/753/ (accessed 12/01/2021, 2021).
[194] "KNEADING BLOCKS." SAHYOG INDUSTRIES. http://www.sahyog-industries.com/industrial-products-kb.htm (accessed 15/05/2020, 2020).
[195] J. Goff, T. Whelan, and D. DeLaney, "The Dynisco Extrusion Processors Handbook," ed: Dynisco, 2000.
[196] H. F. Giles and J. R. Wagner, *Extrusion: The Definitive Processing Guide and Handbook*. Elsevier Science, 2013.
[197] R. Crawford and P. Martin, "Chapter 4 Processing of Plastics," *Plastics Engineering (Third Edition), Butterworth-Heinemann, Oxford,* pp. 245-342, 1998.
[198] I. Sam Janajreh and M. Alshrah, "Remolding of cross-linked polyethylene cable waste: thermal and mechanical property assessment," *Int. J. Therm. Environ. Eng,* vol. 5, pp. 191-198, 2013.

[199] E. ISO, "527-2: 2012," *Plastics–Determination of tensile properties–Part,* vol. 2, 2012.
[200] B. ISO, "ISO 291, 2008, Plastics–Standard atmospheres for conditioning and testing," *British Standards Institution,* 2008.
[201] B. ISO, "178: 2010," *Plastics-Determination of flexural properties (ISO 178: 2010),* 2010.
[202] I. S. Organization, "ISO 180: 2000-Plastics--Determination of Izod impact strength," ed: ISO Geneva, 2000.
[203] A. G. Banerjee, "Computer aided design of side actions for injection molding of complex parts," 2006.
[204] G. Wypych, "8 - THE EFFECT OF FILLERS ON THE MECHANICAL PROPERTIES OF FILLED MATERIALS," in *Handbook of Fillers (Fourth Edition)*, G. Wypych Ed.: ChemTec Publishing, 2016, pp. 467-531.
[205] "Density determination kit instruction manual." Test Equipment Depot. https://www.testequipmentdepot.com/ohaus/pdfs/density-kit_manual.pdf (accessed 03/07/2020, 2020).
[206] A. D792, "Standard Test Methods for Density and Specific Gravity of Plastics by Displacement," ed: ASTM International West Conshohock-en, PA, USA, 2002.
[207] A. Shenoy and D. Saini, "Melt flow index: More than just a quality control rheological parameter. Part I," *Advances in Polymer Technology,* vol. 6, no. 1, pp. 1-58, 1986.
[208] D. ASTM, "1238-10. Standard test method for melt flow rates of thermoplastics by extrusion plastometer," *ICS number code,* vol. 83, p. 20, 2010.
[209] G. B. Carvalho, S. V. Canevarolo Jr, and J. A. Sousa, "Influence of interfacial interactions on the mechanical behavior of hybrid composites of polypropylene/short glass fibers/hollow glass beads," *Polymer Testing,* vol. 85, p. 106418, 2020.
[210] B. YALCIN, S. Amos, B. Urquiola, and I. Gunes, "Effect of Processing Conditions on the Extent of Glass Bubble Survival During Twin Screw Compounding," *Technical Paper,* no. 5, 2012.
[211] M. P. Cunha, L. B. Gonella, M. Poletto, A. M. C. Grisa, and R. N. Brandalise, "Poly (acrylonitrile-co-butadiene-co-styrene) Reinforced with Hollow Glass Microspheres: Evaluation of Extrusion Parameters and Their Effects on the Composite Properties," *Journal of Polymers,* vol. 2016, 2016.
[212] K.-S. Jang, "Low-density polycarbonate composites with robust hollow glass microspheres by tailorable processing variables," *Polymer Testing,* vol. 84, p. 106408, 2020.
[213] "Improving Twin-Screw Compounding Of Reinforced Polyolefins." https://www.ptonline.com/articles/improving-twin-screw-compounding-of-reinforced-polyolefins (accessed 21/09/2020, 2020).
[214] N. A. Rahman, A. Hassan, R. Yahya, and R. Lafia-Araga, "Impact properties of glass-fiber/polypropylene composites: the influence of fiber loading, specimen geometry and test temperature," *Fibers and Polymers,* vol. 14, no. 11, pp. 1877-1885, 2013.
[215] B. Li and W.-H. Zhong, "Review on polymer/graphite nanoplatelet nanocomposites," *Journal of materials science,* vol. 46, no. 17, pp. 5595-5614, 2011.
[216] H. Salmah, C. Ruzaidi, and A. Supri, "Compatibilisation of polypropylene/ethylene propylene diene terpolymer/kaolin composites: the effect of maleic anhydride grafted-polypropylene," *Journal of Physical Science,* vol. 20, no. 1, pp. 99-107, 2009.
[217] N. Yang *et al.*, "Effect of surface modified kaolin on properties of polypropylene grafted maleic anhydride," *Results in physics,* vol. 7, pp. 969-974, 2017.
[218] M. A. Osman and U. W. Suter, "Surface treatment of calcite with fatty acids: structure and properties of the organic monolayer," *Chemistry of materials,* vol. 14, no. 10, pp. 4408-4415, 2002.
[219] Z. Cao, M. Daly, L. Clémence, I. Major, C. L. Higginbotham, and D. M. Devine, "Characteristics of the treated calcium carbonate particles with stearic acid using different treating methods," 2016.

[220] C. W. Jeon, S. Park, J.-H. Bang, S. Chae, K. Song, and S.-W. Lee, "Nonpolar surface modification using fatty acids and its effect on calcite from mineral carbonation of desulfurized gypsum," *Coatings,* vol. 8, no. 1, p. 43, 2018.
[221] H. Böke, S. Akkurt, S. Özdemir, E. H. Göktürk, and E. N. C. Saltik, "Quantification of CaCO3–CaSO3· 0.5 H2O–CaSO4· 2H2O mixtures by FTIR analysis and its ANN model," *Materials Letters,* vol. 58, no. 5, pp. 723-726, 2004.
[222] S. Kirboga and M. Oner, "Effect of the experimental parameters on calcium carbonate precipitation," *Chemical Engineering Transactions,* vol. 32, 2013.
[223] J. D. Rodriguez-Blanco, S. Shaw, and L. G. Benning, "The kinetics and mechanisms of amorphous calcium carbonate (ACC) crystallization to calcite, via vaterite," *Nanoscale,* vol. 3, no. 1, pp. 265-271, 2011.
[224] A. Tironi, M. Trezza, E. Irassar, and A. Scian, "Thermal treatment of kaolin: effect on the pozzolanic activity," *Procedia Materials Science,* vol. 1, pp. 343-350, 2012.
[225] W. Urbaniak-Domagala, "The use of the spectrometric technique FTIR-ATR to examine the polymers surface," *Advanced aspects of spectroscopy,* vol. 3, pp. 85-104, 2012.
[226] M. Carrasco and F. Puertas, "Sodium silicate solutions from dissolution of glass wastes. Statistical analysis," *Materiales de Construcción,* vol. 64, 04/01 2014, doi: 10.3989/mc.2014.05213.
[227] Y. Geng, S. J. Wang, and J.-K. Kim, "Preparation of graphite nanoplatelets and graphene sheets," *Journal of colloid and interface science,* vol. 336, no. 2, pp. 592-598, 2009.
[228] A. S. Patole, S. P. Patole, H. Kang, J.-B. Yoo, T.-H. Kim, and J.-H. Ahn, "A facile approach to the fabrication of graphene/polystyrene nanocomposite by in situ microemulsion polymerization," *Journal of colloid and interface science,* vol. 350, no. 2, pp. 530-537, 2010.
[229] J. Li *et al.*, "Carbon nanowalls grown by microwave plasma enhanced chemical vapor deposition during the carbonization of polyacrylonitrile fibers," *Journal of Applied Physics,* vol. 113, no. 2, p. 024313, 2013.
[230] W. Yang, Z.-Y. Liu, G.-F. Shan, Z.-M. Li, B.-H. Xie, and M.-B. Yang, "Study on the melt flow behavior of glass bead filled polypropylene," *Polymer testing,* vol. 24, no. 4, pp. 490-497, 2005.
[231] E. Araujo, K. Araújo, O. Pereira, P. Ribeiro, and T. Mélo, "Fiberglass wastes/polyester resin composites: Mechanical properties and water sorption," *Polímeros,* vol. 16, pp. 332-335, 12/01 2006, doi: 10.1590/S0104-14282006000400014.
[232] T. Kossentini Kallel, R. Taktak, N. Guermazi, and N. Mnif, "Mechanical and structural properties of glass fiber-reinforced polypropylene (PPGF) composites," *Polymer Composites,* vol. 39, no. 10, pp. 3497-3508, 2018.
[233] S. Teng, A. A. R. Nor, and D. Lan, "Rheological and Thermal Behavior of Polypropylene-Kaolin Composites," *Malaysian Journal of Analytical Sciences,* vol. 18, no. 2, pp. 360-367, 2014.
[234] Z. M. Ariff, A. Ariffin, S. S. Jikan, and N. A. A. Rahim, "Rheological behaviour of polypropylene through extrusion and capillary rheometry," *Polypropylene,* pp. 29-49, 2012.
[235] J. Milewski, "A study of the packing of milled fibreglass and glass beads," *Composites,* vol. 4, no. 6, pp. 258-265, 1973.
[236] O. Oikonomidou, M. Triantou, P. Tarantili, C. Anatolaki, and N. Karnavos, "The effect of extrusion reprocessing on structure and properties of isotactic poly (propylene)," in *Macromolecular Symposia*, 2012, vol. 321, no. 1: Wiley Online Library, pp. 216-220.
[237] K. Wang *et al.*, "Effect of talc content on the degradation of re-extruded polypropylene/talc composites," *Polymer degradation and stability,* vol. 98, no. 7, pp. 1275-1286, 2013.
[238] G. Guerrica-Echevarria, J. Eguiazabal, and J. Nazabal, "Effects of reprocessing conditions on the properties of unfilled and talc-filled polypropylene," *Polymer degradation and stability,* vol. 53, no. 1, pp. 1-8, 1996.
[239] M. Sarrionandia, A. Lopez-Arraiza, J. Aurrekoetxea, and A. Arostegui, "Structure and mechanical properties of a talc-filled polypropylene/ethylene-propylene-diene composite after

reprocessing in the melt state," *Journal of applied polymer science,* vol. 114, no. 2, pp. 1195-1201, 2009.
[240] E. Ramırez-Vargas, D. Navarro-Rodrıguez, A. Blanqueto-Menchaca, B. Huerta-Martınez, and M. Palacios-Mezta, "Degradation effects on the rheological and mechanical properties of multi-extruded blends of impact-modified polypropylene and poly (ethylene-co-vinyl acetate)," *Polymer degradation and stability,* vol. 86, no. 2, pp. 301-307, 2004.
[241] M. H. Martins and M.-A. De Paoli, "Polypropylene compounding with post-consumer material: II. Reprocessing," *Polymer Degradation and Stability,* vol. 78, no. 3, pp. 491-495, 2002.
[242] E. Strömberg and S. Karlsson, "The design of a test protocol to model the degradation of polyolefins during recycling and service life," *Journal of Applied Polymer Science,* vol. 112, no. 3, pp. 1835-1844, 2009.
[243] P. N. Khanam *et al.*, "Melt processing and properties of linear low density polyethylene-graphene nanoplatelet composites," *Vacuum,* vol. 130, pp. 63-71, 2016.
[244] E. Watt, M. A. Abdelwahab, M. R. Snowdon, A. K. Mohanty, H. Khalil, and M. Misra, "Hybrid biocomposites from polypropylene, sustainable biocarbon and graphene nanoplatelets," *Scientific reports,* vol. 10, no. 1, pp. 1-13, 2020.
[245] J. Aurrekoetxea, M. Sarrionandia, I. Urrutibeascoa, and M. L. Maspoch, "Effects of recycling on the microstructure and the mechanical properties of isotactic polypropylene," *Journal of materials science,* vol. 36, no. 11, pp. 2607-2613, 2001.
[246] T.-H. Hsieh, M.-Y. Shen, Y.-S. Huang, Q.-Q. He, and H.-C. Chen, "Mechanical Properties of Glass Bead-Modified Polymer Composite," *Polymers and Polymer Composites,* vol. 26, no. 1, pp. 35-44, 2018, doi: 10.1177/096739111802600105.
[247] J. Al-Sabea, "Tensile and Compressive Properties of Kaolin Rienforced Epoxy," 10/01 2015.
[248] K. Gaska, X. Xu, S. Gubanski, and R. Kádár, "Electrical, mechanical, and thermal properties of LDPE graphene nanoplatelets composites produced by means of melt extrusion process," *Polymers,* vol. 9, no. 1, p. 11, 2017.
[249] A. Bunsell and B. Harris, "Hybrid carbon and glass fibre composites," *Composites,* vol. 5, no. 4, pp. 157-164, 1974.
[250] S.-Y. Fu, B. Lauke, E. Mäder, C.-Y. Yue, and X. Hu, "Tensile properties of short-glass-fiber-and short-carbon-fiber-reinforced polypropylene composites," *Composites Part A: Applied Science and Manufacturing,* vol. 31, no. 10, pp. 1117-1125, 2000.
[251] W. Yang, W. Shi, Z.-M. Li, B.-H. Xie, J.-M. Feng, and M.-B. Yang, "Mechanical properties of glass bead-filled linear low-density polyethylene," *Journal of Elastomers & Plastics,* vol. 36, no. 3, pp. 251-265, 2004.
[252] K. Kalaitzidou, H. Fukushima, H. Miyagawa, and L. Drzal, "Flexural and tensile moduli of polypropylene nanocomposites and comparison of expermental data to Halpin-Tsai and Tandon-Wang models," *Polymer Engineering & Science,* vol. 47, pp. 1796-1803, 11/01 2007, doi: 10.1002/pen.20879.
[253] R. B. Yunus, N. Zahari, M. Salleh, and N. A. Ibrahim, "Mechanical properties of carbon fiber-reinforced polypropylene composites," in *Key Engineering Materials*, 2011, vol. 471: Trans Tech Publ, pp. 652-657.
[254] M. D. H. Beg and K. L. Pickering, "Reprocessing of wood fibre reinforced polypropylene composites. Part I: Effects on physical and mechanical properties," *Composites Part A: Applied Science and Manufacturing,* vol. 39, no. 7, pp. 1091-1100, 2008.
[255] B. Yu, C. Geng, M. Zhou, H. Bai, Q. Fu, and B. He, "Impact toughness of polypropylene/glass fiber composites: interplay between intrinsic toughening and extrinsic toughening," *Composites Part B: Engineering,* vol. 92, pp. 413-419, 2016.
[256] N.-J. Lee and J. Jang, "The effect of fibre content on the mechanical properties of glass fibre mat/polypropylene composites," *Composites Part A: Applied Science and Manufacturing,* vol. 30, no. 6, pp. 815-822, 1999.

[257] N. Sato, T. Kurauchi, S. Sato, and O. Kamigaito, "Microfailure behaviour of randomly dispersed short fibre reinforced thermoplastic composites obtained by direct SEM observation," *Journal of materials science,* vol. 26, no. 14, pp. 3891-3898, 1991.
[258] D. K. Platt, *Engineering and high performance plastics market report: a Rapra market report*. iSmithers Rapra Publishing, 2003.
[259] E. J. Joseph and K. Panneerselvam, "Effect of particulate fillers on mechanical, metallurgical and abrasive behavior of tungsten reinforced HDPE composites: A Taguchi approach," *Materials Today: Proceedings,* 2020.
[260] R. Kumar, K. Kumar, and S. Bhowmik, "Optimization of mechanical properties of epoxy based wood dust reinforced green composite using Taguchi method," *Procedia Materials Science,* vol. 5, pp. 688-696, 2014.
[261] K. Ivić, R. Marinković, and Z. Jurković, "Application of the taguchi method in change management," *Ekonomski vjesnik: Review of Contemporary Entrepreneurship, Business, and Economic Issues,* vol. 24, no. 1, pp. 211-217, 2011.
[262] R. K. Roy, *A primer on the Taguchi method*. Society of Manufacturing Engineers, 2010.
[263] D. Awty-Carroll, S. Ravella, J. Clifton-Brown, and P. Robson, "Using a Taguchi DOE to investigate factors and interactions affecting germination in Miscanthus sinensis," *Scientific reports,* vol. 10, no. 1, pp. 1-11, 2020.
[264] S. Hashemi, O. Olumide, and M. Newaz, "Influence of weldlines on tensile properties of hybrid acrylonitrile butadiene styrene (ABS) composites filled with short glass fibres (GF) and glass beads (GB)," *Journal of materials science,* vol. 43, no. 6, pp. 1987-1996, 2008.
[265] U. Yilmazer, "Tensile, flexural and impact properties of a thermoplastic matrix reinforced by glass fiber and glass bead hybrids," *Composites science and technology,* vol. 44, no. 2, pp. 119-125, 1992.
[266] M. Parhizkar, K. Shelesh-Nezhad, and A. Rezaei, "Mechanical and thermal properties of Homo-PP/GF/CaCO 3 hybrid nanocomposites," *Advances in materials Research,* vol. 5, pp. 121-130, 06/25 2016, doi: 10.12989/amr.2016.5.2.121.
[267] S. Hashemi, P. Elmes, and S. Sandford, "Hybrid effects on mechanical properties of polyoxymethylene," *Polymer Engineering & Science,* vol. 37, no. 1, pp. 45-58, 1997.
[268] L. J. Broutman, *Fracture and Fatigue: Composite Materials, Vol. 5* (no. เล่มที่ 5). Elsevier Science, 2016.
[269] M. Quaresimin, K. Schulte, M. Zappalorto, and S. Chandrasekaran, "Toughening mechanisms in polymer nanocomposites: From experiments to modelling," *Composites Science and Technology,* vol. 123, pp. 187-204, 2016.
[270] J. Spanoudakis and R. Young, "Crack propagation in a glass particle-filled epoxy resin," *Journal of Materials Science,* vol. 19, no. 2, pp. 473-486, 1984.
[271] A. C. Garg and Y.-W. Mai, "Failure mechanisms in toughened epoxy resins—A review," *Composites Science and Technology,* vol. 31, no. 3, pp. 179-223, 1988.
[272] D. J. Green, P. S. Nicholson, and J. D. Embury, "Fracture of a brittle particulate composite," *Journal of Materials Science,* vol. 14, no. 6, pp. 1413-1420, 1979.
[273] F. Lange, "The interaction of a crack front with a second-phase dispersion," *Philosophical Magazine,* vol. 22, no. 179, pp. 0983-0992, 1970.
[274] S. Chandrasekaran, N. Sato, F. Tölle, R. Mülhaupt, B. Fiedler, and K. Schulte, "Fracture toughness and failure mechanism of graphene based epoxy composites," *Composites Science and Technology,* vol. 97, pp. 90-99, 2014.
[275] D. Arencón and J. I. Velasco, "Fracture toughness of polypropylene-based particulate composites," *Materials,* vol. 2, no. 4, pp. 2046-2094, 2009.
[276] A. Zotti, S. Zuppolini, M. Zarrelli, and A. Borriello, "Fracture toughening mechanisms in epoxy adhesives," *Adhesives-Applications and Properties,* vol. 1, p. 257, 2016.
[277] D. Maxwell, R. Young, and A. Kinloch, "Hybrid particulate-filled epoxy-polymers," *Journal of materials science letters,* vol. 3, no. 1, pp. 9-12, 1984.

[278] C. DeArmitt and M. Hancock, "Particulate-Filled Polymer Composites," 2003, pp. 357-424.
[279] A. Moloney, H. Kausch, and H. Stieger, "The fracture of particulate-filled epoxide resins," *Journal of Materials Science,* vol. 18, no. 1, pp. 208-216, 1983.
[280] A. Kinloch, D. Maxwell, and R. Young, "The fracture of hybrid-particulate composites," *Journal of materials science,* vol. 20, no. 11, pp. 4169-4184, 1985.
[281] A. Evans, "The strength of brittle materials containing second phase dispersions," *Philosophical Magazine,* vol. 26, no. 6, pp. 1327-1344, 1972.
[282] C. L. Morelli, A. S. Pouzada, and J. A. Sousa, "Influence of hybridization of glass fiber and talc on the mechanical performance of polypropylene composites," *Journal of applied polymer science,* vol. 114, no. 6, pp. 3592-3601, 2009.
[283] M. A. Abdelwahab, A. Rodriguez-Uribe, M. Misra, and A. K Mohanty, "Injection Molded Novel Biocomposites from Polypropylene and Sustainable Biocarbon," *Molecules,* vol. 24, no. 22, p. 4026, 2019.
[284] A. T. P. Zahavich, B. Latto, E. Takacs, and J. Vlachopoulos, "The effect of multiple extrusion passes during recycling of high density polyethylene," *Advances in Polymer Technology: Journal of the Polymer Processing Institute,* vol. 16, no. 1, pp. 11-24, 1997.
[285] J. J. Lee and C. M. Suh, "Interlaminar fracture toughness and associated fracture behaviour of bead-filled epoxy/glass fibre hybrid composites," *Journal of materials science,* vol. 30, no. 24, pp. 6179-6191, 1995.
[286] Z. Guan, "Influence of PP-g-MA compatibilizer characteristics on mechanical properties of glass fiber reinforced polypropylene composites," *Ph. D. Thesis,* 2014.
[287] C. Orr, J. Cernohous, P. Guegan, A. Hirao, H. Jeon, and C. Macosko, "Homogeneous reactive coupling of terminally functional polymers," *Polymer,* vol. 42, no. 19, pp. 8171-8178, 2001.
[288] S. Patankar, A. Das, and Y. Kranov, "Interface engineering via compatibilization in HDPE composite reinforced with sodium borosilicate hollow glass microspheres," *Composites Part A: Applied Science and Manufacturing,* vol. 40, no. 6-7, pp. 897-903, 2009.
[289] J. Gómez-Monterde, M. Sánchez-Soto, and M. L. Maspoch, "Microcellular PP/GF composites: Morphological, mechanical and fracture characterization," *Composites Part A: Applied Science and Manufacturing,* vol. 104, pp. 1-13, 2018.
[290] M. Sclavons *et al.*, "Quantification of the maleic anhydride grafted onto polypropylene by chemical and viscosimetric titrations, and FTIR spectroscopy," *Polymer,* vol. 41, no. 6, pp. 1989-1999, 2000.
[291] Y. Ou, Z. Yu, J. Zhu, G. Li, and S. Zhu, "Effect of Interfacial Adhesion on Crystallization and Mechanical Properties of Poly (Ethylene Terephthalate)/Glass Bead Composites," *CHINESE JOURNAL OF POLYMER SCIENCE,* vol. 14, pp. 172-182, 1996.
[292] F. Djamel, A. Layachi, S. Gherib, G. Stoclet, K. Masenelli-Varlot, and H. Satha, "Crystallization of glass-fiber-reinforced polyamide 66 composites: Influence of glass-fiber content and cooling rate," *Composites Science and Technology,* vol. 130, 05/01 2016, doi: 10.1016/j.compscitech.2016.05.007.
[293] Y. Wang, L. Cheng, X. Cui, and W. Guo, "Crystallization behavior and properties of glass fiber reinforced polypropylene composites," *Polymers,* vol. 11, no. 7, p. 1198, 2019.
[294] C. Aumnate, N. Rudolph, and M. Sarmadi, "Recycling of polypropylene/polyethylene blends: Effect of chain structure on the crystallization behaviors," *Polymers,* vol. 11, no. 9, p. 1456, 2019.
[295] B. Mahltig and Y. Kyosev, "Inorganic and Composite Fibers: Production, Properties, and Applications," 2018.
[296] S. Rana and R. Fangueiro, *Fibrous and textile materials for composite applications*. Springer, 2016.
[297] C. Cherif, "Textile materials for lightweight constructions," *Technol Methods Mater Proper,* 2016.
[298] "GLOBAL GLASS FIBER & GLASS FIBER REINFORCED PLASTIC (GFRP) COMPOSITES MARKET 2020 BY MANUFACTURERS, REGIONS, TYPE AND APPLICATION, FORECAST TO 2025." Global Info

Research https://www.market-research-reports.com/1053294-glass-fiber-reinforced-plastic-gfrp-composites-manufacturers-regions-type-application-forecast (accessed 16/06/2020, 2020).
[299] "Glass Reinforced Plastics (GRP)." plasticon. https://www.plasticon.co.uk/composites/glass-reinforced-plastics (accessed 06/01/2021, 2021).
[300] V. M. Elmar Witten, "The Market for Glass Fibre Reinforced Plastics (GRP) in 2019 Market developments, trends, outlooks and challenges," The Federation of Reinforced Plastics (AVK), 2019. [Online]. Available: https://www.avk-tv.de/files/20190911_avk_market_report_e_2019_final.pdf
[301] "Omya CaCO3 History " https://www.omya.com/history (accessed 04/04/2020, 2020).

Appendix A: Reinforcing materials

Appendix A: Reinforcing materials

Various reinforcing agents have been selected to be used as the fillers in this research. These fillers have been selected from fillers that have significant high consumption in polymer industries and interesting materials that have been developed more recently. From many fillers using in plastic industries, six different reinforcing agents have been selected as the representative from fibre and particles families. The information of these fillers are examined as follows.

A.1 Fibrous reinforcing materials

A.1.1 Glass fibre

Glass fibre has been known for long time ago where there is some evidence to claim that many Egyptain vessels were made by glass fibres [1]. In the 16th and 17th centuries, glass fibre was used for decorative purposes of the dishes by Venetian glassmakers. The use of glass fibre in textile industry was first reported in 1713 by the French physicist Rene-Antoine Ferho de Reumur [295]. Moreover, it has been reported that dresses were made from a fabric combining silk and glass fibre by Edward Drummond Libby of Toledo in 1890 [295]. Furthermore, continuous glass fibre was first introduced in the electrical connection and became known as “E-glass”. In subsequent years, glass fibre began to be used as a reinforcing material for composite materials. This development of technology and productivity were very fast and hence the use of reinforced polymers has become a new chapter the manufacturing industry. In 1935, the first patent for reinforced plastic resins with glass fibre was appeared [295]. The glass fibre was applied for structural applications and it was used to strengthen the plastic for the production of radomes for aircrafts during the World War II. [295]. Later, galss fibre reinforced plasctics become a common material for automobile parts, large vessels (sweepers) with nonmagnetic properties and in several other engineering applications [295-297].

The structure and composition of glass fibre are ambiguous to explain in exact chemical formulation. But its basic component is silica or silicon dioxide (SiO_2) which derived from sand. Sand consists of an irregular network of silicon atoms which are bonded together by Si-O-Si bonds that consisted of four oxygen atoms, tetrahedrally (see Figure A.1) and also has a random and ordered structure as shown in Figure A.2. Typically, its composition is expressed by the percentage content of the oxides of many metals. The main material for the production

of glass is Quartz sand and its structure is shown in Figure A.3. It contains 99%–99.5% silica and about 1% impurities. The less impurities in the sand, the higher its quality [295].

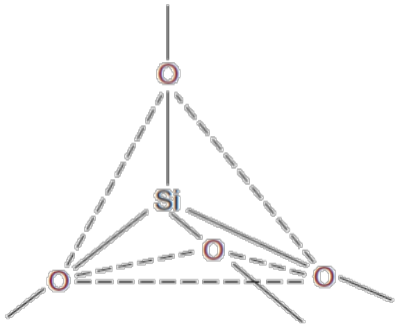

Figure A.1: The basic structural unit of silicates and silicate glasses-the silica teteahedron [295]

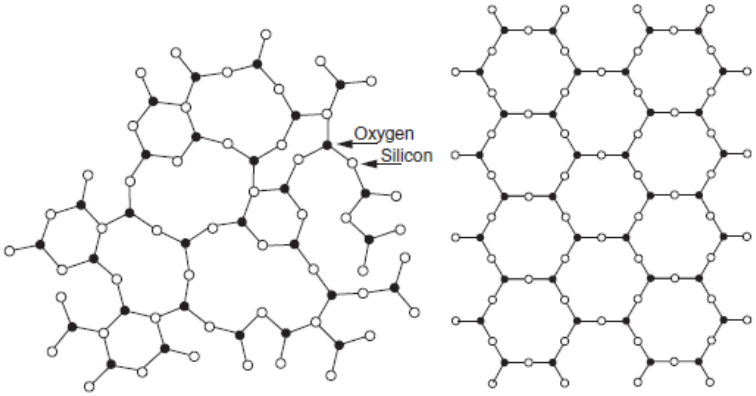

Figure A.2: Random structure of glass and ordered structure crystalline [295]

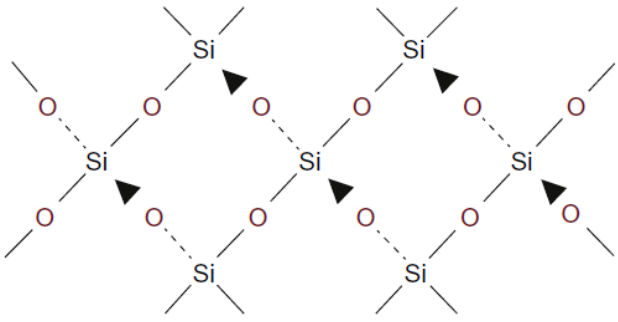

Figure A.3: Schematic of SiO_2 in its crystalline form, quartz [295]

Glass fibres can be classified based on their chemical composition, performance and product characteristics. The chemical composition based classification is usually done by the content of alkali metal oxide as Alkali glass fibre (alkali metal oxide content > 12%), medium-alkali glass fibres (alkali metal oxide content 6-12%), low-alkali glass fibre (alkali metal oxide content

2-6%) and Micro-alkali glass fibre or non-alkali glass fibre (alkali metal oxide content <2%). According to the product characteristics, it can be categorized as Type A (ordinary alkali glass fibres), Type E (electrical purpose), Type M (high elastic), Type AR (high alkali resistance), Type D (low dielectric constant), etc. However, glass fibre can be classified based on its product characteristics which are grouped by a few matrices such as the length of fibre (fixed and continuous fibre), fibre diameter (crude fibre (30 micron in diameter), primary fibre (20 micron in diameter), intermediate fibres (10-20 micron in diameter), textile fibres (3-9 micron in diameter), ultra-fine glass fibre (less than 4 micron in diameter)) [4].

Glass fibre has become one of the major materials in manufacturing composite materials in industries such as in transportation, construction, petrochemical, etc. This is because glass fibre is an excellent inorganic non-metallic material with some promising properties. Nowadays, almost 90% of all glass fibres that are produced in the world is E-grade glass fibre. The remaining 10% includes special-purpose fibres. The mechanical characteristics of glass fibres depend on many factors such as the method of production, the chemical composition of the glass, etc. Glass fibre which has been usually used as reinforcing agents, especially for aerospace applications, has a very high tensile strength. The modulus of elasticity of the fibre can range between 86–87 GPa while the tensile strength is 4500–4800 MPa, both at room temperature. The softening point is in the range of 1015 – 1050 ^{o}C [295]. Some researches revealed the superiority of glass fibres in terms of high tensile strength but lower modulus. Moreover, it exhibits the characteristics of brittle materials. For thermal properties, glass fibre is an inorganic material and hence can exhibit a good flame resistance and heat resistance. Moreover, glass fibre has a low thermal conductivity and a thermal expansion coefficient which are about 0.86 kcal /(m· h· ^{o}C) and 4.8×10^{-6}/^{o}C (in the range of 20 ～ 200 ◦C), respectively [4]. In terms of the chemical corrosion resistance, generally glass fibre is an excellent anticorrosion material. It has corrosion resistance to almost all acids, alkalis, salts and organic solvents. In addition, these properties of glass fibre are greatly influenced by the environmental temperature and humidity [4].

Nowadays, glass fibre has been considered as the main reinforcing agent in polymer composite industry. The global glass fibre and glass fibre reinforced plastic (GFRP) Composites market is valued at 25,690 million USD in 2019 and it is expected to reach 26,290 million USD by the end of 2025. The annual growth rate of composite usage of 0.6% is forecasted during 2020-2025 [298]. GFRP composites are widely used because of its high mechanical strength,

light weight, corrosion and temperature resistance, thermal insulation, smooth internal surface, easiness of forming into complex shapes, ease of repair and its cost effectiveness [299]. With the rapid growth over the past two decades, China has become the world's largest producer and supplier of glass fibre which is the main reinforcing agent for composite market share in the world. In 2018, the top three sectors using GFRP in China were electrical, transportation and construction as shown in Figure A.4.

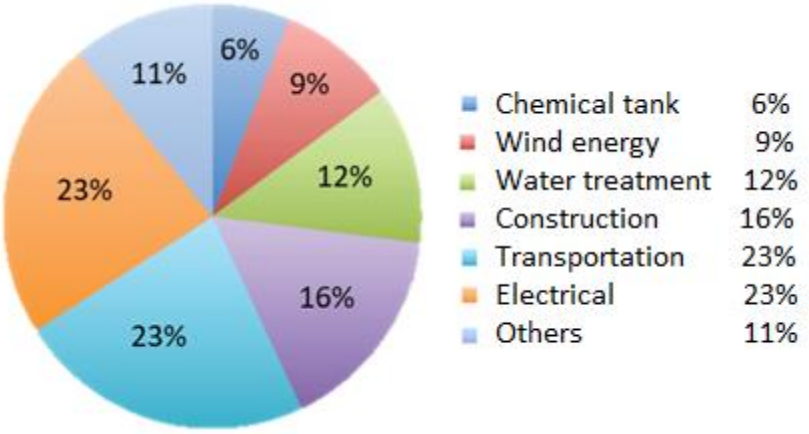

Figure A.4: GFRP Market Share in China in 2018 [22]

Nowadays, the Chinese glass fibre composite industry has a market size twice as big as in the United States. There are approximately 5,000 companies involved in composites manufacturing in China, leading to shipment of 4.62 million metric tons of glass fibre composites annually and had a domestic market demand of 23,487 metric tons in 2017. To promote the wider use of composite materials, the Chinese composites industry is researching low-cost design and manufacturing technologies, structural multifunction integration technologies, environmentally-friendly materials, repair and retrofitting technologies, and recycling technologies [22].

Another important player in global composite market is the United States. Overall, the U.S. composites industry has been valued at 25.2 billion USD in 2018 for a wide variety of products. The glass fibre market in USA grew by 2.9% in 2018, reaching 2.5 billion pounds weight in terms of the volume and 2.1 billion USD in terms of the value. The demand for glass fibre in the U.S. is expected to reach 3 billion pounds weight by 2024, with a compound annual growth rate of 2.8%. With an annual production capacity of 110,000 metric tons, the new facility is expected to be operational by mid-2019 and will help serve the growing wind energy market.

According to the statistics of the German Federation of Reinforced Plastics, the European GFRP market was estimated to be of 1.14 million metric tons in 2019 as shown in Figure 17. Production of thermoplastics, used primarily in the automobile industry, generally still grew more strongly compared to the production of most thermoset materials [22]. The two main areas of applications for GFRP were construction/infrastructure and transport as can be seen in Figure A.5 [300].

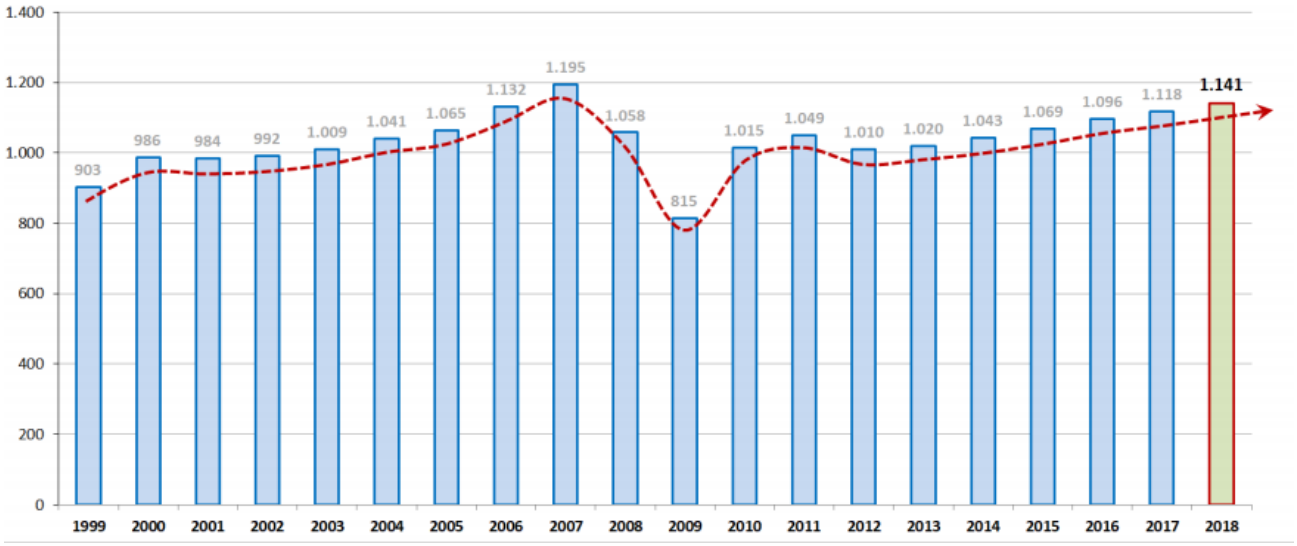

Figure A.5: The European GFRP production volume since 1900 (in kiloton) [300]

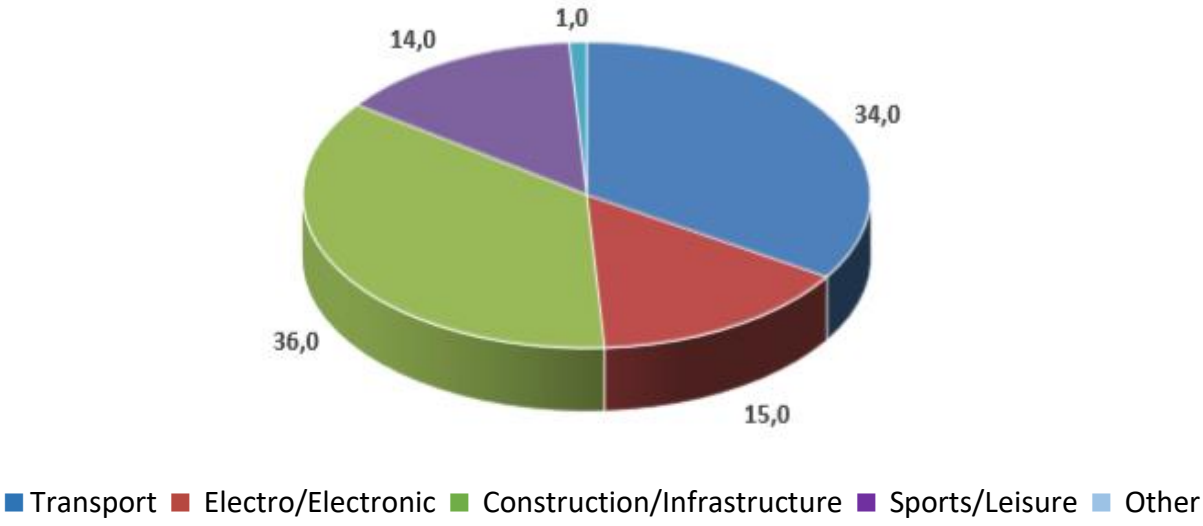

Figure A.6: The GFRP market share in 2019 (% of the total European market) [300]

The composite market in many European countries have been widely expanded while Germany has been dominant market. Glass fibre polymer composite in Germany has a strong focus on the transportation sector and the electro/electronics industry. Germany continues

to be the European leader in composites, with a total production volume of 229,000 metric tons in 2018 [22]. In this region, glass fibre has been considered as the main reinforcing agent. It offers a wide range of advantages for many segments of the transportation sector, including electro mobility. There are various applications that can be adapted and improved by applying glass fibre composites. For example, the infrastructure market is thriving in Turkey, while the oil and gas industry is strong in Norway and Sweden [22]. The other advantages of glass fibre composites include reduced energy consumption, durability and possible minimal maintenance. However, the awareness of the materials is still too limited for them to be widely considered by decision makers.

A.1.2 Carbon fibre

Carbon fibre is the one of the fibrous reinforcing materials which were invented to be used in more sophisticated applications such as structural applications in aerospace industry. The invention of the carbon fibres can be traced back in 1880 [4]. Edison used carbon filament as wire for lamp but carbon fibre filament was very brittle, easily oxidation, and too low brightness; hence later he used tungsten filament. In the 1950s, the development of carbon fibre began to draw attention as new engineering materials. In the 1960s, the high-strength and low-density carbon fibres were developed. After 40 years of efforts, the carbon fibre technology has become more matured in mechanical properties, hence in industrial productions [4].

Carbon fibre is made from carbonization heat treatment of organic fibres such as rayon fibre, polyacrylonitrile (PAN) fibre and its carbon content is 90∼99%. The structure of carbon fibre is similar to graphite crystal which composed of pure carbon. Manufacturing process of carbon fibre have to be done under high pressure and temperature. General synthesis process cannot be applied because there is no suitable solvent which dissolve the carbon element. Moreover, organic fibre with a high carbon content have to be protected under the atmosphere of Nitrogen (N_2) or Argon (Ar) and majority of non-carbon elements are removed by heating. This process is called carbonization [4].

At present, carbon fibre has the rapid development. There are many types of carbon fibre production in the UK and worldwide. Generally, they can be classified by the type of fibre precursor (PAN-based carbon fibre, pitch-based carbon fibre, rayon-based carbon fibre, vapor-grown carbon fibre), manufacturing methods (carbon fibre (800∼1600◦C), graphite

fibres (2000 ～ 3000◦C), oxidative fibres (preoxidation fibre at 200～300◦C, activated carbon fibre), carbon fibre properties (general grade carbon fibre (GP) and high performance carbon fibre (HP); HP includes middle strength type (MT), high strength type (HT), ultra-high strength type (UHT)) and their purpose and function (load structure using carbon fibre, flame resistant (fire) carbon fibre, activated carbon fibre (adsorption activity), conductive carbon fibre, carbon fibre used for lubrication; wear-resistant carbon fibre, corrosion resistant carbon fibre), etc [4].

Carbon fibre has decent performance that meets the requirements of various functions so it has become popular in polymer composite industries. For mechanical properties, carbon fibre has high strength and high modulus. Modulus of carbon fibres increases with the increase of treatment temperature in carbonization process since the crystal can be grown up. However, carbon fibre is quite brittle, thus has bad impact performance. For thermal properties, carbon fibre has good resistance to high and low temperatures and has good thermal conductivity performance as well. Moreover, carbon fibre has the excellent corrosion resistance and better water resistance than the glass fibre [4].

The development of carbon fibre exhibit continuous improvement in performance and market demand. Daniel Pichler, Managing Director from CarbConsult GmbH revealed that the global demand for carbon fibre was approximately 100,000 tons in 2019-2020, and this demand is expected to be increased in future [22].The usage of carbon-fibre reinforced plastic (CFRP) composite is mainly used in aircrafts which require 50% fewer structure maintenance operations [21]. The commercial aircraft segment demand in the market was over 29,000 tons in 2019. Market size of aerospace composites was over 12.7 billion USD in 2019 and has been predicted that it will reach over 9% growth between 2020 and 2026. The exterior application segment dominated around 60% market share in 2019. The North American aerospace composites market held majority of revenue share of over 40% in 2019 [21].

Moreover, the potential future market scenario of carbon fibre reinforced polymer is shown in Figure A.7. Aerospace, wind turbine blades, sporting goods and moulding compounds will continue to grow as more and more programs are engineered to use carbon fibres. Automotive applications has been anticipated as the highest market potential because there are so many developments in these applications and vehicle platforms.

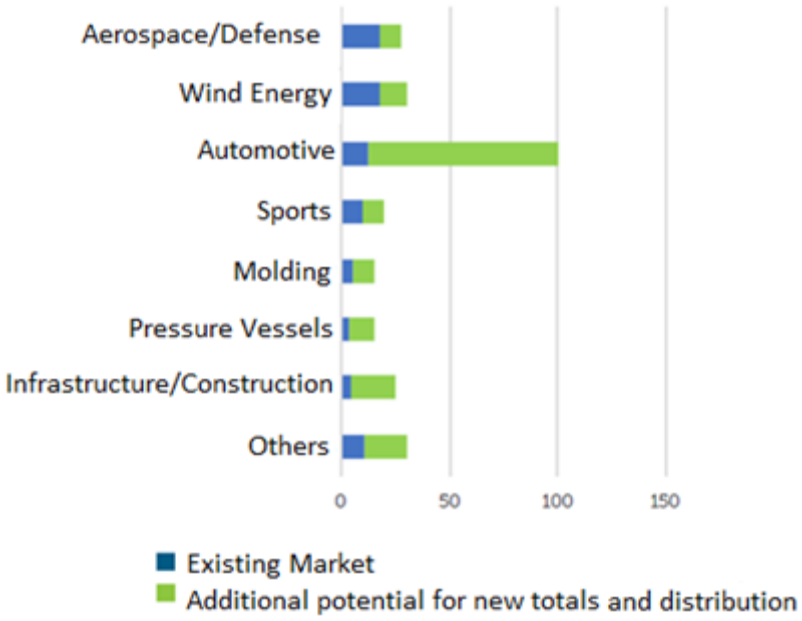

Figure A.7: Potential future market scenario of carbon fibre reinforced polymer [22]

A.2 Particle reinforced materials

A.2.1 Calcium Carbonate ($CaCO_3$)

This is one of the wildly used reinforced materials in the polymers industry ($CaCO_3$). The origin of $CaCO_3$ began to be discussed for paper industry by Bosshard of Omya/Plüss-Staufer AG in 1965 [301]. Calcium carbonate is a white, non-toxic and solid chemical compound. It can be found geologically in the earth's crust as the fifth most common elemental constituent of the earth's crust after oxygen, silicon, aluminum, and iron [182]. It has been found in deposit formed in sedimentary rocks. The process of formation of calcium deposits begins with weathering of land surface due to the changes in chemical or physical condition such as heat, frost, rain, and the effect of sun [182]. It is available as chalk, limestone, marble and in shells of marine creatures. Marine organisms such as mollusks and corals use dissolved calcium and carbon dioxide in water to form $CaCO_3$ which is used in their skeletal structures [182]. Calcium carbonate is migrated from the land to the sea since rainwater carries it from land. Approximately 500,000,000 tons of minerals are carried by rivers to the seas every year out of which about 10-15% of sedimentary rocks containing calcium carbonate are formed. The natural conditions such as an underwater volcanic explosion may affect since they alter the temperature of water and the concentration of carbon dioxide in water and, consequently, its internal use and release to the atmosphere. These forms effect to the structure of crystal of $CaCO_3$. There are three crystalline forms which are shown in Figure A.8 [182].

(a).

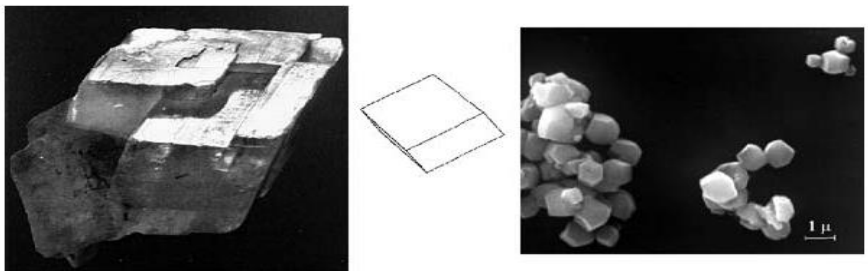

(b).

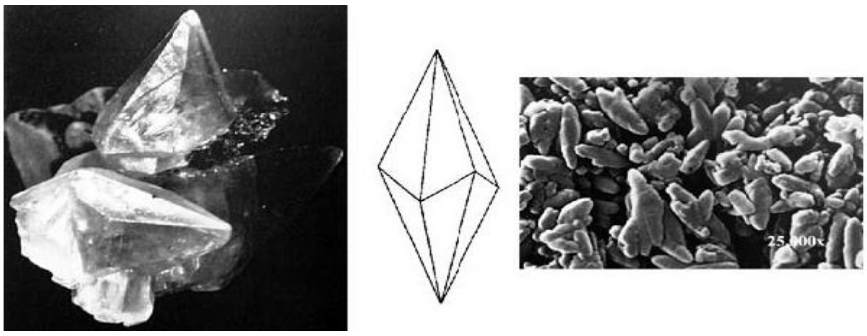

(c).

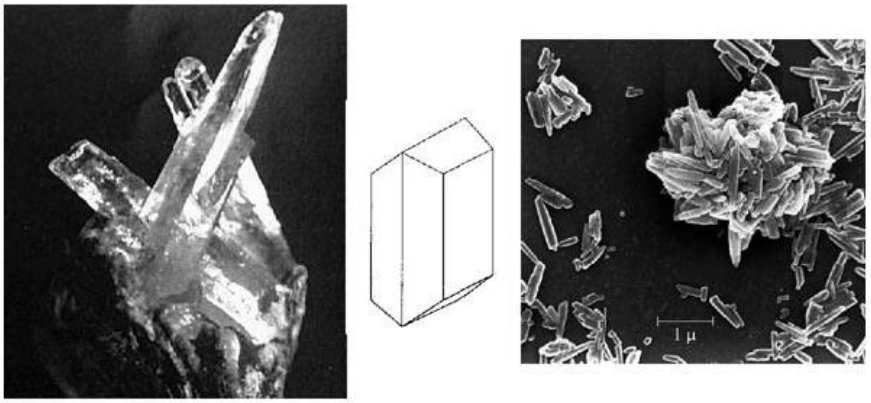

Figure A.8: Different crystalline forms of calcium carbonate (a).Trigonal-rhombohedral calcite (b). Trigonal-scalemohedral calcite (c). Orthorhombic aragonite [182]

Different forms of $CaCO_3$ have different structures such as Calcite (Calcspar) has trigonal rhombohedral or trigonal scalenohedral form while Aragonite has orthorhombic crystal structure, etc [182]. Moreover, minerals associated with $CaCO_3$ can be easily differentiated by their physical properties such as density (aragonite 2.9 g/cm^3 and calcite 2.7 g/cm^3), refractive index (aragonite 1.7, calcite with two refractive indices of 1.49 and 1.66 which causes a double refraction effect), and hardness (aragonite 3.5-4 and calcite 3) [182].

Three major $CaCO_3$ manufacturing processes as used are milling, precipitation, and coating. More than 90% calcium carbonate is processed by milling. The milling method requires to obtain the particle size distribution. In the wet milling process, the material is obtained in slurry form which is more economical and environmentally friendly. The first operation is

calcination which is performed in a kiln at 900 ^{o}C. At this stage, $CaCO_3$ is decomposed to calcium oxide and carbon dioxide which is used in the further step. Then, calcium oxide is mixed with water in a process called slaking. This converts calcium oxide to lime for purification operation for purity improvement [182].

The demand for $CaCO_3$ in the plastics industry is expected to grow vastly especially in the automobile industry for bumpers and other body parts of cars in coming years [87]. $CaCO_3$ has been used in waste water treatment, painting and coating industries. The applications of $CaCO_3$ particles are determined by a number of parameters, including specific surface area, morphology, size, brightness, oil adsorption, and purity. Particle morphology plays an important role in industrial applications. Moreover, it shows benefits including improved brightness, opacity, strength and printability [182]. There are many supported reasons for this popularity such as cost saving, including safe and abundant mineral and eco-friendliness. This material is suitable for a wide range of applications such as automotive components, home appliances, and industrial applications [87, 93]. Not only the objective of the usage of calcium carbonate as reinforcing materials was for environmental advantages but it also increased mechanical properties and other sophisticated features such as electric resistance, enhance surface finishing and thermodynamic stability, etc [87]. For the improvement of mechanical properties, there are so many reports revealed that calcium carbonate can enhance the impact strength, modulus including ductilibility [87, 182]. In PP composite in comparison of talc, calcium carbonate and kaolin, it was evident that $CaCO_3$ gave improvement in toughness and was found to have better nucleating properties than kaolin [182].

The $CaCO_3$ market size was 17 billion US dollars in 2018 and was predicted to register over 28 billion US dollars between 2018 and 2027. This growth can be attributed to the rise in the demand for $CaCO_3$ in various end-use industries such as plastic, paper, paints, and building & construction [177]. Demand for $CaCO_3$ continues to increase for paper coating applications as well as mineral fillers for plastics industries. Among the global consumers of $CaCO_3$, Asia is expected to occupy a major share, particularly in the paper industries, in the near future [87].

A.2.2 Kaolin

Kaolin has been also known by the common term of clay. The term kaolin is used to refer to the mineral called “Kaolinite”. Typically, the theoretical kaolin composition is $Al_2O_3.2SiO_2.2H_2O$ which consists of 46.3% SiO_2, 39.8% Al_2O_3 and13.9% H_2O. The individual

kaolin particle consists of an alumina octahedral sheet bound on one side to a silica tetrahedral sheet, stacked alternately. The two sheets of kaolinite form a tight fit with the oxygen atoms forming the link between the two layers (Figure A.9) [94]. Consequently, kaolin is often shown to be in the structure called “booklets”, which are stacks of plates, one on top of the other and connected through hydrogen bonding. Kaolins can be classified into primary or secondary forms. Primary kaolins are formed by modifications of crystalline rocks such as granite while the secondary kaolin deposits are sedimentary and are formed by erosion of primary deposits.

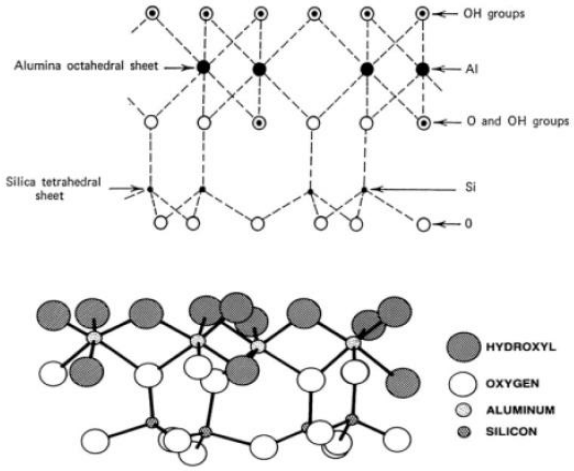

Figure A.9: Structure of Kaolin [94]

Kaolin has been used in plastic industry as the extremely versatile functional filler. There are a lot of reports revealed that it can improve mechanical property of thermoplastics [96, 184]. Moreover, Kaolin can improve the dimensional stability and surface finishing which are a common problem with high aspect ratio fibrous reinforcements.

There are various attempts on developing kaolin as filler in polymer by several researchers [96, 184]. Some scholars exposed that the addition of a treated kaolin filler improved the mechanical properties of polymer composites [96]. Moreover, kaolin has been also selected as flame retardant agent since kaolin in a suitable amount can improve the flame retardancy of PP matrix. This is because the formation of more compact char layers and chemical bond can reduce smoke release and flame propagation [184]. Moreover, the addition of kaolin can enhance electrical properties (volume resistivity, dielectric strength, and dielectric loss).

A.2.3 Glass Bead

Although glass fibre has been considered as a popular reinforced material in polymer composites industry but there are a number of researches that have been investigated the incorporation of glass bead in polymer composites to improve performance. Glass beads are made from any form of glass including broken pieces from glass work. The glass is crushed or ball mill. Then it is sieved and fed to a special furnace. After that coupling agent is applied directly after formation of the sphere for surface treatment. Then, these proper glass beads with satisfactory degree of roundness and size will be passes through vibrating sieving machine and finish grading process.

The structure of glass bead are similar to glass fibre since both of them are made from the glass. The glass beads are from size reduction of glass such as ball mill and crushing while glass fibre is made from molten glass and formed into glass fibers by a process known as fiberization [295]. The main purpose of the addition of glass bead into polymer are dimensional stability, high abrasion resistance, hardness improvement and high heat resistance. Generally, the improvement of strength, modulus and creep may be less than glass fibre at a comparable content because the shape of spherical filler. However, glass beads are beneficial in terms of compressive strength and reinforcing effect which do not rely on filler orientation [165]. In investigations on glass bead reported that the addition of glass bead in proper content can increase glass transition temperature (T_g) higher than that of unfilled polymer. Moreover, the improvement of performance is mostly governed by several factors such as particle size, particle shape, roundness, dispersion and surface treatment, etc.

A.2.4 Graphene nanoplatelets (GNPs)

Currently, graphene nanoplatelets (GNPs) are a type of attractive carbon materials which has been received a significant attention in the 21st century so far. GNPs consist short stacks of the individual layers of graphite [179]. Each stack is a planar monolayer of sp^2-hybridized carbon atoms arranged in a regular hexagonal pattern [191]. Graphene has been considered as the basic structural unit of all other graphitic allotropes of carbon (as shown in Figure A.10 a-c), including fullerenes (Figure A.10a), carbon nanotubes (CNTs) (Figure A.10b), graphite (Figure A.10c), [191].

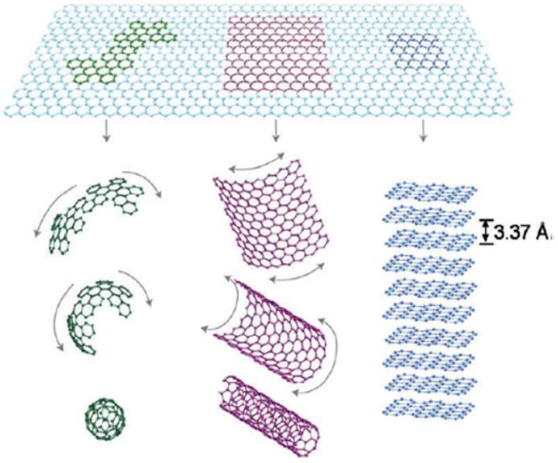

Figure A.10: Graphene in the building block of all graphitic form
(a): fullerenes, (b): Carbon Nanotubes (CNTs), (c) : graphite [191]

Recently, GNPs has been considered as one of interesting materials due to its ability to enhance many aspects of the final properties of neat polymers. One of outstanding features of GNPs is that its excellent thermal conductivity and electrical conductivity. Normally, GNPs has been widely studied as filler that can improve the electrical and thermal conductivity [107, 179, 186, 187]. There are researches investigating factors that affect to the performance of its ability to enhance conductivity. Effects of dispersion of GNPs, size, loading content, proportion of various GNPs size were studied.

Furthermore, many researches revealed that GNPs can help to improve mechanical properties such as tensile modulus [107, 108, 113, 179, 186, 188-191]. The surface area and aspect ratio of GNPs are higher than other carbon nanostructures [191]. Many scientific groups have paid attention on these characteristic and tried to utilize GNPs in various applications such as gas barrier, electrical conductivity and thermal properties.

However, if a particular polymer is incompatible with GNPs that may course to create improper properties. Many attempts have been made to overcome this issue by chemically modifying various functional groups on surface or graphene's structure. These modified functional groups can be enhanced the compatibility between graphene and polymers. This can improve the dispersibility in polymer matrix by governing the van der Waals forces [187]. From this principal, numerous academic groups have evaluated the possibility of graphene and its derivatives as the fillers that can improve mechanical, thermal, electrical and gas barrier properties of polymers [179].

Appendix B: Raw Material Data Sheets

Appendix B.1: Polymer materials datasheets

TECHNICAL DATA SHEET

Product Name
SCG PP

Product Type
Polypropylene Impact Copolymer

Product Grade
P739ET

Product Description

SCG PP P739ET is a high flow rate impact copolymer polypropylene resin. It is designed for compounding and injection molding process. This resin is recommended for compounds that require good surface aesthetics and low flow mark after injection process. It is suitable for various automotive parts.

Typical Application

- Automotive exterior/interior parts
- Home appliances parts
- Complicated industrial parts
- Compounding

Product Characteristics

- High flowability
- Stiffness and impact balance

International

- Directive 2002/95/EC (RoHS1)
- Directive (EU) 2015/863 amending annex II to Directive 2011/65/EU (RoHS2)
- Directive 2000/53/EC on ELV
- REACH Regulation (EC) No 1907/2006

Physical Properties

Property	Test Method	Typical Value	Unit
Melt Flow Rate	ISO 1133 @ 230°C, 2.16 kg	55	g/10 min
Density	ISO 1183	0.910	g/cm^3
Tensile Modulus	ISO 527	1,270	MPa
Tensile Strength at Yield	ISO 527	27	MPa
Charpy Impact Strength	ISO 179 @ 23°C	6.5	kJ/m^2
Rockwell Hardness	ISO 2039-2	90	°C
Heat Deflection Temperature	ISO 75 @ 0.45 MPa	90	°C

Note: the given values are typical value measured on the product. Values herein are not to be constructed as a product specification.

SCG Performance Chemicals Co., Ltd.
1 Siam Cement Road, Bangsue, Bangkok, 10800 Thailand
Tel.: +66 2586 1111 ext. 5352 Fax: +66 2586 3676
E-mail: automotive@scg.com

Published: August 2018

www.scgchemicals.com

Quality Circular Polymers

Containers, Crates, Garden Furniture, Luggage, TWIM

lyondellbasell
Advancing Possible

TYPICAL PROPERTIES				MECHANICAL							ADDITIONAL INFO			TYPICAL APPLICATIONS	SPECIFIC CHARACTERISTICS
		Density	MFR 230°C, 2,16kg	Tensile Modulus	Tensile Stress at Yield	Tensile Elongation at Break	Flexural Modulus	Charpy Impact Notched			COLOR	RECYCLED PC %	RESTRICTION		
		23°C						23 °C	0 °C	-20 °C					
Test Method		ISO 1183	ISO 1133-1	ISO 527	ISO 527	ISO 527	ISO 527	ISO 179/1eA							
Units		g/cm³	g/10 min	MPa	MPa	%	MPa	kJ/m²							
PP HETEROPHASIC COPOLYMER, QCP															
Moplen	QCP840P	1,050	12	2250	27	60	2100	4.0			Grey	>75%	See disclaimer below	Containers, crates, furniture, pails, bin dividers	High stiffness, 20% Talc filled
Moplen	QCP840P Black	1,060	14	2300	27	15	2300	4.0			Black	>75%	See disclaimer below	Containers, crates, furniture, pails, bin dividers	High stiffness, 20% Talc filled
Moplen	QCP249P	0.935	15	1100	22	150	1090	10.5			Grey	>80%	See disclaimer below	Containers, crates, furniture, pails, baby strollers	NU, High impact resistance
Moplen	QCP249P Ivory	0.935	15	1100	22	150	1090	10.5			Ivory	>80%	See disclaimer below	Containers, crates, furniture, pails	NU, High impact resistance
Moplen	QCP249P Black	0.935	15	1100	22	150	1090	10.5			Black	>80%	See disclaimer below	Containers, crates, furniture, pails, baby strollers	NU, High impact resistance
Moplen	QCP189P	0.918	15	800	19	30	800	30		>7	Grey	>85%	See disclaimer below	High impact containers, luggage, furniture	AS, Very high impact even at low temperature
Moplen	QCP300P	0.915	16	1300	27	40	1200	6.5			Grey	>95%	See disclaimer below	Containers, pails, crates, furniture, caps	Medium fluidity
Moplen	QCP300P Ivory	0.915	16	1300	27	40	1200	6.5			Ivory	>95%	See disclaimer below	Containers, pails, crates, furniture, caps	
Moplen	QCP300P Black	0.917	16	1200	27	50	1150	6.0			Black	>95%	See disclaimer below	Containers, pails, crates, furniture, caps	Medium fluidity
Moplen	QCP300R	0.915	21	1250	26	30	1150	6.5			Grey	>95%	See disclaimer below	Containers, pails, crates, furniture, caps	Medium fluidity
Moplen	QCP300R Ivory	0.915	21	1250	26	30	1150	6.5			Ivory	>95%	See disclaimer below	Containers, pails, crates, furniture, caps	
Moplen	QCP300R Black	0.914	20	1200	27	25	1150	5.5			Black	>95%	See disclaimer below	Containers, pails, crates, furniture, caps	Medium fluidity
Moplen	QCP300S	0.915	35	1150	26	25	1100	6.0			Grey	>95%	See disclaimer below	Crates, boxes, pallets, pails, compounds, caps	Good fluidity
Moplen	QCP300S Ivory	0.915	35	1150	26	25	1100	6.0			Grey	>95%	See disclaimer below	Crates, boxes, pallets, pails, compounds, caps	Good fluidity
Moplen	QCP300S Black	0.916	35	1150	26	25	1050	6.0			Black	>95%	See disclaimer below	Crates, boxes, pallets, pails, compounds, caps	Good fluidity
Moplen	QCP540S	0.950	35	1400	24	25	1300	6.0			Grey	>85%	See disclaimer below	Crates, boxes, pallets, pails, compounds, caps	NU, Good fluidity
Moplen	QCP540S Black	0.950	35	1400	24	25	1300	6.0			Black	>85%	See disclaimer below	Crates, boxes, pallets, pails, compounds, caps	NU, Good fluidity
Moplen	QCP840S	1,050	40	2075	25	<10	2180	3.0			Grey	>75%	See disclaimer below	High stiffness containers	Good fluidity, high stiffness, 20% Talc filled
Moplen	QCP840S Black	1,050	40	2075	25	<10	2180	3.0			Black	>75%	See disclaimer below	High stiffness containers	Good fluidity, high stiffness, 20% Talc filled
Moplen	QCP300T	0.915	50	1150	26	20	1100	6.0			Grey	>95%	See disclaimer below	Large containers, boxes, compounds	High fluidity
Moplen	QCP300T Black	0.915	50	1150	26	20	1100	6.0			Black	>95%	See disclaimer below	Large containers, boxes, compounds	High fluidity
Moplen	QCP300U	0.915	70	1250	26	10	1150	5.0			Grey	>95%	See disclaimer below	Large containers, boxes, DVD boxes, compounds	Very high fluidity
Moplen	QCP300U Ivory	0.915	70	1250	26	10	1150	5.0			Ivory	>95%	See disclaimer below	Large containers, boxes, DVD boxes, compounds	Very high fluidity
Moplen	QCP300U Black	0.915	70	1150	25	10	1050	4.5			Black	>95%	See disclaimer below	Large containers, boxes, DVD boxes, compounds	Very high fluidity

**Restrictions: this product is not intended for highly regulated applications including food contact, potable water contact, medical and pharmaceutical applications.*

Legend: NA=Not Applicable; NU=Nucleated; AS=Antistatic; TWIM=Thin Wall Injection Molding; TSL=Toys,Sports and Leisure; NB=No Break; IMR=Inter Material Replacement

You can find out more about us by visiting our website at: www.lyondellbasell.com
Before using a LyondellBasell product, customers and other users should make their own independent determination that the product is suitable for the intended use. They should also ensure that they can use the LyondellBasell product safely and legally. (Material Safety Data Sheets are available from LyondellBasell at www.lyondellbasell.com) This document does not constitute a warranty, express or implied, including a warranty of merchantability or fitness for a particular purpose. No one is authorized to make such warranties or assume any liabilities on behalf of LyondellBasell except in writing signed by an authorized LyondellBasell employee. Unless otherwise agreed in writing, the exclusive remedy for all claims is replacement of the product or refund of the purchase price at LyondellBasell's option, and in no event shall LyondellBasell be liable for special, consequential, punitive, or exemplary damages.
Adflex, *Adstif*, *Clyrell*, , *Moplen* are trademarks owned or used by LyondellBasell group companies. *Clyrell* and *Moplen* are registered in the U.S. Patent and Trademark Office.

addivant™
SOLUTIONS TO BREAKTHROUGH

Technical Information
www.addivant.com
Effective: 4/1/2013

POLYBOND® 3200

Polymer Modifier

POLYBOND® 3200 is a maleic anhydride modified polypropylene homopolymer.

CAS Number 9003-07-0

Typical Physical Properties of POLYBOND® 3200

Property	Typical Value	Test Based On
Appearance	Off-white Pellet	Visual
Melt Flow Rate @ 190°C, 2.16Kg	115 g/10 min	ASTM D-1238
Maleic Anhydride Content	High*	ASTM D-6047
Density @ 23°C	0.91 g/cm^3	ASTM D-792
Bulk Density	0.6 g/ cm^3	ASTM D-1895B
Melting Point	157°C	DSC

*** High = Maleic Anhydride Content typically in the range of 0.8 to 1.2%.**

Applications

- High efficiency coupling agent for glass-filled polypropylene providing improved physical properties including strength
- Higher coupling efficiency vs. lower functionality products reducing raw material costs
- Coupling agent for cellulose fiber-filled polypropylene leading to reduced water uptake and higher flexural/tensile strengths
- Compatibilizer for polypropylene/polyamide blends giving enhanced hydrolytic stability and strength properties
- Coupling agent for mineral-filled polypropylene offering improved strength and impact properties
- Coupling agent and process aid for halogen-free, flame retardant (HFFR) wire & cable compounds giving improved dispersion of flame retardant along with improved mechanical properties
- Tie-layer component giving improved compatibility between multilayer polar and non-polar materials

Food Contact

POLYBOND® 3200 is approved for use under a several sections of the USA FDA 21CFR regulations as well as the European Food Regulations. Check with the Product Safety and Regulatory Affairs Department of Addivant™ for current status.

Regulatory Status

The components of POLYBOND® 3200 are listed on USA TSCA inventory. For information on other inventory listings, see Section 15 (Regulatory Information) of the MSDS for POLYBOND® 3200.

Storage & Handling Precautions

Keep POLYBOND® 3200 dry prior to processing. Loss of anhydride functionality may occur due to conversion to acid groups by reaction with atmospheric moisture. Tie liners of open boxes when not in use to prevent exposure to moisture. If exposure occurs, POLYBOND® 3200 can be dried in a hopper dryer or oven for three hours at 105°C to remove moisture. A slight pungent odor is normal during processing of POLYBOND® 3200. Purge equipment with polypropylene before and after running POLYBOND® 3200.

For additional handling and toxicological information consult the Addivant™ Material Safety Data Sheet

The information contained herein relates to a specific Addivant™ product and its use, and is based on information available as of the date hereof. Additional information relating to the product can be obtained from the pertinent Material Safety Data Sheets. Nothing in this Technical Data Sheet shall be construed to modify any of Addivant™ standard terms and conditions of sale under which the product is sold by Addivant™. NOTHING IN THIS TECHNICAL DATA SHEET SHALL BE CONSTRUED TO CONSTITUTE A REPRESENTATION OR WARRANTY, EXPRESS OR IMPLIED, REGARDING THE PRODUCT'S CHARACTERISTICS, USE, QUALITY, SAFETY, MERCHANTABILITY OR FITNESS FOR A PARTICULAR PURPOSE, AND ANY AND ALL SUCH REPRESENTATIONS AND WARRANTIES ARE HEREBY EXPRESSLY DISCLAIMED. Nothing contained herein shall constitute permission or recommendation to practice any intellectual property without the permission of the owner.

Addivant™ and the Addivant™ logo are trademarks of Addivant™ Corporation or one of its subsidiaries.

Copyright © 2013 Addivant™ Corporation. All rights reserved.

Appendix B.2: Reinforced materials datasheets

The Role of Calcium Carbonate in Adhesives & Sealants

Omya is a leading global producer of industrial minerals, mainly fillers and pigments derived from calcium carbonate and dolomite, and a worldwide distributor of specialty chemicals.

The company's major markets are forest products (fiber based products such as paper, board and tissue), polymers, building materials (paints, coatings, sealants, adhesives and construction) as well as life sciences (food, feed, pharmaceuticals, cosmetics, environment and agriculture).

Founded in 1884 in Switzerland, Omya now has a global presence extending to more than 180 locations in over 50 countries and 8,000 employees.

Reduces

Our calcium carbonates can reduce the content, and thus dependency of polymer based binder products in formulations. This reduces the carbon footprint (greenhouse gas emissions) of the overall package.

Replaces

Our calcium carbonates help to replace mineral fillers & pigments with high oil absorption, and carbon footprint (greenhouse gas emissions) and therefore reduce polymer based binders.

Resistant

Our calcium carbonates increase the resistance and durability of coating films, as well as adhesive & sealant joints, and thus the life cycle of the final products and goods.

Workability

Our calcium carbonates improve the workability of coatings, adhesives, sealants, inks, plasters and renders, leading to increased working life of application tools and less energy consumption.

Product Overview

	Particle Size	Products	Effect of $CaCO_3$
Surface Treated	30 –100 nm	Viscoexcel® Hakuenka® Vigot®	Rheological/Mechanical Modifier
	< 1 µm	Omyacoll® P100 Omyalite® 95T Omyabond® 520	Functional Filler
	~ 2 µm	Omyacarb® 1T Omyacarb® 2T Omya® BLH	Filler
Untreated	5 µm	various types of: Omyacarb®	Extender
	< 100 µm		

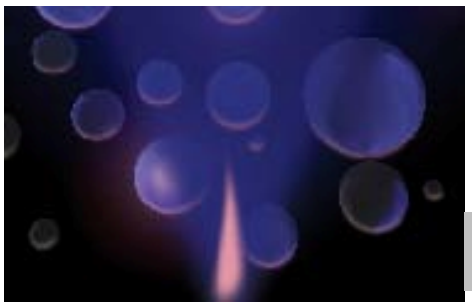

Potters-Ballotini Co. Ltd.
an affiliate of The PQ Corporation

Low Alkaline Glass Beads

Low Alkaline Glass Beads (E-glass beads) have been developed as fillers for **engineering plastic**, **painting & coating**.

Feathers

- **Good fluidity** and **dispersion**
- **Isotropic fillers** cause **no stain**
- **Low alkaline solubility**
- **Selection** of **Coupling Agent Coating**

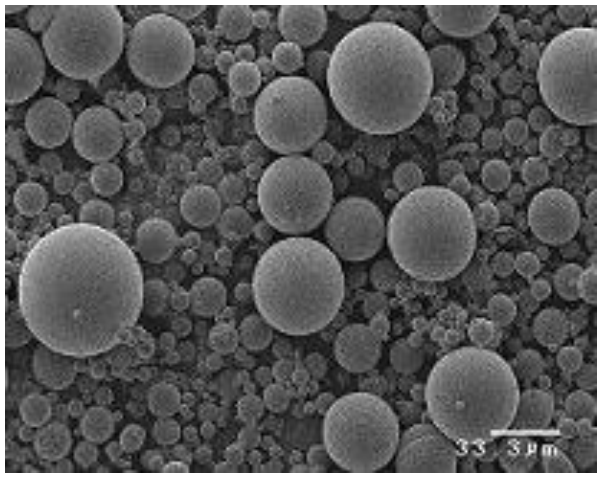

Applications

- **Dimensional Stability**
- **Low Warpage**
- **Hardness**
- **High Abrasion Performance**
- **High Heat Resistance**

Product	Material	Ave. Particle size （μm）	Particle range （μm）
EGB731	**Low Alkaline Borosilicate Glass**	20	45～2
EGB210		18	38～2

Particle Size Distribution (Electric Resistance Method)

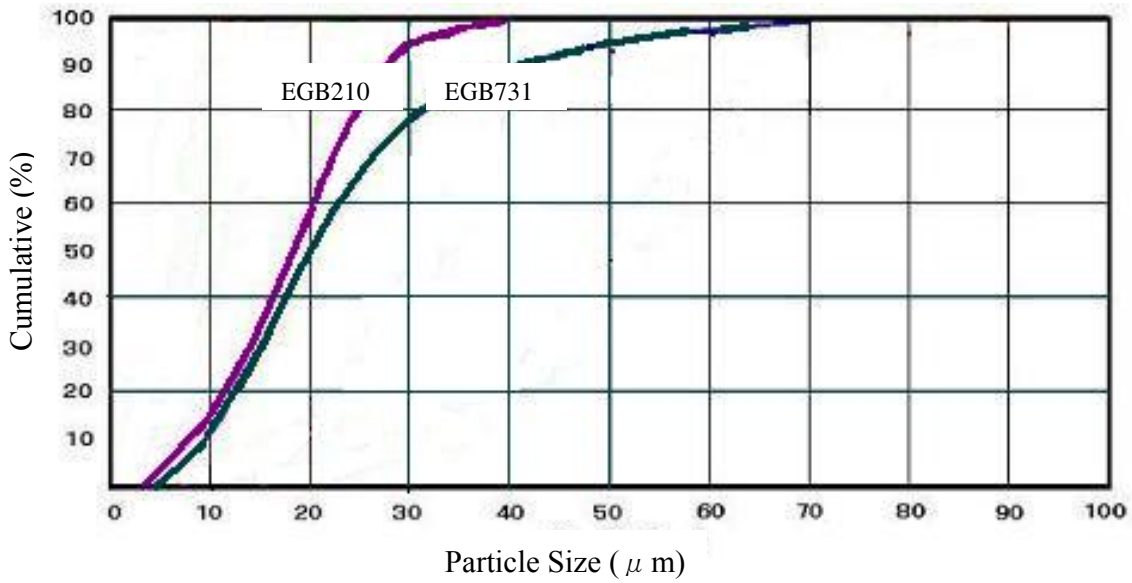

【Details】

Feathers

- **Good fluidity** and **dispersion**: Low Alkaline Glass Beads are good dispersion and provide excellent fluidity performance to resin compounds by feather of sphere particle and controlled particle size distribution.

- **Isotropic fillers** cause **no stain**: Low Alkaline Glass Beads are isotropic fillers by feather of sphere particle. Glass beads do not cause strain generally caused by anisotropic fillers such as glass fibers and micas.

- **Low alkaline solubility**: **Low alkaline composition** provides lower alkaline solubility than soda lime glass.

- **Selection** of **Coupling Agent Coating**: In order to enhance best interaction between polymer resin and glass beads, glass beads with proper coupling agent coating can be selected.

Applications

- **Dimensional Stability**: Low Alkaline Glass Beads provide dimensional stability to engineering plastic by low uniform shrinkage effect.

- **Low Warpage**: Low Alkaline Glass Beads support lower warpage of engineering plastic by low uniform shrinkage effect.

- **Hardness**: Hardness of Low Alkaline Glass Beads provides surface hardness to resin compounds.

- **High Abrasion Performance**: Hardness of Low Alkaline Glass Beads supports high abrasion performance of coating resin compounds.

- **High Heat Resistance**: Heat resistance of glass material supports high heat resistance of engineering plastic, painting and coating resin compound.

Chemical Composition & Physical properties

Composition	(%) Sample data
SiO_2	55.5
Al_2O_3	14.0
B_2O_3	5.7
Fe_2O_3	0.2
Na_2O,K_2O	0.5
MgO	1.0
CaO	23.1
Total	100.0

Properties	Average data
Density	2.6
Refractive Index（nD）	1.53 ～ 1.57
Hardness（New Mohs' scale）	6.5
Softening Point（℃）	830
Thermal Expansion Coefficient（× 10^{-7}/℃）	51
Thermal Conductivity (kcal/mh℃)	0.89
Specific Heat (kcal/kg℃)	0.20

Potters-Ballotini Co.Ltd.
10F, KYODO BLDG. (MANSEI)
2-2-17, SOTOKANDA, CHIYODA-KU
TOKYO 101-0021, JAPAN

TEL: (+81-3) 5298-2541
Fax: (+81-3) 5298-2544
E-mail: info@pqj.co.jp

HOFFMANN MINERAL
Unternehmensgruppe Hoffmann

SILFIT Z 91

TECHNICAL DATA SHEET – Field of application: ELASTOMERS

1. Description

SILFIT Z 91 is a natural combination of corpuscular silica and lamellar kaolinite, which has been subjected to a heat treatment. The components and the thermal process lead to a product that offers special performance benefits as a functional filler.

Characteristics:

Appearance:	free-flowing powder
Color CIELAB scale:	
L*	95
a*	- 0.1
b*	1.0
Sieve residue > 40 µm:	10 mg/kg
Volatile matter at 105°C:	0.2%
Density:	2.6 g/cm³
Particle size distribution	
D_{50} :	2 µm
D_{97} :	10 µm
Surface area BET:	8 m²/g
Oil absorption:	55 g/100 g
pH value:	6.5
Equilibrium moisture content at 25 °C and	
50 % relative humidity	0.12 %
80 % relative humidity	0.22 %
90 % relative humidity	0.54 %

Packaging:

Paper bags	à 25 kg
PE bags:	≤ 20 kg
EVA bags:	≤ 20 kg
Big Bags:	600 – 900 kg
Bulk:	on demand

Shelf life:
Unlimited if stored properly under dry conditions.

2. Applications

In elastomer applications **SILFIT Z 91** can be used as a functional filler either on its own or in combination with other non-reinforcing or reinforcing fillers.

Fields of application:

In general **SILFIT Z 91** is suitable for any rubber products used for technical applications.

Its particular properties are that it provides a balanced relationship between tensile strength, tear strength, low compression set and excellent extrusion properties.

It is particularly suitable for very bright or white compounds.

SILFIT Z 91 also provides advantages in the following instances:

- very high dispersion requirements:
  - compounds with a high oil content
  - automotive profiles with very low surface defect rates
  - products with extremely thin walls (membranes)
  - very high surface quality requirements (roller coverings and offset blankets)
- prevention of filler caused mold fouling during the injection process or deposits in the orifice die (Plating) during extrusion
- very low chloride content (washing machine gaskets)

Methods of processing:
Any process commonly used in the rubber industry

Elastomers:
BIIR, BR, CIIR, CR, HNBR, IIR, IR, NBR, NR, PNR, SBR;
CM, CSM, EPM, EPDM, EVM, Q

Dosage:
Generally in the range from 50 to 300 phr, depending on application, formulation and requirements

3. Benefits

- low sieve residues
- good and rapid incorporation
- very good dispersion, also in critical compounds
- good flow properties
- excellent surfaces
- excellent extrusion properties
- no negative influence on curing rate
- low tensile and compression set
- high electrical resistance
- good aging properties
- high chemical resistance
- complies with the standards on articles in contact with foodstuffs of the BfR and FDA
- matting effect

SILFIT Z 91 also provides the following benefits **compared with Sillitin/Sillikolloid**:

- lower moisture content, less moisture absorption
- lower chloride content
- very high brightness
- very high color-neutrality
- improved dispersion behavior like the Sillitin puriss grades
- slightly improved extrusion properties
- markedly improved compression set possible
- best combination of extrusion properties and compression set (within the range of non surface treated grades)
- outstandingly low dielectric losses in high voltage cable insulations

VM-9/07.19/06584980

HOFFMANN MINERAL GmbH • P.O. Box 14 60 • 86619 Neuburg (Donau) • Germany • Phone +49 8431 53-0 • Fax +49 8431 53-330
Internet: www.hoffmann-mineral.com • E-Mail: info@hoffmann-mineral.com

4. Comparison of properties:

		Sillitin							Silfit	Sillikolloid
		V 85	V 88	N 82	N 85	N 87	Z 86	Z 89	Z 91	P 87
Color-neutrality		●●	●●●●●	●	●●	●●●	●●	●●●●	●●●●●●	●●
Extrusion	Profile quality	●	●	●●●	●●	●●	●●●	●●●	●●●°	●●●●
	Collapse resistance	●	●	●●●	●●	●●	●●●	●●●	●●●	●●●●
	Matting effect	●●●●	●●●●	●●●	●●●	●●●	●●	●●	●●	●
Viscosity		●	●	●●●	●●	●●	●●●	●●●	●●●	●●●●
Tensile strength		●	●	●●●	●●	●●	●●●	●●●	●●●	●●●●
Tear resistance		●	●	●●●	●●	●●	●●●	●●●	●●●	●●●●
Compression set		●	●	●●●	●●	●●	●●●	●●●	●°	●●●●
Rebound elasticity		●●●●	●●●●	●●●	●●●	●●●	●●	●●	●●	●
Abrasion loss		●●●●	●●●●	●●	●●●	●●●	●●	●●	●●	●

• = low ••••••= high

5. Application examples:

- **Plating**
  Prevention of filler caused mold fouling during the injection process or deposits in the orifice die (plating) during extrusion
  Technical report: “Die Plating”
- **Car body seals**
  - excellent extrusion properties
  - quick cure
  - higher tensile strength, higher tear resistance and markedly better compression set compared with calcined clay in non-conductive compounds
  - generally low compression set, also testing according to Volkswagen VW PV 3307
  - prevention of filler caused deposits in the orifice die (plating) during extrusion

  Technical report: “Silfit Z 91 in Car Body Seals”
- **Washing machine gaskets**
  - higher tensile strength and higher tear resistance versus calcined clay
  - replacement of precipitated silica without deteriorating properties, faster cure and lower swelling in water and detergent lyes
  - prevention of filler caused mold fouling
  - very low chloride content

  Technical report: “Silfit in Grey Colored Washing Machine Gaskets”
- **White building profiles (window and facade seals)**
  - good extrusion properties, slightly higher tensile strength, lower compression set and more neutral white color (less yellow tint) versus calcined clay

  Technical report: “Calcined Neuburg Siliceous Earth in White Building Profiles”
- **Medium to high voltage cable insulation**
  - better dielectric loss factor tan δ, lower sieve residue, higher tensile strength versus calcined clay

  Technical report: “Calcined Neuburg Siliceous Earth in Medium and High Voltage Cable Insulation”

All mentioned technical reports and even more are available at www.hoffmann-mineral.com

Our applications engineering advice and the information contained in this memorandum are based on experience and are made to the best of our knowledge and belief, they must be regarded however as non-binding advice without guarantee. Working and employment conditions over which we have no control exclude any damage claim arising from the use of our data and recommendations. Furthermore we cannot assume any responsibility for patent infringements, which might result from the use of our information.

xGnP® Graphene Nanoplatelets – Grade M

xGnP® Graphene Nanoplatelets are unique nanoparticles consisting of short stacks of graphene sheets having a platelet shape. Each grade contains particles with a similar average thickness and surface area.

Grade M particles have an average thickness of approximately *6 to 8 nanometers* and a typical surface area of *120 to 150 m^2/g*. Grade M is available with average particle diameters of ***5***, ***15,*** or ***25*** microns.

Characteristics of Bulk Powder

Property	*Typical Value*
Appearance	Black granules
Bulk Density	0.03 to 0.1 g/cc
Oxygen Content*	< 1 percent
Residual Acid Content*	< 0.5 wt%

**Note: nanoplatelets have naturally occurring functional groups like ethers, carboxyls, or hydroxyls that can react with atmospheric humidity to form acids or other compounds.*

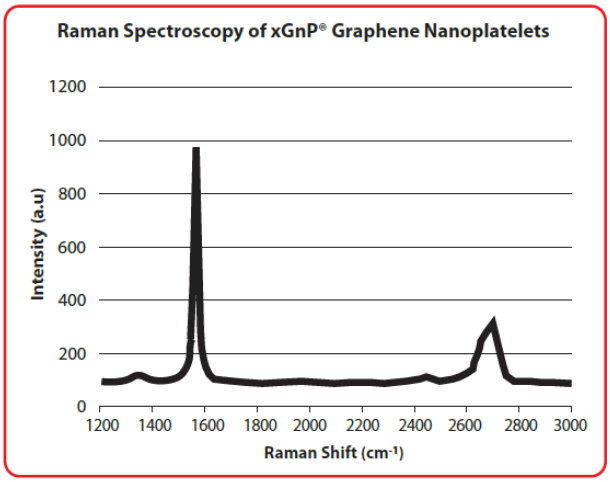

	Parallel To Surface	Perpendicular To Surface
Density (g/c^3)	2.2	2.2
LOI – Loss on Ignition (wt %)	≥ 99.0	≥ 99.0
Thermal Conductivity (W/m.K)	3,000	6
Thermal Expansion (m/m/K)	4 - 6 x 10^{-6}	0.5 - 1.0 x 10^{-6}
Tensile Modulus (MPa)	1,000	NA
Tensile Strength (MPa)	5	NA
Electrical Conductivity (S/m)	10^{7}	10^{2}

XG Sciences, Inc. believes the information in this technical data sheet to be accurate at publication. XG Sciences, Inc. does not assume any obligation or liability for the information in this technical data sheet. No warranties are given. All implied warranties of fitness for a particular purpose are expressly excluded. No freedom from infringement of any patent owned by XG Sciences or other is to be inferred. XG Sciences encourages its customers to review their manufacturing processes and applications for xGnP Graphene Nanoplatelets from the standpoint of human health and environmental quality to ensure that this material is not utilized in ways that it is not intended or tested.

XG Sciences Inc.
3101 Grand Oak Drive
Lansing, MI 48911

+1 517 703 1110
info@xgsciences.com
www.xgsciences.com

KCC Corporation

Glass Fiber - Product Information

Chopped Strand

Chopped Strand Characteristics

Chopped Strand(CS) is produced by collimating the continuous fibers into strands and either chopping directly under bushing.

KCC CS is specifically used in extrusion and injection molding process with thermoplastic and thermosetting resin matrix. Various KCC CS products combine with PA(Polyamide), PC(Polycarbonate), PET(Polyethylene terephthalate), PP(Polypropylene), Phenolic Resin and etc.

KCC CS is excellent in feeding with low fuzz generation and superior dispersion in the extruder.

Product Code

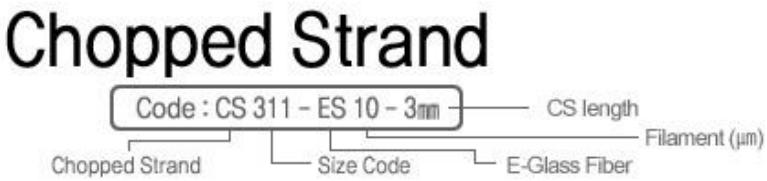

Available products

Product name	Application	Sizing	Moisture (%)	% Loss on Ignition	Filament Dia.	Bulky density	Length (mm)
CS311	PA, Phenol	Silane-based	Max. 0.1	0.70 ± 0.15	10.0 ± 1 (㎛)	Min. 0.60	3, 4.5
CS321	PC, PET, PBT			0.80 ± 0.15	10.0 ± 1 (㎛)		3
CS331	PP			0.85 ± 0.15	13.0 ± 1 (㎛)		4
CS391	Anti-Ethylene Glycol			0.70 ± 0.15	10.0 ± 1 (㎛)		3

Packing

Bags per pallet	1 Bag
Pallet dimensions, LxWxH (㎜)	1140*1140*1345

Pallet net weight (kg)	900 / 1,000
Pallets per 20ft container	18

ELG Carbon Fibre Ltd.
RECYCLED CARBON FIBRE

CARBISO™ MF Milled Fibre

Carbiso™ MF is recycled carbon fibre milled to 80µ or 100µ made from standard modulus fibre.

Milled fibres are used in demanding applications to increase mechanical properties and provide tailored electrical and thermal conductivity of the chosen matrix.

The milled carbon fibres have excellent dispersibility as the fibres are unsized and are compatible with most thermoset and thermoplastic matrices.

Carbiso™ MF Milled Fibre

Nomenclature for Carbiso™ MF products

Example:

CARBISO™ MF SM45R-100

BRAND NAME	PRODUCT TYPE	FIBRE CLASSIFICATION	DIMENSION
CARBISO™	MF Milled Fibre	SM45R Standard modulus fibre with a strength of 4-5Gpa, reclaimed unsized fibre	06-50 100 micron average fibre length

For additional details please see ELG Technical Note 1702: Product Nomenclature

Material data of Carbiso™ MF

Typical properties	Units	MF SM45R-80 / MF SM45R-100
Carbon fibre content	%	>98
Fibre diameter	μm	7
Fibre length	μm	80/100
Sizing Content	%	0
Bulk Density	g/l	400
Metal Contamination*	g/1000g	<0.5/1000
Packaging (Pillow bag)	kg	17.5
Tensile Strength**	MPa	4150
Tensile Modulus**	GPa	230-255

* Our milled fibres have passed through our metal detection and separation systems, metal contamination figures are a guide.

** Mechanical properties quoted are values measures by impregnated strand tests in accordance with ISO:ASTM D4018 – 17

Alternative fibre lengths available on request

The information presented in this document is provided in good faith, but no warranty is given or is to be implied regarding its accuracy or relevance to any particular application. Users must satisfy themselves regarding the suitability and safety of their use of the information and products in the application concerned.

ELG Carbon Fibre Ltd. Cannon Business Park, Gough Road, Coseley, West Midlands, WV14 8XQ

+44 1902 406010 www.ELGCF.com

Appendix B.3: Commercial PP/glass fibre reinforced resins datasheets

SABIC® PPCOMPOUND G3230A

PP SHORT GLASS FIBER REINFORCED

DESCRIPTION

SABIC® PPcompound G3230A is a 30% short glass fiber reinforced Polypropylene for under-the-hood and structural applications. The base material is a PP homopolymer and is available in standard black. The glass fibres are chemically coupled to the PP matrix. This material has been designed to combine a good performance profile with fast processing.

SABIC® PPcompound G3230A is a designated automotive grade.

IMDS ID: 109612410

TYPICAL PROPERTY VALUES

Revision 20171214

PROPERTIES	TYPICAL VALUES	UNITS	TEST METHODS
POLYMER PROPERTIES			
Melt Flow Rate			
at 230 °C and 2.16 kg	11	dg/min	ISO 1133
Density (1)	1130	kg/m³	ISO 1183
Filler content	30	%	SABIC method
Mould shrinkage (2)			
24 hours after injection moulding	0.6	%	SABIC method
MECHANICAL PROPERTIES (1)			
Tensile test			
stress at break	93	MPa	ISO 527/1A
strain at break	3	%	ISO 527/1A
Flexural test			
Flexural modulus	6900	MPa	ISO 178/1A
Charpy Impact Strength Notched			
at 23 °C	12	kJ/m²	ISO 179/1eA
THERMAL PROPERTIES (1)			
Heat deflection temperature			
at 1.80MPa (HDT/A)	150	°C	ISO 75/A
Coeff. of linear thermal expansion			
-30 °C to 100 °C	40	µm/mK	ISO 11359-2

© 2017 Copyright by SABIC. All rights reserved

(1) Injection molded sample ISO527-1A
(2) Injection molded plaque 65x65x3.2mm

QUALITY

SABIC is fully certified in accordance with the internationally accepted quality standard ISO9001.

STORAGE AND HANDLING

Avoid prolonged storage in open sunlight, high temperatures (<50 °C) and/or high humidity as this could well speed up alteration and consequently loss of quality of the material and/or its packaging. Keep material completely dry for good processing.

DISCLAIMER

Any sale by SABIC, its subsidiaries and affiliates (each a “seller”), is made exclusively under seller’s standard conditions of sale (available upon request) unless agreed otherwise in writing and signed on behalf of the seller. While the information contained herein is given in good faith, SELLER MAKES NO WARRANTY, EXPRESS OR IMPLIED, INCLUDING MERCHANTABILITY AND NONINFRINGEMENT OF INTELLECTUAL PROPERTY, NOR ASSUMES ANY LIABILITY, DIRECT OR INDIRECT, WITH RESPECT TO THE PERFORMANCE, SUITABILITY OR FITNESS FOR INTENDED USE OR PURPOSE OF THESE PRODUCTS IN ANY APPLICATION. Each customer must determine the suitability of seller materials for the customer’s particular use through appropriate testing and analysis. No statement by seller concerning a possible use of any product, service or design is intended, or should be construed, to grant any license under any patent or other intellectual property right.

© 2017 Copyright by SABIC. All rights reserved

MACOMASS
Compounds Masterbatches

Data Sheet

Article:	**MM-PP HF 24**
Description:	PP 50% glass-fibre reinforced
Processing:	Injection molding
Colour	90005 natur
Article number:	210495478

Date: 01.08.2017

General Properties	Norm	Unit	Value
MFR 230°C/2,16 kg	ISO 1133	g/10min	2.0 ± 0.5
Density	ISO 1183	g/cm^3	1.33 ± 0.02
Mechanical Properties			
Tensile strength	ISO 527-2	N/mm^2	≥ 80
Elongation at break	ISO 527-2	%	≥ 2
Elastic modulus	ISO 178	N/mm^2	≥ 8000
Impact strength	ISO 179	kJ/m^2	≥ 28
Notched impact strength	ISO 179	kJ/m^2	≥ 5

Processing Parameters		
Drying	°C / h	80 / 2
Cylinder Temperature	°C	200-240
Processing Temperature	°C	220-250
Mold Temperature	°C	30-60

These indications are approximate values, depending on the processing machine. Adjustments while the processing can be necessary.

Remarks

This information is based on experience and is to be regarded as a guidance only. It is given without obligation. We recommend that the suitability of this product is checked for the intended application by the customer. On the basis of our conditions of sale, we only assume a warranty for the supply of consistent quality and according to the agreed specification.

MACOMASS Verkaufs AG – Schwalbenrainweg 46 – DE-63741 Aschaffenburg – Phone: +49 6021 3506-0 – E-Mail: macomass@macomass.de

Appendix C Experimental raw data for chapter 4

Appendix C Experimental raw data for chapter 4

Table C.1 Measured melt flow index of neat PP and PP based composites

Composites	Melt Flow Index (g/10 min)	SD
Neat PP	55.50	4.79
Extruded neat PP	60.69	7.65
PP/CC10	51.12	7.05
PP/CC15	46.20	3.64
PP/CC20	45.48	9.28
PP/CC25	45.24	7.56
PP/CC30	42.96	5.95
PP/GB10	51.84	6.39
PP/GB15	50.52	5.30
PP/GB20	50.40	7.84
PP/GB25	49.44	4.88
PP/GB30	47.52	6.38
PP/KL10	45.12	3.44
PP/KL20	39.00	3.01
PP/KL30	34.08	2.16
PP/GN10	36.34	2.42
PP/GN20	14.00	1.33
PP/GN30	8.22	0.71
PP/GF10	51.00	4.33
PP/GF15	48.12	6.32
PP/GF20	41.04	3.12
PP/GF25	40.92	2.56
PP/GF30	37.68	5.50
PP/CF10	45.09	5.77
PP/CF20	40.97	7.85
PP/CF30	27.00	4.33

Table C.2 Tensile properties of neat PP based composites

Composites	Tensile strength (MPa)				%Elongation				Tensile Modulus (MPa)	
	@Yield	SD	@Break	SD	@Yield	SD	@Break	SD		
Neat PP	30.8	0.6	21.8	0.6	4.64%	0.16%	148.8%	37.9%	1708.6	38.9
Extruded PP	30.5	0.4	21.3	0.8	5.34%	0.21%	87.0%	32.4%	1518.9	50.3
PP/CC10	27.6	1.4	19.9	1.1	3.97%	0.17%	41.8%	9.7%	1851.1	73.3
PP/CC15	27.5	0.6	19.7	1.1	3.34%	0.24%	29.4%	2.6%	2105.3	54.5
PP/CC20	26.8	0.3	20.0	0.7	3.13%	0.04%	33.6%	6.7%	2116.6	30.3
PP/CC25	25.0	0.3	20.9	0.5	3.10%	0.07%	35.2%	4.4%	2138.3	52.1
PP/CC30	25.4	1.2	21.5	1.9	2.57%	0.07%	27.3%	8.4%	2294.7	118.3
PP/GB10	31.7	2.9	21.1	3.9	4.32%	0.05%	20.4%	2.2%	1871.7	173.7
PP/GB15	31.1	0.5	22.8	2.6	4.41%	0.21%	24.6%	6.7%	1919.3	31.5
PP/GB20	30.5	0.5	23.9	0.8	4.23%	0.11%	24.2%	2.5%	2034.3	39.5
PP/GB25	32.3	0.4	25.8	1.0	3.82%	0.11%	20.9%	3.6%	2138.0	32.0
PP/GB30	31.7	0.4	25.4	1.2	3.55%	0.08%	20.2%	2.5%	2344.6	40.6
PP/KL10	32.6	1.4	25.2	3.3	3.82%	0.07%	20.9%	3.1%	2003.3	98.0
PP/KL20	31.6	1.2	25.7	1.5	3.24%	0.12%	12.8%	0.8%	2089.5	94.0
PP/KL30	32.1	0.4	28.0	1.0	2.47%	0.11%	4.9%	1.0%	2421.7	219.0
PP/GN10	31.6	1.3	28.3	1.2	4.14%	0.14%	10.8%	2.1%	1835.6	223.0
PP/GN20	31.5	0.8	29.2	0.9	3.17%	0.11%	6.2%	0.6%	2578.5	76.9
PP/GN30	32.0	0.9	29.8	1.0	3.23%	0.09%	6.6%	0.9%	2612.0	99.0
PP/GF10	36.2	0.9	31.0	1.7	3.90%	0.42%	11.9%	0.7%	2300.6	29.0
PP/GF15	35.8	1.0	32.7	2.0	3.82%	0.21%	8.2%	0.9%	2366.5	152.5
PP/GF20	42.3	0.6	39.3	1.1	3.46%	0.19%	6.1%	0.2%	3079.1	195.6
PP/GF25	41.5	1.2	39.1	0.9	3.56%	0.12%	6.8%	0.4%	3207.6	103.2
PP/GF30	44.6	0.7	42.4	1.0	3.17%	0.20%	5.3%	0.3%	3758.2	71.3
PP/CF10	35.7	0.6	26.3	1.6	3.57%	0.14%	19.1%	2.1%	2689.6	125.6
PP/CF20	39.0	0.3	34.9	0.6	3.59%	0.12%	12.1%	0.5%	4030.4	88.0
PP/CF30	45.9	1.8	43.3	1.9	3.44%	0.10%	6.6%	0.3%	5456.3	189.1

Table C.3 Flexural strength and modulus of neat PP, extruded PP and PP based composites

Composites	Flexural Strength (MPa)		Flexural Modulus (MPa)	
	Average	SD	Average	SD
Neat PP	36.6	2.3	1240.3	30.4
Extruded PP	35.7	0.9	1227.3	60.7
PP/CC10	50.0	6.7	1411.8	42.1
PP/CC15	45.2	5.0	1412.7	12.5
PP/CC20	45.9	14.0	1597.6	19.5
PP/CC25	45.7	3.9	1618.8	26.9
PP/CC30	41.9	2.0	1804.7	30.2
PP/GB10	49.6	3.5	1348.7	44.3
PP/GB15	48.7	1.4	1374.6	19.0
PP/GB20	52.7	1.2	1461.0	26.5
PP/GB25	55.8	6.2	1547.3	33.9
PP/GB30	51.5	3.1	1822.7	74.0
PP/KL10	38.8	0.1	1394.2	4.2
PP/KL20	39.1	0.1	1546.3	23.4
PP/KL30	41.2	0.1	1747.1	13.8
PP/GN10	37.3	0.1	1467.1	15.8
PP/GN20	41.0	0.8	2252.0	48.1
PP/GN30	45.4	0.3	2975.1	47.2
PP/GF10	41.5	0.2	1624.4	13.5
PP/GF15	44.9	0.1	1889.3	46.3
PP/GF20	52.4	0.7	2300.8	31.3
PP/GF25	52.9	0.9	2511.7	87.8
PP/GF30	58.7	0.2	3081.2	52.8
PP/CF10	44.9	0.4	2190.9	60.2
PP/CF20	51.4	0.8	3247.4	160.5
PP/CF30	60.0	1.9	4709.4	216.7

Table C.4 Izod impact of neat PP, extruded PP and PP based composites

Composites	Izod impact strength	
	kJ/m^2	SD
Neat PP	5.11	0.29
Extruded PP	4.50	0.20
PP/CC10	4.88	0.26
PP/CC15	4.86	0.36
PP/CC20	4.73	0.28
PP/CC25	4.64	0.11
PP/CC30	4.68	0.25
PP/GB10	5.39	0.34
PP/GB15	5.27	0.13
PP/GB20	5.09	0.32
PP/GB25	5.07	0.13
PP/GB30	5.00	0.22
PP/KL10	5.21	0.29
PP/KL20	5.16	0.28
PP/KL30	4.12	0.24
PP/GN10	4.46	0.43
PP/GN20	3.58	0.28
PP/GN30	3.33	0.09
PP/GF10	5.01	0.08
PP/GF15	5.16	0.08
PP/GF20	5.33	0.16
PP/GF25	5.36	0.10
PP/GF30	5.61	0.17
PP/CF10	4.68	0.21
PP/CF20	5.00	0.22
PP/CF30	4.90	0.07

Table C.5 The percentages of change of mechanical properties of PP based composites

Composites	The percentage of change of PP based composite		
	Tensile modulus	Flexural modulus	Izod impact strength
Neat PP			
Extruded PP	-11%	-1%	-8%
PP/CC10	8%	14%	-5%
PP/CC15	23%	14%	-5%
PP/CC20	24%	29%	-7%
PP/CC25	25%	31%	-9%
PP/CC30	34%	46%	-8%
PP/GB10	10%	9%	6%
PP/GB15	12%	11%	3%
PP/GB20	19%	18%	0%
PP/GB25	25%	25%	-1%
PP/GB30	37%	47%	-2%
PP/KL10	17%	12%	2%
PP/KL20	22%	25%	1%
PP/KL30	42%	41%	-19%
PP/GN10	7%	18%	-13%
PP/GN20	51%	82%	-30%
PP/GN30	53%	140%	-35%
PP/GF10	35%	31%	-2%
PP/GF15	39%	52%	1%
PP/GF20	80%	86%	4%
PP/GF25	88%	103%	5%
PP/GF30	120%	148%	10%
PP/CF10	57%	77%	-8%
PP/CF20	136%	162%	-2%
PP/CF30	219%	280%	-4%

Table C.6 The rating and percentage of change of PP composites

Rating	Mechanical properties			MFI	Density
	Tensile Modulus	Flexural Modulus	Izod impact strength		
5	> 400%		> 100%	> 82%	>45%
4	301% – 400%		76% – 100%	64% – 82%	34% – 44%
3	201% – 300%		51% – 75%	43% – 63%	23% – 33%
2	101% – 200%		26% – 50%	22% – 42%	12% – 22%
1	1% – 100%		1% – 25%	1% – 21%	1% – 11%
0	0		0	0	0
-1	< (-1%) – (-100%)		< (-1%) – (-20%)	< (-1%) – (-21%)	< (-1%) – (-11%)
-2	< (-101%) – (-200%)		< (-21%) – (-40%)	< (-22%) – (-42%)	< (-12%) – (-22%)
-3	< (-201%) – (-300%)		< (-41%) – (-60%)	< (-43%) – (-63%)	< (-23%) – (-33%)
-4	< (-301%) – (-400%)		< (-61%) – (-80%)	< (-64%) – (-82%)	< (-34%) – (-44%)
-5	< (-400%)		< (-81%) – (-100%)	< - 82%	< - 45%

Table C.7 The rating and percentage of change of PP composites' cost

Rating	Cost
5	> 100%
4	76% – 100%
3	51% – 75%
2	26% – 50%
1	1% – 25%
0	0
-1	< (-1%) – (-20%)
-2	< (-21%) – (-40%)
-3	< (-41%) – (-60%)
-4	< (-61%) – (-80%)
-5	< (-81%) – (-100%)

Table C.8 The description of rating for process implication

Rating	Description		
	Additional equipment	Additional methodology	Compound process handling
5	Required	Required	Difficult
4	Not required	Required	Difficult
3	Not required	Not required	Difficult
2	Required	Required	Easy
1	Not required	Required	Easy
0	Not required	Not required	Easy

Table C.9 The rating of PP based composites

Composites	Tensile Modulus	Flexural Modulus	Izod impact strength	MFI	Density	Cost	Process complication
Neat PP	0.00	0.00	0.00	0.00	0.00	0.00	0.00
PP/CC10	0.10	0.17	-0.23	-0.48	0.36	-0.47	1.00
PP/CC15	0.29	0.17	-0.24	-1.02	0.79	-0.71	1.00
PP/CC20	0.30	0.36	-0.37	-1.10	1.74	-0.94	1.00
PP/CC25	0.31	0.38	-0.46	-1.13	1.98	-1.18	1.00
PP/CC30	0.43	0.57	-0.42	-1.38	2.52	-1.41	1.00
PP/GB10	0.12	0.11	0.28	-0.40	0.40	0.21	2.00
PP/GB15	0.15	0.14	0.16	-0.55	0.72	0.32	2.00
PP/GB20	0.24	0.22	-0.02	-0.56	1.38	0.41	2.00
PP/GB25	0.31	0.31	-0.03	-0.67	1.79	0.53	2.00
PP/GB30	0.47	0.59	-0.11	-0.88	2.87	0.62	2.00
PP/KL10	0.22	0.16	0.10	-1.14	0.40	-0.09	3.00
PP/KL20	0.28	0.31	0.05	-1.82	1.30	-0.18	4.00
PP/KL30	0.52	0.51	-0.97	-2.36	2.04	-0.26	4.00
PP/GN10	0.09	0.23	-0.63	-2.11	0.26	5.00	4.00
PP/GN20	0.64	1.02	-1.50	-4.57	0.95	5.00	5.00
PP/GN30	0.66	1.75	-1.74	-5.00	1.03	5.00	5.00
PP/GF10	0.43	0.39	-0.10	-0.50	0.28	-0.24	1.00
PP/GF15	0.48	0.65	0.05	-0.81	0.69	-0.32	1.00
PP/GF20	1.00	1.07	0.22	-1.59	1.19	-0.44	1.00
PP/GF25	1.10	1.28	0.25	-1.61	1.54	-0.56	1.00
PP/GF30	1.50	1.86	0.50	-1.96	2.01	-0.68	1.00
PP/CF10	0.72	0.96	-0.42	-1.15	0.55	5.00	2.00
PP/CF20	1.70	2.02	-0.11	-1.60	0.75	5.00	2.00
PP/CF30	2.74	3.50	-0.21	-3.14	1.47	5.00	2.00

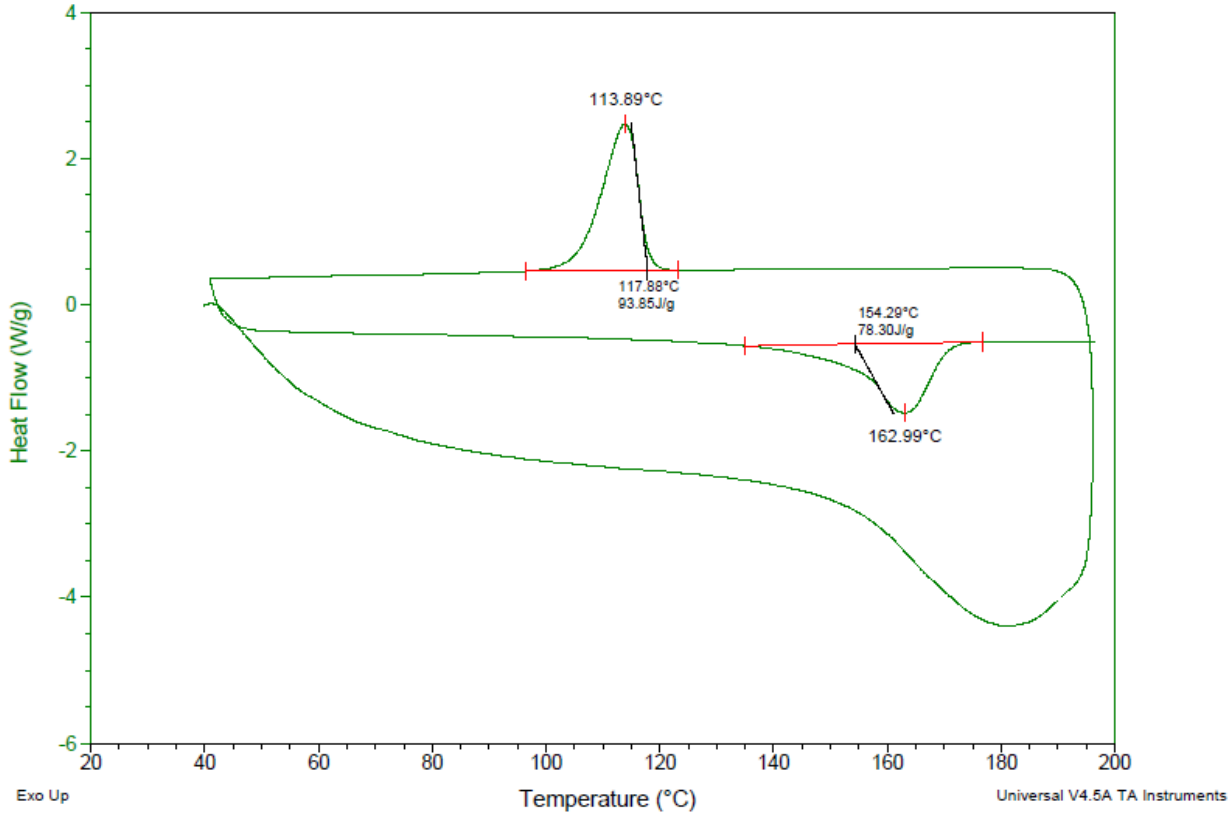

Figure C.1 DSC thermogram of neat PP with heat, cool, heat mode

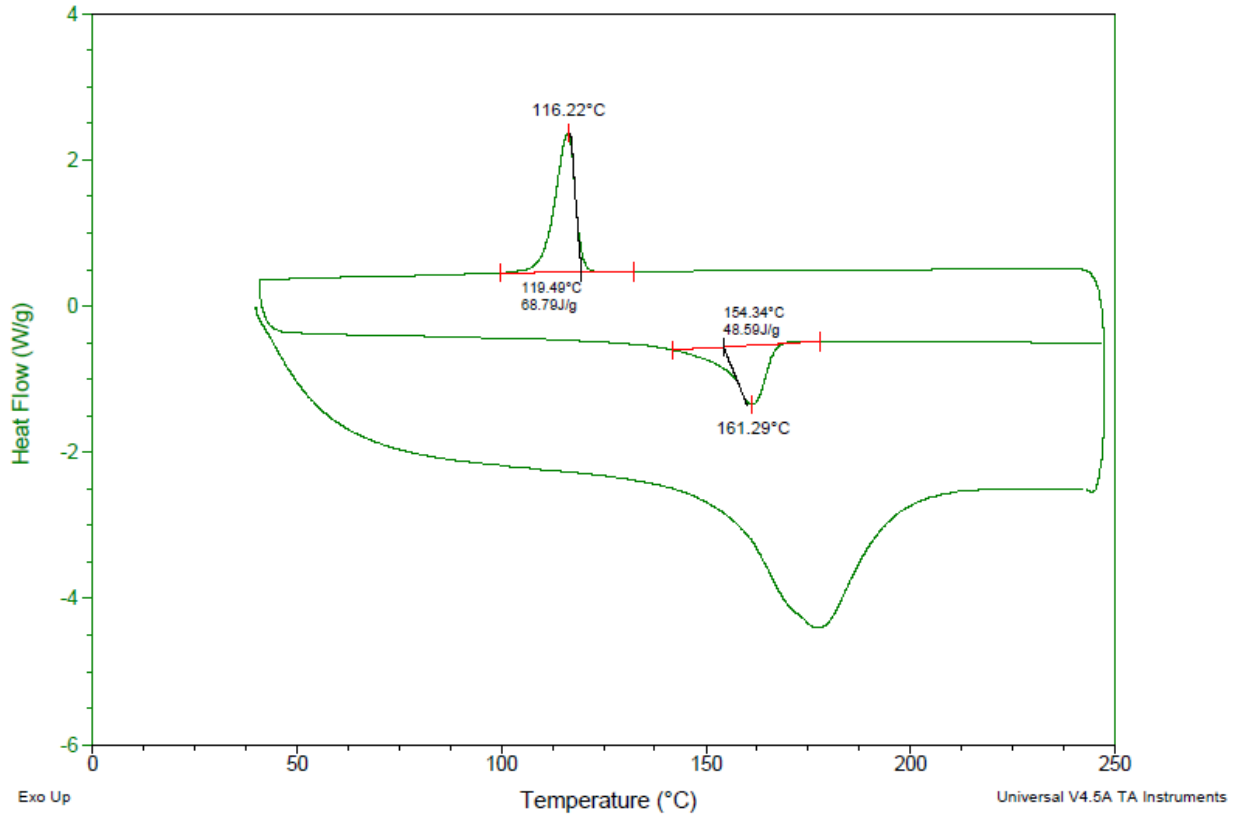

Figure C.2 DSC thermogram of PP/CC30 with heat, cool, heat mode

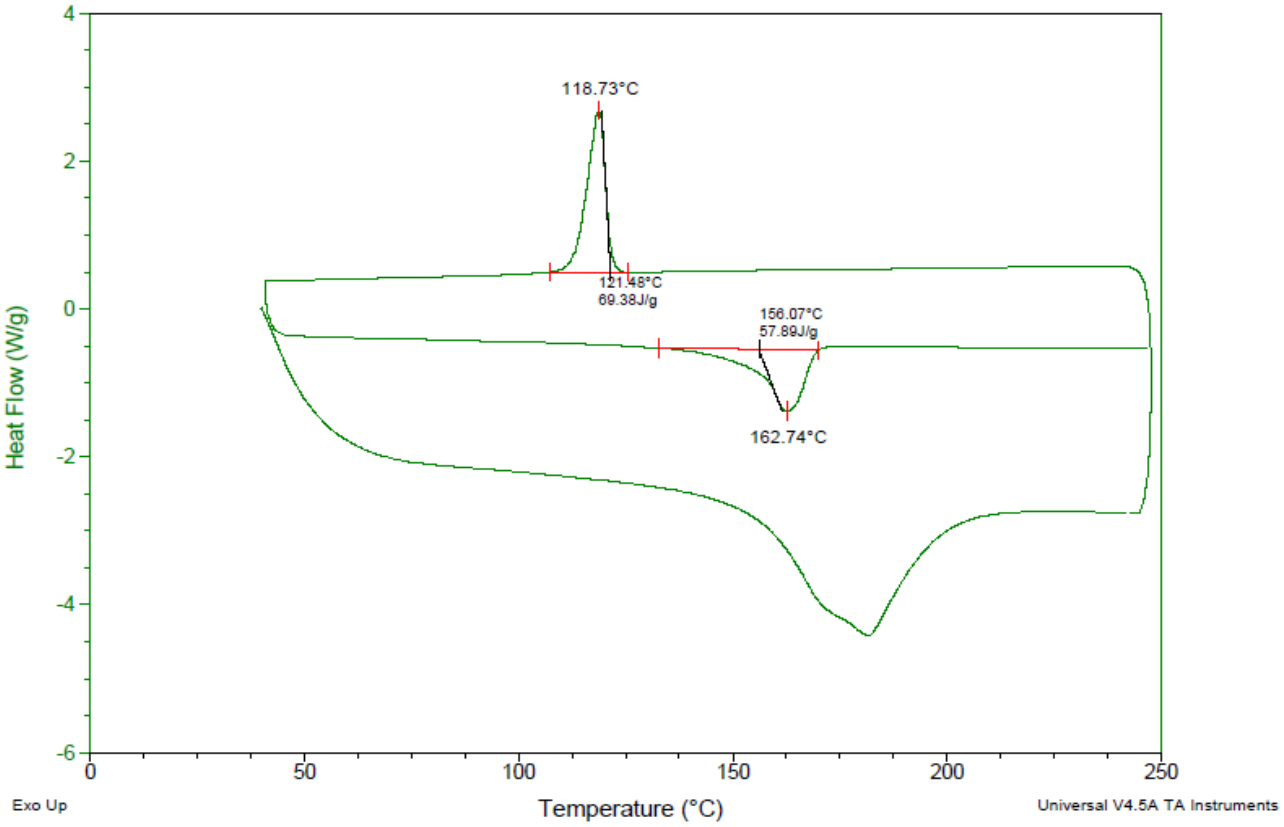

Figure C.3 DSC thermogram of PP/GB30 with heat, cool, heat mode

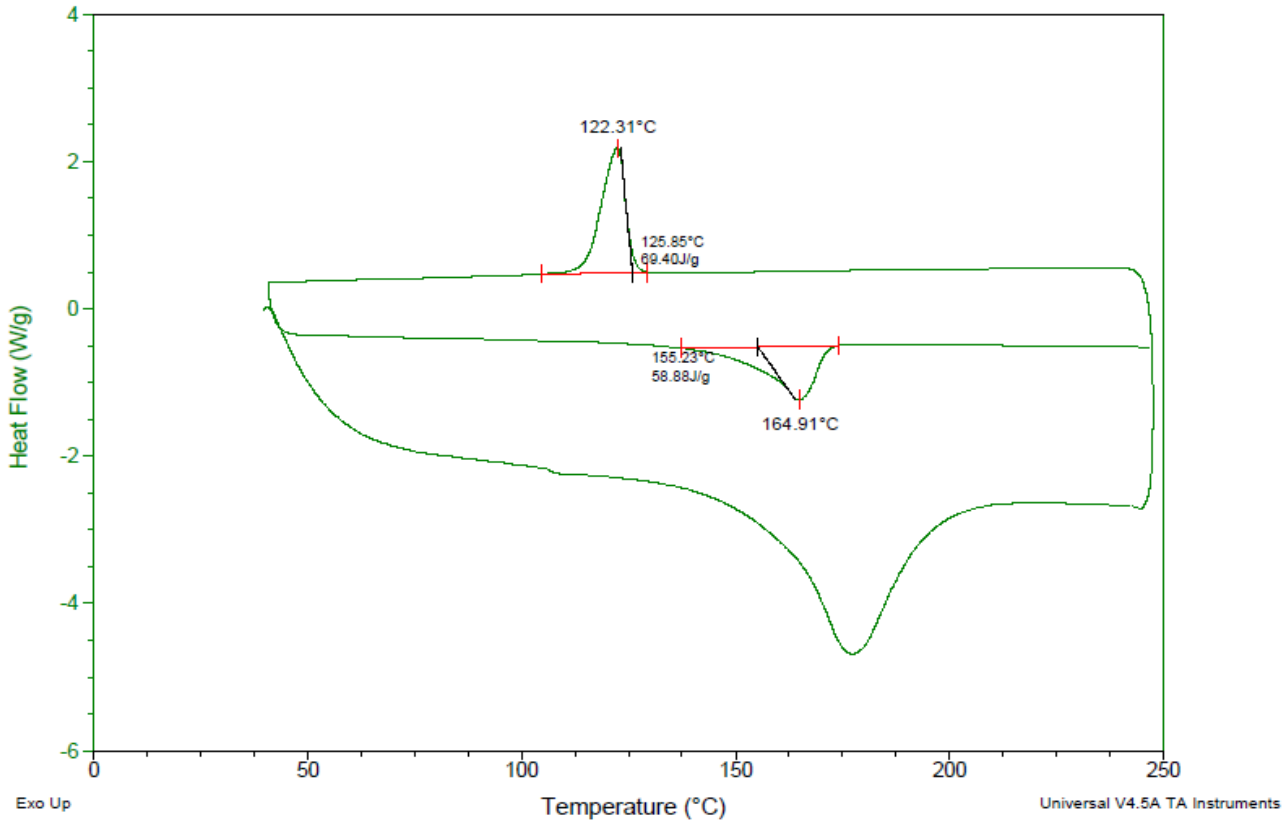

Figure C.4 DSC thermogram of PP/KL30 with heat, cool, heat mode

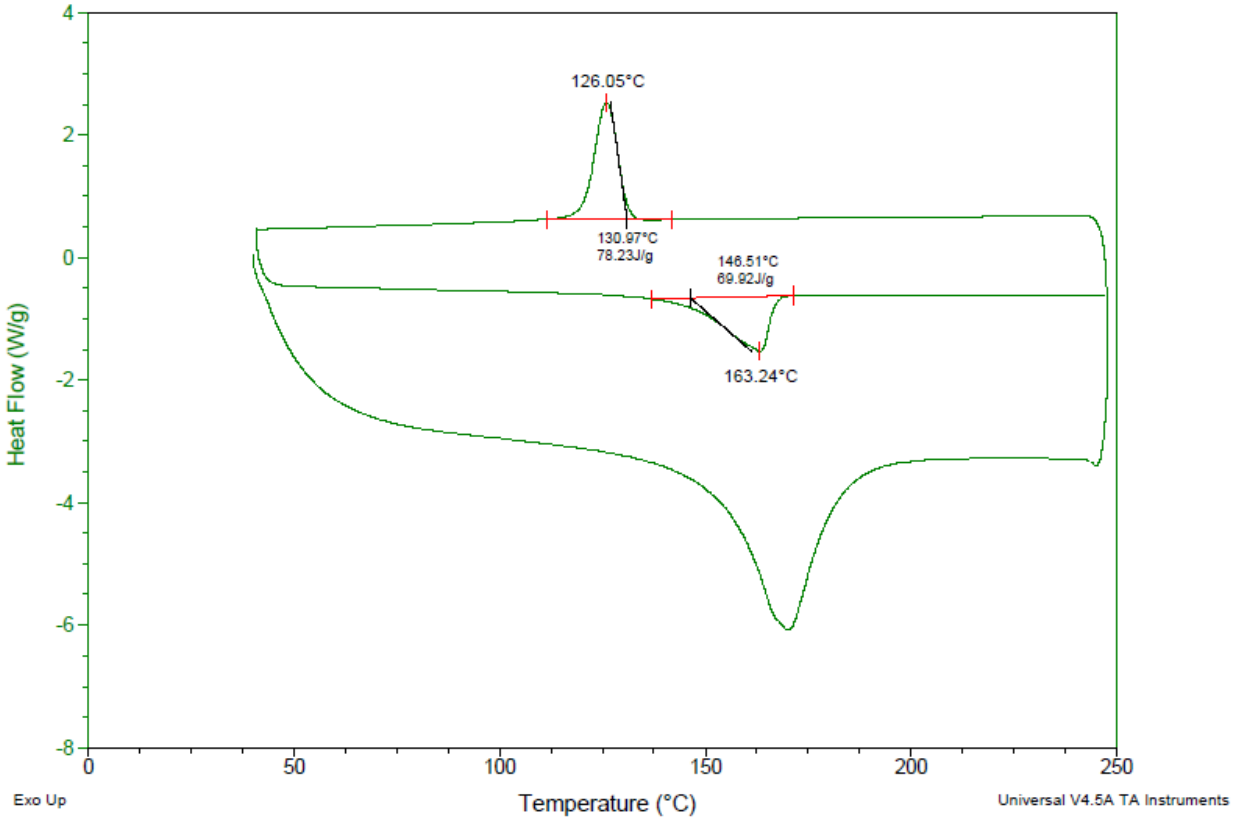

Figure C.5 DSC thermogram of PP/GN30 with heat, cool, heat mode

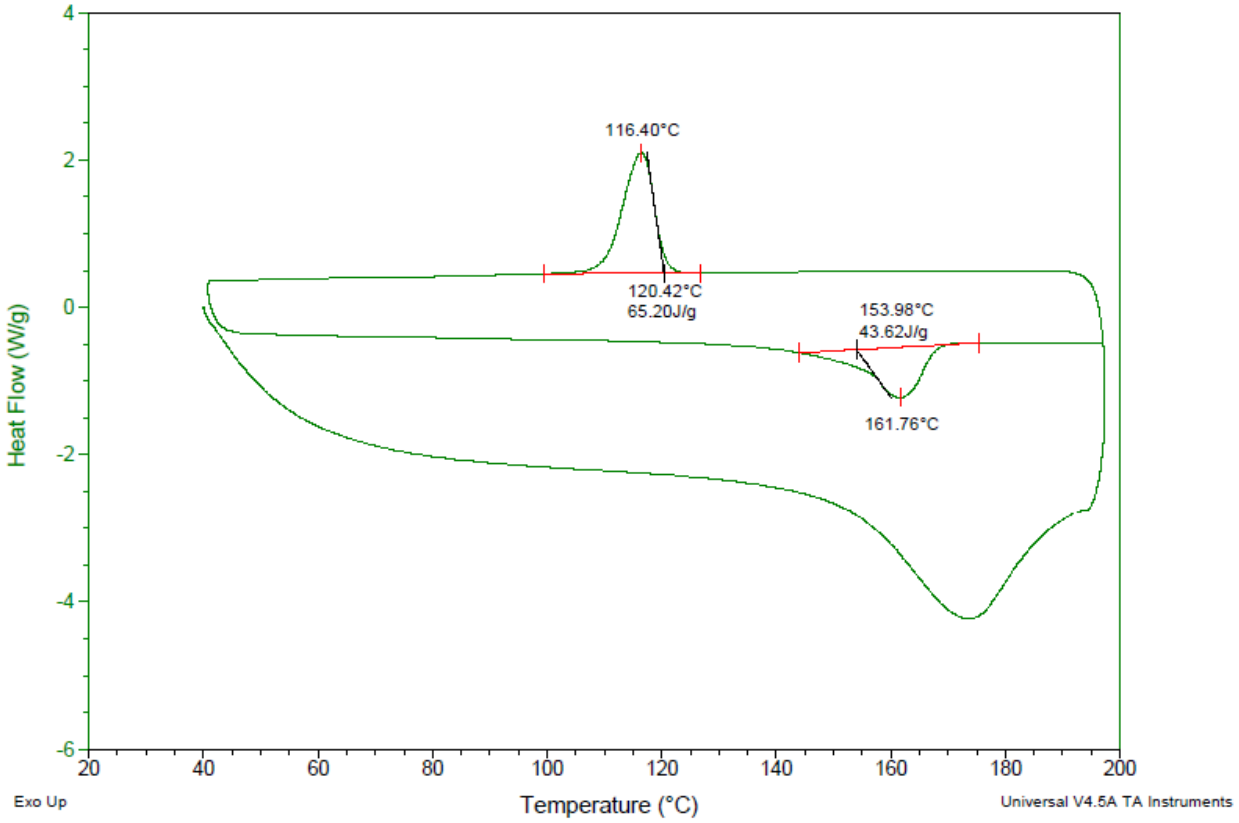

Figure C.6 DSC thermogram of PP/GF30 with heat, cool, heat mode

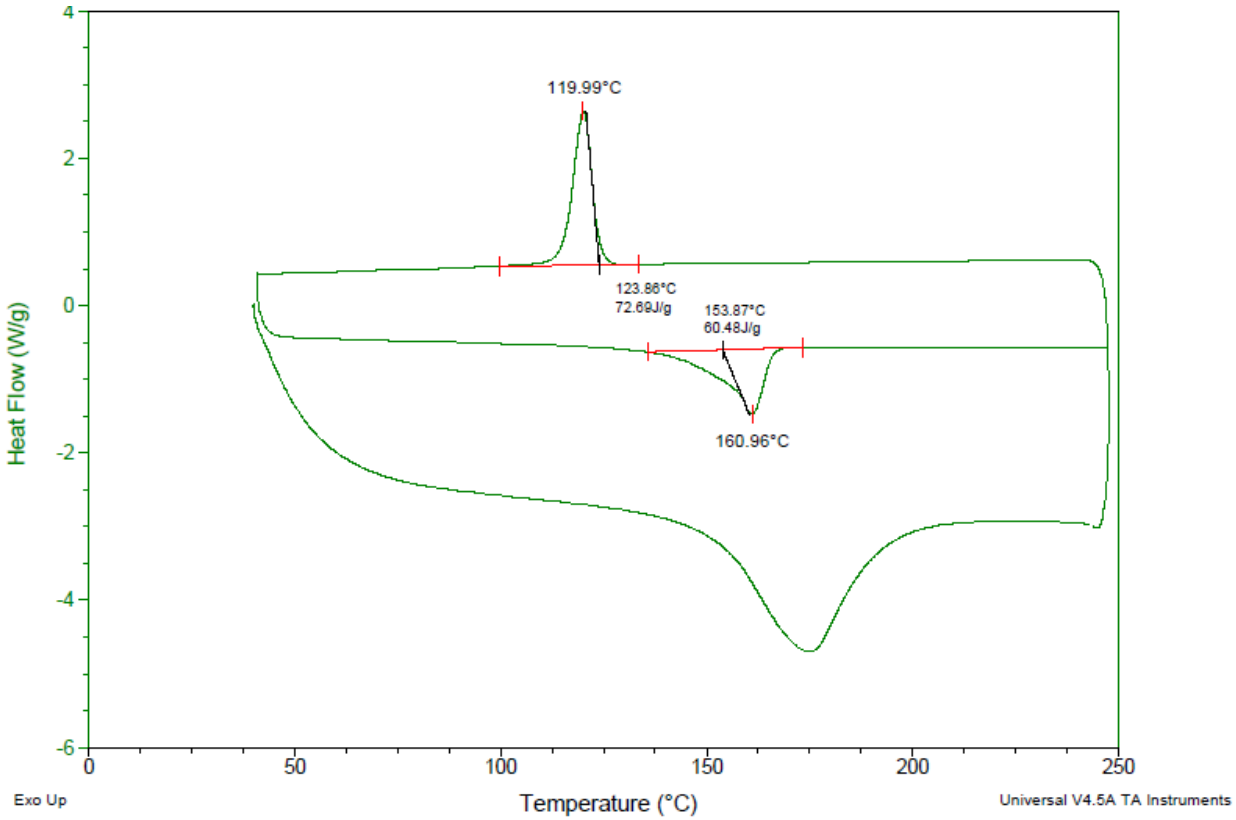

Figure C.7 DSC thermogram of PP/CF30 with heat, cool, heat mode

Appendix D Experimental raw data for chapter 5

Appendix D Experimental raw Data for Chapter 5

Table D.1 Tensile modulus of extruded PP and neat PP based hybrid composites

Composites	Tensile modulus (MPa)	SD
Extruded PP	1518.9	50.3
HC1 (PP/GB1/GF10)	2217.8	56.1
HC2 (PP/GB1/GF30)	3718.1	65.3
HC3 (PP/GB2/GF10)	2234.6	32.7
HC4 (PP/GB2/GF30)	3847.4	130.0
HC5 (PP/GB5/GF10)	2411.4	27.7
HC6 (PP/GB5/GF30)	3937.4	147.4
HC7 (PP/GB10/GF10)	2435.8	28.6
HC8 (PP/GB10/GF30)	4505.8	82.4

Table D.2 Flexural modulus of extruded PP and neat PP based hybrid composites

Composites	Flexural modulus (MPa)	SD
Extruded PP	1227.3	60.7
HC1 (PP/GB1/GF10)	1881.9	41.3
HC2 (PP/GB1/GF30)	3645.4	92.7
HC3 (PP/GB2/GF10)	1985.2	26.8
HC4 (PP/GB2/GF30)	3662.2	69.1
HC5 (PP/GB5/GF10)	2319.3	20.1
HC6 (PP/GB5/GF30)	3800.2	22.6
HC7 (PP/GB10/GF10)	2353.3	19.5
HC8 (PP/GB10/GF30)	4501.5	29.1

Table D.3 Izod impact strength of extruded PP and neat PP based hybrid composites

Composites	Izod impact strength (kJ/m^2)	SD
Extruded PP	4.50	0.20
HC1 (PP/GB1/GF10)	4.16	0.33
HC2 (PP/GB1/GF30)	5.11	0.29
HC3 (PP/GB2/GF10)	4.25	0.23
HC4 (PP/GB2/GF30)	5.14	0.25
HC5 (PP/GB5/GF10)	4.27	0.14
HC6 (PP/GB5/GF30)	5.17	0.30
HC7 (PP/GB10/GF10)	5.08	0.25
HC8 (PP/GB10/GF30)	5.73	0.13

Table D.4 Measured melt flow index of neat PP and PP based hybrid composites

Composites	Melt Flow Index (g/10 min)	SD
Neat PP	55.50	4.79
HC1 (PP/GB1/GF10)	45.84	6.4
HC2 (PP/GB1/GF30)	39.12	5.2
HC3 (PP/GB2/GF10)	45.60	3.7
HC4 (PP/GB2/GF30)	39.42	3.9
HC5 (PP/GB5/GF10)	45.78	5.9
HC6 (PP/GB5/GF30)	39.72	2.9
HC7 (PP/GB10/GF10)	43.14	4.5
HC8 (PP/GB10/GF30)	34.08	2.8

Table D.5 Measured density of neat PP based hybrid composites

Composites	Density (g/cm^3)	SD
Neat PP, Extruded PP	0.910	0.014
HC1 (PP/GB1/GF10)	0.930	0.009
HC2 (PP/GB1/GF30)	1.071	0.016
HC3 (PP/GB2/GF10)	0.938	0.017
HC4 (PP/GB2/GF30)	1.074	0.020
HC5 (PP/GB5/GF10)	0.979	0.007
HC6 (PP/GB5/GF30)	1.103	0.004
HC7 (PP/GB10/GF10)	1.003	0.006
HC8 (PP/GB10/GF30)	1.152	0.026

Table D.6 The rating of PP based hybrid composite

	The improvement of mechanical properties			MFI	Density	Cost
	Tensile Modulus	Flexural Modulus	Izod impact strength			
Extruded PP	0.00	0.00	0.00	0.00	0.00	0.00
HC1	0.58	0.67	-0.38	-1.06	0.24	-0.20
HC2	1.81	2.46	0.67	-1.80	1.97	-0.65
HC3	0.59	0.77	-0.28	-1.09	0.34	-0.18
HC4	1.92	2.48	0.71	-1.77	2.00	-0.63
HC5	0.73	1.11	-0.27	-1.07	0.85	-0.12
HC6	1.99	2.62	0.74	-1.74	2.36	-0.56
HC7	0.75	1.15	0.63	-1.36	1.13	-0.01
HC8	2.46	3.33	1.36	-2.36	2.95	-0.46

Table D.7 Tensile modulus of additional hybrid composites, PP/GF40wt% and PP/GF50wt%

Composites	Tensile modulus (MPa)	SD
Extruded PP	1518.9	50.3
HC1 (PP/GB1/GF10)	2217.8	56.1
HC2 (PP/GB1/GF30)	3718.1	65.3
HC3 (PP/GB2/GF10)	2234.6	32.7
HC4 (PP/GB2/GF30)	3847.4	130.0
HC5 (PP/GB5/GF10)	2411.4	27.7
HC6 (PP/GB5/GF30)	3937.4	147.4
HC7 (PP/GB10/GF10)	2435.8	28.6
HC8 (PP/GB10/GF30)	4505.8	82.4
HC9 (PP/GB7.5/GF30)	3951.3	52.4
HC10(PP/GB15/GF30)	4581.1	82.5
HC11 (PP/GB20/GF30)	4636.1	63.7
HC12 (PP/GB25/GF35)	4791.8	109.9
HC13 (PP/GB10/GF40)	5310.4	128.3
PP/GF40	4069.2	138.29
PP/GF50	5260.2	160.84

Table D.8 Flexural modulus of additional hybrid composites, PP/GF40wt% and PP/GF50wt%

Composites	Flexural modulus (MPa)	SD
Extruded PP	1227.3	60.7
HC1 (PP/GB1/GF10)	1881.9	41.3
HC2 (PP/GB1/GF30)	3645.4	92.7
HC3 (PP/GB2/GF10)	1985.2	26.8
HC4 (PP/GB2/GF30)	3662.2	69.1
HC5 (PP/GB5/GF10)	2319.3	20.1
HC6 (PP/GB5/GF30)	3800.2	22.6
HC7 (PP/GB10/GF10)	2353.3	19.5
HC8 (PP/GB10/GF30)	4501.5	29.1
HC9 (PP/GB7.5/GF30)	3866.2	46.9
HC10(PP/GB15/GF30)	4514.7	105.4
HC11 (PP/GB20/GF30)	4724.7	173.0
HC12 (PP/GB25/GF35)	4884.7	71.9
HC13 (PP/GB10/GF40)	5277.1	114.6
PP/GF40	3861.8	77.9
PP/GF50	4982.3	107.7

Table D.9 Izod impact strength of additional hybrid composites, PP/GF40wt% and PP/GF50wt%

Composites	Izod impact strength (kJ/m^2)	SD
Extruded PP	4.50	0.20
HC1 (PP/GB1/GF10)	4.16	0.33
HC2 (PP/GB1/GF30)	5.11	0.29
HC3 (PP/GB2/GF10)	4.25	0.23
HC4 (PP/GB2/GF30)	5.14	0.25
HC5 (PP/GB5/GF10)	4.27	0.14
HC6 (PP/GB5/GF30)	5.17	0.30
HC7 (PP/GB10/GF10)	5.08	0.25
HC8 (PP/GB10/GF30)	5.73	0.13
HC9 (PP/GB7.5/GF30)	5.29	0.14
HC10(PP/GB15/GF30)	5.72	0.16
HC11 (PP/GB20/GF30)	5.75	0.40
HC12 (PP/GB25/GF35)	5.81	0.26
HC13 (PP/GB10/GF40)	6.03	0.20
PP/GF40	5.65	0.35
PP/GF50	5.95	0.31

Table D.10 Measured melt flow index of neat PP and PP based hybrid composites

Composites	Melt Flow Index (g/10 min)	SD
Neat PP	55.50	4.79
HC1 (PP/GB1/GF10)	45.84	6.4
HC2 (PP/GB1/GF30)	39.12	5.2
HC3 (PP/GB2/GF10)	45.60	3.7
HC4 (PP/GB2/GF30)	39.42	3.9
HC5 (PP/GB5/GF10)	45.78	5.9
HC6 (PP/GB5/GF30)	39.72	2.9
HC7 (PP/GB10/GF10)	43.14	4.5
HC8 (PP/GB10/GF30)	34.08	2.8
HC9 (PP/GB7.5/GF30)	37.98	2.56
HC10(PP/GB15/GF30)	33.36	0.94
HC11 (PP/GB20/GF30)	33.00	1.26
HC12 (PP/GB25/GF35)	31.20	1.54
HC13 (PP/GB10/GF40)	30.66	1.98

Table D.11 Measured density of neat PP based hybrid composites

Composites	Density (g/cm^3)	SD
Neat PP, Extruded PP	0.910	0.014
HC1 (PP/GB1/GF10)	0.930	0.009
HC2 (PP/GB1/GF30)	1.071	0.016
HC3 (PP/GB2/GF10)	0.938	0.017
HC4 (PP/GB2/GF30)	1.074	0.020
HC5 (PP/GB5/GF10)	0.979	0.007
HC6 (PP/GB5/GF30)	1.103	0.004
HC7 (PP/GB10/GF10)	1.003	0.006
HC8 (PP/GB10/GF30)	1.152	0.026
HC9 (PP/GB7.5/GF30)	1.127	0.050
HC10(PP/GB15/GF30)	1.213	0.037
HC11 (PP/GB20/GF30)	1.241	0.007
HC12 (PP/GB15/GF35)	1.235	0.013
HC13 (PP/GB10/GF40)	1.231	0.029

Table D.12 The rating of neat PP based composite

	The improvement of mechanical properties			MFI	Density	Cost
	Tensile Modulus	Flexural Modulus	Izod impact strength			
Extruded PP	0.00	0.00	0.00	0.00	0.00	0.00
HC8 (PP/GB10/GF30)	2.46	3.33	1.36	-2.36	2.95	-0.46
HC9 (PP/GB7.5/GF30)	2.00	2.69	0.87	-1.93	2.65	-0.51
HC10 (PP/GB15/GF30)	2.52	3.35	1.35	-2.37	3.70	-0.36
HC11 (PP/GB20/GF30)	2.57	3.56	1.38	-2.48	4.05	-0.25
HC12 (PP/GB15/GF35)	2.69	3.73	1.45	-2.68	3.96	-0.47
HC13 (PP/GB10/GF30)	3.12	4.12	1.69	-2.74	3.92	-0.68

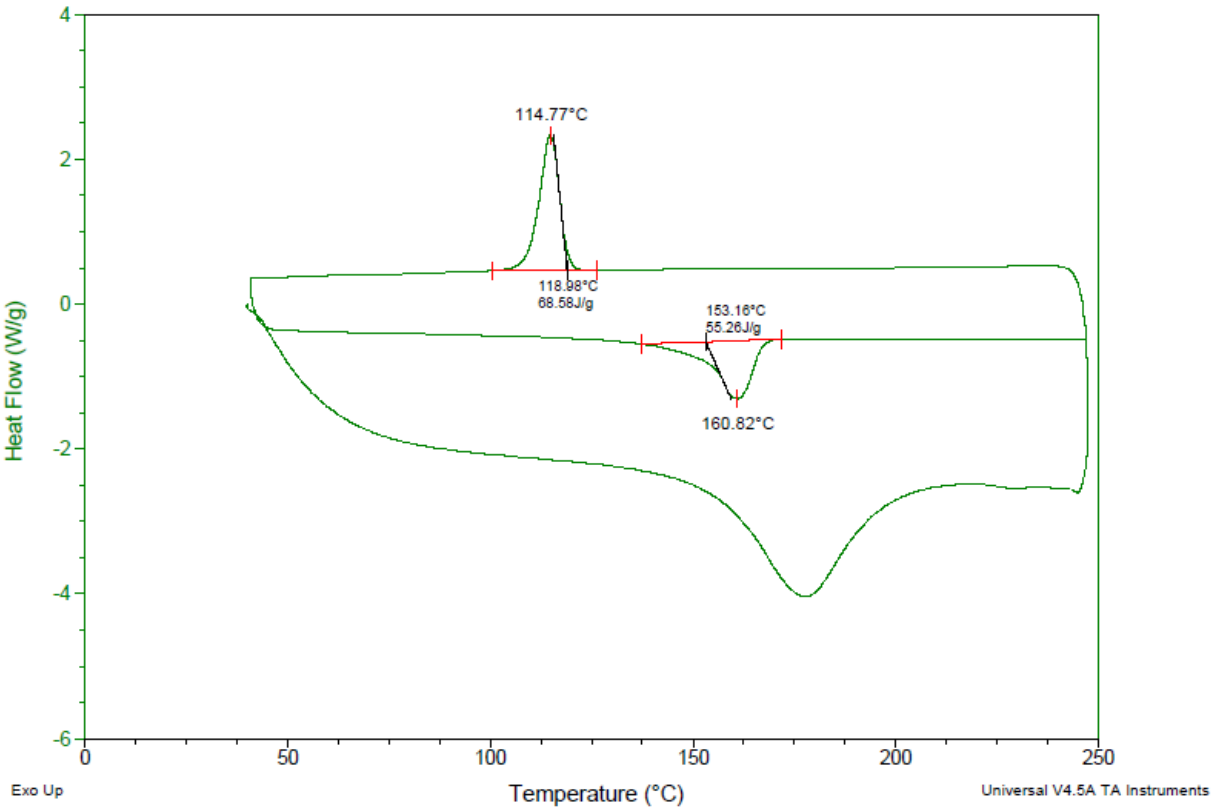

Figure D.1 DSC thermogram of HC2 with heat, cool, heat mode

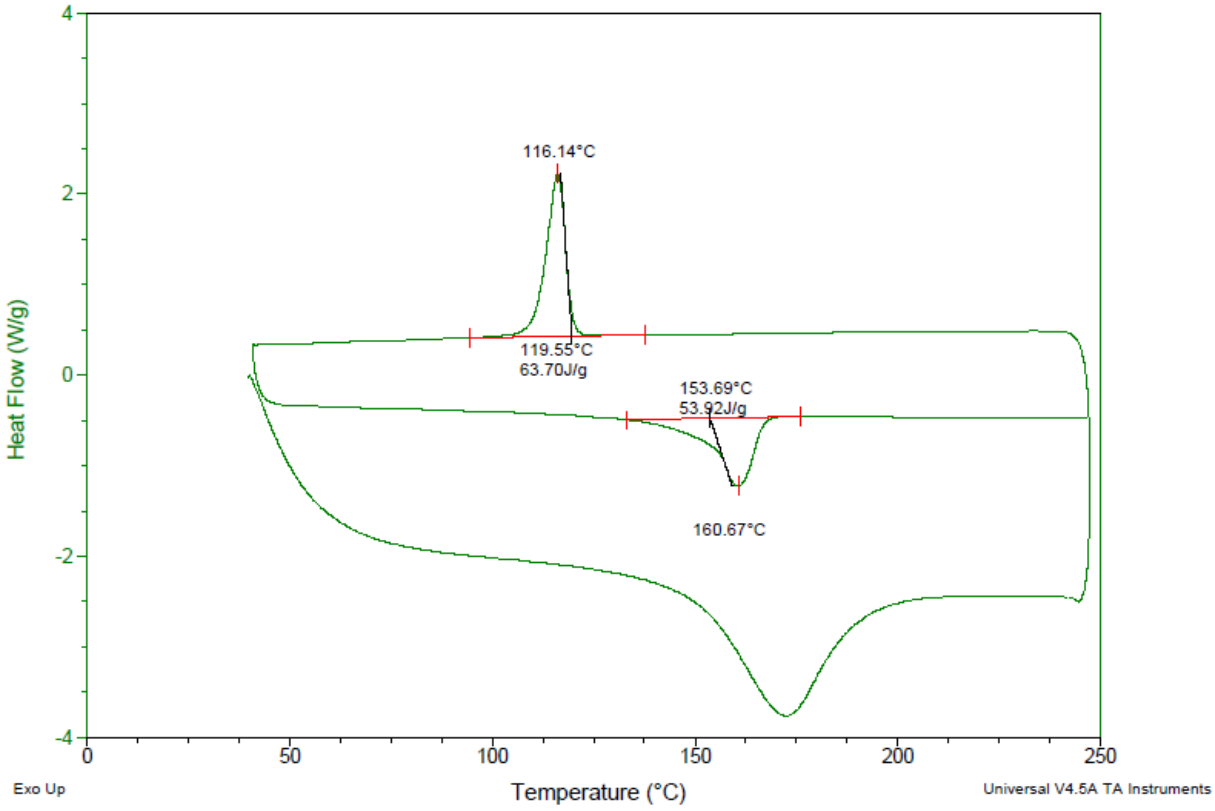

Figure D.2 DSC thermogram of HC6 with heat, cool, heat mode

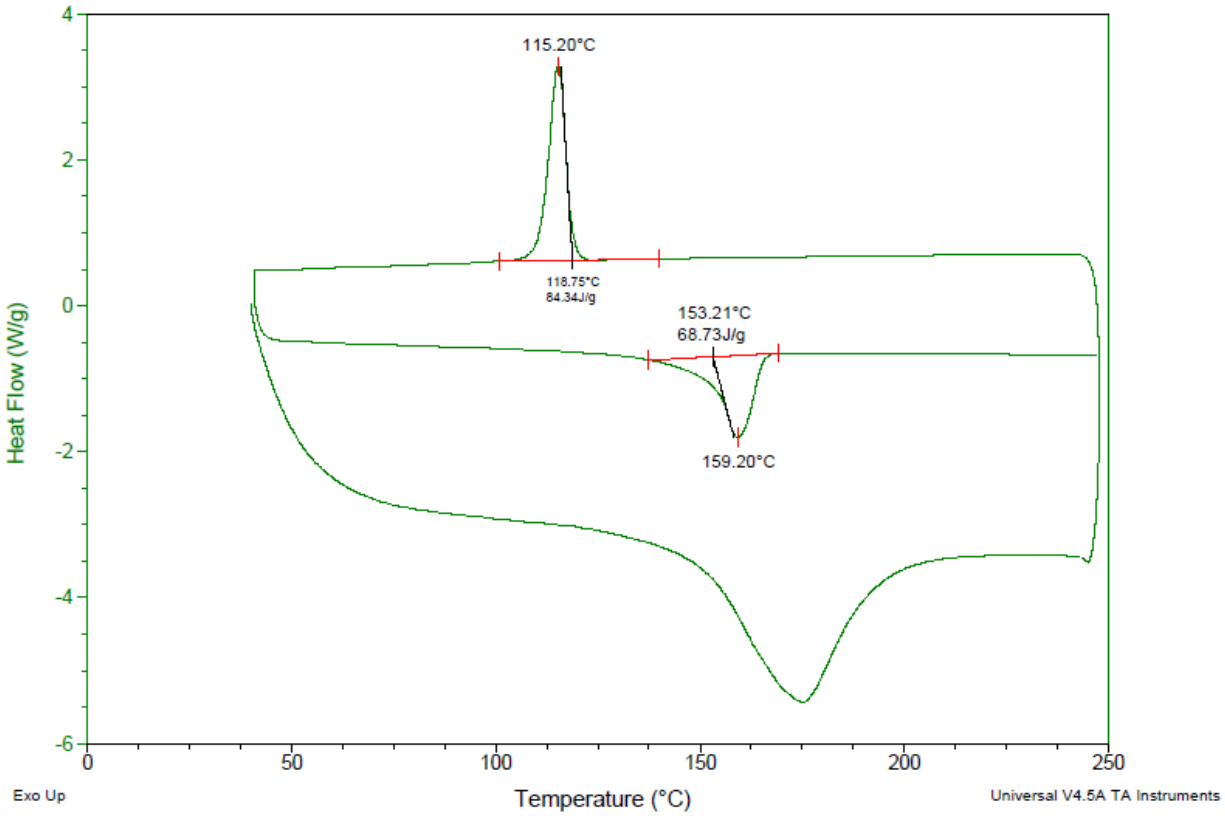

Figure D.3 DSC thermogram of HC7 with heat, cool, heat mode

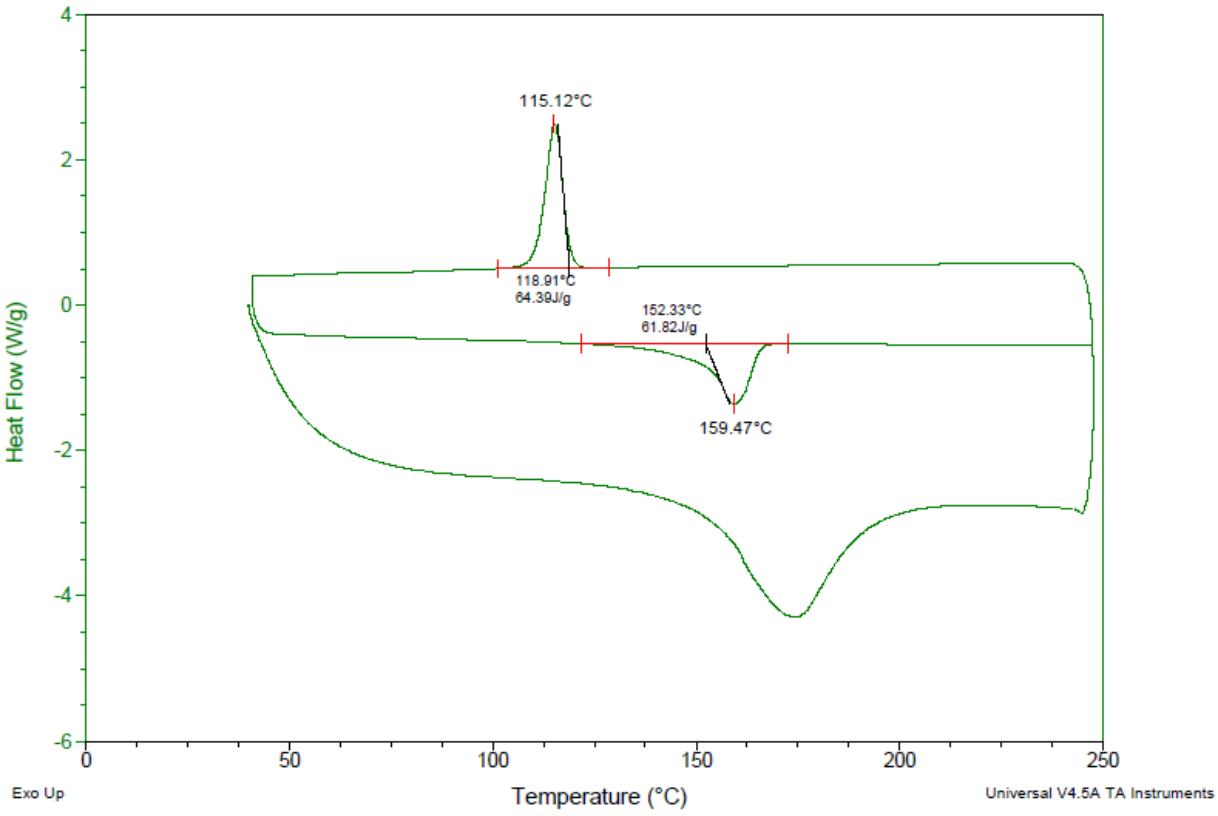

Figure D.4 DSC thermogram of HC8 with heat, cool, heat mode

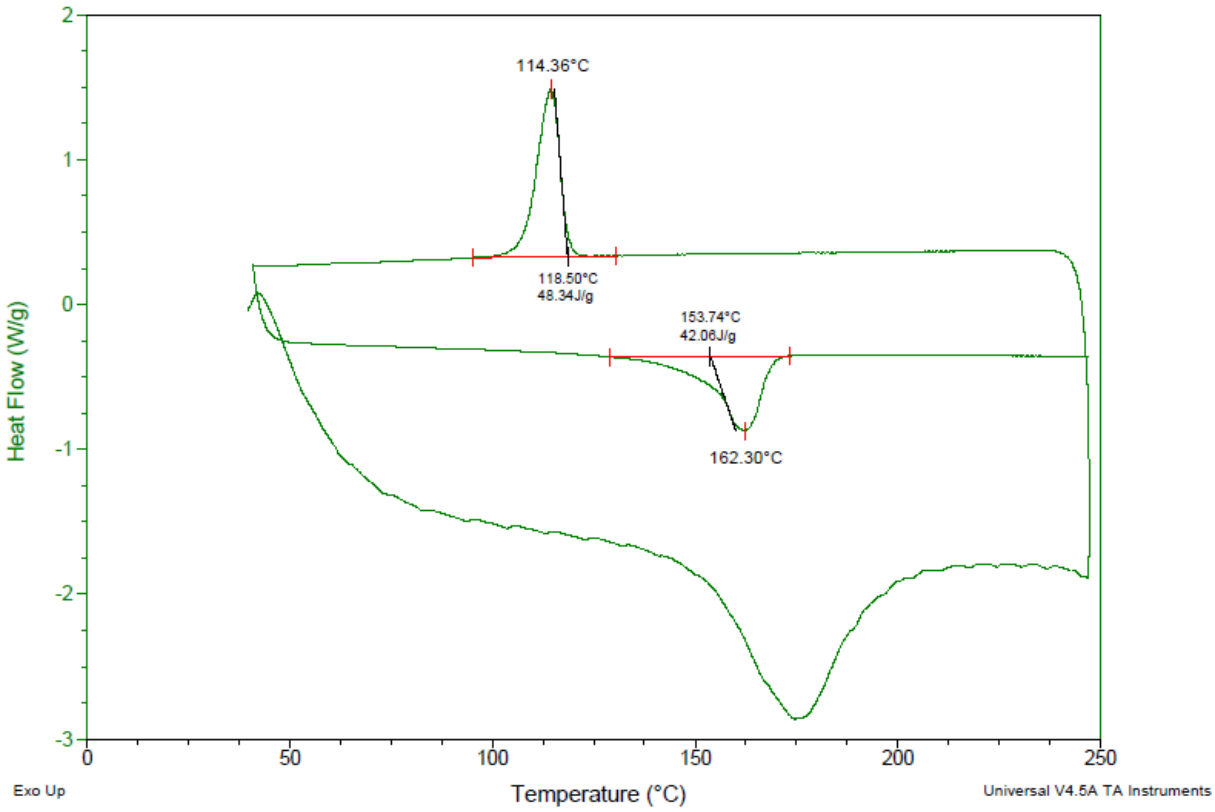

Figure D.5 DSC thermogram of HC10 with heat, cool, heat mode

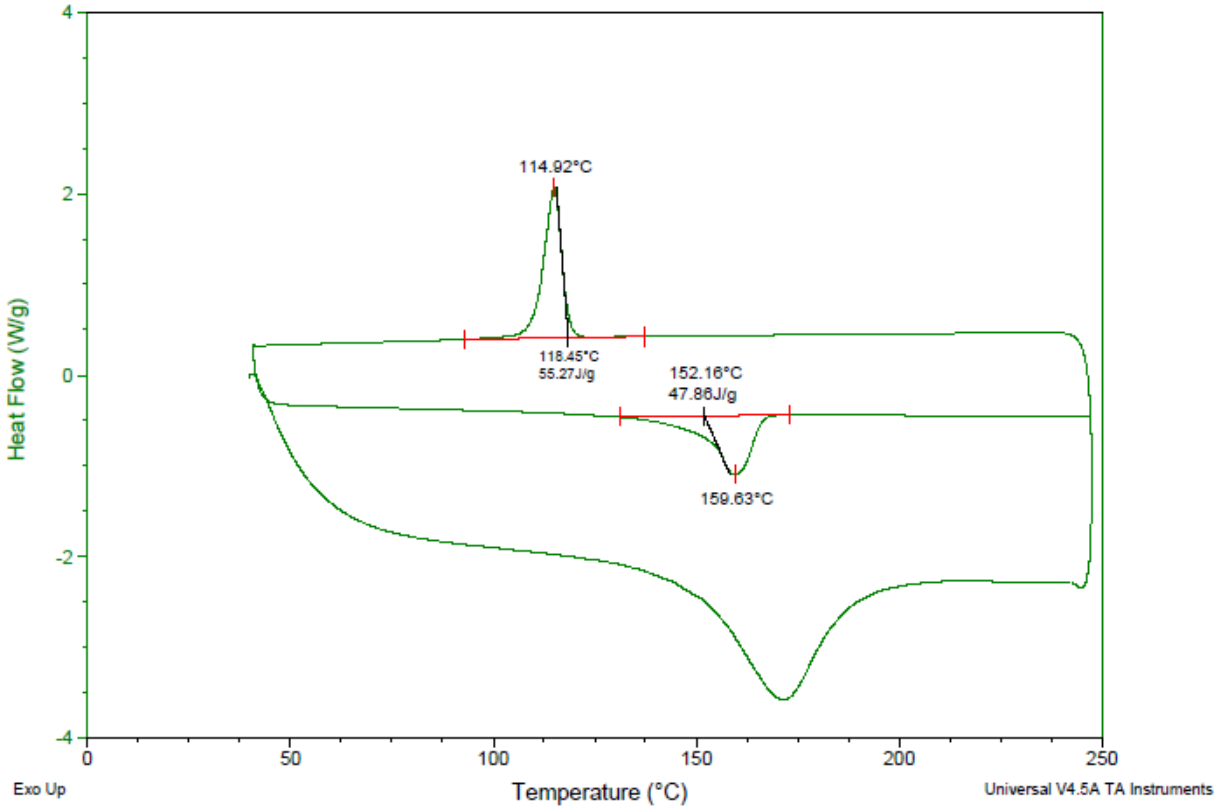

Figure D.6 DSC thermogram of HC13 with heat, cool, heat mode

Appendix E: Experimental raw data for chapter 6

Appendix E: Experimental raw Data for Chapter 6

Table E.1: Tensile modulus of neat PP, HC13, rPP based hybrid composites

Composites	Tensile modulus (MPa)	SD
Neat PP	1708.6	38.9
F13	5310.4	128.3
rHC1	4859.2	167.7
rHC2	4753.9	161.4
rHC3	4668.9	137.0
rHC4	4466.2	169.0
rHC5	4225.2	195.4
rHC6	4201.8	109.5

Table E.2: Flexural modulus of neat PP, HC13, rPP based hybrid composites

Composites	Flexural modulus (MPa)	SD
Neat PP	1240.3	30.4
F13	5277.1	169.8
rHC1	5222.6	83.2
rHC2	5221.3	35.4
rHC3	5084.0	38.5
rHC4	4839.3	112.4
rHC5	4586.7	86.4
rHC6	4557.6	61.5

Table E.3: Izod impact strength of neat PP, HC13, rPP based hybrid composites

Composites	Izod impact strength (kJ/m^2)	SD
Neat PP	5.11	0.29
F13	6.03	0.18
rHC1	5.51	0.22
rHC2	5.42	0.07
rHC3	5.31	0.24
rHC4	5.29	0.23
rHC5	5.25	0.14
rHC6	5.20	0.10

Table E.4: Measured melt flow index of neat PP and rPP based hybrid composites

Composites	Melt Flow Index (g/10 min)	SD
Neat PP	55.50	4.79
F13	30.66	1.98
rHC1	31.32	1.61
rHC2	31.38	2.60
rHC3	30.93	2.89
rHC4	27.28	2.28
rHC5	23.64	1.65
rHC6	20.44	1.62

Table E.5: Measured density of rPP based hybrid composites

Composites	Density (g/cm^3)	SD
Neat PP	0.910	0.014
F13	1.231	0.029
rHC1	1.229	0.014
rHC2	1.228	0.022
rHC3	1.230	0.025
rHC4	1.234	0.029
rHC5	1.229	0.016
rHC6	1.230	0.042

Table E.6: The rating of rPP based hybrid composite

	The improvement of mechanical properties			MFI	Density
	Tensile Modulus	Flexural Modulus	Izod impact strength		
HC13	2.64	4.07	0.90	-2.74	3.92
rHC1	2.30	4.01	0.40	-2.66	3.89
rHC2	2.23	4.01	0.31	-2.66	3.88
rHC3	2.17	3.87	0.20	-2.71	3.91
rHC4	2.02	3.63	0.18	-3.11	3.95
rHC5	1.84	3.37	0.14	-3.51	3.89
rHC6	1.82	3.34	0.09	-3.86	3.91

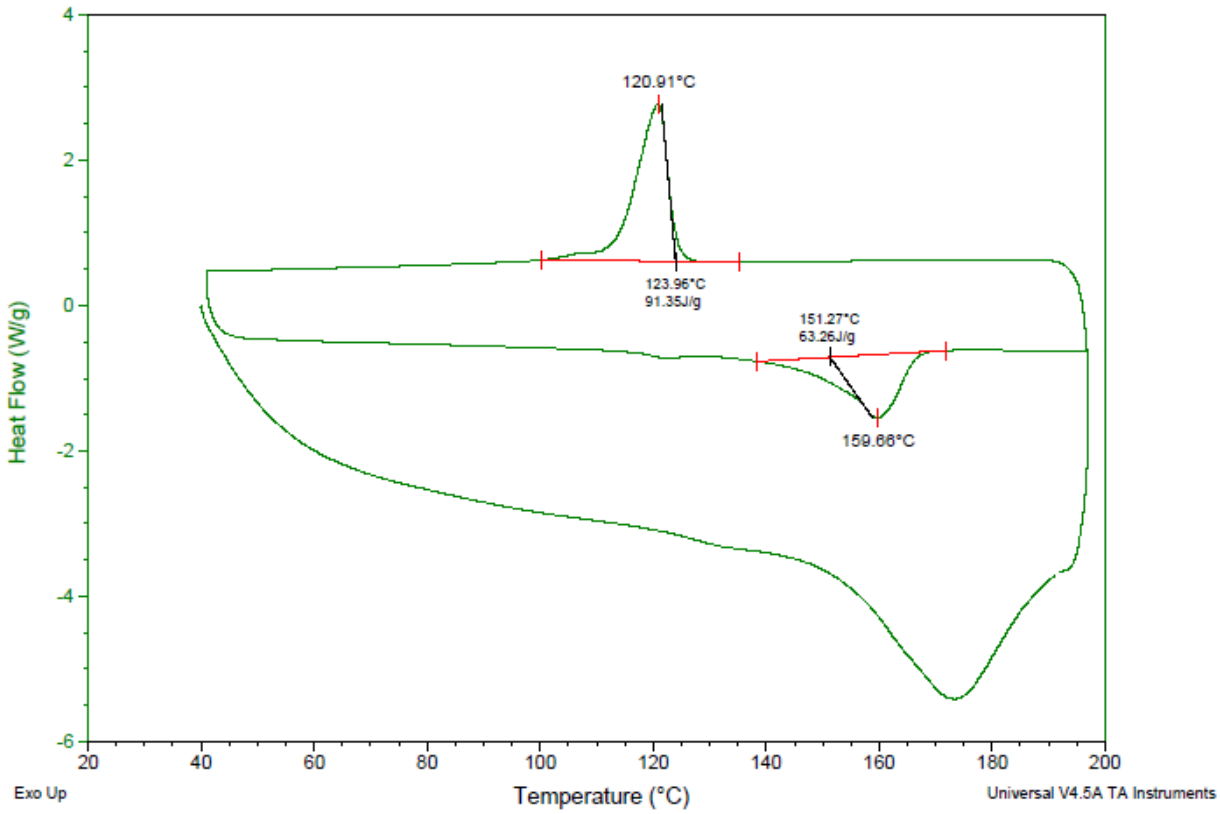

Figure E.1: DSC thermogram of rPP with heat, cool, heat mode

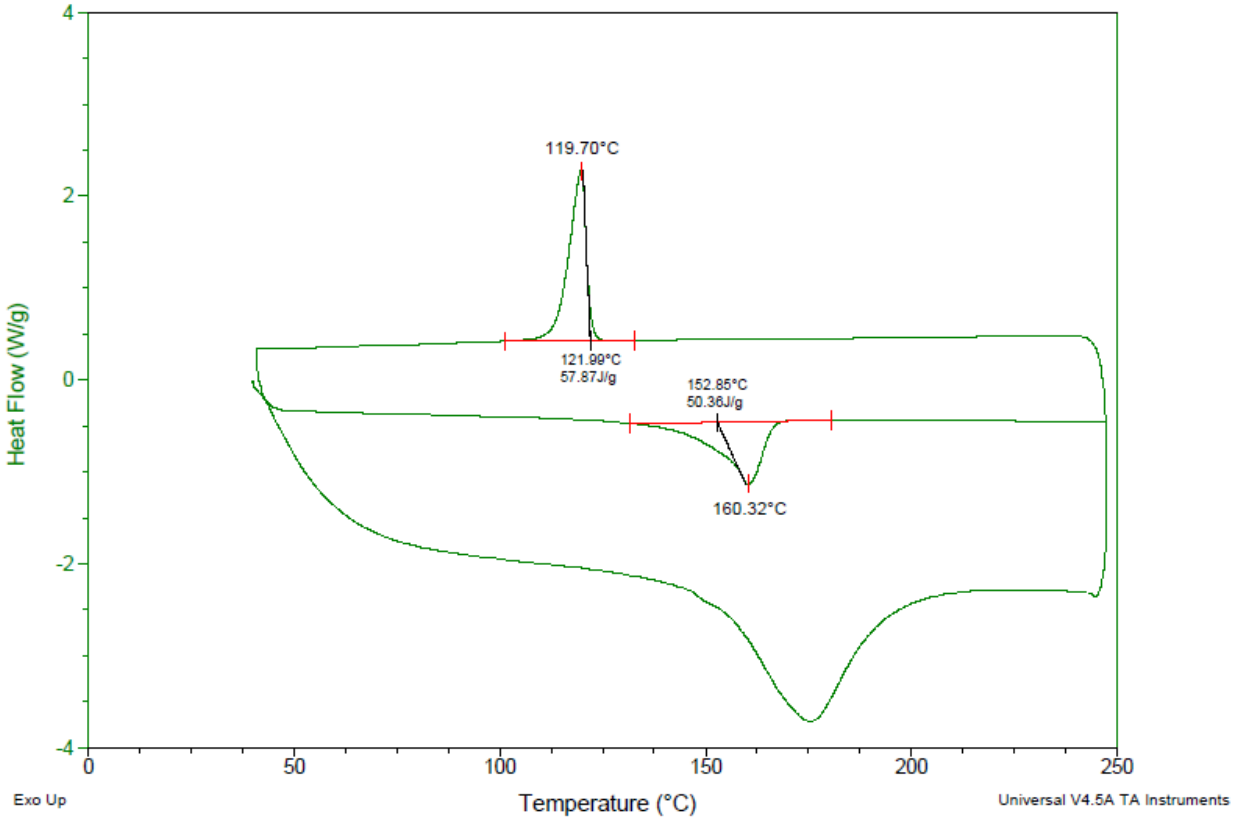

Figure E.2: DSC thermogram of rHC1 with heat, cool, heat mode

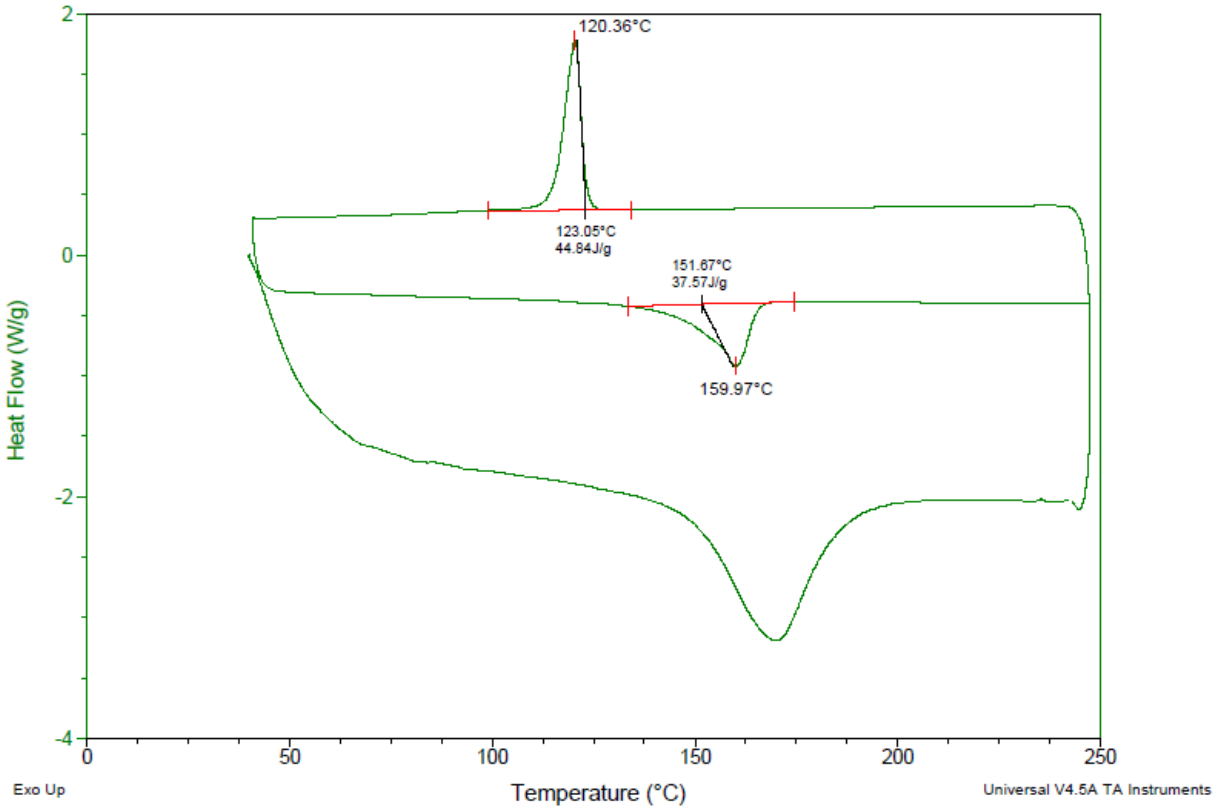

Figure E.3: DSC thermogram of rHC3 with heat, cool, heat mode

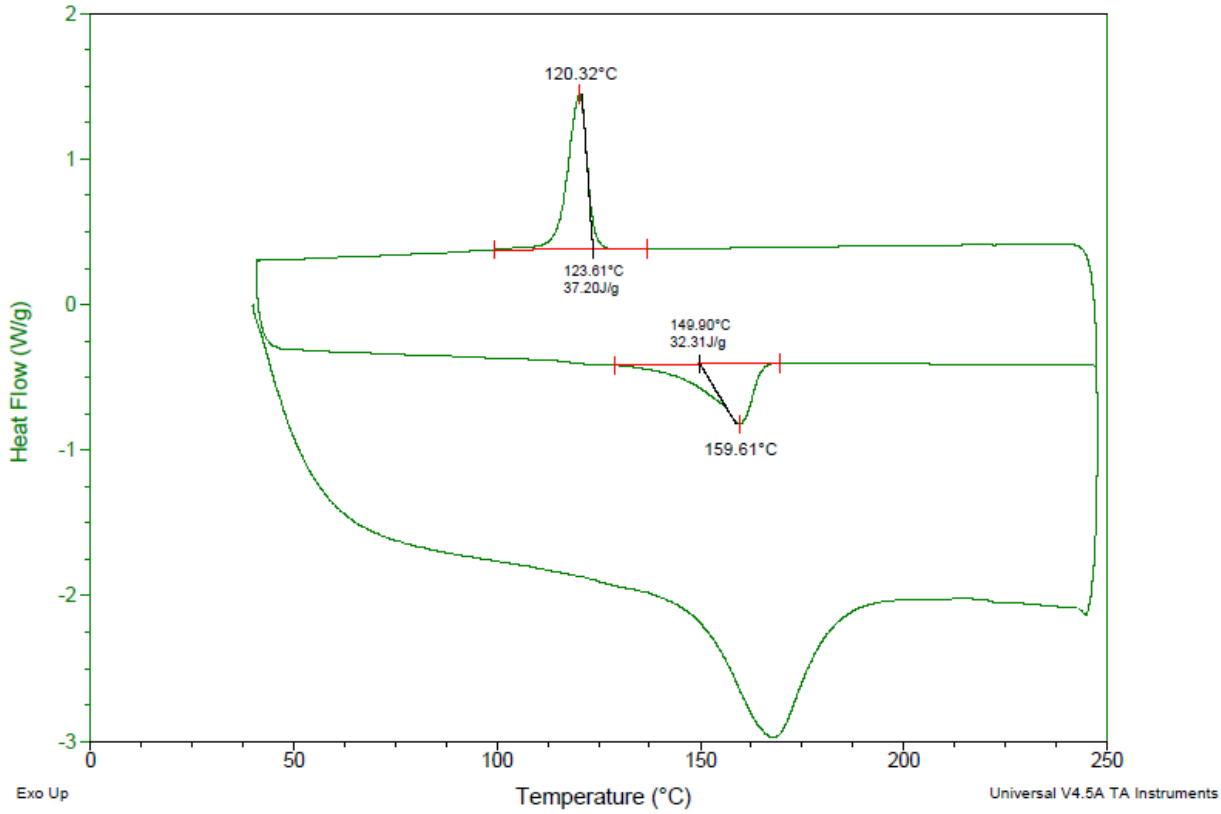

Figure E.4: DSC thermogram of rHC4 with heat, cool, heat mode

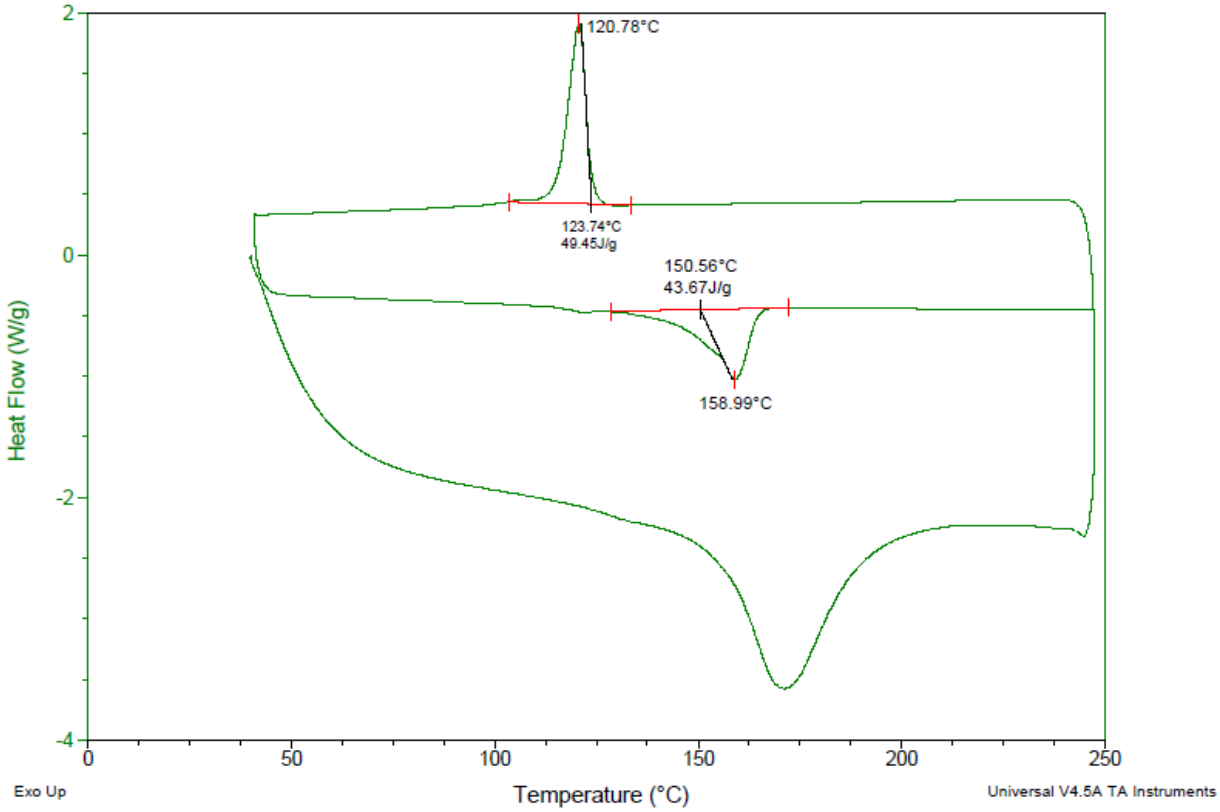

Figure E.5: DSC thermogram of rHC5 with heat, cool, heat mode

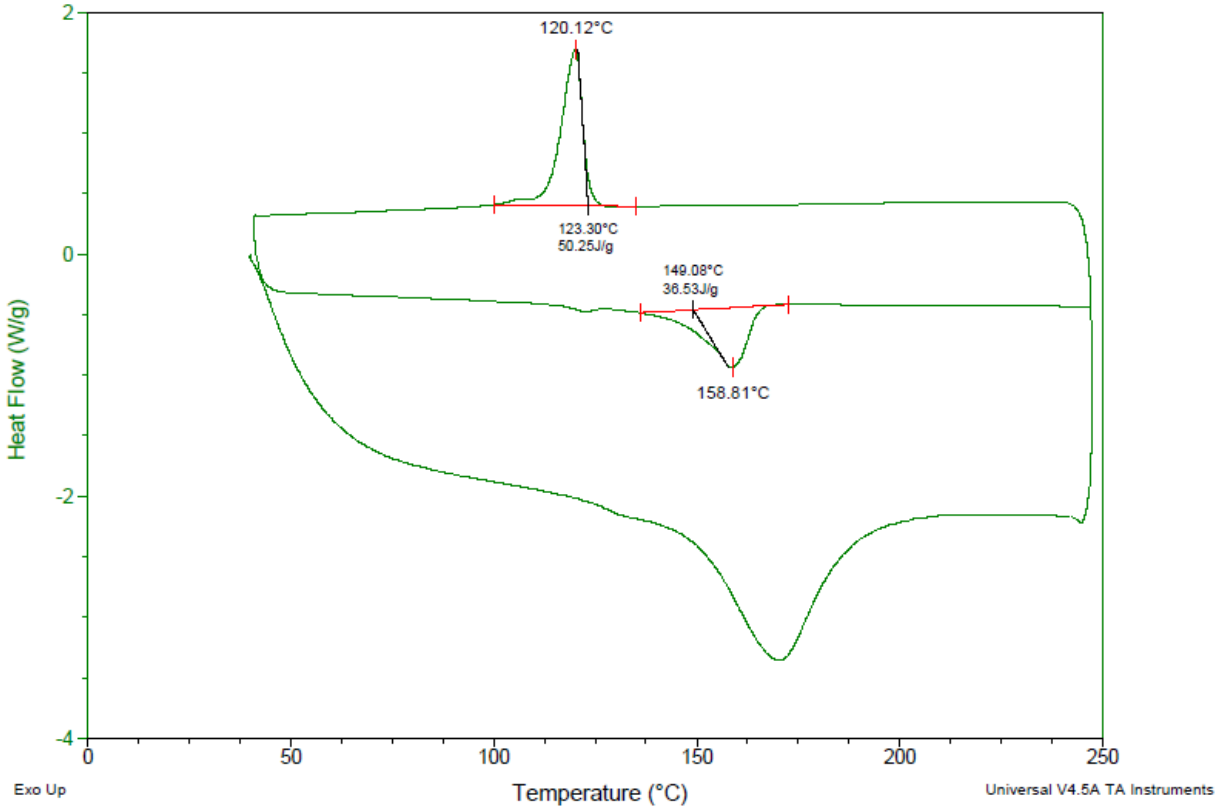

Figure E.6: DSC thermogram of rHC6 with heat, cool, heat mode